Top 2 of 2

DOT/FAA/CT-ACD33090/9

PROCEEDINGS OF THE MLS MATH MODEL USER GROUP MEETING, June 27-28 1990

Jesse D. Jones
Linda Pasquale
Coordinators

August 1990

Engineering, Research, and Development Service
Concepts Analysis Division
FAA Technical Center
Atlantic City International Airport, N.J. 08405

PROCEEDINGS

OF THE

MLS MATH MODEL

USER GROUP MEETING

JUNE 27-28, 1990

FAA TECHNICAL CENTER
ATLANTIC CITY INTERNATIONAL AIRPORT
NEW JERSEY 08405

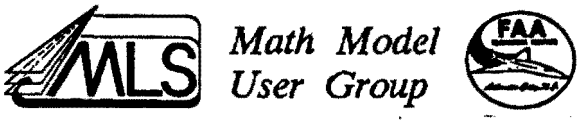


TABLE OF CONTENTS

	Page
MEETING AGENDA	v
ATTENDENCE LIST	vii
MLS PROGRAM OVERVIEW - Richard Arnold	1
MODEL VALIDATION - Mike DiBenedetto	33
RUNWAY HUMP SHADOWING - Al Lopez	73
RUNWAY HUMP SHADOWING - Kent Chamberlin	103
THEORY OF DME/P - Robert Kelly	131
EL SITING CRITERIA - Al Lopez	141
MODELING CONSIDERATIONS - Jim Evans	157
A SPECIAL APPLICATION - Jan-Hein van Dronkelaar	173

MLS MATHEMATICAL MODEL USER GROUP MEETING
AGENDA

JUNE 27-28, 1990
FAA TECHNICAL CENTER
ATLANTIC CITY INTERNATIONAL AIRPORT, NJ 08405

DAY 1 - June 27, 1990

Morning Session - 9:00 to 12:00

Welcome	
MLS Program Overview	Richard Arnold, FAA
Model Validation	Mike DiBenedetto, Ohio Univ.

Lunch - 12:00 to 1:00

Afternoon Session - 1:00 to 4:00

Runway Hump Shadowing	Al Lopez, ARL Associates
Runway Hump Shadowing	Kent Chamberlin, Univ. of N. H.
General Discussion	

DAY 2 - June 28, 1990

Morning Session - 9:00 to 12:00

Theory of DME/P	Robert Kelly, Bendix
EL Siting Criteria	Al Lopez, ARL Associates

Lunch - 12:00 to 1:00

Afternoon Session - 1:00 to 4:00

Modeling Considerations	Jim Evans, Lincoln Laboratory
A Special Application	Jan-Hein van Dronkelaar, NLR
General Discussion	

V

MLS MATH MODEL USER GROUP MEETING - JUNE 27-28, 1990

ATTENDANCE LIST

Mr. Glen Adams
MiTech Inc.
600 Maryland Avenue, S.W.
Suite 695
Washington, D.C. 20024
202-484-4780

Mr. Richard Arnold
FAA National Headquarters, AND-30
800 Independence Ave., S.W.
Washington, D.C. 20591
202-267-8709

Mr. Dennis Atkeson
Avionics Engineering Center
Department of Electrical and
Computer Engineering
Stocker Center
Ohio University, Athens, OH 45701-2979
614-593-1532

Mr. Rick Cassell
MiTech, Inc.
600 Maryland Ave., S.W.
Suite 695
Washington, D.C. 20024
202-484-4780

Dr. Kent Chamberlin
Dept. of Electrical and Computer Engineering
Kingsbury Hall
University of New Hampshire
Durham, NH 03824-3591
603-862-3766

Mr. Elmer Clausen
Bell Aerospace Textron
P.O. Box 1
Buffalo, NY 14240-0001
716-298-6597

Mr. Mike DiBenedetto
Avionics Engineering Center
Department of Electrical and
Computer Engineering
Stocker Center
Ohio University, Athens, OH 45701-2979
614-593-1515

Mr. Jan-Hein van Dronkelaar
National Aerospace Laboratory
P.O. Box 90502
Anthony Fokkerweg 2
1059 CM Amsterdam
The Netherlands
31-020-113-583

Mr. Gerald Einarsson
Microwave Landing System Project
Transport Canada
110 O'Connor St., Rm. 736
Ottawa, Ontario K1A ON8
613-993-9308

Dr. Moe Elgamal
Microwave Landing System Project
Transport Canada
110 O'Connor St., Rm. 736
Ottawa, Ontario K1A ON8
613-993-4811

Dr. Jim Evans
MIT Lincoln Laboratory, Room HW-10
244 Wood Street
Lexington, MA 02173-9108
617-981-7433

Mr. Seymour Everett
FAA National Headquarters, ASE-300
800 Independence Ave., S.W.
Washington, D.C. 20591
202-267-8621

Mr. Richard Frazita
Scan Tek, Inc.
P.O. Box 2177
St. James, NY 11780
516-584-9554

Mr. Ron Frerking
AT&T, Fed. Systems Advanced Tech.
Room E3K18
P.O. Box 20046
Greensboro, NC 27420-0046
919-279-5802

Mr. Anthony Greco
1842 EEG/EETWE
Scott Air Force Base
IL 62225-6348
618-256-6339

Ms. Patricia Hatzis
MMLS Engineering Group, G312
The MITRE Corporation
Burlington Road
Bedford, MA 01730
617-271-8911

Ms. Danette Havel
Avionics Engineering Center
Department of Electrical and
Computer Engineering
Stocker Center
Ohio University, Athens, OH 45701-2979
614-593-1527

Mr. Bob Ibach
Wilcox Electric, Inc.
2001 N. E. 46th Street
Kansas City, MO 64116
816-453-2600

Ms. Marjorie Luke Johnson
ARINC Research Corporation
2551 Riva Road
Annapolis, MD 21401
301-266-2268

Mr. Jesse Jones
FAA Technical Center, ACD-330
Atlantic City International Airport
NJ 08405
609-484-4573

Mr. Robert Kelly
Allied-Signal Aerospace Co.
Bendix Communications Division
1300 East Joppa Road
Baltimore, MD 21204
301-583-4299

Mr. Michael Kleintz
DLR
Institut für Hochfrequenztechnik
D-8031 Oberpfaffenhofen
Post Wessling / Obb.
Federal Republic of Germany
49-08153-28-379

Mr. Alex Lakhtman
CTA Incorporated
English Creek Center, Suite 204
McKee City, NJ 08232
609-645-5022

Mr. Harry Lenzing
AT&T, Bell Labs
Room 2F211
Holmdel, NJ 07733
201-949-4961

Mr. Al Lopez
ARL Associates
Four Sarina Drive
Commack, NY 11725
516-499-2987

Mr. Paul Manning
Transportation Systems Center
Kendall Square
Cambridge, MA 02142
617-494-3417

Mr. Anthony McAndrew
ARINC Research Corporation
2551 Riva Road
Annapolis, MD 21401
301-266-4434

Ms. Linda Pasquale
FAA Technical Center, ACD-330
Atlantic City International Airport
NJ 08405
609-484-6806

Mr. Rick Pierce
Bell Aerospace Textron
P.O. Box 1
Buffalo, NY 14240-0001
716-298-6908

Mr. James Rambone
FAA Technical Center, ACD-330
Atlantic City International Airport
NJ 08405
609-484-5373

Dr. B. Röde
DLR
Institut für Hochfrequenztechnik
D-8031 Oberpfaffenhofen
Post Wessling / Obb.
Federal Republic of Germany
49-08153-28-351

Mr. Glyn Romrell
E-Systems
2268 South 3270 West
Salt Lake City
UT 84119
801-974-7217

Dr. Hollis Ryan
CTA Incorporated
English Creek Center, Suite 204
McKee City, NJ 08232
609-645-5070

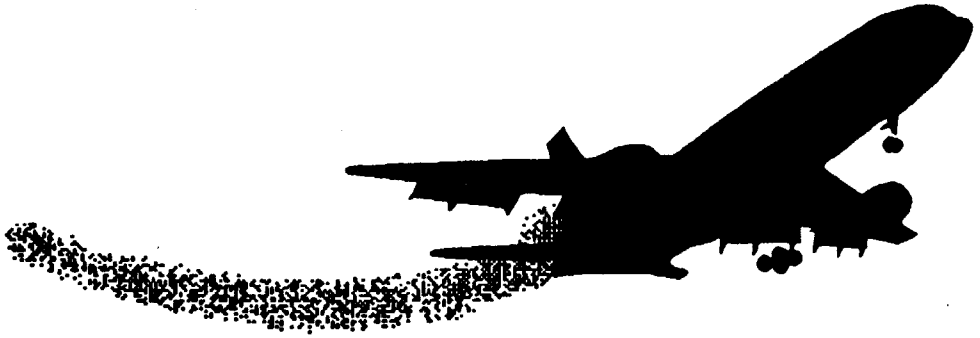
Mr. Rial Sloan
FAA National Headquarters, ANN-150
800 Independence Ave., S.W.
Washington, D.C. 20591
202-267-6660

Mr. Douglas Vickers
Avionics Engineering Center
Department of Electrical and
Computer Engineering
Stocker Center
Ohio University, Athens, OH 45701-2979
614-593-1510

Mr. Edmund Zyzys
FAA Technical Center, ACD-330
Atlantic City International Airport
NJ 08405
609-484-6816

RICHARD ARNOLD
FAA, MLS PROGRAM MANAGER

MLS PROGRAM OVERVIEW



FAA MLS PROGRAM
OVERVIEW

CURRENT AND PROJECTED PRECISION APPROACHES

- 750 CURRENT ILS
- 1250 MLS AUTHORIZED
- 1400 + QUALIFIED LOCATIONS
- 2000 + PROJECTED BY 2010
- DOES NOT ACCOUNT FOR ROTORCRAFT LOCATIONS

WHY MLS ?

- FREQUENCIES
- ATC BENEFITS
- G/A PRECISION APPROACHES
- CAT II/III APPROACHES
- ROTORCRAFT

MLS DEMONSTRATION PROGRAM

- NINE ECONOMIC AND OPERATIONAL EVALUATIONS
- ALL PROJECTS STARTED
- INTERIM RESULTS AVAILABLE

1387/M3113 01/10689 4

FREQUENCY ANALYSIS

- ***Objective: Determine the imminence and severity of ILS/MLS frequency congestion and FM interference***
- **COMPUTER MODEL DEVELOPED**
- **CONTAINS**
  - **ANTENNA CONFIGURATIONS**
  - **ALL ILS VOR LOCATIONS**
  - **CELLULAR STRUCTURE**
- **TO BE ACCOMPLISHED**
  - **EARTH CURVATURE**
  - **DIFFRACTION MODEL**
  - **MLS MODEL**
- **ILS RESULTS EARLY FALL**

EVALUATION OF WIDEBODY CURVED/ SEGMENTED APPROACHES

- ***Objective: Solve human and technical issues for curved approaches***
- ***NLR STUDY***
  - ***747 SIMULATOR***
  - ***20 747 LINE CREWS***
  - ***320 APPROACHES***
  - ***FINAL SEGMENT LENGTH - .7 TO 3.0 NM***

EVALUATION OF WIDEBODY CURVED/ SEGMENTED APPROACHES (CONT)

- *NLR CONCLUSION*
  - *NO MISSED APPROACHES*
  - *APPROACH STABILITY AFFECTED BY FAF*
  - *ALL PILOTS ACCEPTED 3NM FINAL*
  - *MODERATE INCREASE IN PILOT EFFORT*
  - *FOLLOW - ON FALL '90 - 20 CREWS-ANOMALIES*
- *MCDONNELL DOUGLAS MD-11 SIMULATOR*
  - *CONTROL LAWS, AERODYNAMICS, COCKPIT DISPLAYS, CERTIFICATION*

EVALUATION OF ADVANCED PROCEDURES

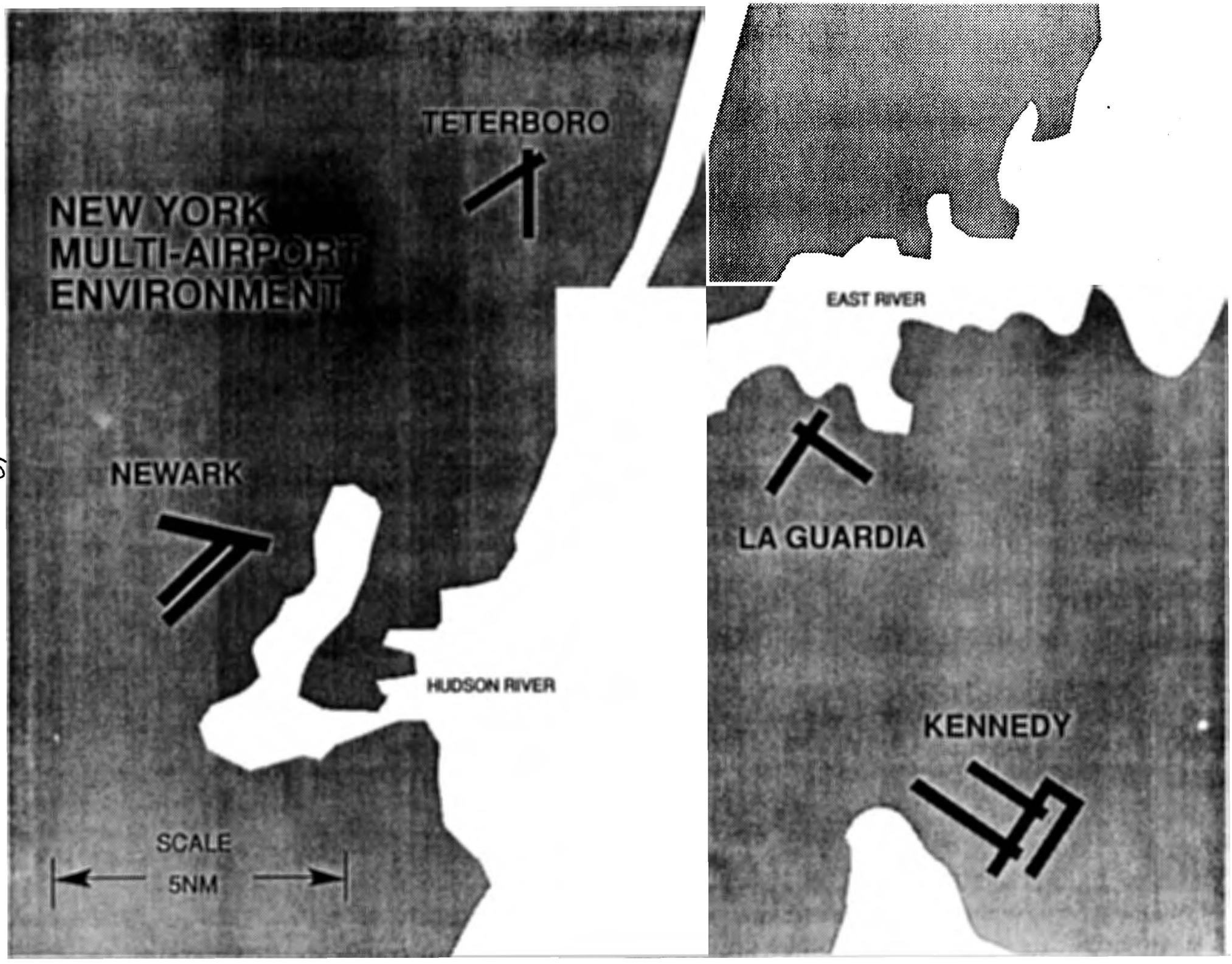
- *Objective: Determine economic and operational benefits of MLS in multi-airport environments*

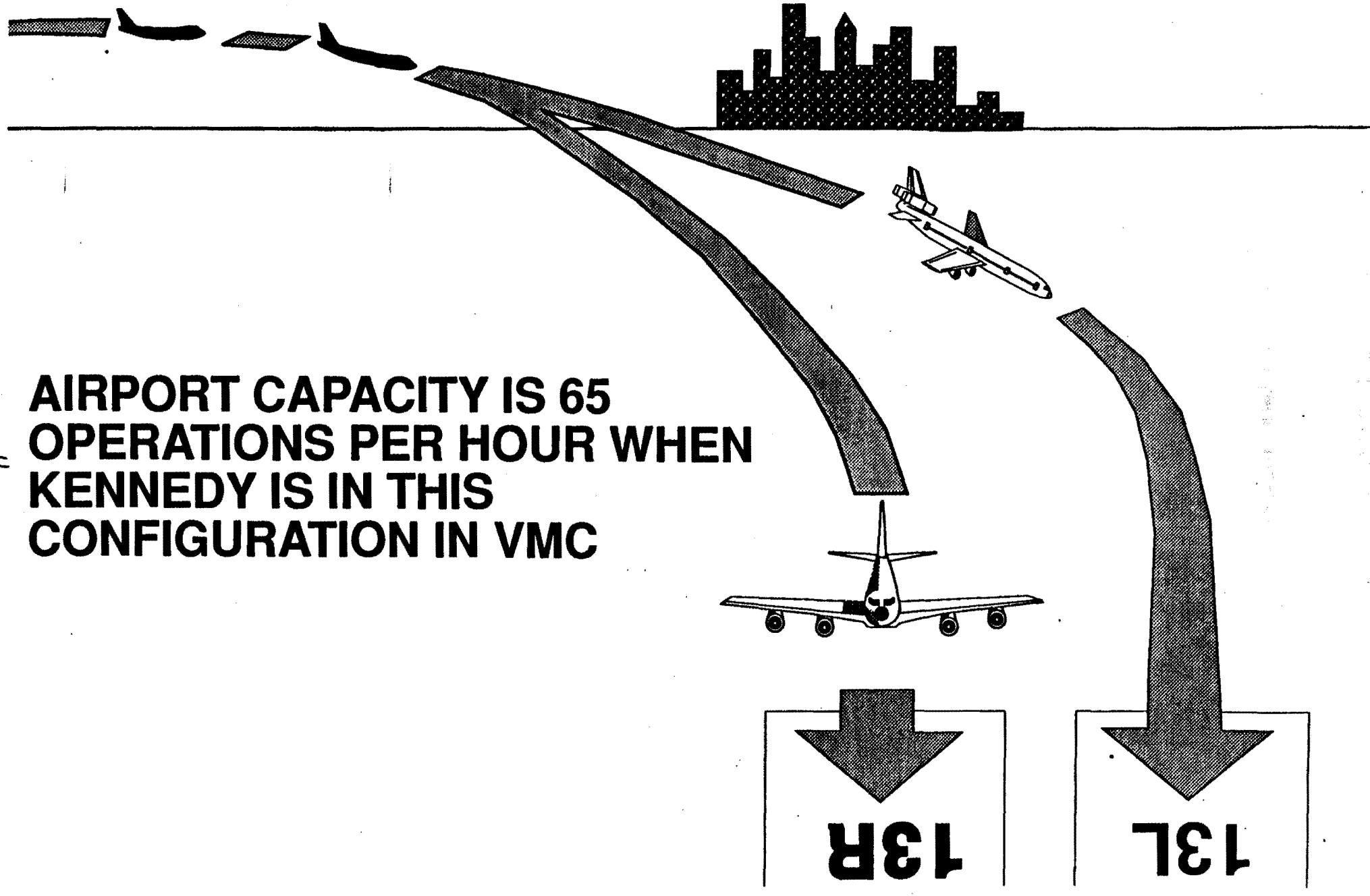
- *NASA AMES PRELIMINARY RESULTS*

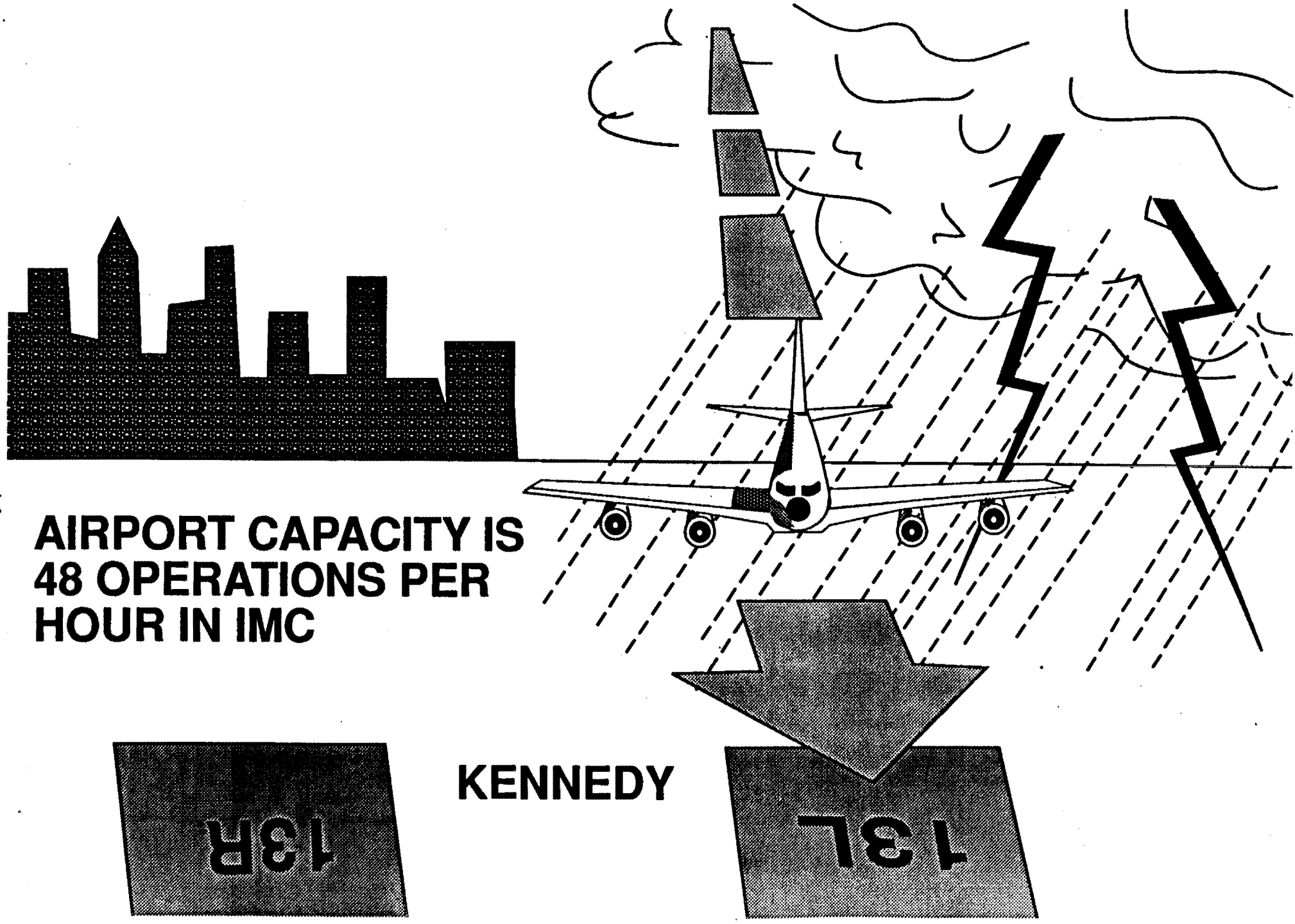
  - *LGA SIMULATION INDICATES REDUCED FLIGHT TIME, INCREASE FLOW RATE*
  - *TETERBORO DELAYS ELIMINATED*

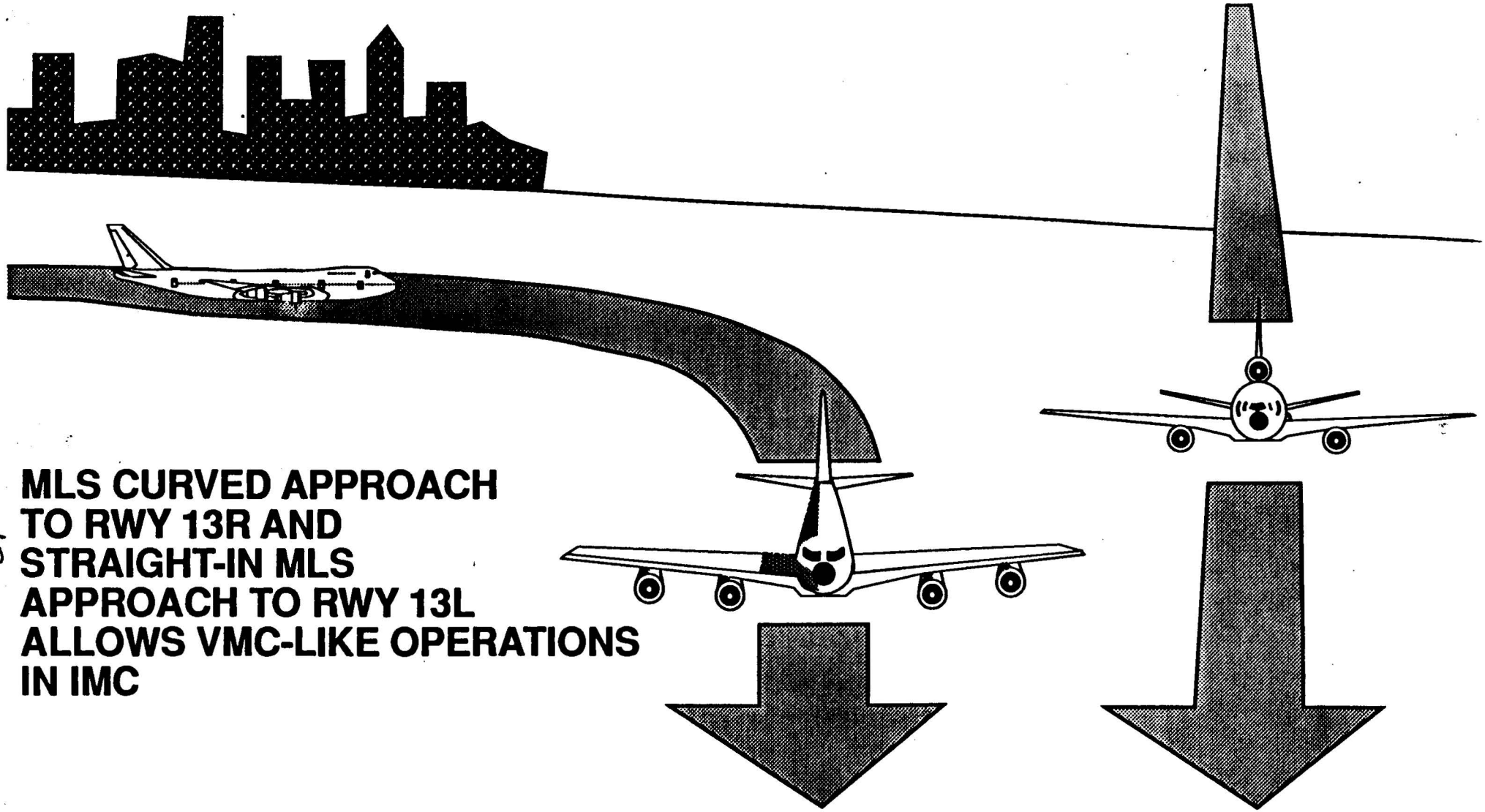
- *NASA AMES PLANS*

  - *SIMULATE ENTIRE NY AREA*
  - *SIMULATE CHICAGO, SAN FRANCISCO*


TETERBORO
NEW YORK
MULTI-AIRPORT
ENVIRONMENT
NEWARK
HUDSON RIVER
SCALE
5NM
EAST RIVER
LA GUARDIA
KENNEDY


AIRPORT CAPACITY IS 65
OPERATIONS PER HOUR WHEN
KENNEDY IS IN THIS
CONFIGURATION IN VMC
13R
13L

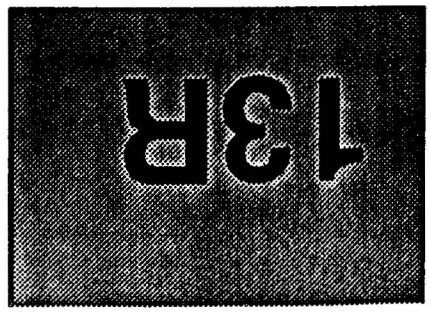

AIRPORT CAPACITY IS
48 OPERATIONS PER
HOUR IN IMC
13R
KENNEDY
13L



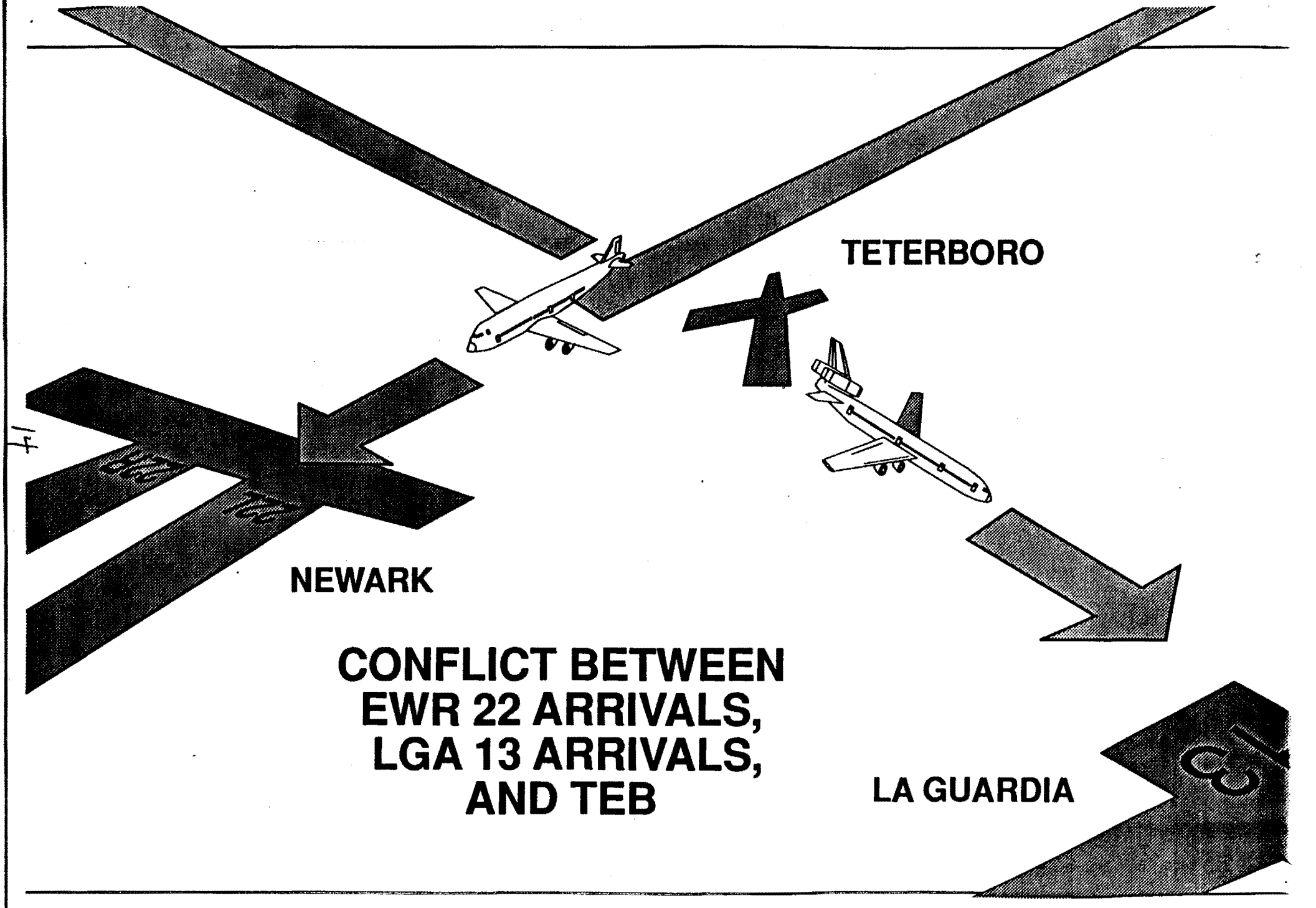
MLS CURVED APPROACH TO RWY 13R AND STRAIGHT-IN MLS APPROACH TO RWY 13L ALLOWS VMC-LIKE OPERATIONS IN IMC

13

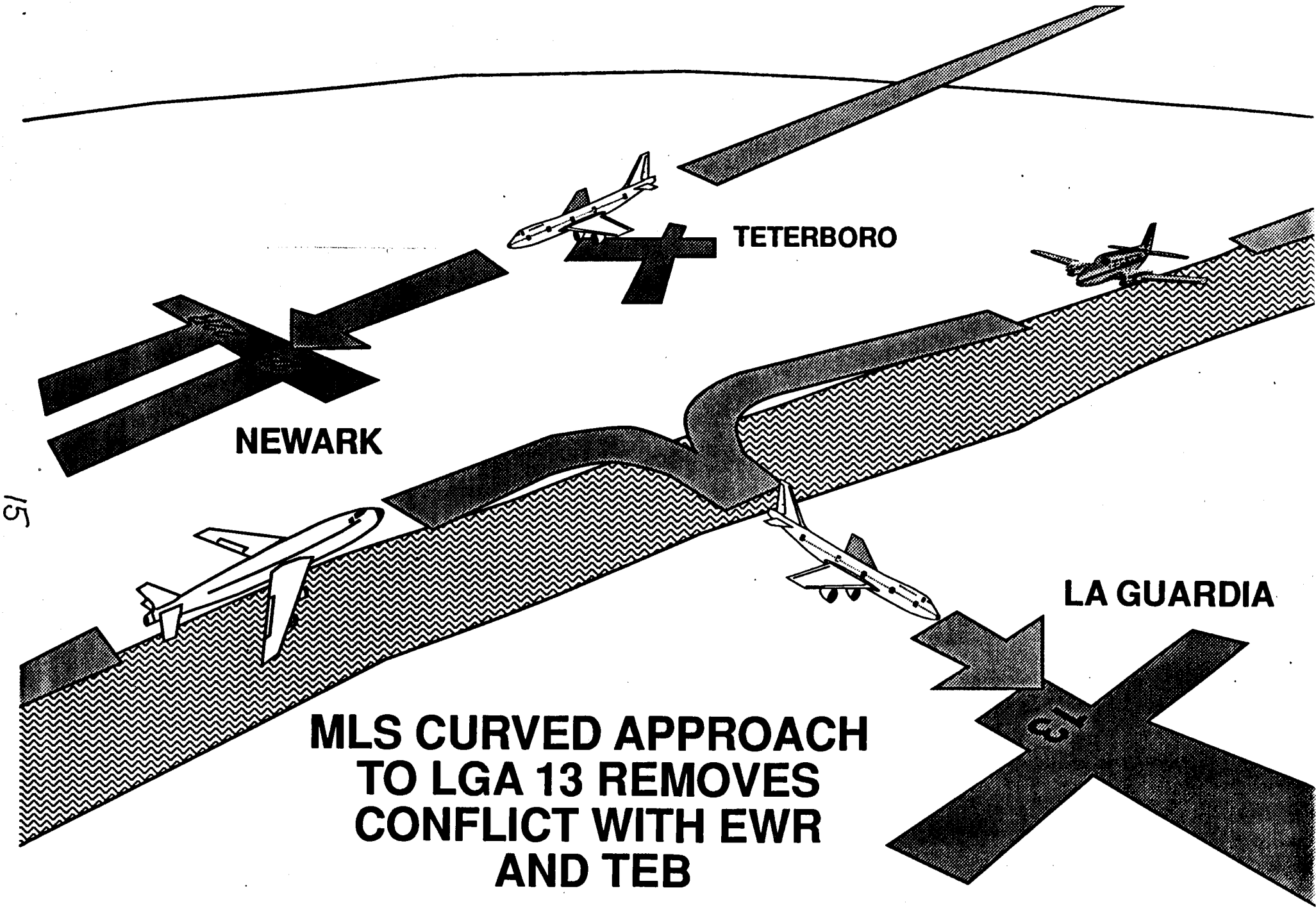
KENNEDY







CONFLICT BETWEEN EWR 22 ARRIVALS, LGA 13 ARRIVALS, AND TEB



MLS CURVED APPROACH TO LGA 13 REMOVES CONFLICT WITH EWR AND TEB

GENERAL AVIATION/COMMUTER CAPACITY ENHANCEMENT

- ***Objective: Increase flow rate by moving commuter/GA aircraft off main runways***
- **AIRPORT/AIRSPACE ANALYSES**
- **INSTALL MLS AT MIDWAY 22L, JFK 13R, PHILADELPHIA 27L, LGA 13, ASPEN**

COMPARISON OF MLS TO ILS PERFORMANCE

- *Objective: Quantify MLS technical advantages*
- SIMULTANEOUS DATA COLLECTION
- FINDINGS
  - ILS DISTURBED BY OVERFLIGHTS
  - MLS UNAFFECTED
  - MLS SMOOTHER THAN CAT I ILS
  - MLS ACCURACY
- MCDONNELL DOUGLAS MD 11
- FAA TECH CENTER

ASSESSMENT OF REDUCED MLS MINIMA

- ***Objective: Validate MLS capability for lower DH and RVR***
- **DEVELOPMENT OF STANDARDS, COCKPIT PROCEDURES, AND AIRCRAFT SYSTEMS**
- **RUNWAY VISUAL ENVIRONMENT**
- **FAA TECH CENTER, FLIGHT STANDARDS**

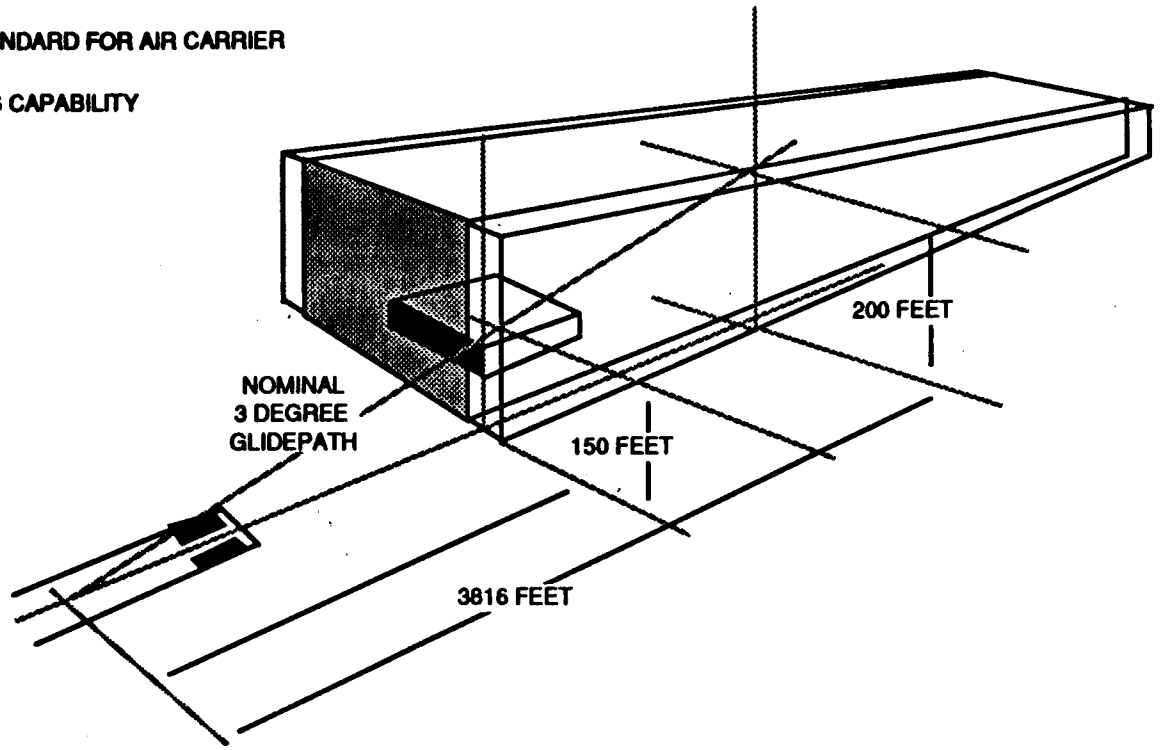
MLS 150-FOOT DECISION HEIGHT

- **PROBABILITY OF A SUCCESSFUL LANDING INCREASED WITH MLS - DME/P WHILE REDUCING DECISION HEIGHT**

○ STANDARD FOR AIRSPACE

● STANDARD FOR AIR CARRIER

● MLS CAPABILITY



61

ASSESSMENT OF MLS AVIONICS COSTS

- ***Objective: Develop costing models for airlines and industry***
- **DETAILED INDUSTRY SURVEY**
- **RETROFIT VS NEW**
- **TRANSPORTATION SYSTEMS CENTER (TSC)**

DEVELOPMENT OF DME/P INTERROGATORS

- ***Objective: Provide units for Evaluation Program***
- **SIX UNITS BY DECEMBER - SEL**
- **TWO PROTOTYPES - OPTION 20**
- **CONTRACT AWARD APRIL '90 - DELIVERY APRIL '91**
- **TSC**

CATEGORY II/III FLIGHT DEMONSTRATION AND PROCUREMENT

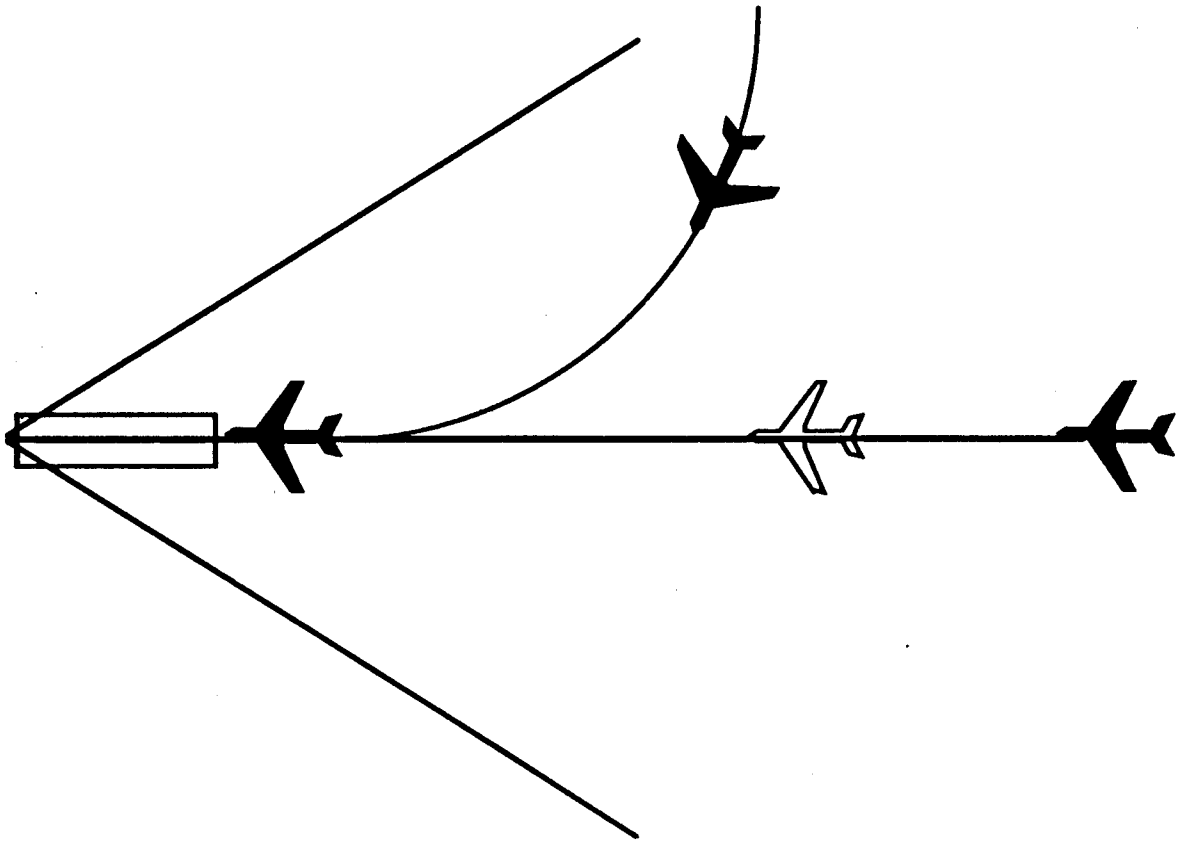
- ***Objective: Assure certification of airborne equipment***
- **UPGRADE FAA AIRCRAFT**
- **MD -11 CERTIFICATION CAT I COLLECTION FOR CAT III**
- **FAA TECH CENTER**

OTHER PROJECTS/ACTIVITIES

OTHER PROJECTS

- MLS CAT III FUTURE REQUIREMENTS
  - ASSESS DEMAND FOR CAT III LANDING SYSTEMS
  - TSC
- GHOSTING
  - MITRE
- USE OF GPS FOR PRECISION APPROACH
  - FEASIBILITY
  - TIMEFRAME
  - USER COST

ADVANCED ATC DEVELOPMENT
MLS APPLICATIONS - GHOSTING CONCEPT



DOD ACTIVITIES

- DOD PRECISION LANDING STANDARD FOR YR 2000
- CONTRACT WITH CMC TO DESIGN AND PRODUCE 1078 UNITS
- CONTRACT IN 1992 FOR 8700 DUAL MLS/ILS RECEIVERS
- BELL CONTRACT FOR UP TO 132 TACTICAL SYSTEMS
- 405 FIXED-BASE SYSTEMS THROUGH THE FAA

CURRENT ENVIRONMENT

- INDUSTRY/FAA COOPERATION
  - ATA INDUSTRY LEAD
  - 5 OVERSIGHT COMMITTEES COMPOSED OF USER GROUPS, AIRLINES, AND INDUSTRY
  - OBJECTIVE: JOINTLY DESIGN AND MANAGE EVALUATION PROGRAMS

27

CURRENT ENVIRONMENT
(CONT)

- FOREIGN INITIATIVES
  - CANADA
    - $ 448 M APPROVED PROGRAM
    - 42 SYSTEMS
  - USSR
    - CAT III SYSTEM OPERATING
    - 27 CAT III SYSTEMS BY JAN '98
    - 500 CAT I BY 2000

FIRST PRODUCTION CONTRACT STATUS

- HAZELTINE CONTRACT - JAN 84
  - 178 SYSTEMS
  - PRICE $79.4M - PROGRESS PAYMENTS $42.0M

- 30 MONTH DELIVERY DELAY
  - TWO SYSTEMS DELIVERED
  - UNAUTHORIZED SLOWDOWN - AUG 88

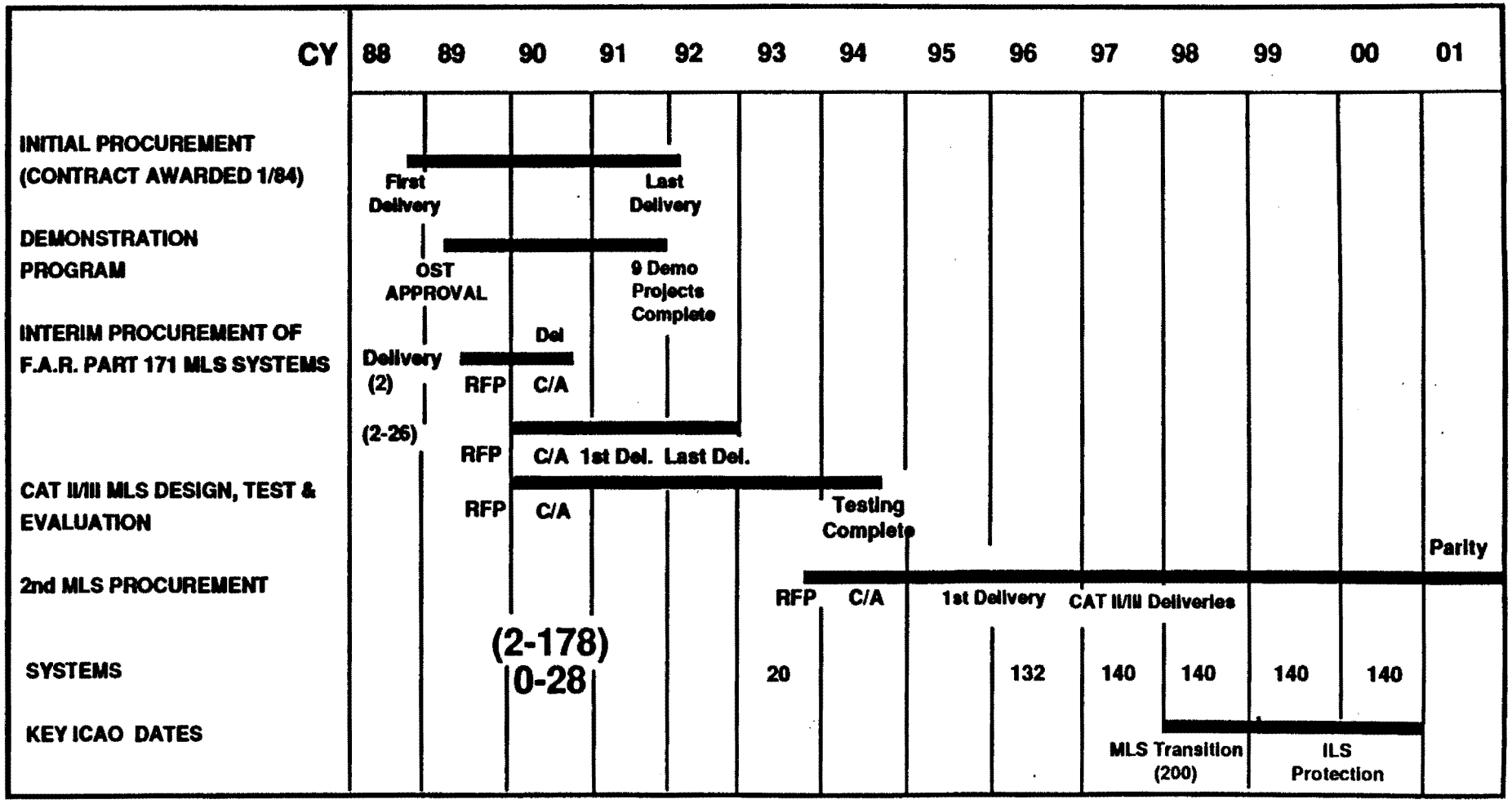
- NEGOTIATIONS/SHOW CAUSE LETTER - JUL 2/89

- TERMINATION LETTER - AUG 7/89

MLS ACQUISITION SCHEDULE

- TWO SYSTEMS CONTRACT AWARD - APRIL '90
- 2-26 SYSTEMS - CONTRACT AWARD - EARLY '91
- CATEGORY III PROTOTYPE
  - 2 CONTRACTORS - SEPARATE DESIGNS
  - 6 - 12 SYSTEMS - SYSTEMS PER CONTRACTOR PRODUCTION CONTRACT - SAME CONTRACTORS AWARD '94 FIRST DELIVERY '96

MLS PROGRAM SCHEDULE



MIKE DiBENEDETTO
OHIO UNIVERSITY

MODEL VALIDATION

Ohio University
Model Validation Activities

by

Michael F. DiBenedetto

34

Presented to

MLS Mathematical Model User Group

June 27-28, 1990

FAA Technical Center
Atlantic City International Airport, NJ

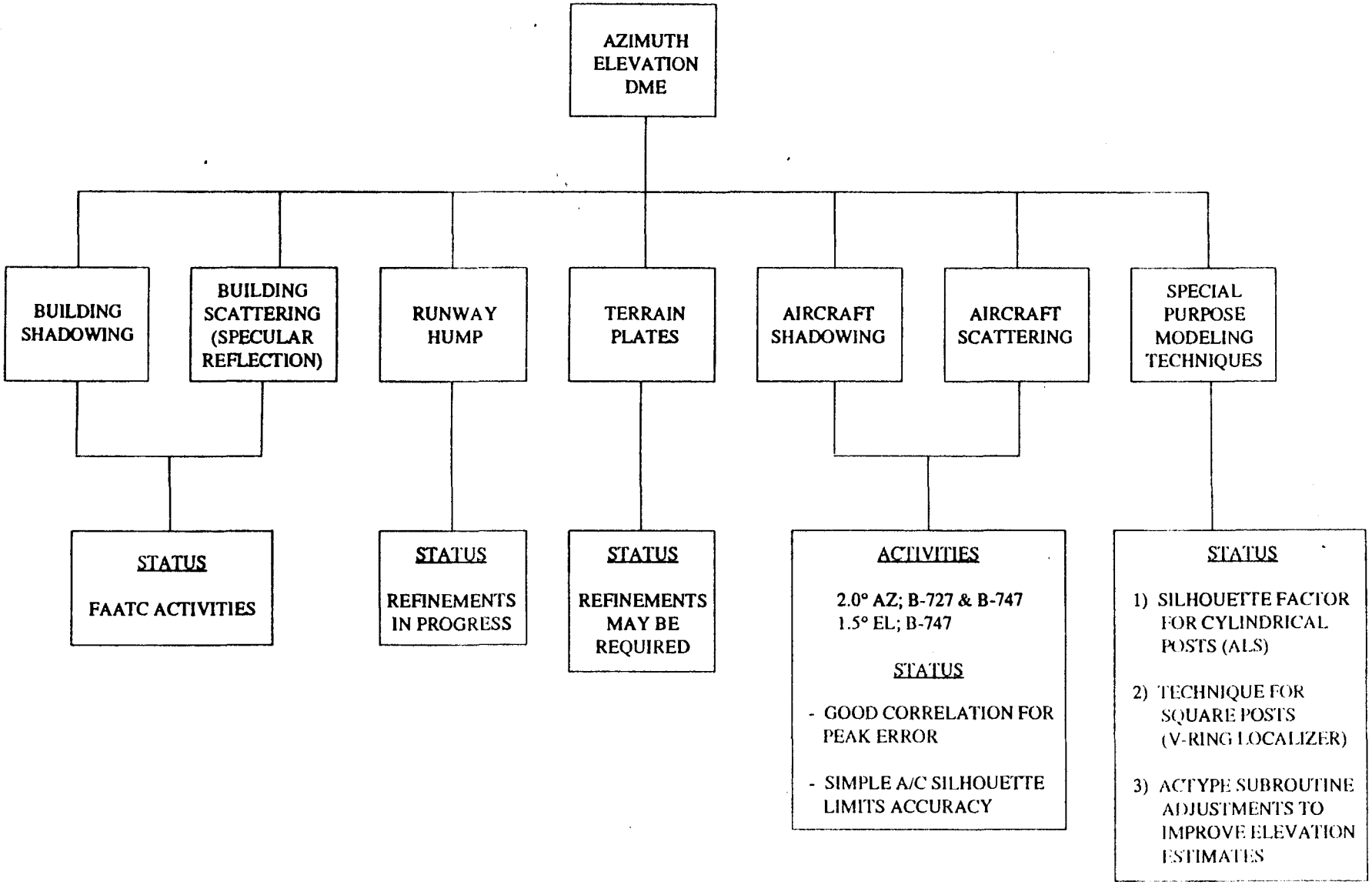
MODEL VALIDATION

Objective: Validate model for developing siting criteria and assessing system performance for a given airport environment.

APPLICATIONS WHICH PROVIDED VALIDATION OPPORTUNITIES

-Refinement of MLS critical areas
-Development of MLS/ILS collocation criteria
-Development of MLS/ALS collocation criteria
-Development of DME/P critical areas for advanced procedures (Future work)
-MLS demonstration program, predictions of system performance for given airport environment

ASPECTS OF MODEL TO BE VALIDATED



MODEL VALIDATION PROCESS

1) Pre-model to select geometries that will produce meaningful measurements

2) Determine geometries accurately

3) Two or three measurements should be made along each receiver path until repeatibility is obtained
   -verifies measurement
   -knowing measurement variability useful in validation work

4) Factors influencing the correlation of measured and model results
   -limitation on reproducing the receiver path, airborne measurements flight path option useful for future validation efforts
   -limitations on reproducing test geometries and conditions with model
   -tracking system error: $\pm$ 0.02^{o} for O.U. tracker
   -error sources not accounted for by the model
   -how much of the test site environment should be included? (error isolation)
   -ground roughness required for elevation work

VALIDATION OF AIRCRAFT SHADOWING/SCATTER ROUTINE

Objective: Validate effects predicted for interfering aircraft

Activities

ACY B-727 and 2.0° degree beamwidth azimuth

SDF B-747 and 2.0° beamwidth azimuth
B-747 and 1.5° beamwidth elevation

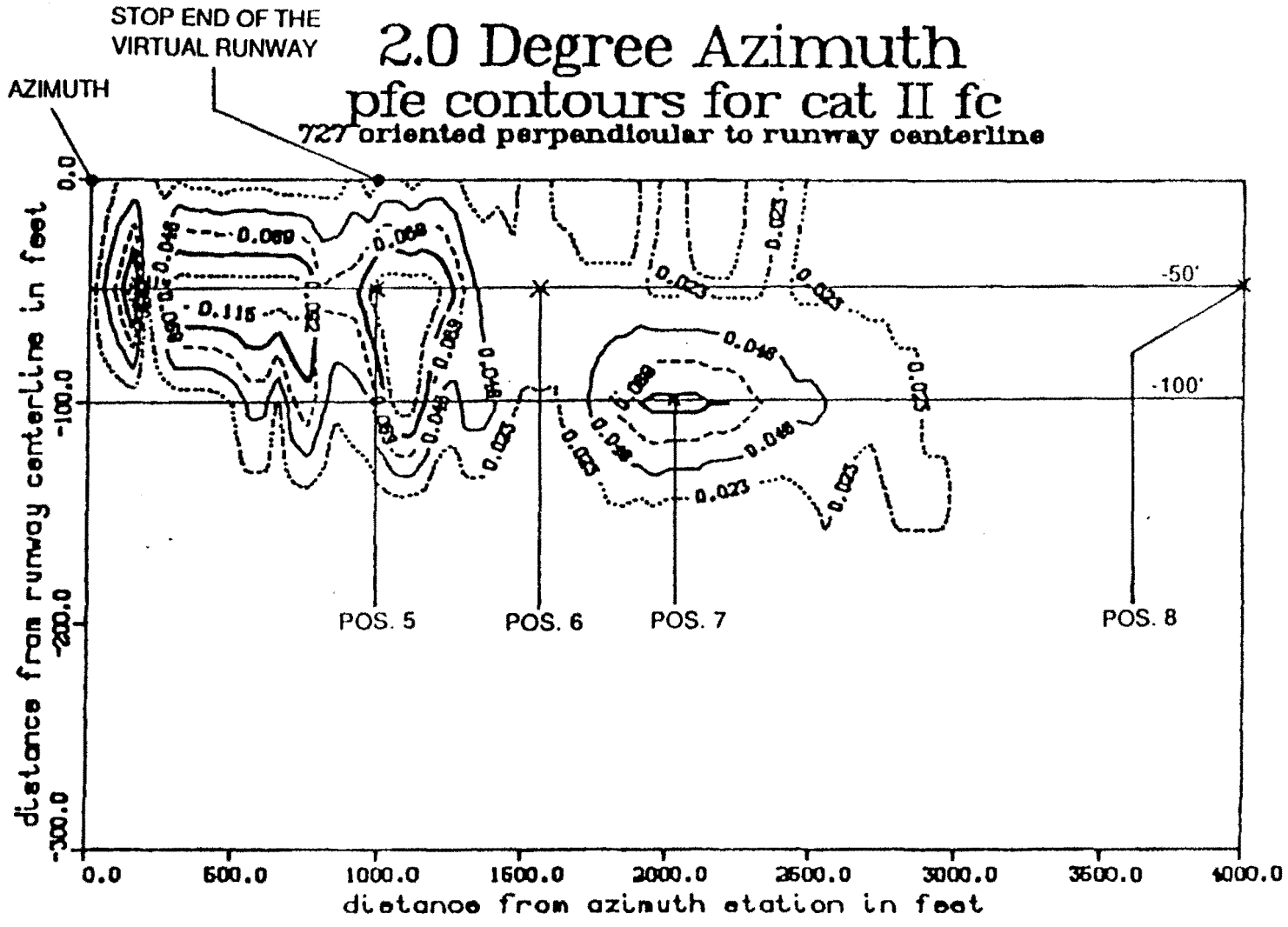
Validation Results

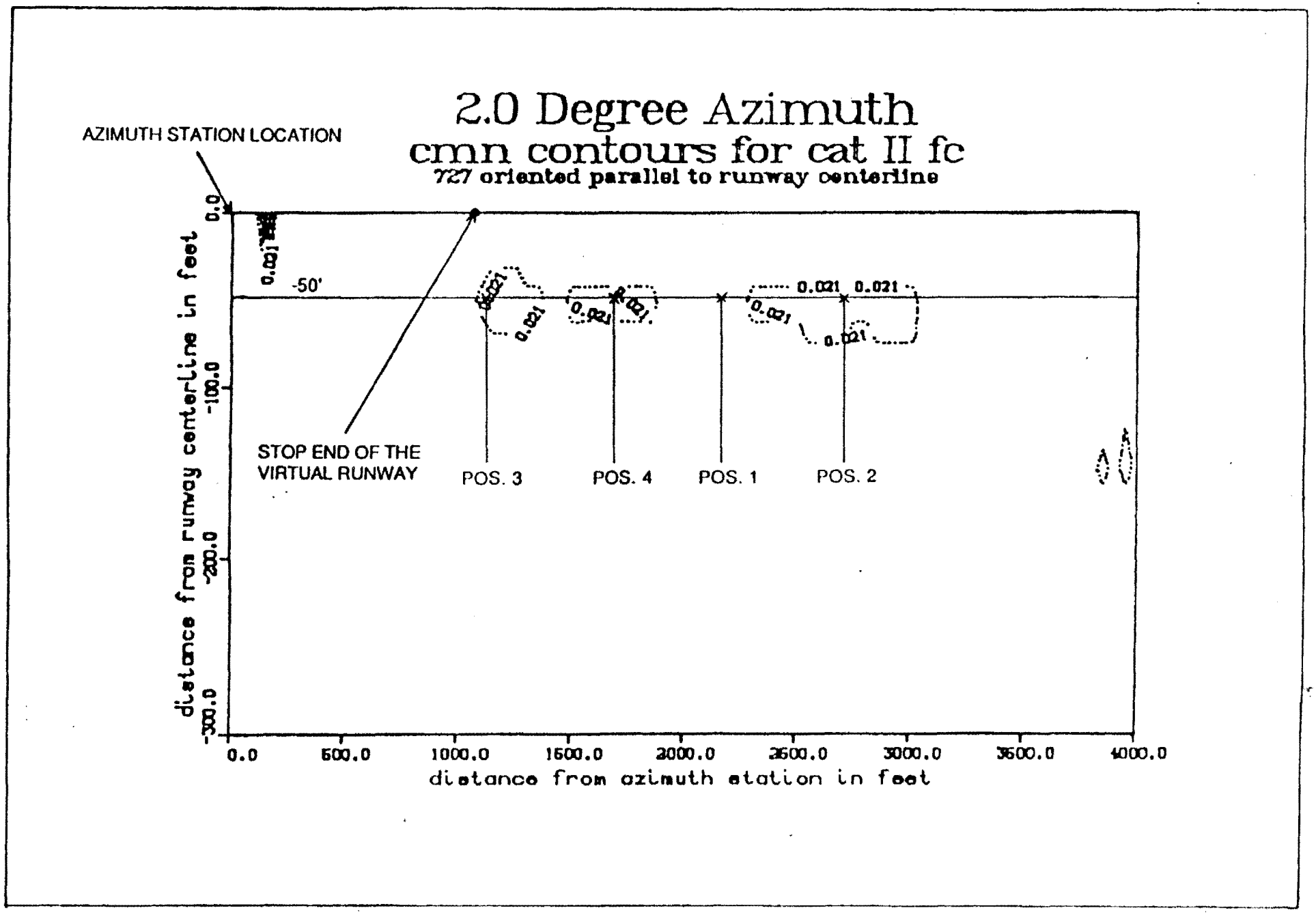
ACY parallel aircraft orientation
- errors masked by system noise, most locations tested
- errors measure 1-2X of tracker accuracy

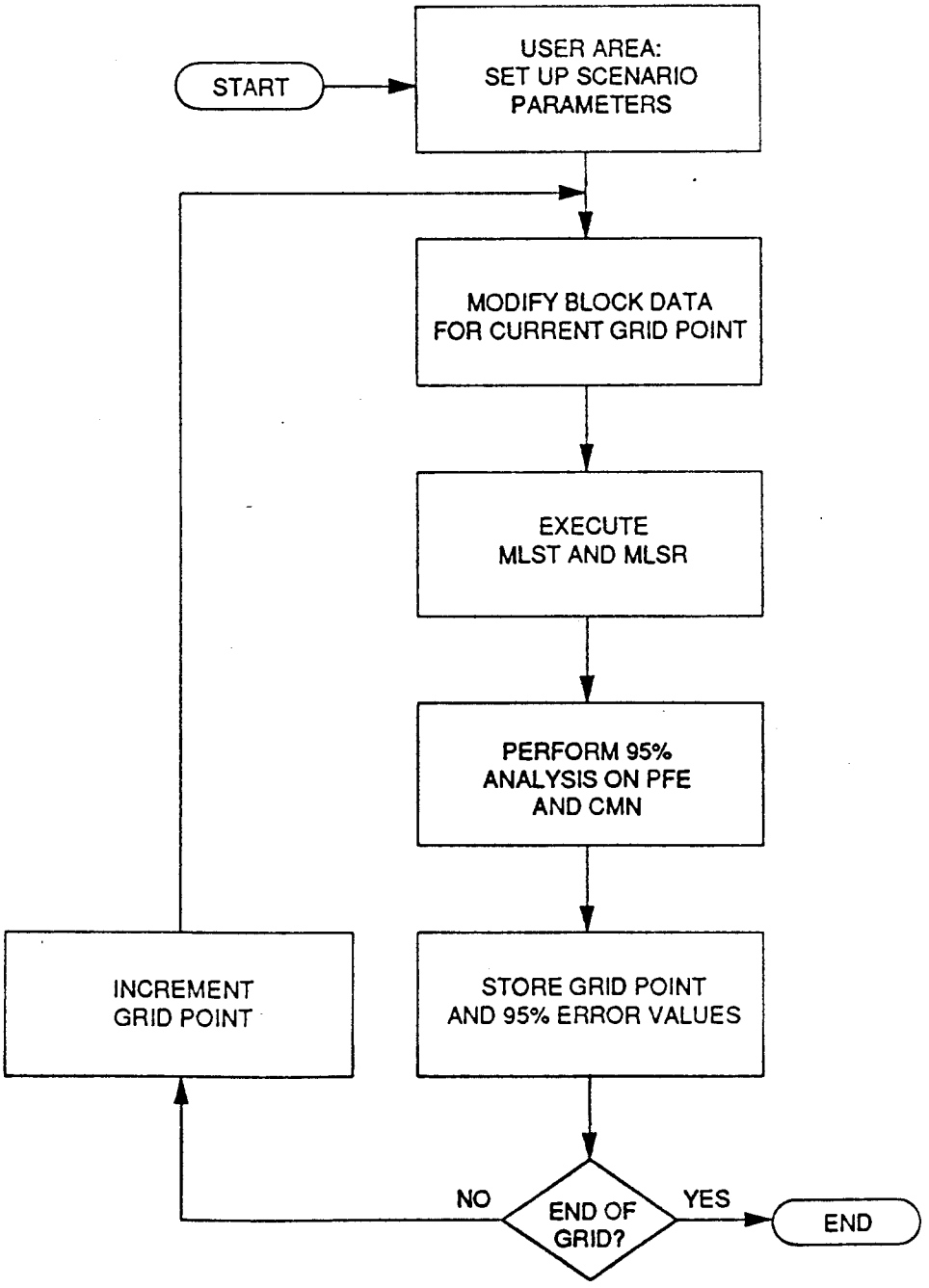
perpendicular orientation
- good correlation for peak errors
- sensitivity to receiver path
- limited ability to account for tail fin "tilt"

SDF parallel aircraft orientation
- good correlation for peak errors
- secondary signature characteristics missing
- added engine pods, improved correlation
- runway hump and shadowing at same time?

perpendicular orientation
- good correlation for peak errors
- sensitivity to receiver path
- adjustment of aircraft tail parameter (optional)
- runway hump and shadowing at same time?


STOP END OF THE
VIRTUAL RUNWAY
AZIMUTH
2.0 Degree Azimuth
pfe contours for cat II fc
727 oriented perpendicular to runway centerline
-50'
-100'
POS. 5
POS. 6
POS. 7
POS. 8
0.089
0.115
0.046
0.023
distance from runway centerline in feet
0.0
-100.0
-200.0
-300.0
0.0
500.0
1000.0
1500.0
2000.0
2500.0
3000.0
3500.0
4000.0
distance from azimuth station in feet

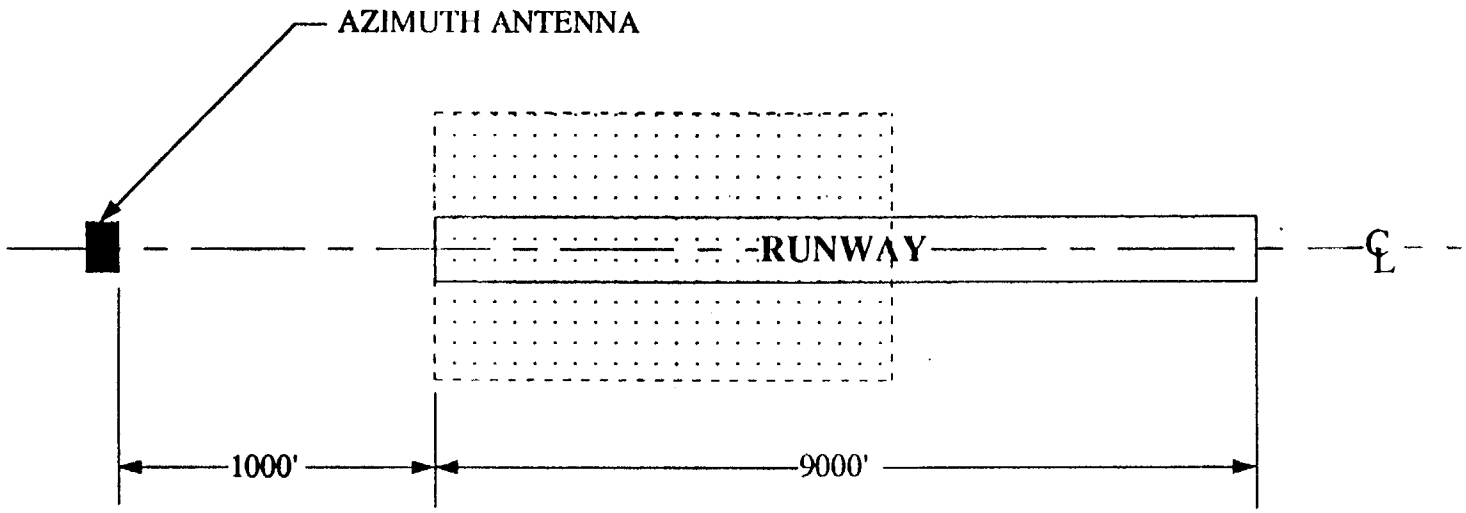

2.0 Degree Azimuth
cmn contours for cat II fc
727 oriented parallel to runway centerline
AZIMUTH STATION LOCATION
STOP END OF THE VIRTUAL RUNWAY
POS. 3
POS. 4
POS. 1
POS. 2
-50'
0.021
distance from runway centerline in feet
0.0
-100.0
-200.0
-300.0
0.0
500.0
1000.0
1500.0
2000.0
2500.0
3000.0
3500.0
4000.0
distance from azimuth station in feet



CONTOUR PACKAGE (CONTROLLING EXEC CONMLS)

004 003 / 002 E29

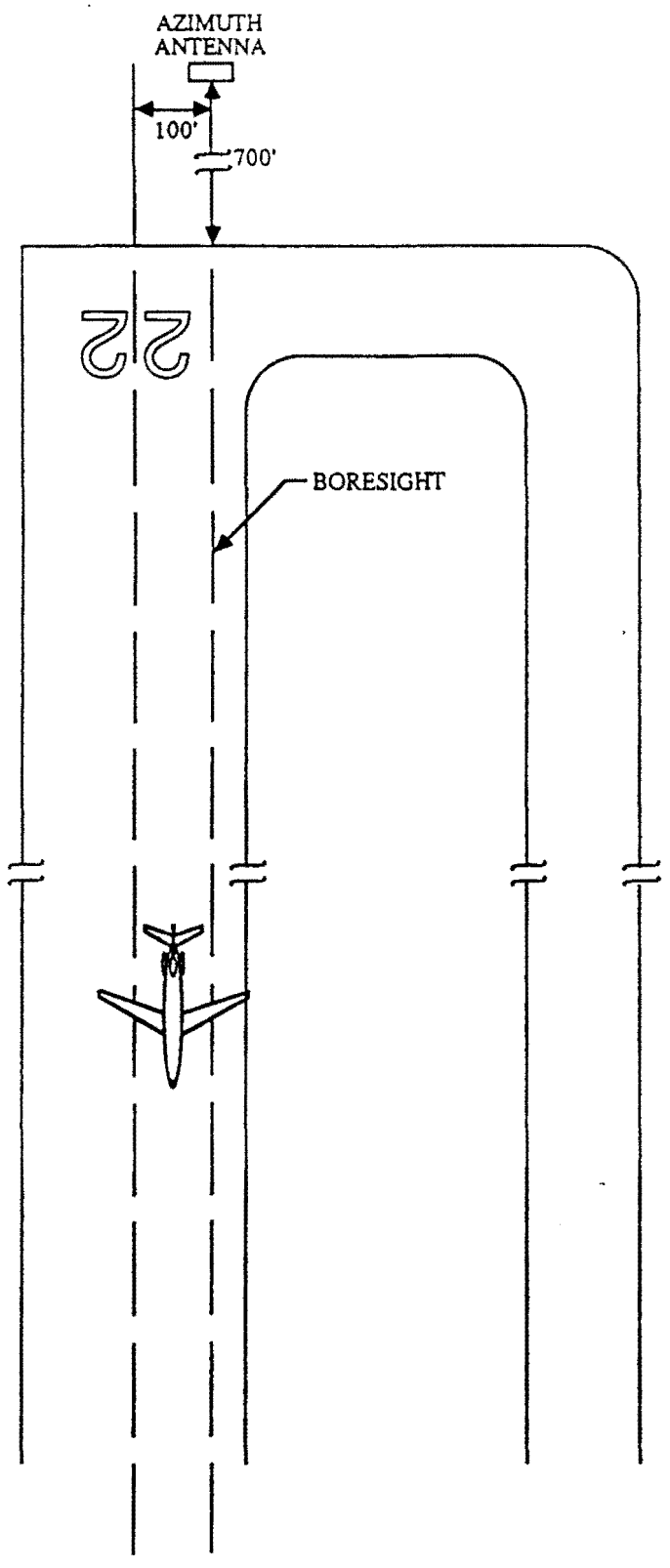
SAMPLE INTERFERING AIRCRAFTS SEARCH GRID

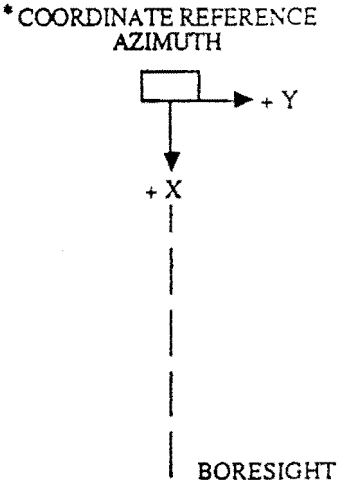


001 003 / 002 E39

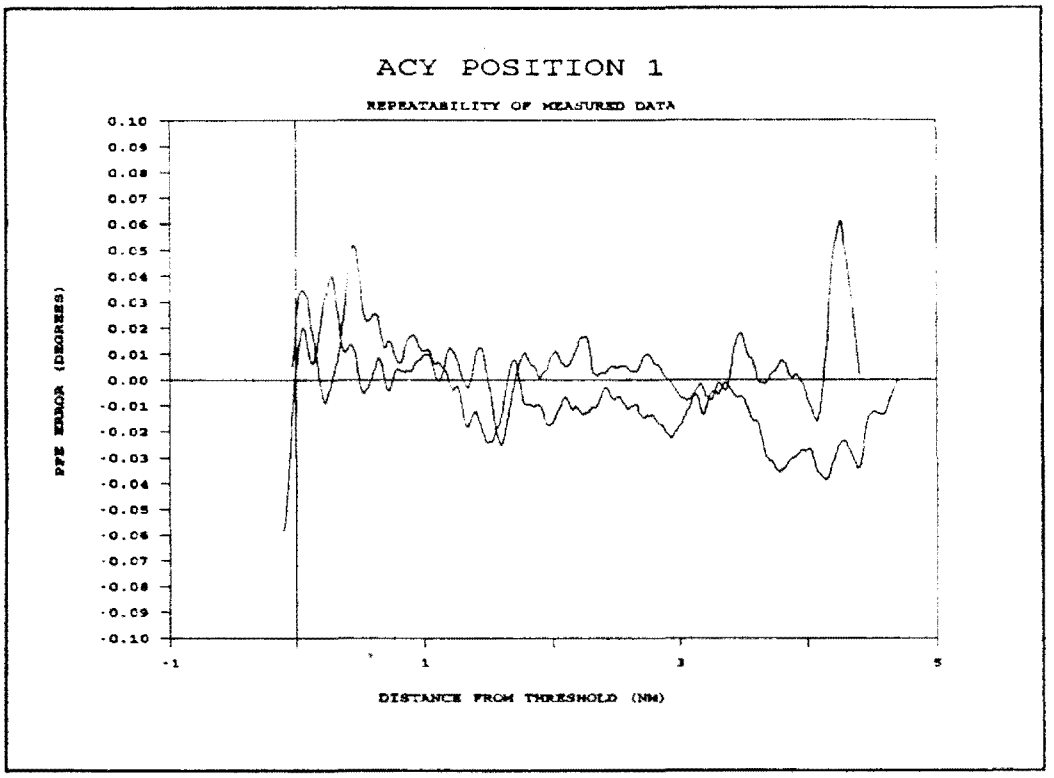
POSITION 1, ACY

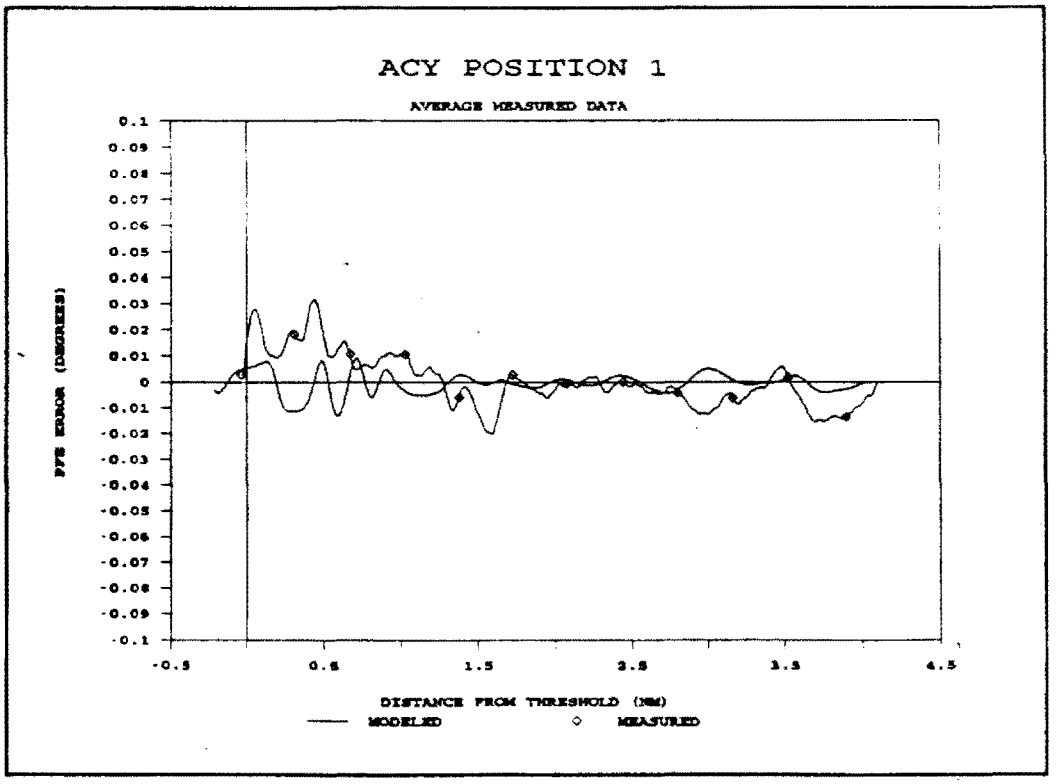
NOSE (X,Y)*	TAIL (X,Y)*
(2221,-50)	(2088,-50)





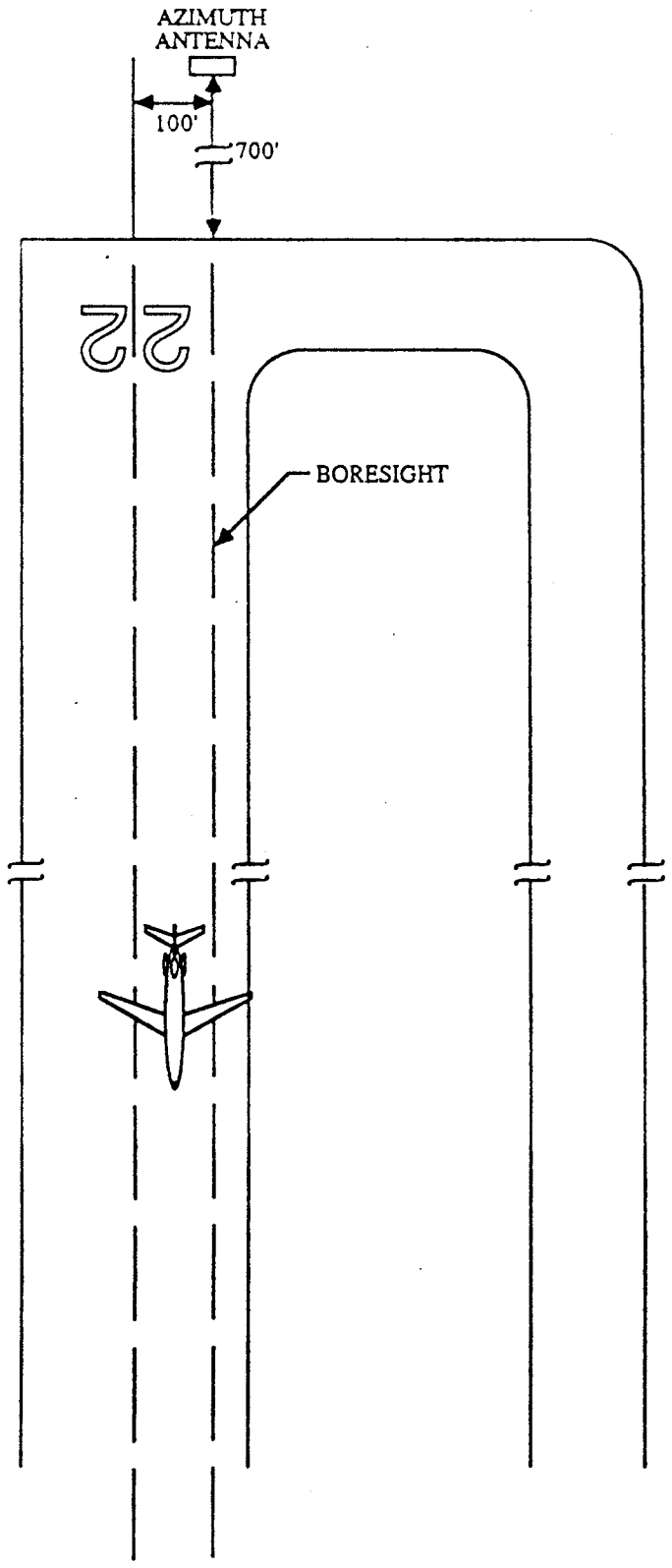
Aircraft Position 1.

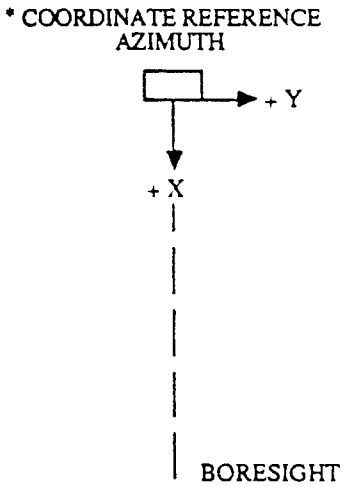

ACY POSITION 1
REPEATABILITY OF MEASURED DATA
PFE ERROR (DEGREES)
0.10
0.09
0.08
0.07
0.06
0.05
0.04
0.03
0.02
0.01
0.00
-0.01
-0.02
-0.03
-0.04
-0.05
-0.06
-0.07
-0.08
-0.09
-0.10
-1
1
3
5
DISTANCE FROM THRESHOLD (NM)


ACY POSITION 1
AVERAGE MEASURED DATA
PFE ERROR (DEGREES)
0.1
0.09
0.08
0.07
0.06
0.05
0.04
0.03
0.02
0.01
0
-0.01
-0.02
-0.03
-0.04
-0.05
-0.06
-0.07
-0.08
-0.09
-0.1
-0.5
0.5
1.5
2.5
3.5
4.5
DISTANCE FROM THRESHOLD (NM)
MODELED
MEASURED

POSITION 3, ACY

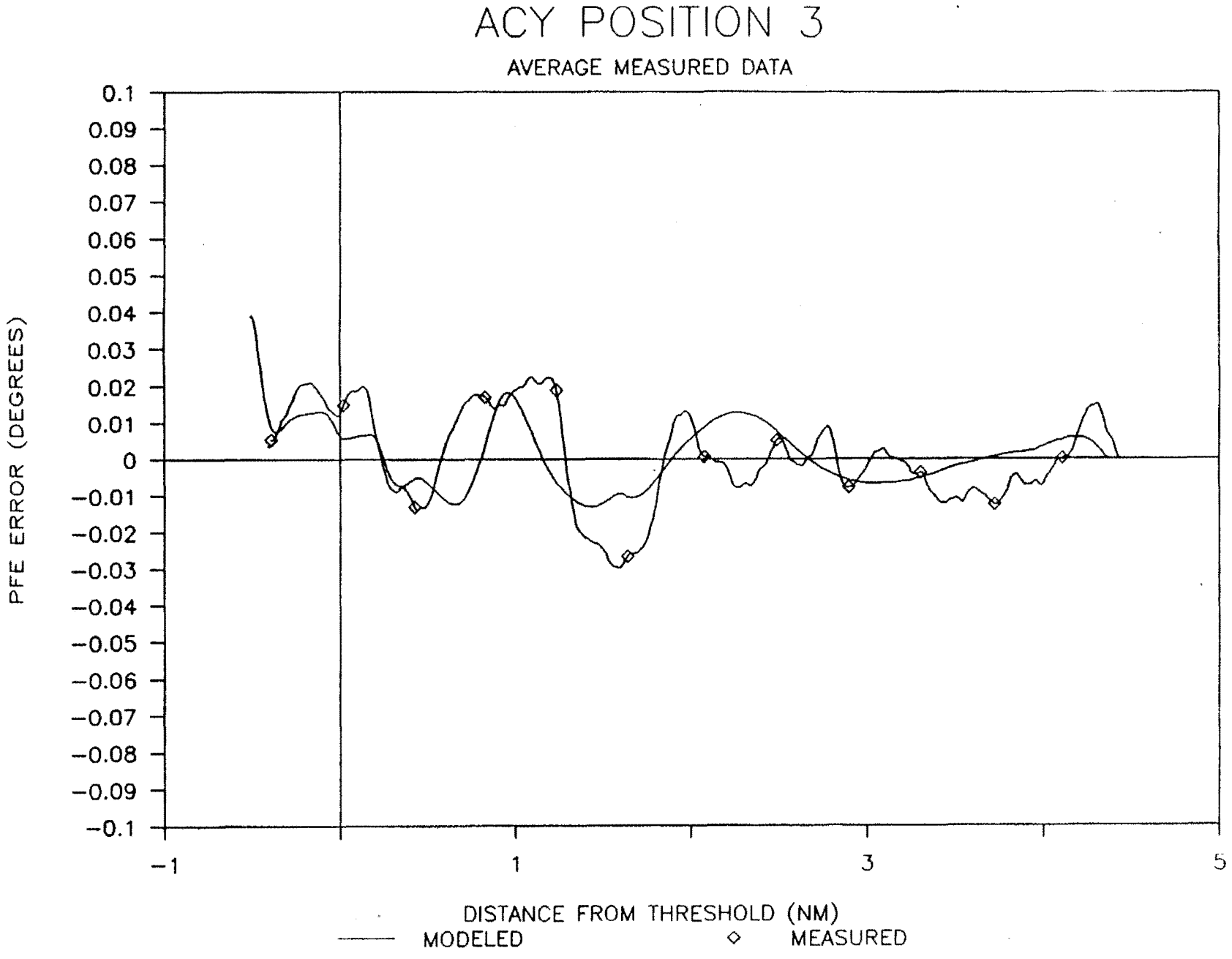
NOSE (X,Y)*	TAIL (X,Y)*
(1202,-50)	(1069,-50)

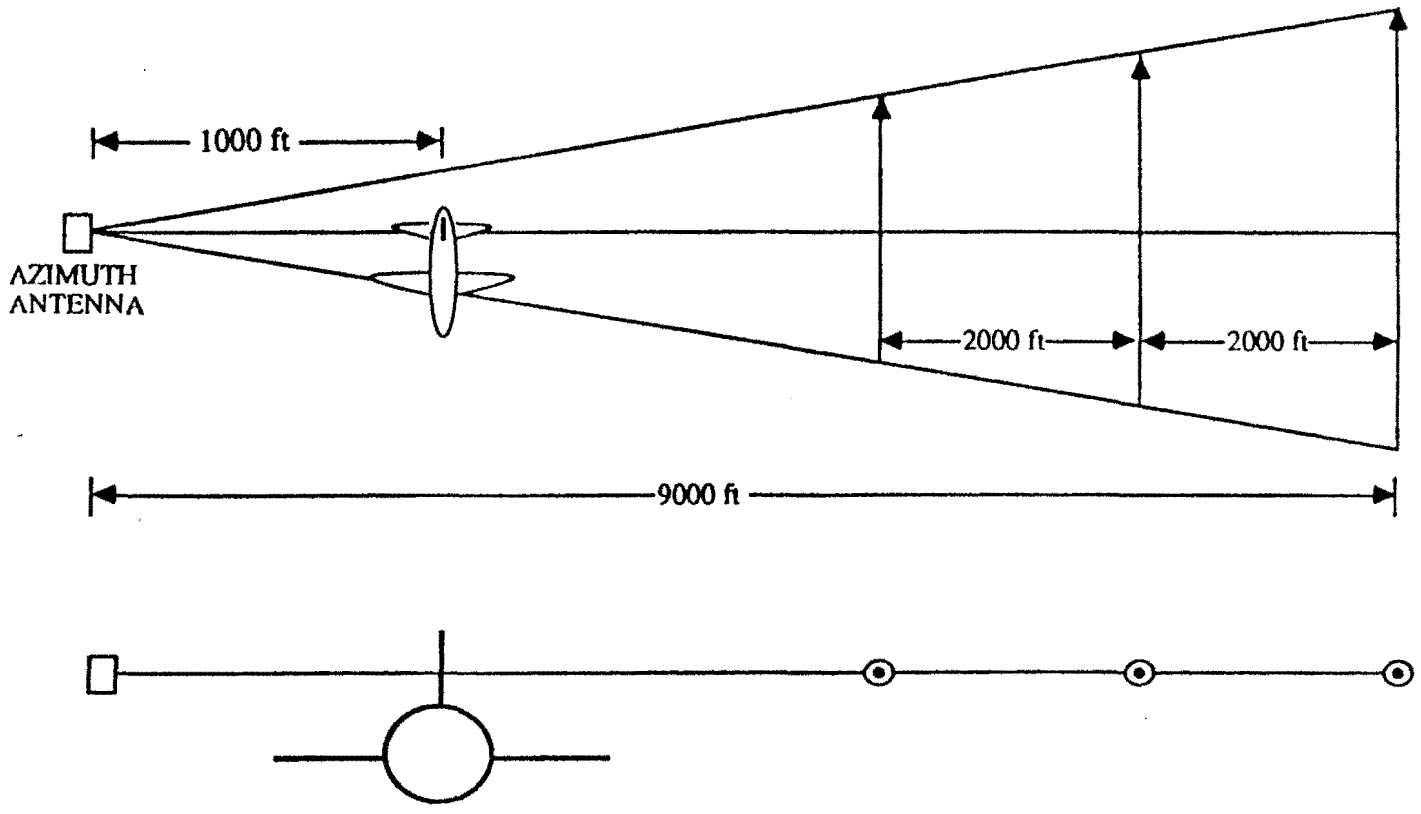




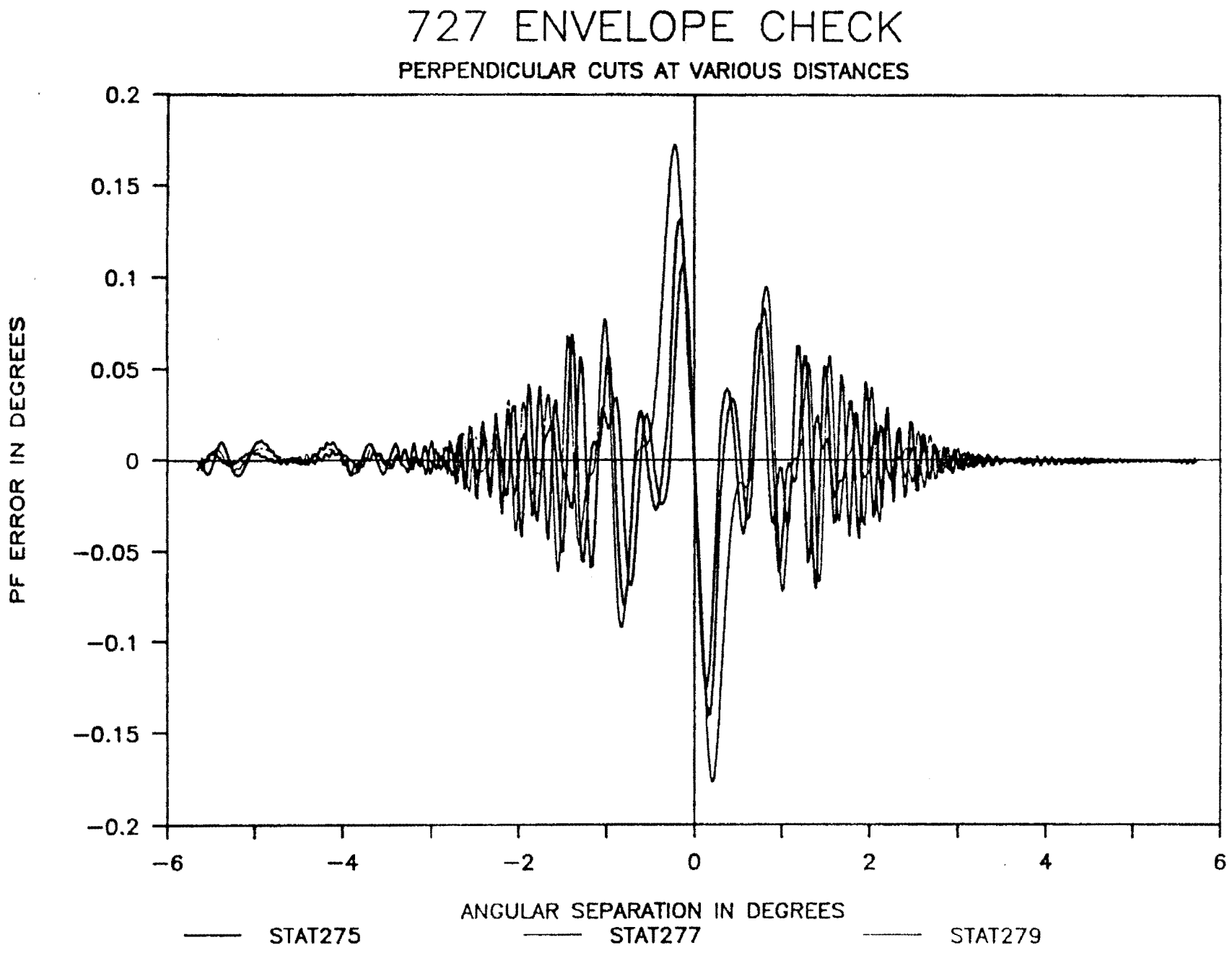
Aircraft Position 3.

84

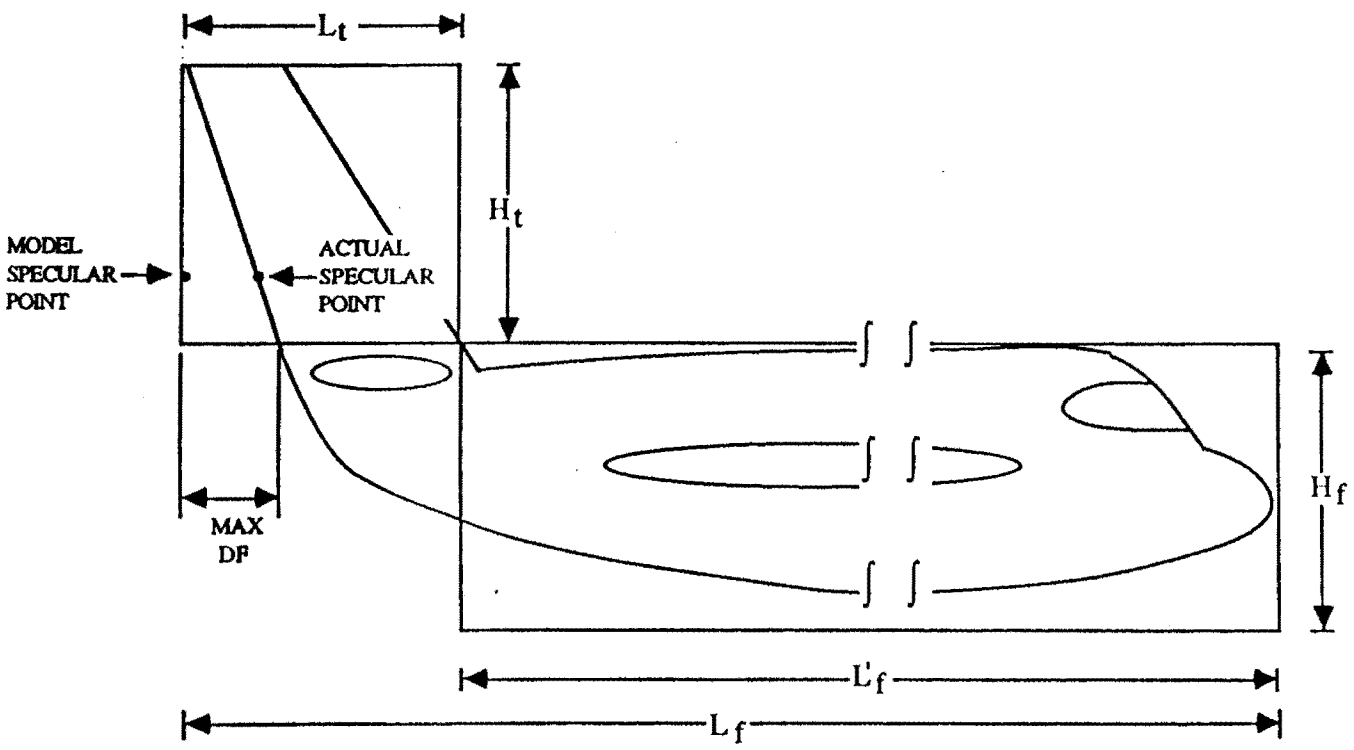

ACY POSITION 3
AVERAGE MEASURED DATA
PFE ERROR (DEGREES)
0.1
0.09
0.08
0.07
0.06
0.05
0.04
0.03
0.02
0.01
0
−0.01
−0.02
−0.03
−0.04
−0.05
−0.06
−0.07
−0.08
−0.09
−0.1
−1
1
3
5
DISTANCE FROM THRESHOLD (NM)
MODELED
MEASURED



Geometry used to generate error signature for B-727 tailfin shadowing.



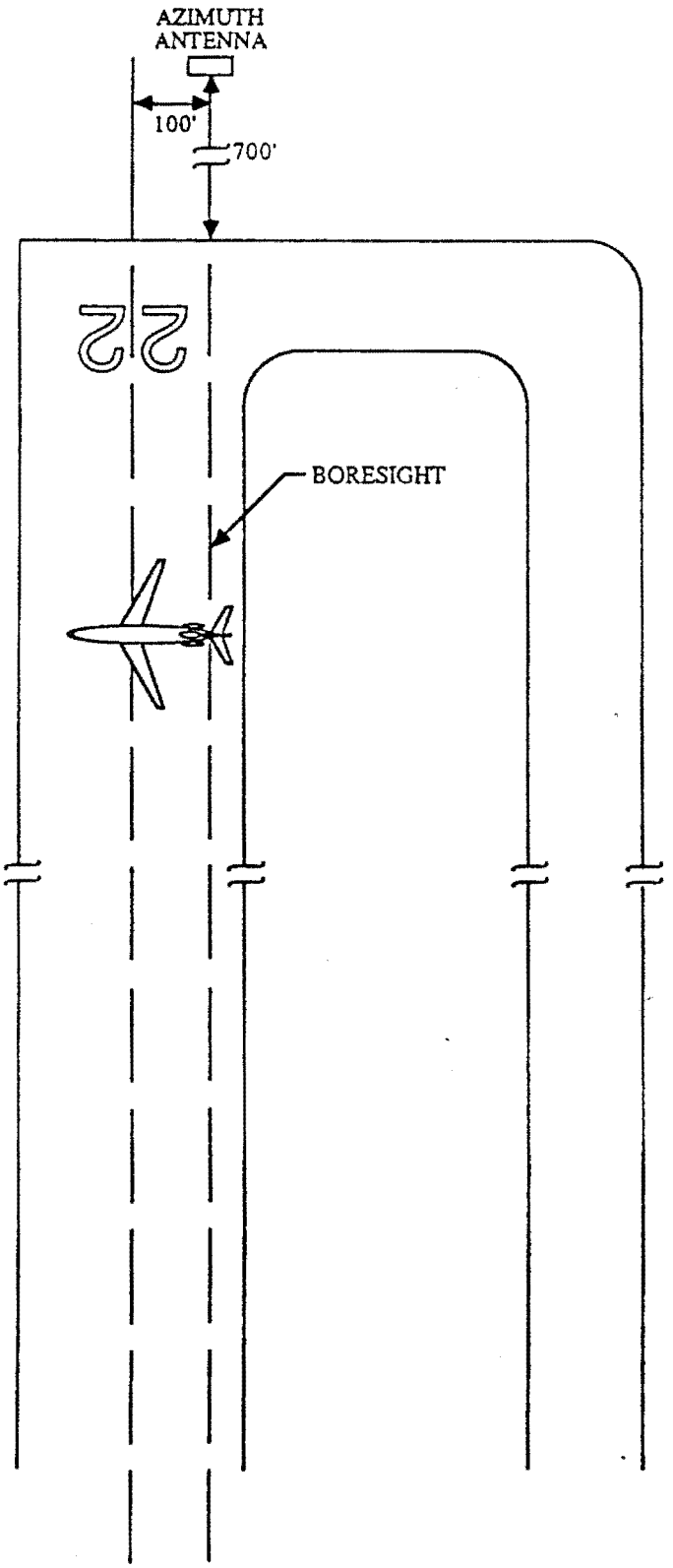
Error signature for B-727 tailfin shadowing.

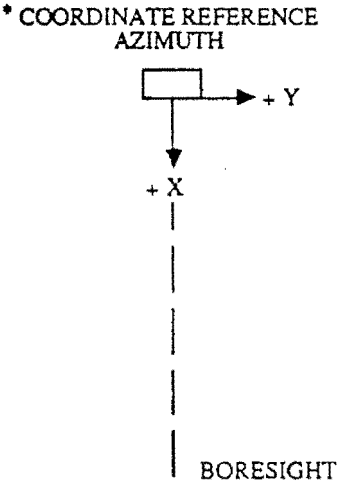


Actual aircraft tailfin versus model representation, shadowing case.

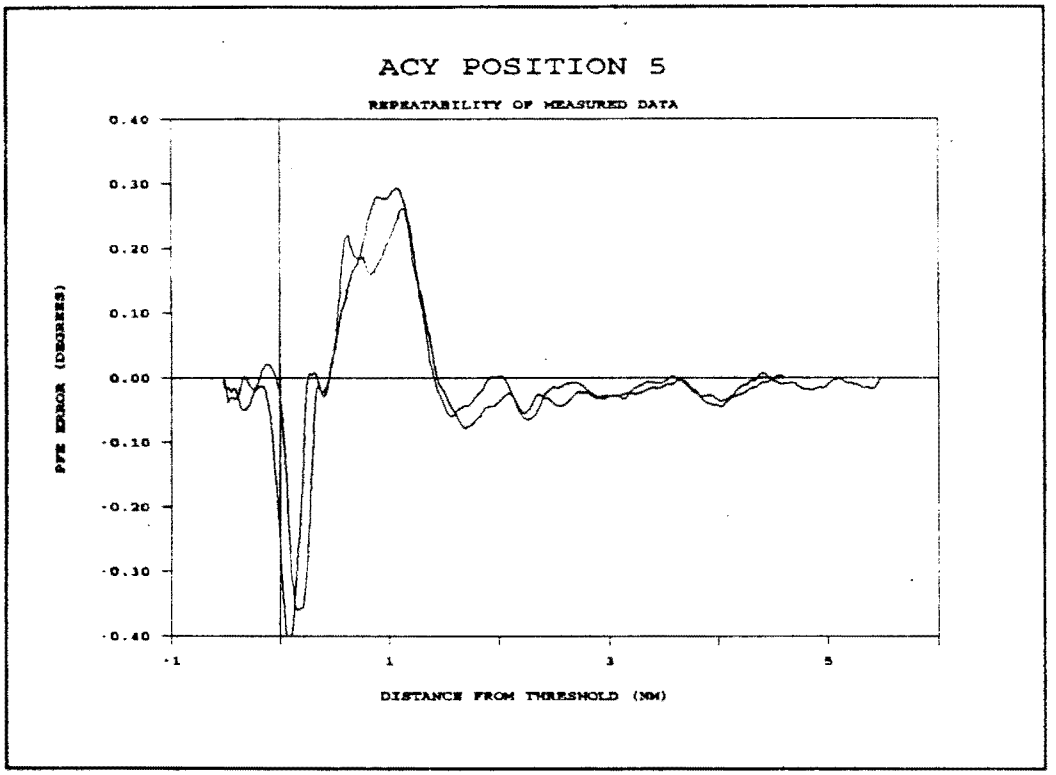
POSITION 5, ACY

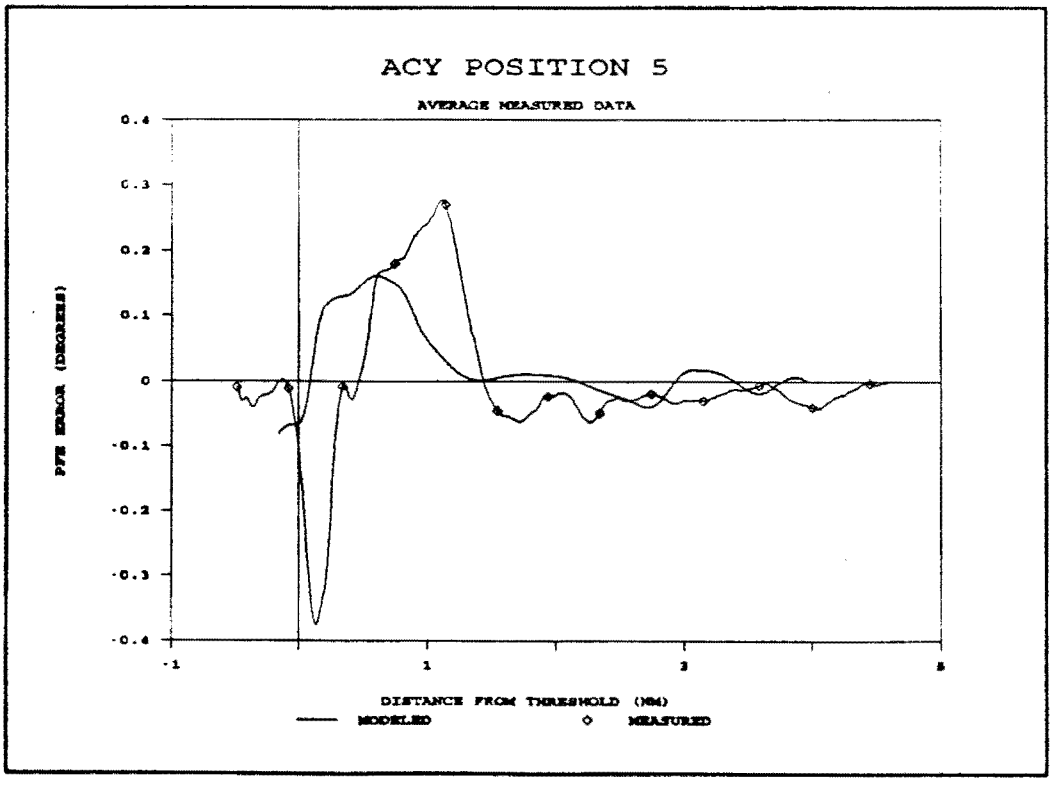
NOSE (X,Y) *	TAIL (X,Y) *
(964,-106)	(964,27)





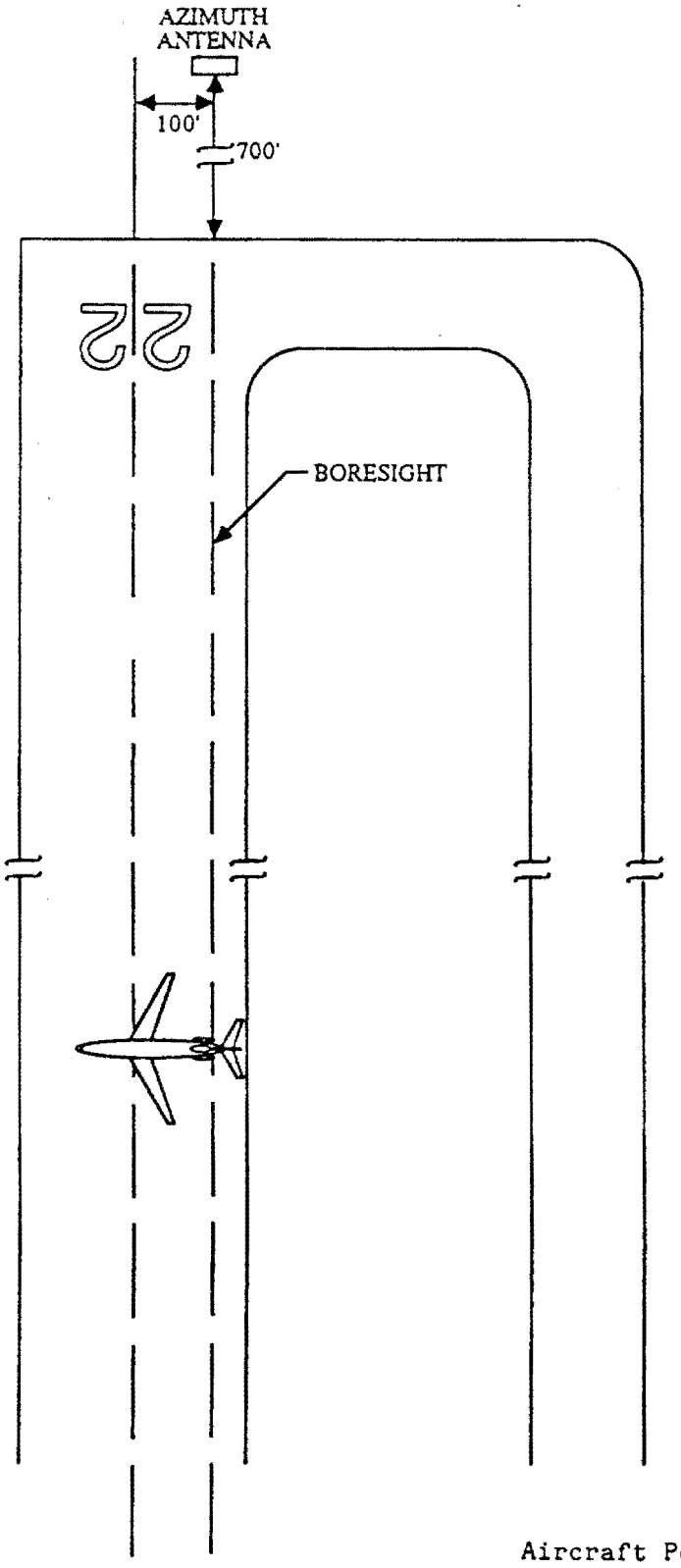
Aircraft Position 5.

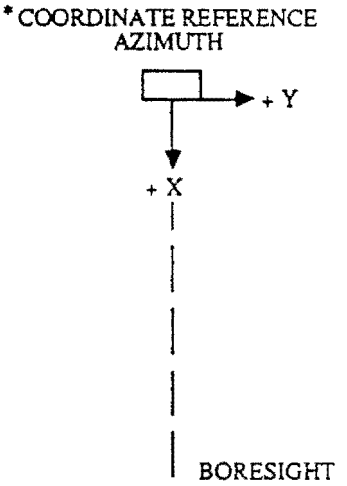

ACY POSITION 5
REPEATABILITY OF MEASURED DATA
PFE ERROR (DEGREES)
0.40
0.30
0.20
0.10
0.00
-0.10
-0.20
-0.30
-0.40
-1
1
3
5
DISTANCE FROM THRESHOLD (NM)


ACY POSITION 5
AVERAGE MEASURED DATA
PFE ERROR (DEGREES)
0.4
0.3
0.2
0.1
0
-0.1
-0.2
-0.3
-0.4
-1
1
3
5
DISTANCE FROM THRESHOLD (NM)
MODELED
MEASURED

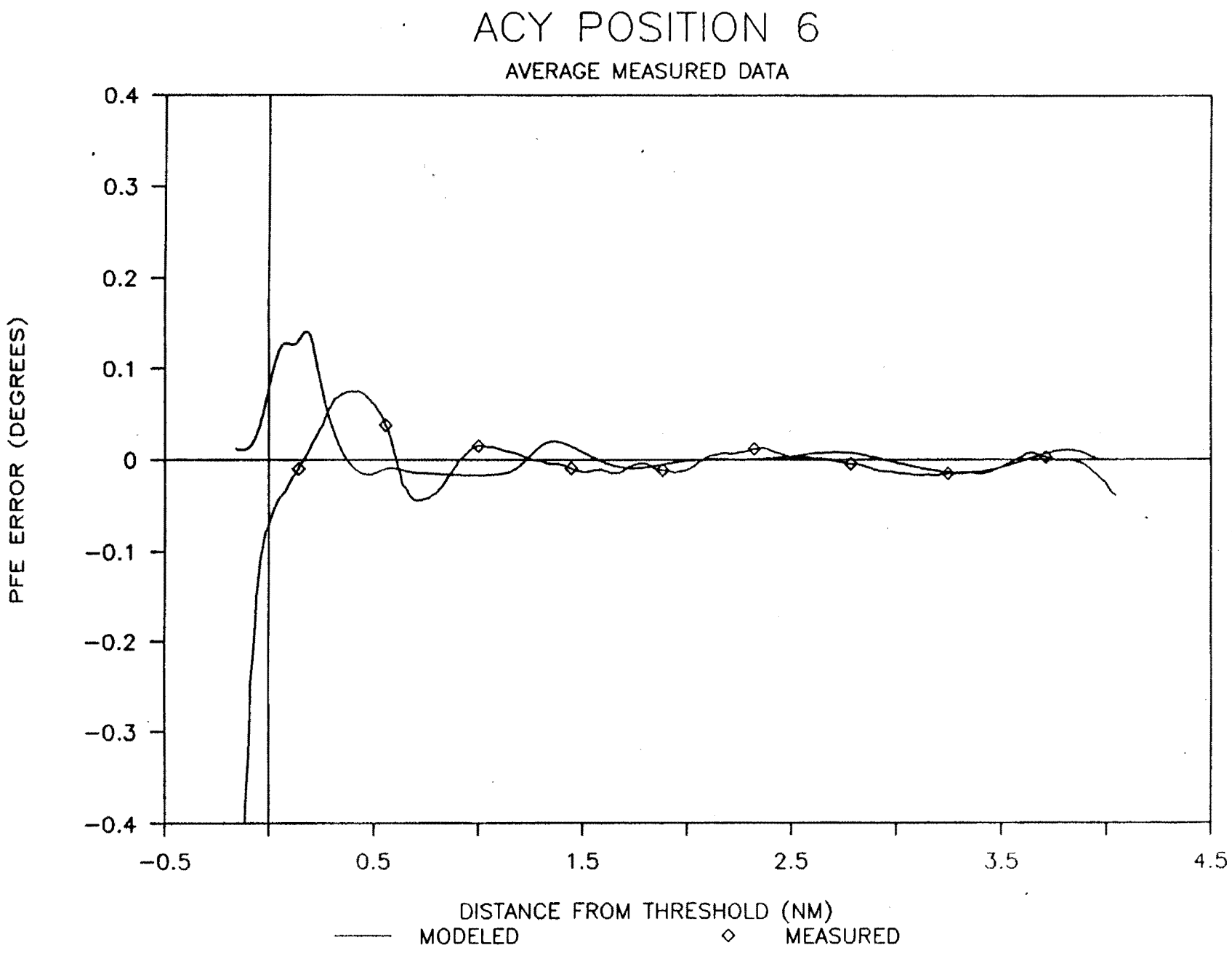
POSITION 6, ACY

NOSE (X,Y)*	TAIL (X,Y)*
(1571,-106)	(1571,27)

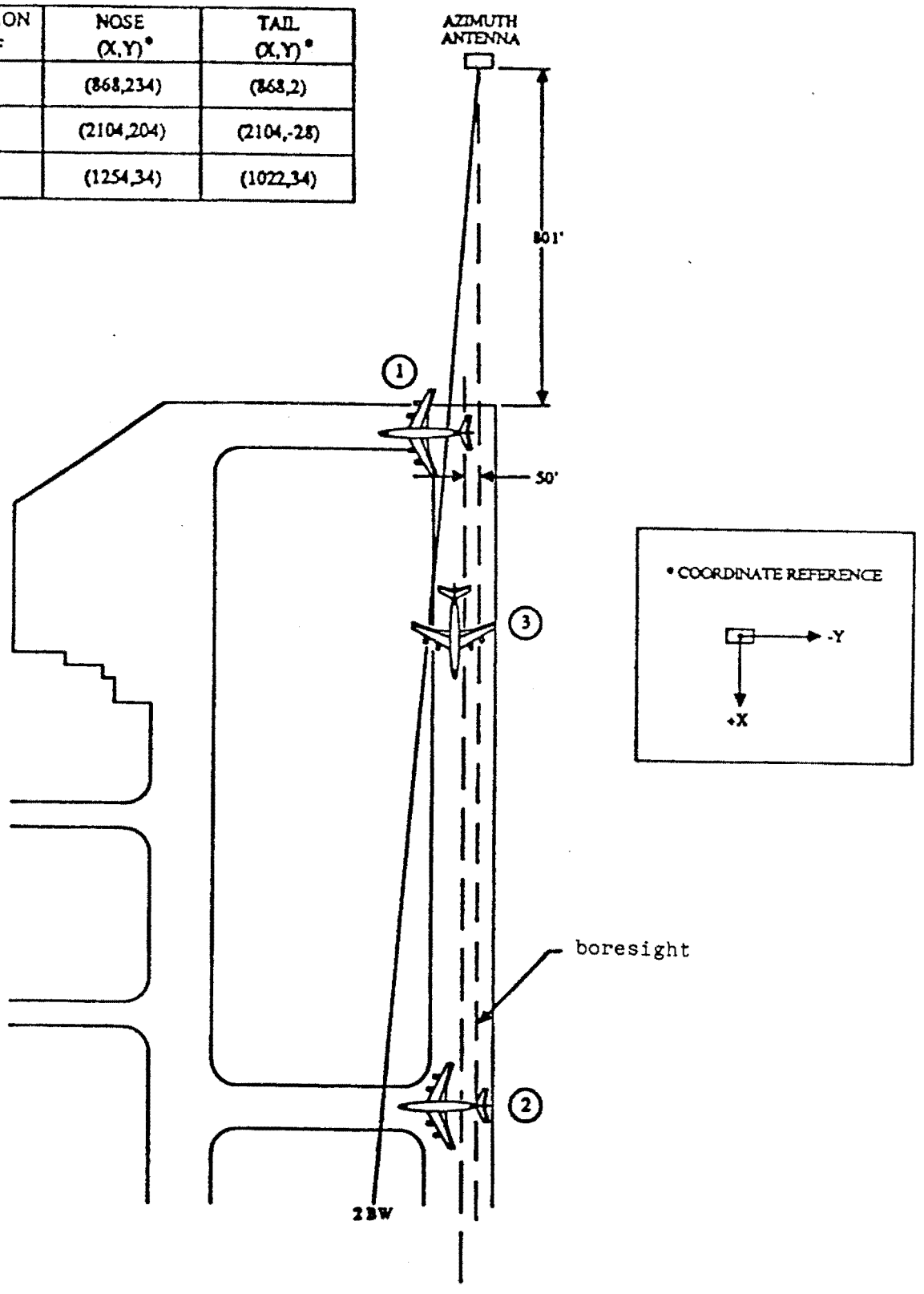




Aircraft Position 6.


ACY POSITION 6
AVERAGE MEASURED DATA
PFE ERROR (DEGREES)
0.4
0.3
0.2
0.1
0
−0.1
−0.2
−0.3
−0.4
−0.5
0.5
1.5
2.5
3.5
4.5
DISTANCE FROM THRESHOLD (NM)
MODELED
MEASURED

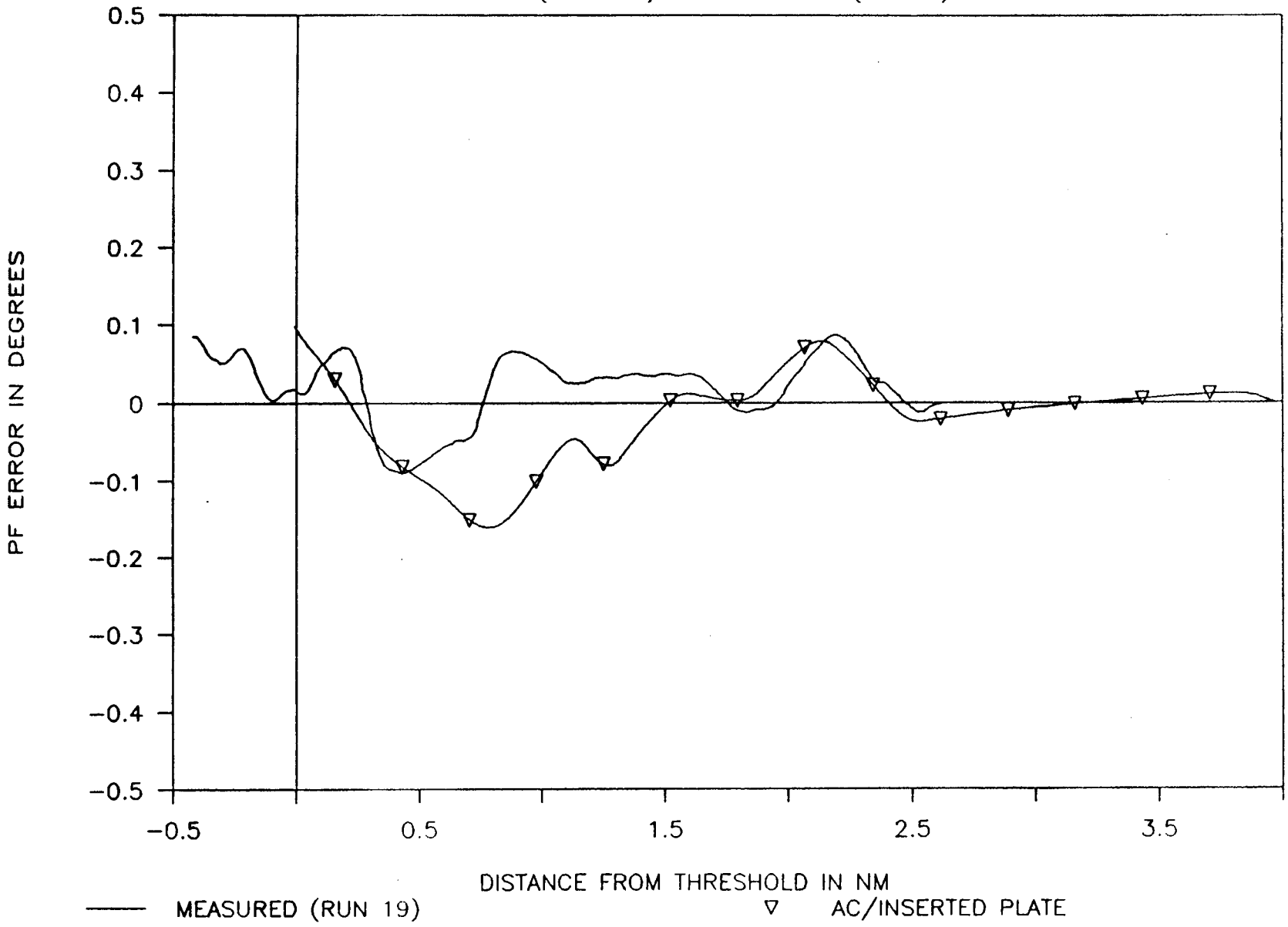
POSITION SDF	NOSE (X,Y)*	TAIL (X,Y)*
1	(868,234)	(868,2)
2	(2104,204)	(2104,-28)
3	(1254,34)	(1022,34)

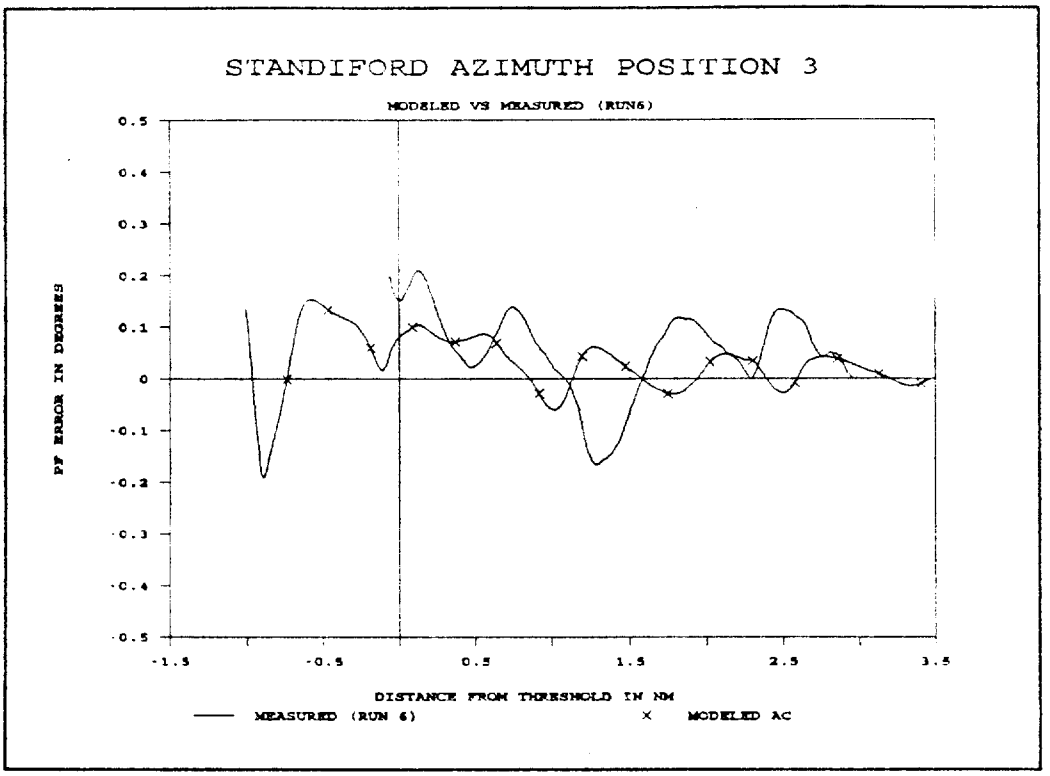


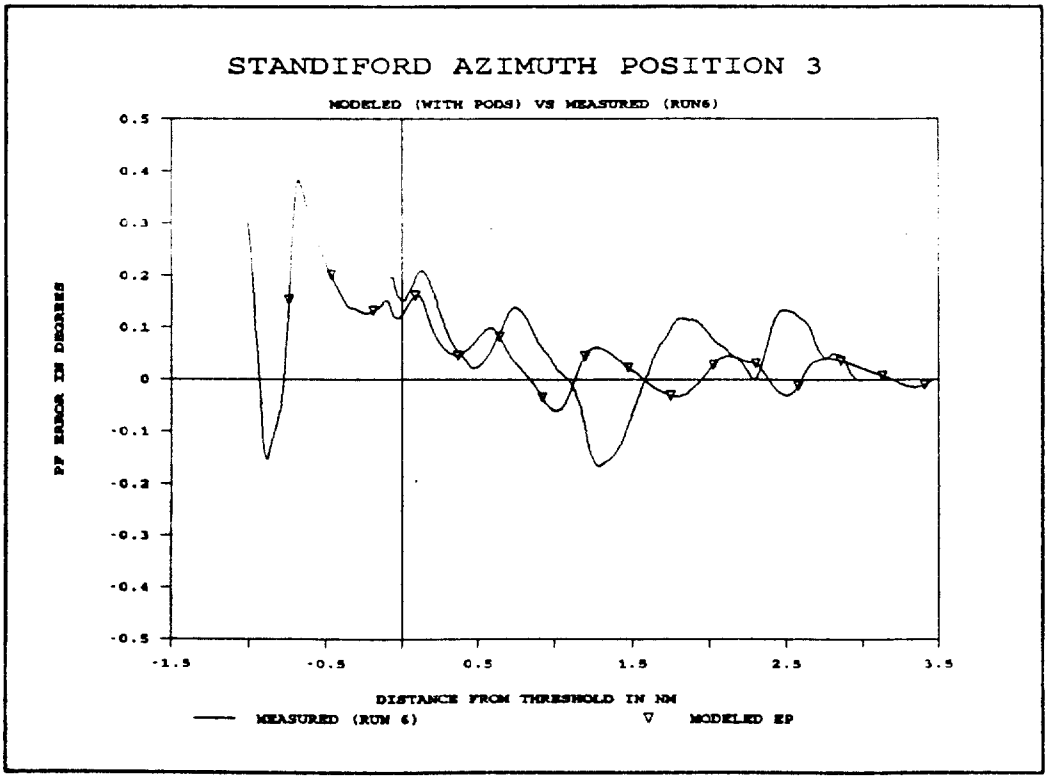
Azimuth aircraft Positions 1, 2, and 3.

STANDIFORD AZIMUTH POSITION 1

MODELED (+ PLATE) VS. MEASURED (RUN19)

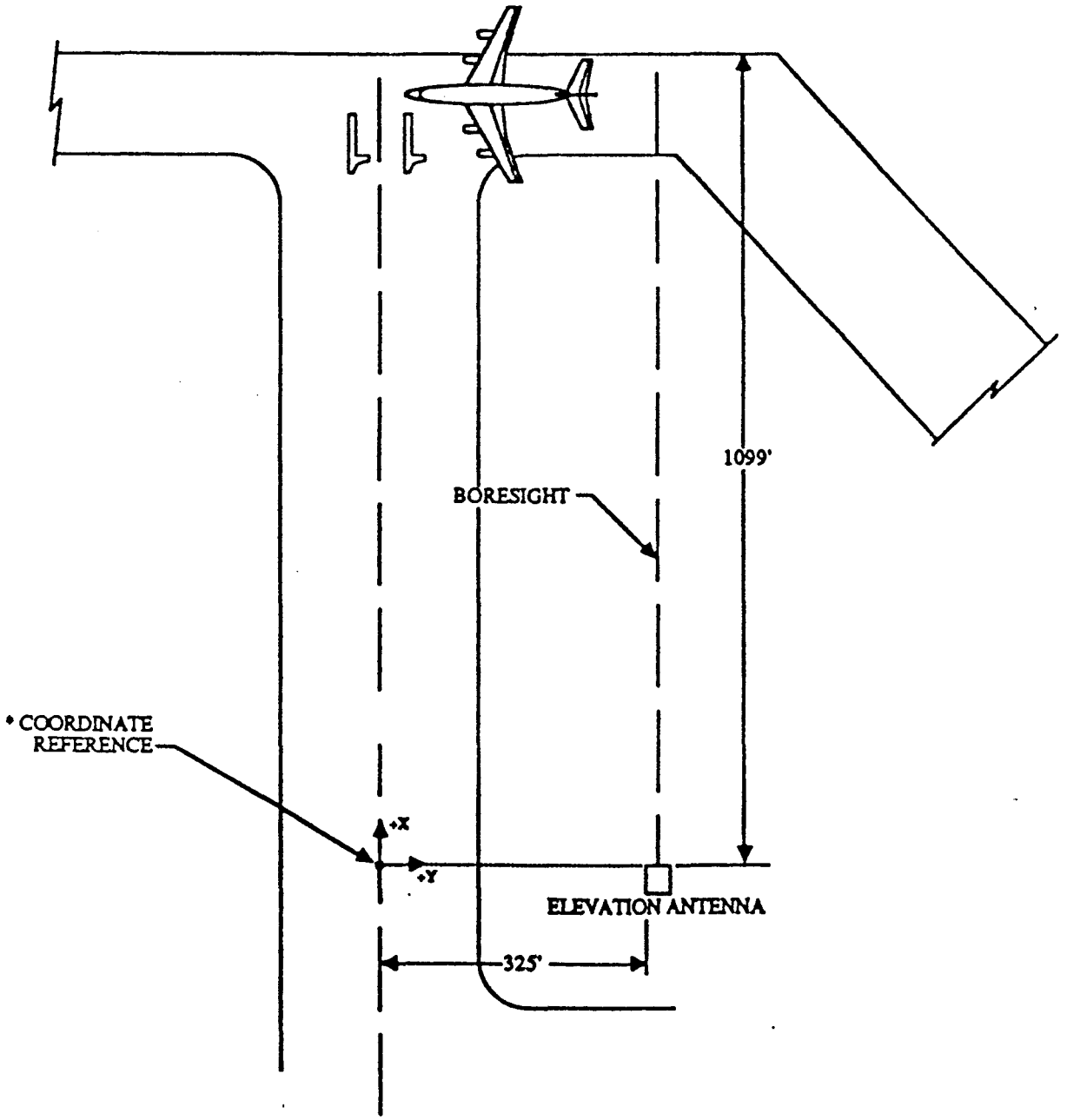



STANDIFORD AZIMUTH POSITION 3
MODELED VS MEASURED (RUN6)
PF ERROR IN DEGREES
0.5
0.4
0.3
0.2
0.1
0
-0.1
-0.2
-0.3
-0.4
-0.5
-1.5
-0.5
0.5
1.5
2.5
3.5
DISTANCE FROM THRESHOLD IN NM
MEASURED (RUN 6)
MODELED AC

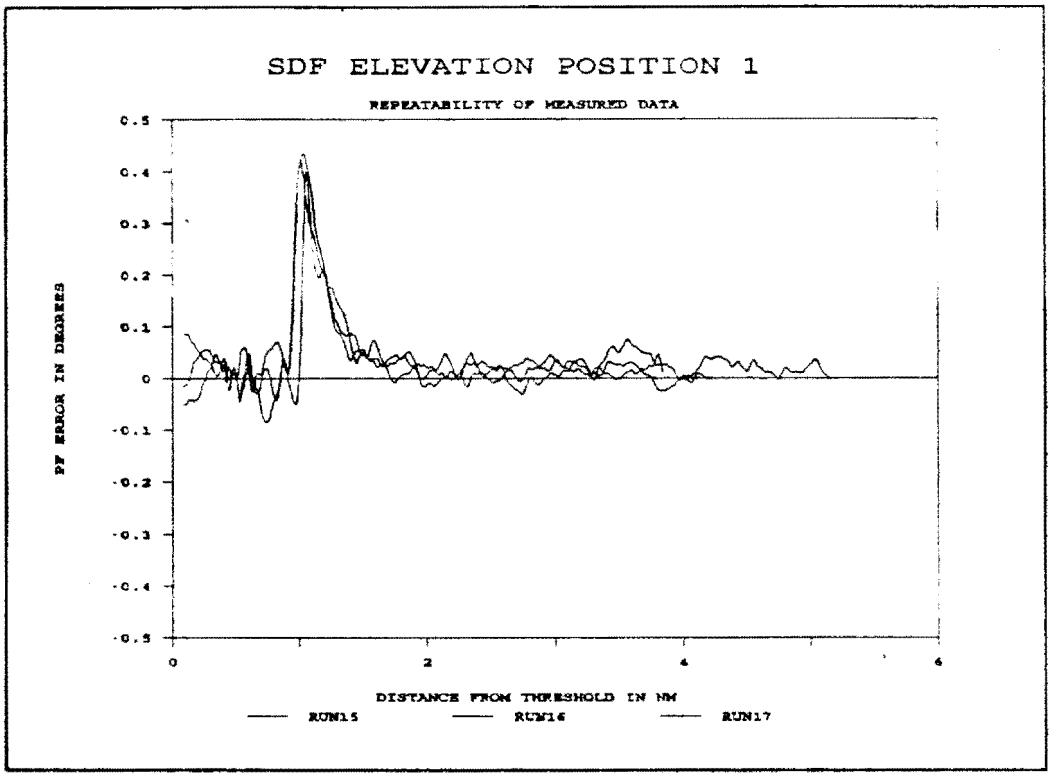

STANDIFORD AZIMUTH POSITION 3
MODELED (WITH PODS) VS MEASURED (RUN6)
PF ERROR IN DEGREES
0.5
0.4
0.3
0.2
0.1
0
-0.1
-0.2
-0.3
-0.4
-0.5
-1.5
-0.5
0.5
1.5
2.5
3.5
DISTANCE FROM THRESHOLD IN NM
MEASURED (RUN 6)
MODELED EP

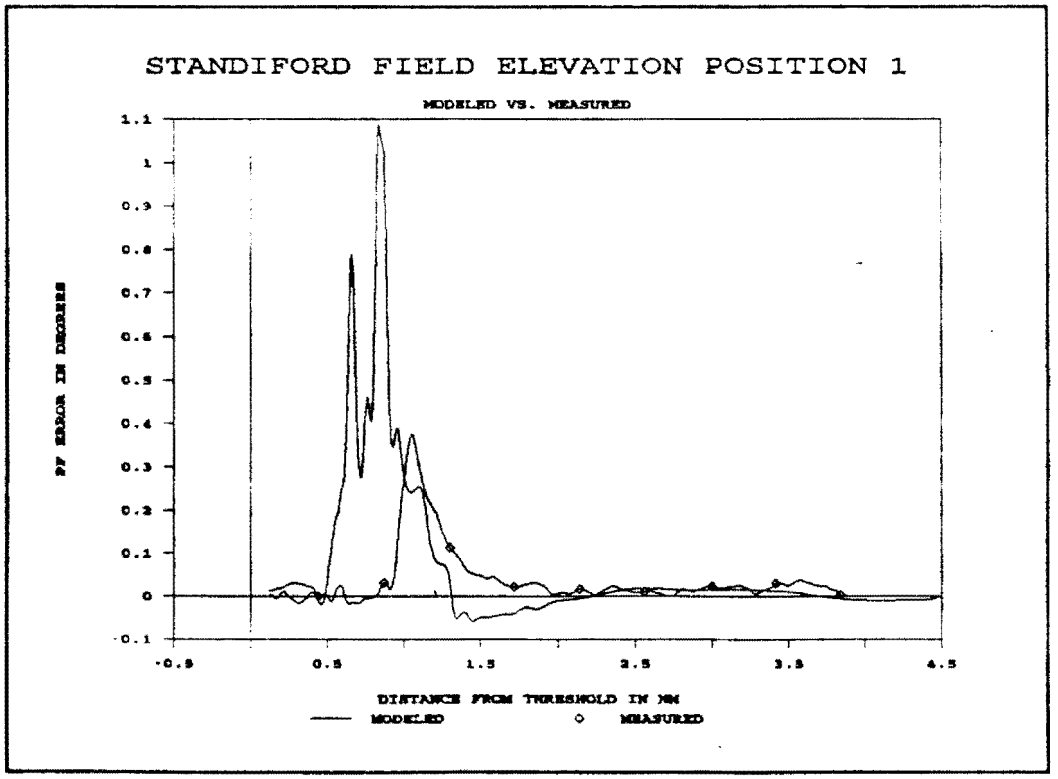
POSITION 1, SDF

NOSE (X,Y)*	TAIL (X,Y)*
(1069,64)	(1069,296)

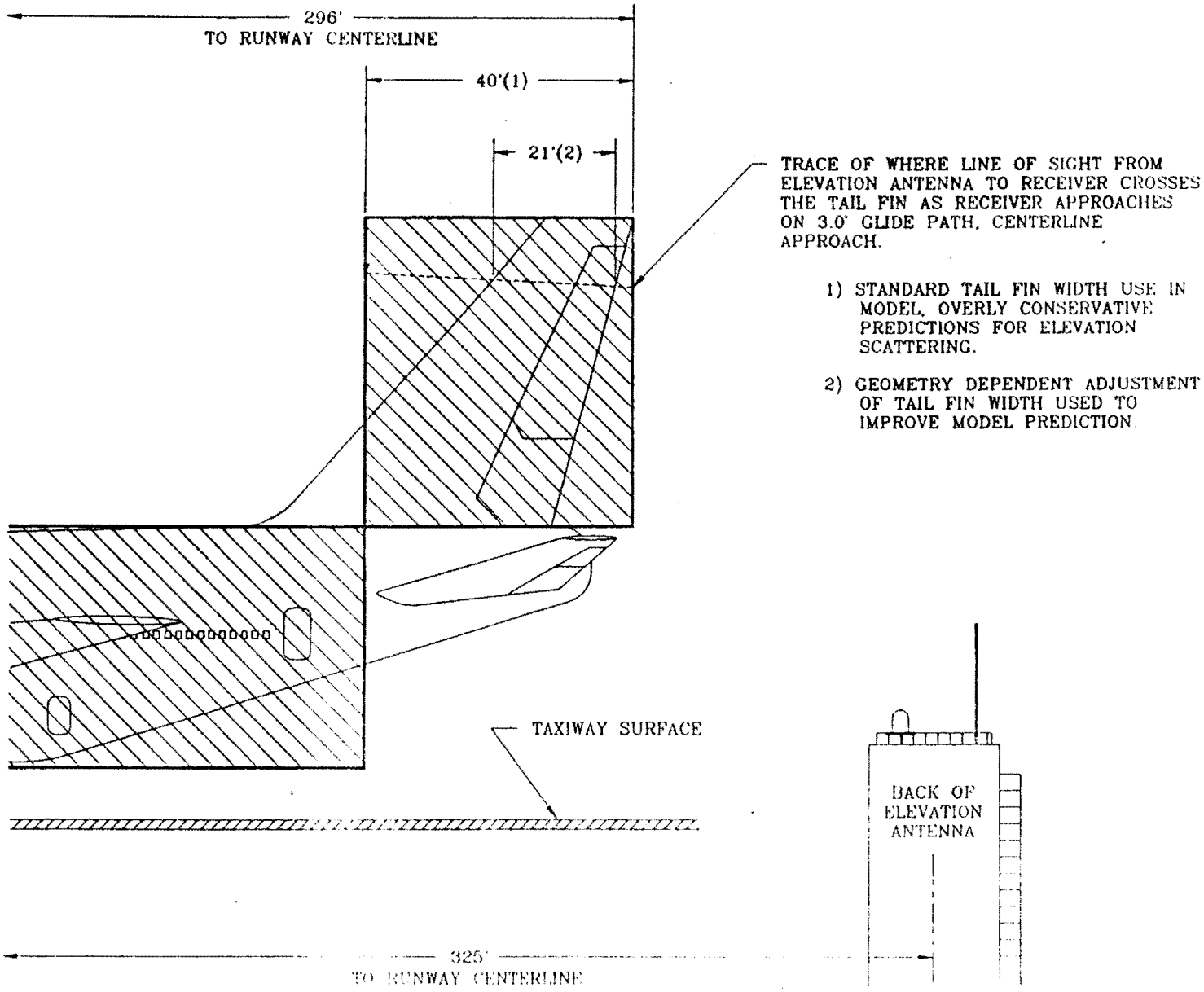


Elevation aircraft Position 1.


SDF ELEVATION POSITION 1
REPEATABILITY OF MEASURED DATA
PF ERROR IN DEGREES
0.5
0.4
0.3
0.2
0.1
0
-0.1
-0.2
-0.3
-0.4
-0.5
0
2
4
6
DISTANCE FROM THRESHOLD IN NM
RUN15
RUN16
RUN17


STANDIFORD FIELD ELEVATION POSITION 1
MODELED VS. MEASURED
PF ERROR IN DEGREES
1.1
1
0.9
0.8
0.7
0.6
0.5
0.4
0.3
0.2
0.1
0
-0.1
-0.5
0.5
1.5
2.5
3.5
4.5
DISTANCE FROM THRESHOLD IN NM
MODELED
MEASURED

SDF ELEVATION POSITION 1

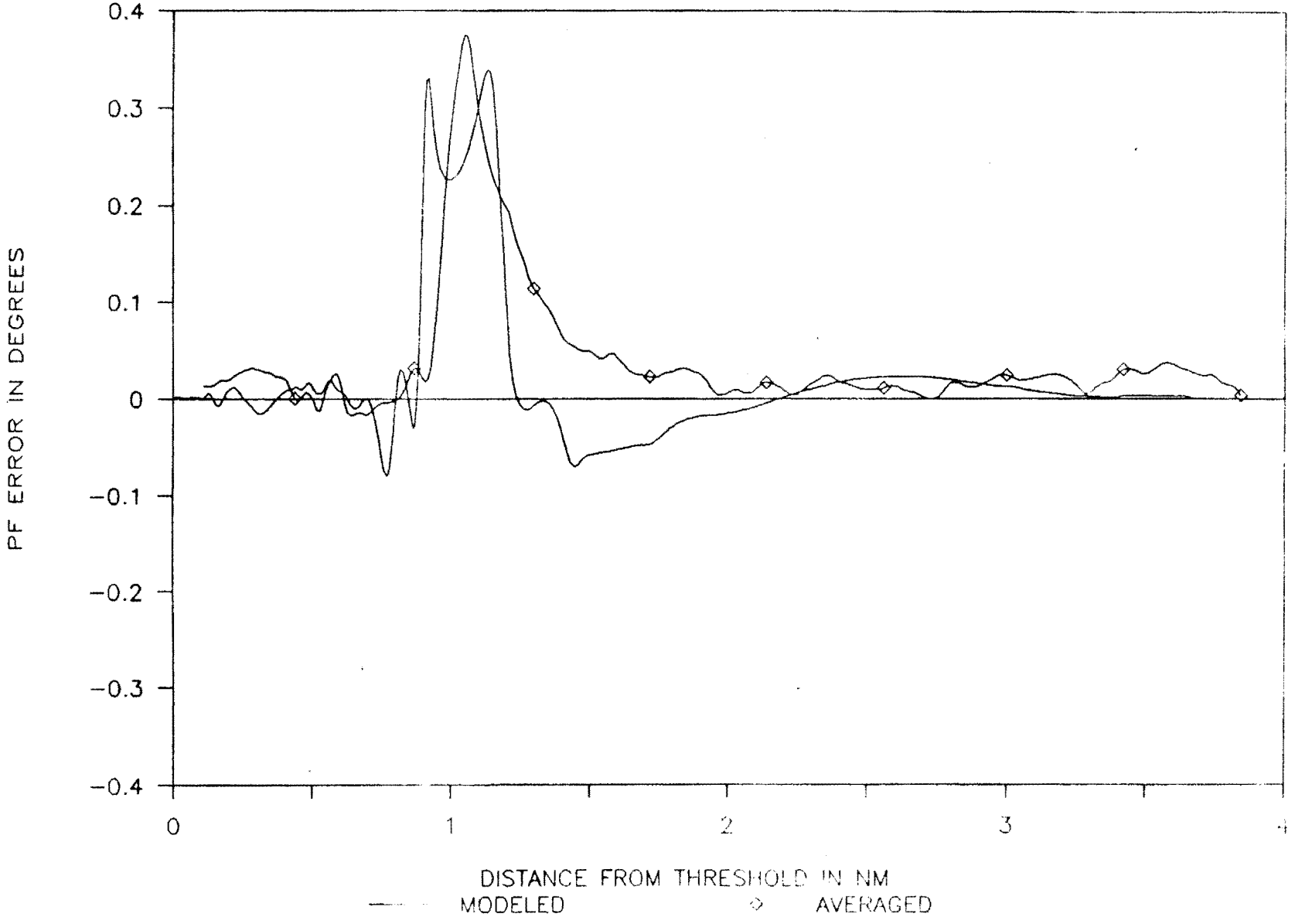


19

038003

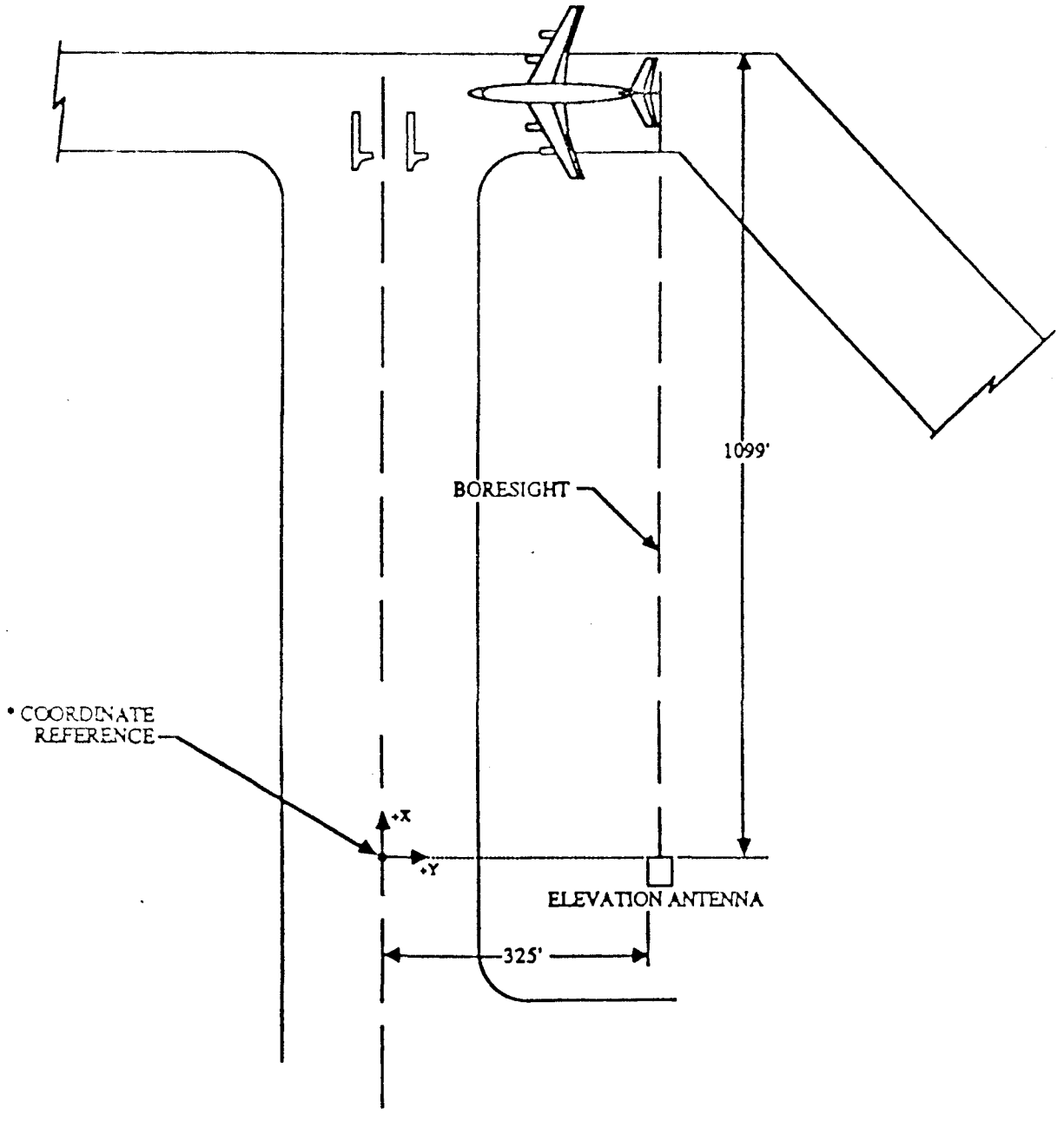
STANDIFORD FIELD ELEVATION POSITION 1

MODIFIED TAILFIN RESULTS VS. AVERAGED



POSITION 2, SDF

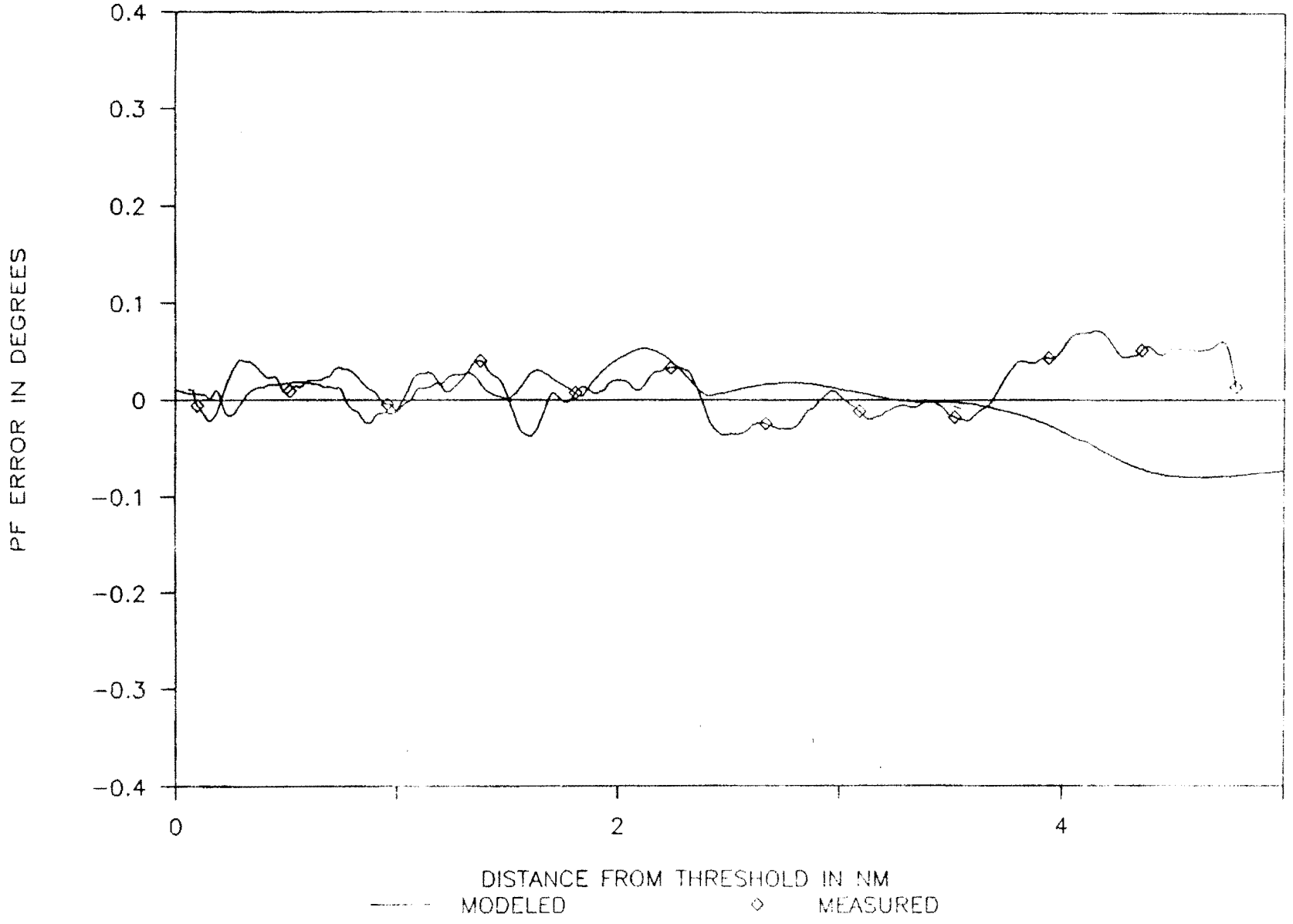
NOSE (X,Y)*	TAIL (X,Y)*
(1069,124)	(1069,358)



Elevation aircraft Position 2.

STANDIFORD FIELD ELEVATION POSITION 2

MODELED VS. MEASURED



MODELING TECHNIQUES FOR SPECIAL STRUCTURES

Objective: To validate the prediction of effects due to objects which have cross-sectional dimensions comparable to the wavelength at MLS frequencies and are within the near-field of the antenna.

- Emphasis on the effects of ILS/ALS structures on the azimuth guidance signal

- Validation of techniques for modeling cylindrical and square posts

Validation Activities

ACY Measured effect of 2 inch light pole on 2.0° beamwidth azimuth antenna

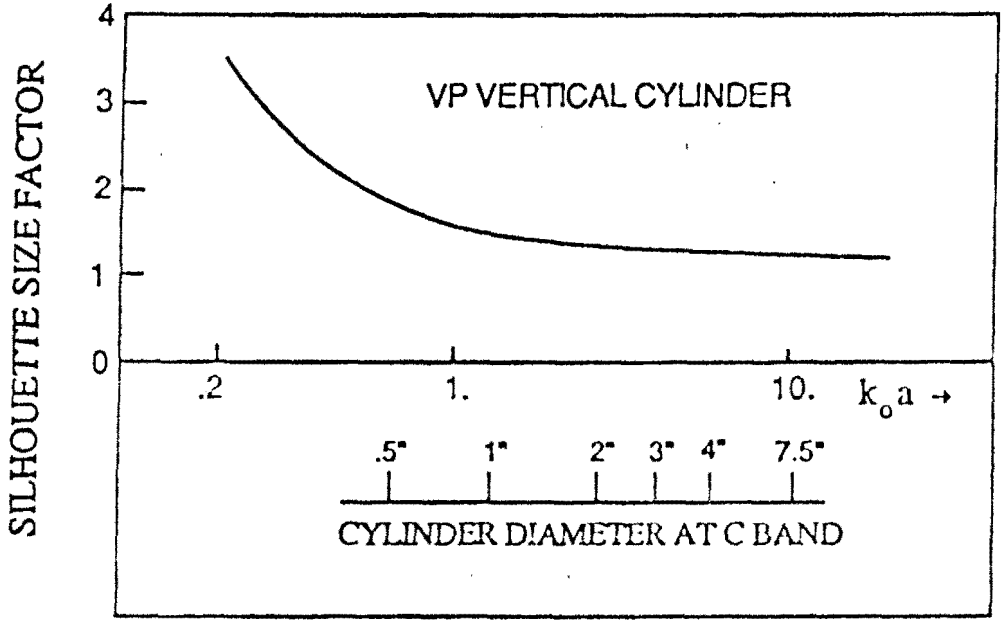
UNI Measured effect of ALSF MALS pole on 3.0° beamwidth azimuth antenna

Results

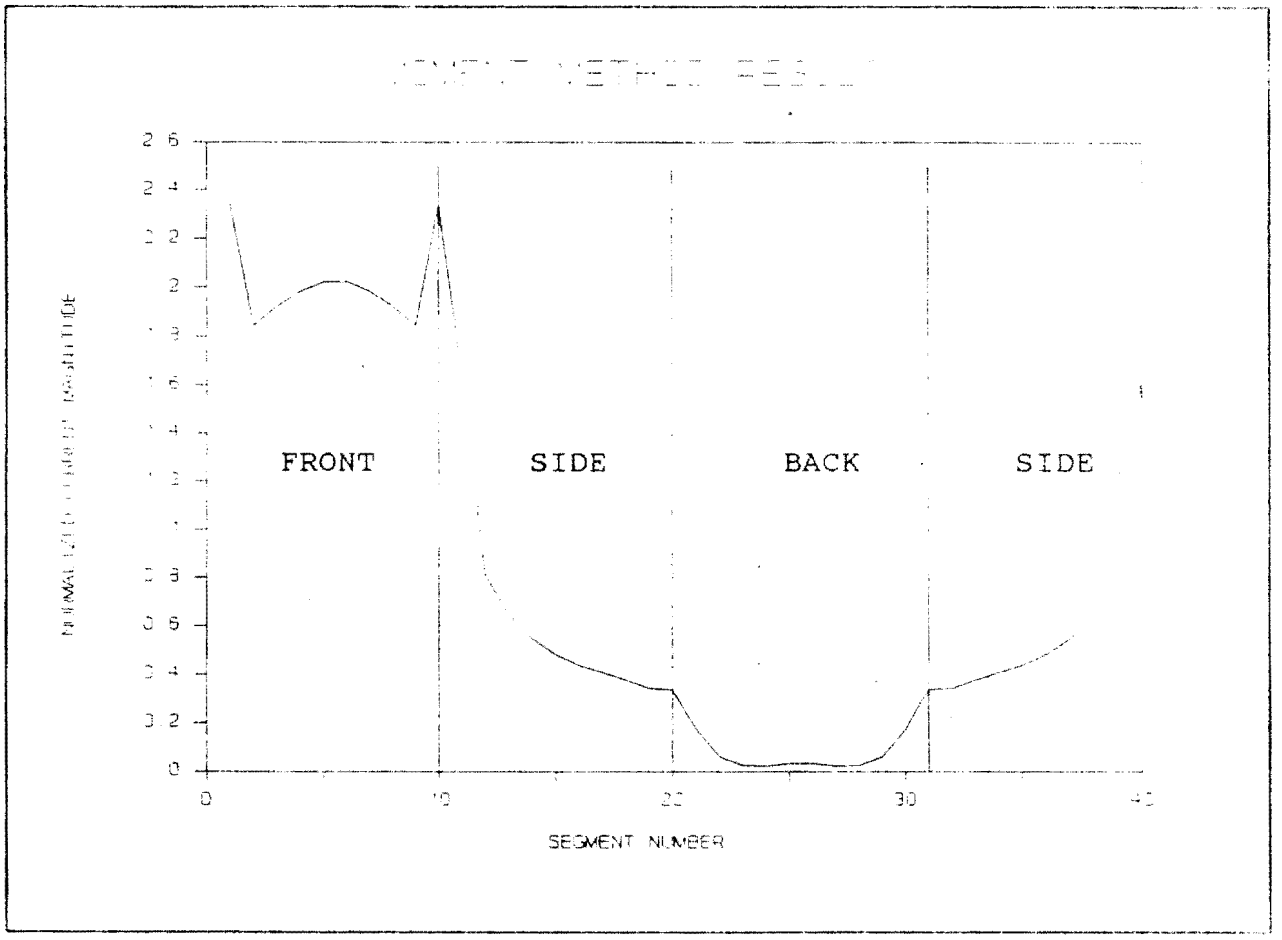
Validation of silhouette factor for modeling cylindrical post

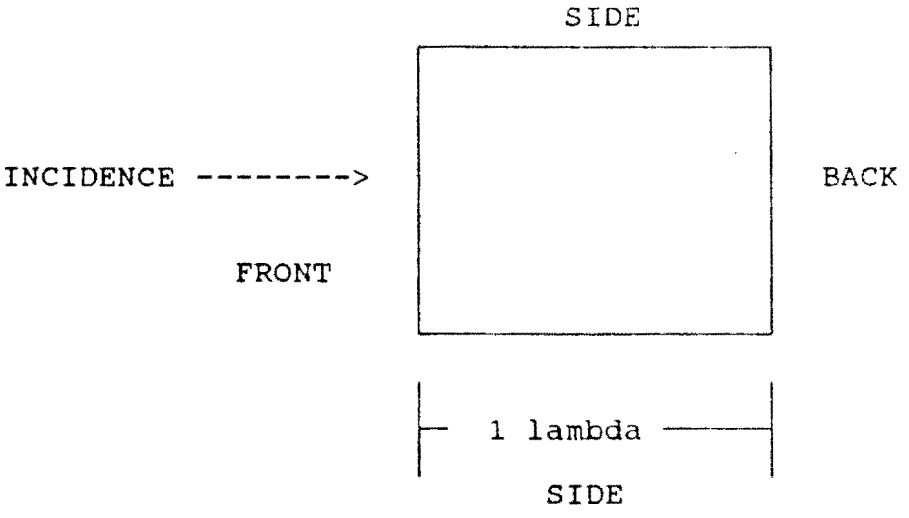
Development of a technique for modeling square posts

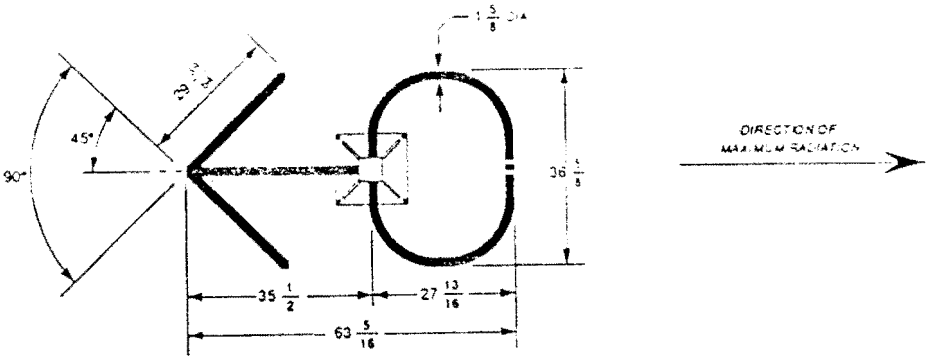
SILOUETTE FACTOR FOR MODELING VERTICAL CYLINDER WITH RECTANGULAR PLATE



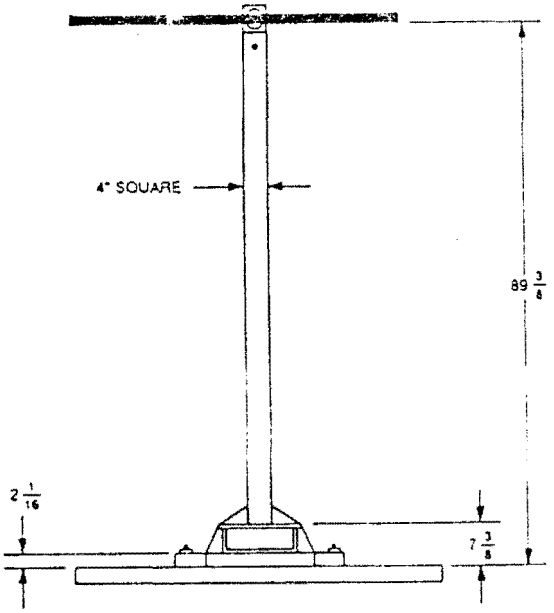
MOMENT METHOD RESULT: CURRENT INDUCED ON A SQUARE CYLINDER DUE TO NORMALLY INCIDENT TRANSVERSE-MAGNETIC WAVE





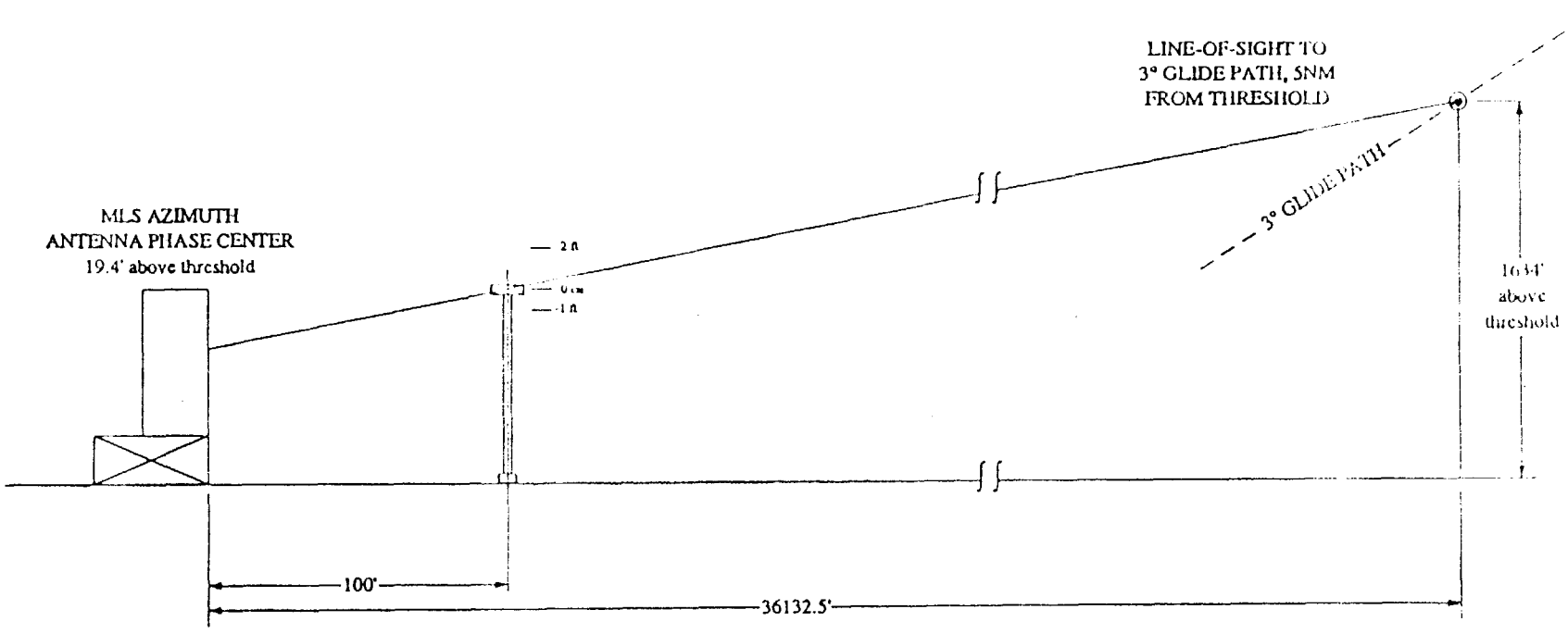


PLAN VIEW



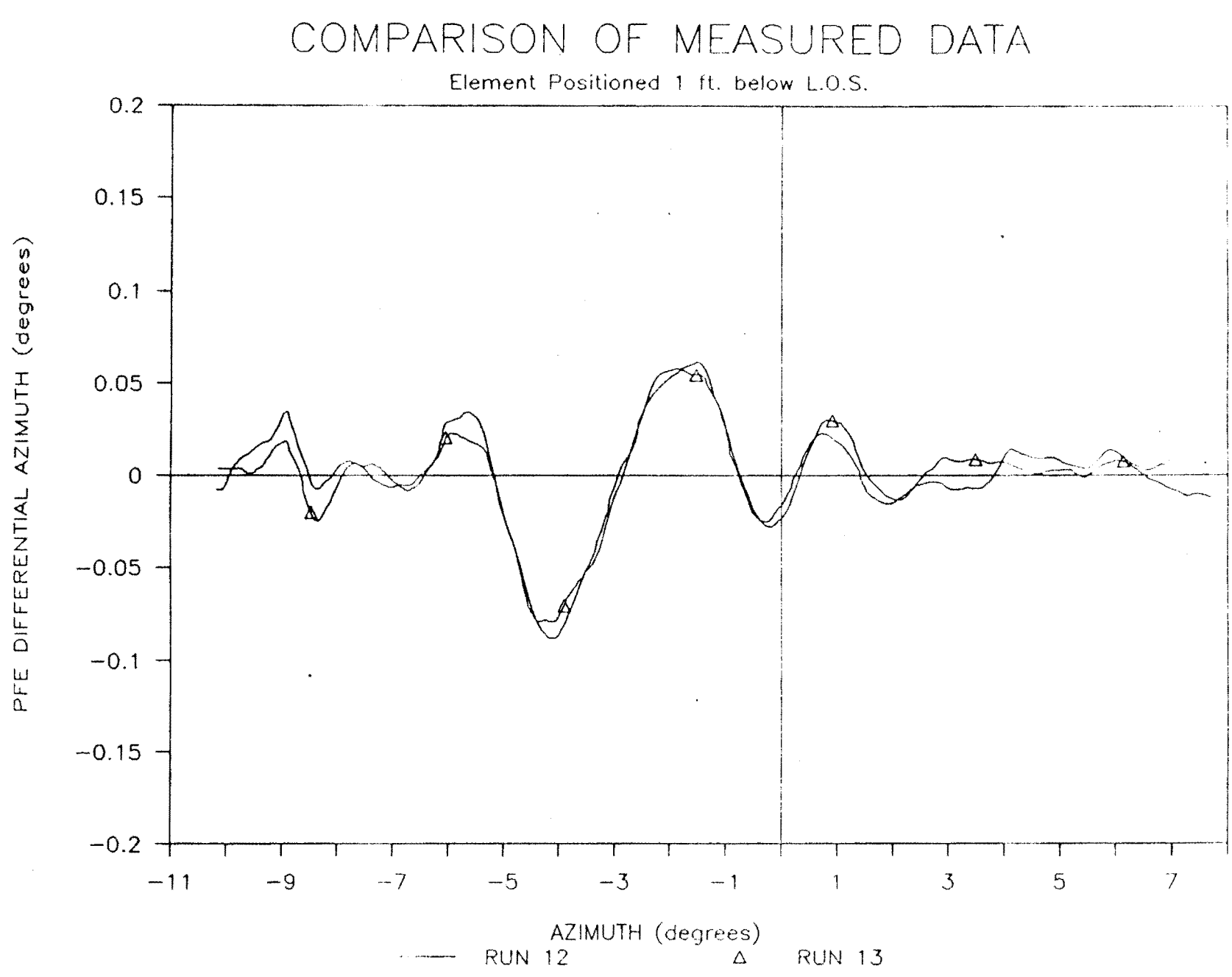
PROFILE VIEW

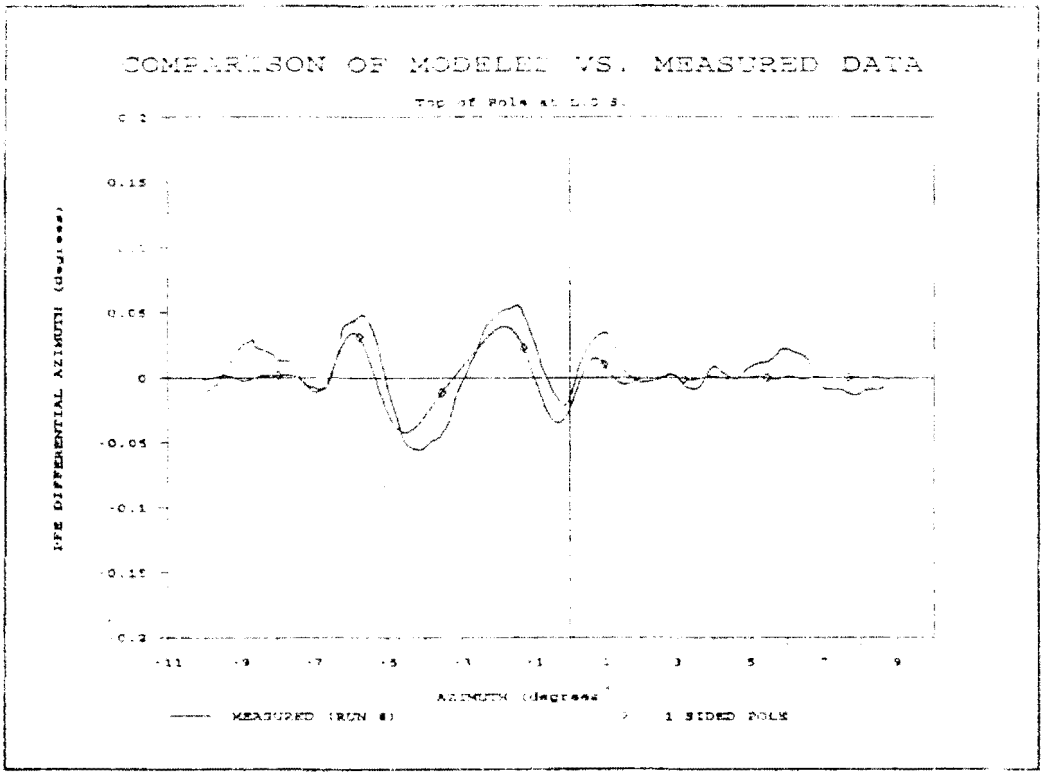
V-Ring Antenna Outline Drawing

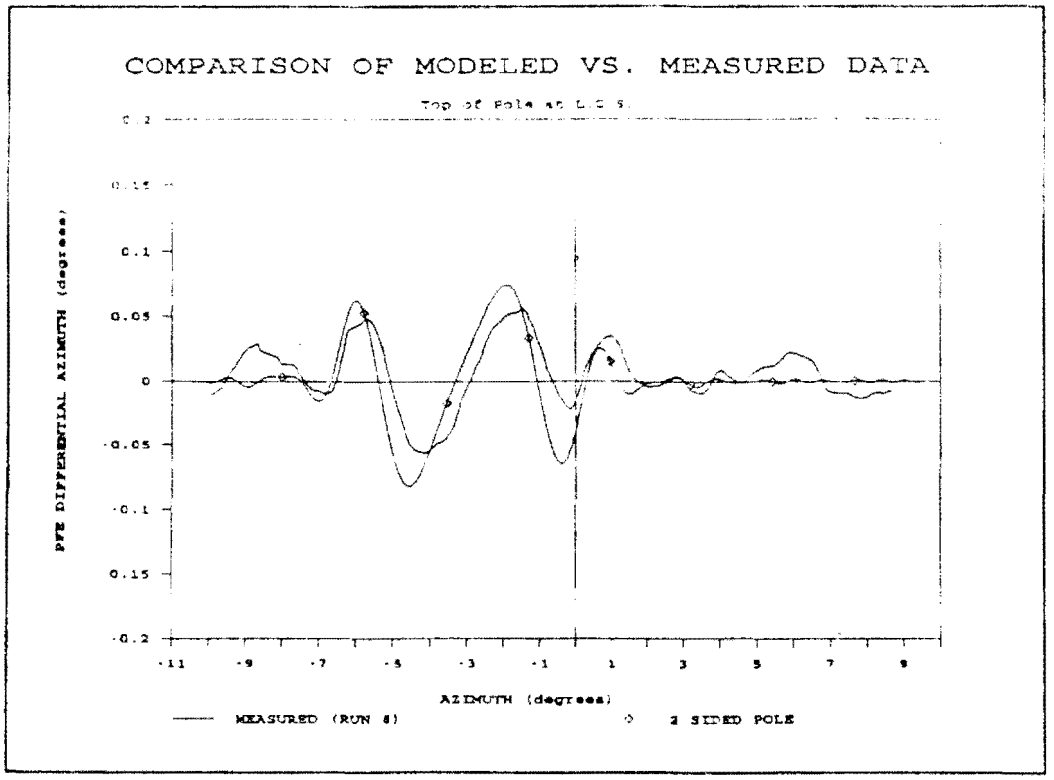


NOT TO SCALE

Profile of flight path with respect to the localizer antenna height.


COMPARISON OF MEASURED DATA
Element Positioned 1 ft. below L.O.S.
PFE DIFFERENTIAL AZIMUTH (degrees)
0.2
0.15
0.1
0.05
0
−0.05
−0.1
−0.15
−0.2
−11
−9
−7
−5
−3
−1
1
3
5
7
AZIMUTH (degrees)
RUN 12
RUN 13


COMPARISON OF MODELED VS. MEASURED DATA
Top of Pole at L.C.S.
PFE DIFFERENTIAL AZIMUTH (degrees)
0.15
0.05
0
-0.05
-0.1
-0.15
-0.2
-11
-9
-7
-5
-3
-1
1
3
5
7
9
AZIMUTH (degrees)
MEASURED (RUN 8)
1 SIDED POLE


COMPARISON OF MODELED VS. MEASURED DATA
Top of Pole at L.C.S.
PFE DIFFERENTIAL AZIMUTH (degrees)
0.1
0.05
0
-0.05
-0.1
0.15
-0.2
-11
-9
-7
-5
-3
-1
1
3
5
7
9
AZIMUTH (degrees)
MEASURED (RUN 8)
2 SIDED POLE

AL LOPEZ
ARL ASSOCIATES

RUNWAY HUMP SHADOWING

ESTIMATING POWER DENSITY ABOVE RUNWAYS WITH COMPLEX CENTERLINE PROFILES

ALFRED R. LOPEZ

FOUR SARINA DRIVE
COMMACK, NY 11725

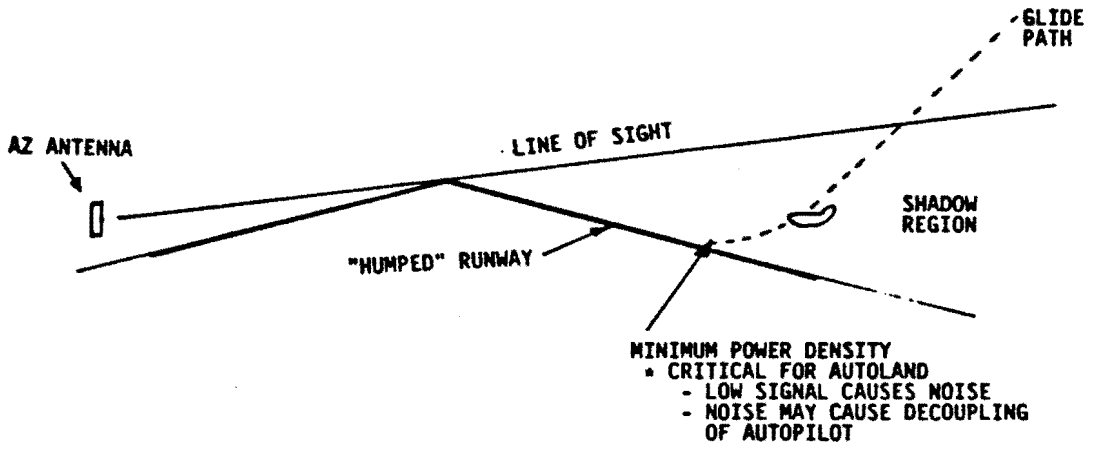
- o INTRODUCTION
- o BASIC PROBLEM
- o REVIEW OF INITIAL PAPER
- o EXTENSION OF INITIAL WORK
  - WEDGE ATTENUATION FACTOR AS BUILDING BLOCK
  - INVERTED WEDGE
- o RESULTS
- o SUMMARY

INTRODUCTION

A METHOD, WHICH HAS SPECIAL APPLICATION TO THE MICROWAVE LANDING SYSTEM, HAS BEEN DEVELOPED FOR ESTIMATING POWER DENSITY ABOVE RUNWAYS WITH COMPLEX CENTERLINE PROFILES. THE METHOD USES A BUILDING BLOCK APPROACH WHERE THE FUNDAMENTAL FLAT GROUND MODEL IS AUGMENTED WITH FACTORS THAT ACCOUNT FOR THE ATTENUATION ATTRIBUTED TO THE PARTICULAR CENTERLINE PROFILE FEATURES. THIS PAPER IS ACTUALLY A SEQUEL TO A PAPER THAT WAS PUBLISHED IN THE AP TRANSACTIONS IN THE JUNE 1987 ISSUE WITH THE TITLE "APPLICATION OF WEDGE DIFFRACTION THEORY TO ESTIMATING POWER DENSITY AT AIRPORT HUMPED RUNWAYS." APPLICATION OF A SINGLE WEDGE SURFACE, AS DESCRIBED IN THE ORIGINAL PAPER, PROVED TO BE ADEQUATE FOR ESTIMATING POWER DENSITY AT SEVERAL AIRPORT RUNWAYS. HOWEVER, AT SEVERAL OTHER RUNWAYS THE CENTERLINE PROFILE COMPLEXITY WAS SUCH THAT THE SINGLE WEDGE SURFACE PROVED TO BE INADEQUATE.

AS INDICATED IN THE OUTLINE, I PLAN TO FIRST PROVIDE SOME BACKGROUND ON THE APPLICATION THAT MOTIVATED THE STUDY, THEN REVIEW SOME OF THE KEY CONCEPTS PRESENTED IN THE INITIAL PAPER, AND THEN PRESENT THE NEW MATERIAL.

AIRPORT "HUMPED" RUNWAYS

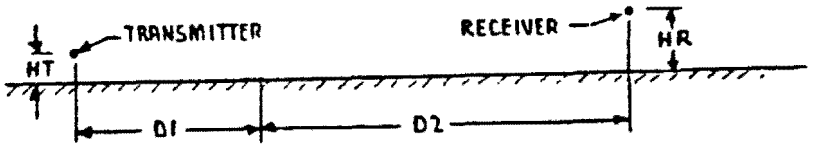


BASIC PROBLEM

I BELIEVE ONE OF THE REAL BENEFITS OF THE MICROWAVE LANDING SYSTEM, WHICH IS SCHEDULED TO REPLACE THE EXISTING INSTRUMENT LANDING SYSTEM BY THE YEAR 2000, WILL BE TO MAKE AUTOMATIC LANDINGS ROUTINE. A CRITICAL POINT IN AN AUTOLAND APPROACH IS THE POINT WHEN THE LANDING GEAR MAKES INITIAL CONTACT WITH THE RUNWAY SURFACE; AT THIS POINT THE SIGNAL LEVEL IS AT A MINIMUM VALUE. THIS SITUATION IS SHOWN IN THIS VIEWGRAPH FOR THE CASE WHERE THE AIRCRAFT IS LANDING IN A SHADOW ATTRIBUTED TO THE RUNWAY PROFILE. IF THE SIGNAL-TO-NOISE RATIO IS LOW AT THE TOUCHDOWN POINT THEN THE RESULTING NOISE IN THE ANGLE GUIDANCE MAY CAUSE THE AUTOPILOT TO DECOUPLE. AT THIS CRITICAL POINT THE CONSEQUENCE OF SUCH AN EVENT IS SUBSTANTIAL INCREASE IN THE HAZARD OF LANDING OR EXECUTING A MISSED APPROACH.

THE PROBLEM IS TO SITE THE ANTENNAS SUCH THAT SUFFICIENT POWER DENSITY IS PROVIDED ON RUNWAYS WITH CENTERLINE PROFILES THAT REDUCE THE SIGNAL LEVEL. MEAUREMENTS OF POWER DENSITY AT ACTUAL SITES ARE POSSIBLE, BUT THEY ARE COSTLY. THEREFORE A MEANS FOR ACCURATELY ESTIMATING POWER DENSITY AT ACTUAL SITES IS DESIREABLE.

FLAT GROUND POWER DENSITY FORMULA



TRANSMITTER ERP IN DIRECTION PARALLEL TO GROUND

$$P_{FG} = \underbrace{\frac{P\,G}{4\pi(D1+D2)^2}}_{\text{FREE SPACE FACTOR}} \underbrace{4\sin^2\left(\frac{2\pi\,HT}{\lambda}\sin\theta\right)}_{\text{GROUND REFLECTION FACTOR}}$$

$$\sin\theta \approx HR/(D1+D2)$$

IF $\quad \frac{HT}{\lambda}\frac{HR}{D1+D2} < \frac{1}{8}$

THEN $\quad \boxed{P_{FG} = P\,G\,\frac{4\pi}{\lambda^2}\left(\frac{HT}{D1+D2}\right)^2\left(\frac{HR}{D1+D2}\right)^2}$

REVIEW

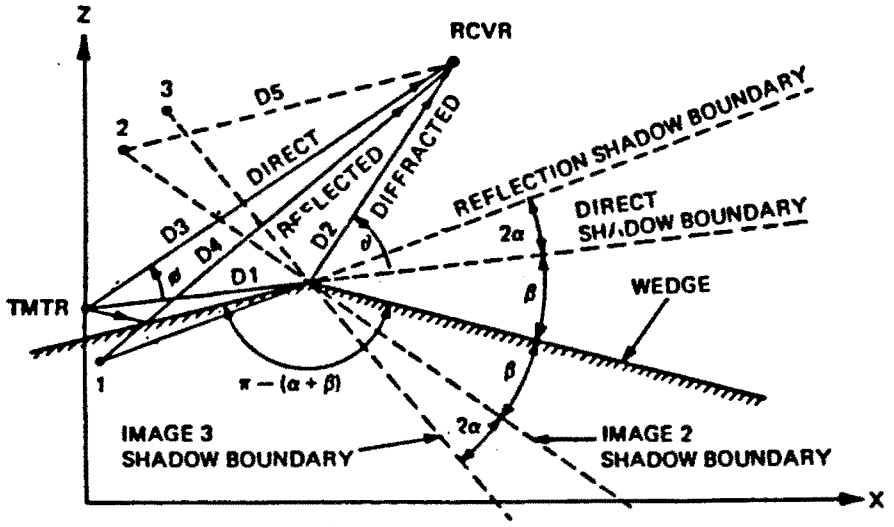
IN THE INITIAL PAPER THE BASIC REFERENCE FORMULA FOR POWER DENSITY WAS THE FLAT GROUND FORMULA.

A SIMPLE DERIVATION OF THIS FORMULA IS PRESENTED IN THIS VIEWGRAPH.

THE DIMENSIONING IS CONSISTENT WITH A 0-DEGREE ANGLE WEDGE WITH A VERTEX D1 UNITS FROM THE TRANSMITTER.

THE REFLECTION FACTOR IS SIMPLY THE POWER PATTERN FOR THE TRANSMITTER AND ITS IMAGE. THE IMAGE IS ASSUMED TO HAVE UNITY AMPLITUDE AND 180 DEGREES OF PHASE.

WEDGE DIFFRACTION GEOMETRY



REVIEW

ONE OF THE KEY RESULTS PRESENTED IN THE INITIAL PAPER IS A SIMPLE FORMULATION FOR WEDGE DIFFRACTION UNDER CERTAIN CONDITIONS:

IF THE WEDGE ANGLE IS SMALL AND THE TRANSMITTER IS NEAR ONE OF THE WEDGE SURFACES,
THEN A GOOD APPROXIMATION OF THE TOTAL FIELD IS PROVIDED BY A FORMULA THAT INCLUDES
ONE DIRECT COMPONENT,
AT MOST, TWO SINGLY REFLECTED COMPONENTS,
AND FOUR DIFFRACTED COMPONENTS

THE RELEVANT GEOMETRY IS SHOWN IN THIS VIEWGRAPH. THE FOUR DIFFRACTION COMPONENTS ARE RELATED TO THE TRANSMITTER AND THE THREE IMAGES SHOWN. THEY HAVE MAXIMUM AMPLITUDE AT THE CORRESPONDING SHADOW BOUNDARIES.

THE BASIC FORMULAS ARE PRESENTED IN THE FOLLOWING VIEWGRAPH.

BASIC FORMULAS

DIRECT DIFFRACTED

$$E(\theta) = \overbrace{E1(\theta)}^{} - \underbrace{E2(\theta)}_{} - \overbrace{E3(\theta) + E3(\theta - 2\alpha) + E3(-\theta - 2\beta) - E3(-\theta - 2\alpha - 2\beta)}^{}$$

REFLECTED

$$E1(\theta) = \frac{D1 + D2}{D3} V(\theta) u(\theta) \exp\left(j \frac{2\pi}{\lambda} (D1 + D2 - D3)\right)$$

$$E2(\theta) = \frac{D1 + D2}{D4} V'(\theta - 2\alpha) u(\theta - 2\alpha) \exp\left(j \frac{2\pi}{\lambda} (D1 + D2 - D4)\right)$$

$$+ \frac{D1 + D2}{D5} V'(\theta + 2\beta) u(-\theta - 2\beta) \exp\left(j \frac{2\pi}{\lambda} (D1 + D2 - D5)\right)$$

$$E3(\theta) = \left(\frac{\tanh(v)}{2v} - \frac{v}{4} \exp(-1.5v)\right) \operatorname{sgn}(\theta) \exp\left(-j \frac{\pi}{4} \tanh(v/2.4)\right)$$

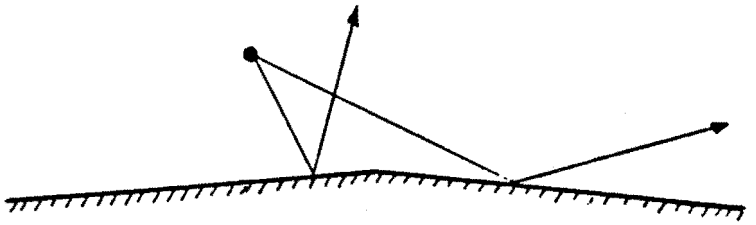
REVIEW

AS SHOWN, THE TOTAL FIELD CONSISTS OF THREE BASIC TERMS, DIRECT, REFLECTED, AND DIFFRACTED. THE DEFINITION OF VARIABLES AND FUNCTIONS ARE GIVEN IN THE ORIGINAL PAPER. THIS VIEWGRAPH PRESENTS THE BASIC FORM OF THE EQUATIONS.

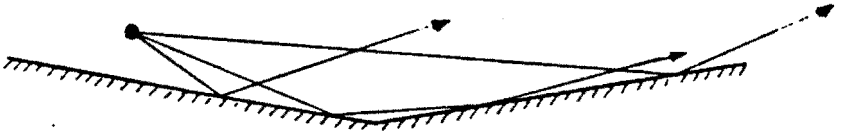
THE REFLECTED TERM CONSISTS OF TWO SINGLY REFLECTED COMPONENTS. FOR THE MORE COMPLEX RUNWAY CENTERLINE SITUATIONS, WHICH IS THE SUBJECT MATTER OF THIS PAPER, AN INVERTED WEDGE MODEL IS USEFUL. FOR THIS CASE, A DOUBLY REFLECTED COMPONENT MUST BE ADDED TO THE REFLECTED TERM.

ANOTHER KEY RESULT OF THE INITIAL PAPER IS THE BOTTOM EQUATION, WHICH IS AN ELEMENTARY-FUNCTION APPROXIMATION FOR THE DIFFRACTION INTEGRAL. THIS FORMULATION SIMPLIFIES THE COMPUTATIONS.

REFLECTION COMPONENTS FOR INVERTED WEDGE



WEDGE -- SINGLY REFLECTED COMPONENTS



INVERTED WEDGE -- SINGLY AND DOUBLY REFLECTED COMPONENTS

INVERTED WEDGE

THIS VIEWGRAPH SHOWS THE INVERTED WEDGE, WHICH HAS TWO SINGLY REFLECTED COMPONENTS AND ONE DOUBLY REFLECTED COMPONENT.

ALSO SHOWN IS THE NORMAL WEDGE, WHICH HAS TWO SINGLY REFLECTED COMPONENTS.

THE COMPUTER PROGRAM LISTING IN THE ORIGINAL PAPER DID NOT INCLUDE THE DOUBLY REFLECTED COMPONENT. THE LISTING IN THE SYMPOSIUM DIGEST INCLUDES THIS COMPONENT.

WEDGE ATTENUATION FACTOR

IF THE RECEIVER IS BELOW AND MORE THAN A FRESNEL ZONE FROM THE DIRECT SIGNAL SHADOW BOUNDARY THEN THE POWER DEMSITY IS GIVEN BY THE FOLLOWING EQUATION

WEDGE POWER DENSITY — FLAT GROUND POWER DENSITY

$$P(HT, HR) = (P)(G)\frac{4\pi}{\lambda^2}\left(\frac{HT}{D1+D2}\right)^2\left(\frac{HR}{D1+D2}\right)^2\frac{1}{\pi^4}\left(\frac{\sqrt{\lambda/D}}{\alpha+\beta}\right)^6$$

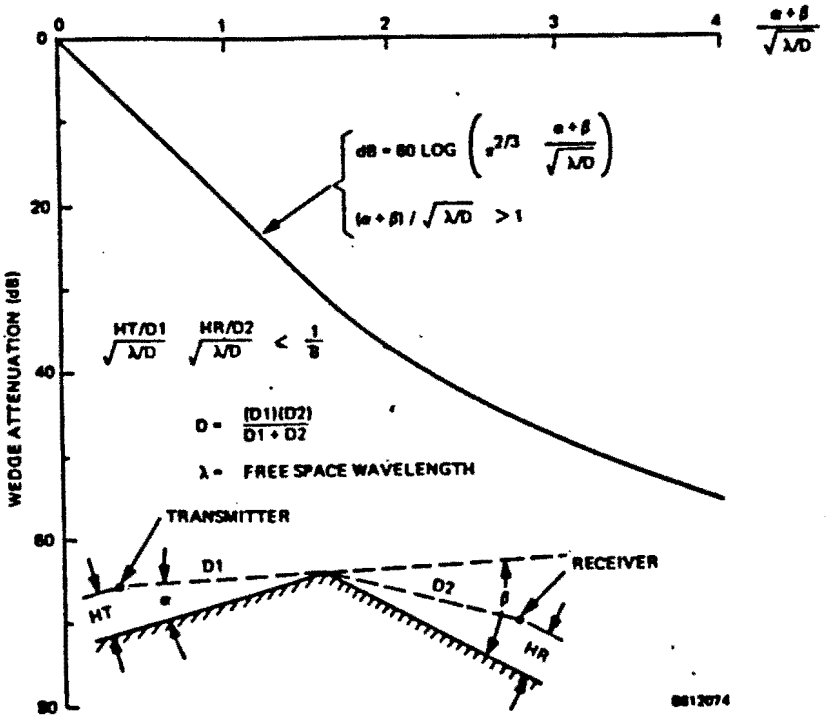
$$WA = \frac{1}{\pi^4}\left(\frac{\sqrt{\lambda/D}}{\alpha+\beta}\right)^6$$

REVIEW

ONE OF THE MORE INTERESTING RESULTS OF THE ORIGINAL PAPER IS THE DEFINITION OF THE WEDGE ATTENUATION FACTOR. AS SHOWN IN THIS VIEWGRAPH THE FACTOR RELATES THE RATIO OF THE WEDGE TO FLAT GROUND POWER DENSITIES AND THE WEDGE ANGLE. THE FACTOR WAS DERIVED FOR THE CASE WHERE THE RECEIVER WAS IN THE DEEP SHADOW REGION WHERE THE ASYMPTOTIC APPROXIMATION FOR THE DIFFRACTION INTEGRAL IS VALID. THE RESULT CAN BE GENERALIZED TO INCLUDE THE REGION NEAR THE SHADOW BOUNDARY.

THE RELATIONSHIP OF WEDGE ATTENUATION VERSUS WEDGE ANGLE IS SHOWN IN THE FOLLOWING VIEWGRAPH.

WEDGE ATTENUATION VERSUS WEDGE ANGLE (REFERENCE CASE OF FLAT GROUND)



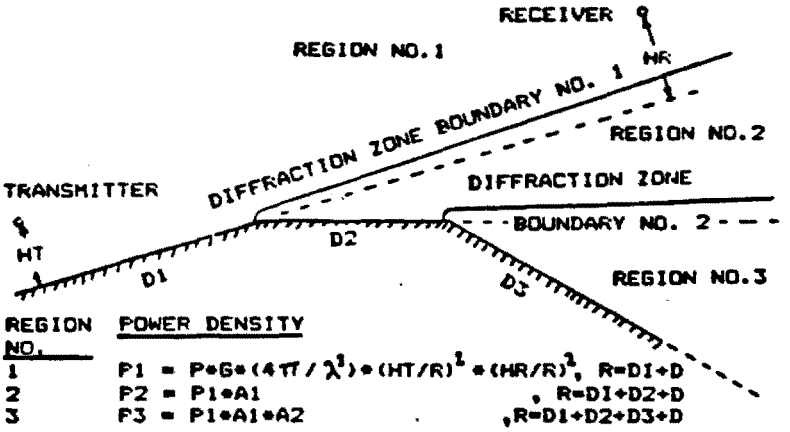
WEDGE FACTOR AS BUILDING BLOCK

A PLOT OF WEDGE ATTENUATION VERSUS THE NORMALIZED WEDGE ANGLE IS PRESENTED IN THIS VIEWGRAPH. THE ATTENUATION IS WITH RESPECT TO THE FLAT GROUND CASE.

THE WEDGE ATTENUATION FACTOR CAN BE USED AS A BUILDING BLOCK FOR ESTIMATING POWER DENSITY NEAR THE RUNWAY SURFACE FOR SITUATIONS WHERE THE RUNWAY PROFILE CAN BE APPROXIMATED BY A SET OF CONNECTED WEDGES.

THIS TURNS OUT TO BE A VERY HELPFUL APPROACH IN THAT IT PROVIDES INSIGHT WITH RESPECT TO THE AFFECT OF EACH WEDGE.

POWER DENSITY ABOVE RUNWAYS WITH COMPLEX RUNWAY CENTERLINES



REGION NO.	POWER DENSITY	
1	$P1 = P*G*(4\pi/\lambda^2)*(HT/R)^2*(HR/R)^2$	$R=D1+D$
2	$P2 = P1*A1$	$R=D1+D2+D$
3	$P3 = P1*A1*A2$	$R=D1+D2+D3+D$

WHERE: P = TRANSMITTER POWER
G = TRANSMITTER GAIN
λ = FREE SPACE WAVELENGHT
D = DISTANCE ALONG EXTENDED WEDGE SURFACE'
A1 = WEDGE NO.1 ATTENUATION FACTOR
A2 = WEDGE NO.2 ATTENUATION FACTOR

BASIC APPROACH FOR CONNECTED WEDGES

THIS VIEWGRAPH SHOWS THE BASIC APPROACH FOR THE CASE WHERE THE RUNWAY PROFILE CAN BE APPROXIMATED BY A SET OF CONNECTED WEDGES.

THE BASIC BUILDING BLOCKS ARE THE FLAT GROUND MODEL AND THE WEDGE ATTENUATION FACTOR.

AS SHOWN IN THE VIEWGRAPH, THREE REGIONS ARE DEFINED.
THE DIFFRACTION ZONE BOUNDARIES SEPARATE THE REGIONS.

- IN REGION ONE, ONLY THE FLAT GROUND MODEL IS REQUIRED TO COMPUTE THE POWER DENSITY.
- IN REGION TWO, THE FLAT GROUND MODEL IS MULTIPLIED BY A WEDGE FACTOR.
- IN REGION THREE, THE FLAT GROUND MODEL IS MULTIPLIED BY TWO WEDGE FACTORS.

AN EXAMPLE IS GIVEN IN THE FOLLOWING VIEWGRAPH.

DENVER RUNWAY 17R -- COMPUTED POWER DENSITY
TEN FEET ABOVE THRESHOLD

Factor	Units	Transmitter MSL (ft) 5293	5295	5298
Transmitter power	dB W	13	13	13
Antenna gain	dB	8	8	8
$4\pi/\lambda^2$	dB $1/m^2$	35.5	35.5	35.5
$(HT/R)^2$	dB	-65.1	-63.0	-60.5
$(HR/R)^2$	dB	-62.1	-62.1	-62.1
Wedge No. 1	dB	-14.0	-13.0	-10.8
Wedge No. 2	dB	-11.9	-11.9	-11.9
Wedge No. 3	dB	12.0	12.0	12.0
Power density	dB W/m^2	-84.6	-81.5	-76.3

DENVER RUNWAY 17R CENTERLINE PROFILE

PT. NO.	0	1	2	3	4
X CORD.	0	1170	3370	7270	12670
MSL	5286	5294	5291	5261	5245



DENVER RUNWAY 17R

THE PROFILE FOR THE DENVER RUNWAY 17R CAN BE APPROXIMATED BY FOUR STAIGHT LINE SEGMENTS FORMING THREE CONNECTED WEDGES. ACCORDING TO THE PROPOSED METHOD, THE POWER DENSITY CAN BE ESTIMATED AT A POINT TEN FEET ABOVE THE RUNWAY THRESHOLD (POINT NO. 4) BY MULTIPLYING THE FLAT GROUND RESULT BY THREE WEDGE FACTORS.

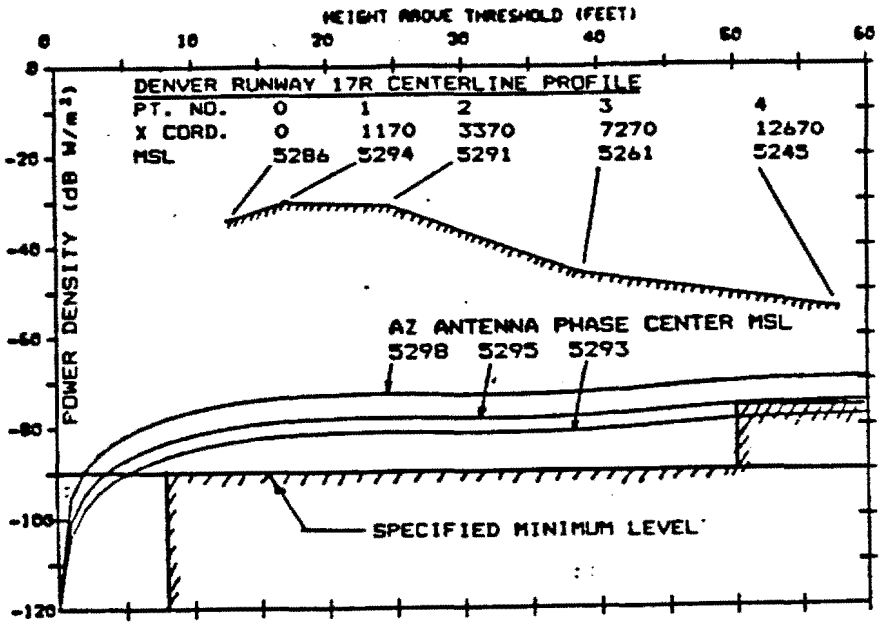
THE RESULTS ARE SHOWN IN THE VIEWGRAPH FOR THREE TRANSMITTER ANTENNA HEIGHTS. IT IS NOTED THAT FACTOR MULTIPLICATION IS CONVERTED TO ADDITION OF DB'S.

THE WEDGE FACTORS WERE EVALUATED BY EXECUTING THE COMPUTER PROGRAM FOR EACH OF THE THREE WEDGES AND DETERMINING THE DB DIFFERENCE BETWEEEN THE ACTUAL AND FLAT GROUND RESULTS. FOR EACH WEDGE THE TRANSMITTER AND RECEIVER WERE LOCATED AS FOLLOWS:

WEDGE NO	TRANSMITTER LOCATION	RECEIVER LOCATION
1.	AT P0 AND HT=12,9,7	AT P2 AND HR=1
2.	AT P1 AND HT=1	AT P3 AND HR=1
3.	AT P2 AND HT=1	AT P4 AND HR=10

NOTE THAT THE THIRD WEDGE IS INVERTED, WHICH RESULTS IN NEGATIVE ATTENUATION.

DENVER RUNWAY 17R -- COMPUTED POWER DENSITY FROM 0 TO 60 FEET ABOVE THRESHOLD

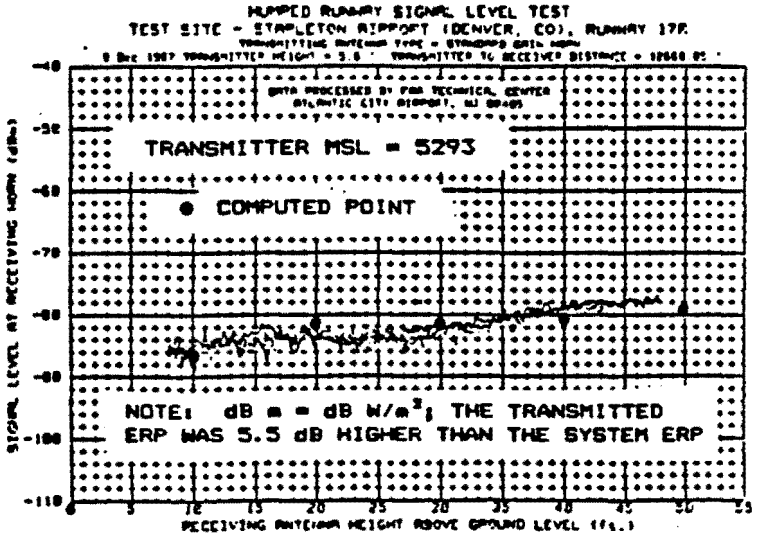


DENVER RUNWAY 17R

CONTINUOUS PLOTS OF POWER DENSITY VERSUS HEIGHT ABOVE THE RUNWAY THRESHOLD, AS SHOWN IN THIS VIEWGRAPH, WERE OBTAINED BY LOCATING A TRANSMITTER ABOVE POINT NO.2 SUCH THAT THE POWER DENSITY WAS EQUAL TO THE VALUE COMPUTED FOR THE RECEIVER AT THE 10 FT HEIGHT. THIS HEIGHT WAS THEN USED AS INPUT TO THE COMPTUER PROGRAM TO GENERATE THE PLOTS.

IT IS INTERESTING TO NOTE THAT THE SPECIFIED MINIMUM POWER DENSITY AT THE 50 FT HEIGHT IS THE DRIVER FOR THE HEIGHT OF THE TRANSMITTER ANTENNA.

DENVER RUNWAY 17R
COMPARISON OF MEASUREMENTS AND COMPUTATIONS

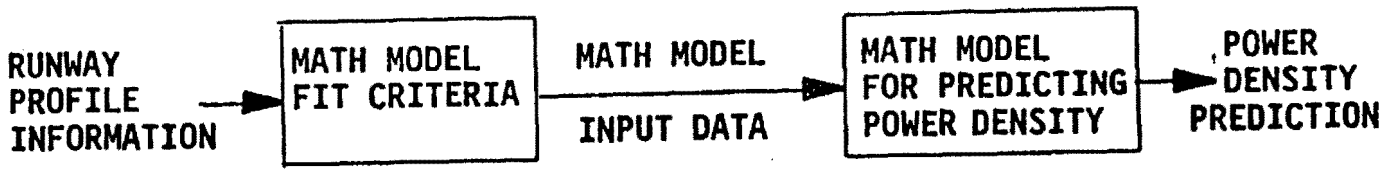


DENVER RUNWAY 17R

MEASUREMENTS WERE MADE BY A TEAM OF FAA AND HAZELTINE PERSONNEL AT DENVER DURING THE PERIOD OF DEC. 7-11, 1987. A SAMPLE OF THE MEASUREMENT RESULTS ARE SHOWN IN THIS VIEWGRAPH. INCLUDED ARE THE COMPUTED POINTS BASED ON THE PROPOSED METHOD FOR ESTIMATING POWER DENSITY.

THE AGREEMENT BETWEEN THE MEASUREMENTS AND THE ESTIMATES WAS GOOD.

KEY ELEMENT FOR MATH MODEL PREDICTION PROCESS



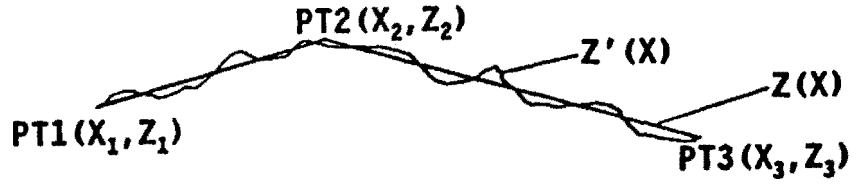
INPUT

KEY ELEMENT IN PROCESS

OUTPUT

98

EXAMPLE:
LEAST SQUARES FIT



GIVEN: LOCATION OF PT1 AND PT3.
FIND X_2 AND Z_2 SUCH THAT

$$\int_{X_1}^{X_3} (Z(X)-Z'(X))^2 \, dX$$ IS A MINIMUM.

ARLopez 900625

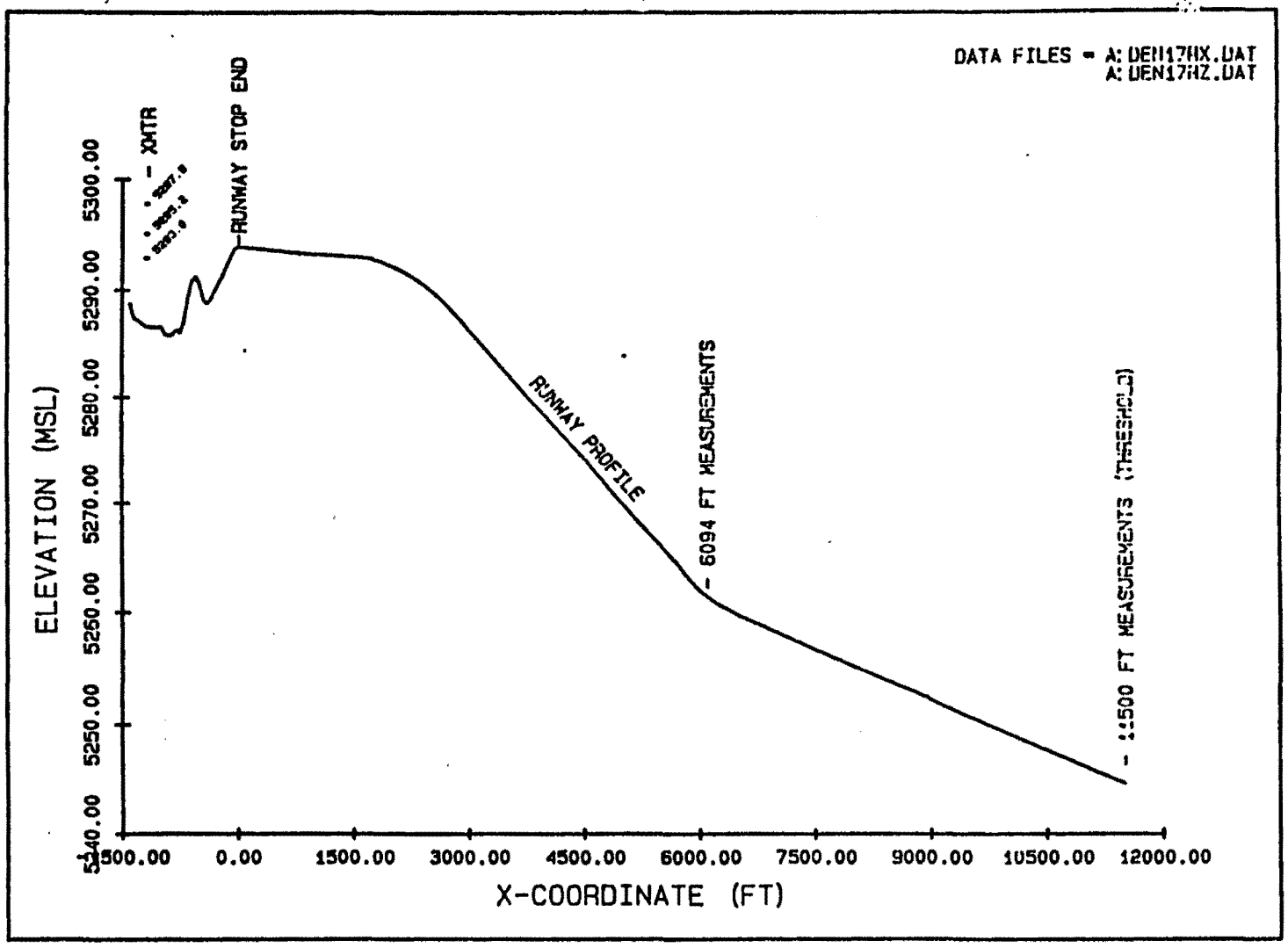


FIGURE 1. DENVER RUNWAY 17R/35L CENTERLINE TERRAIN PROFILE.

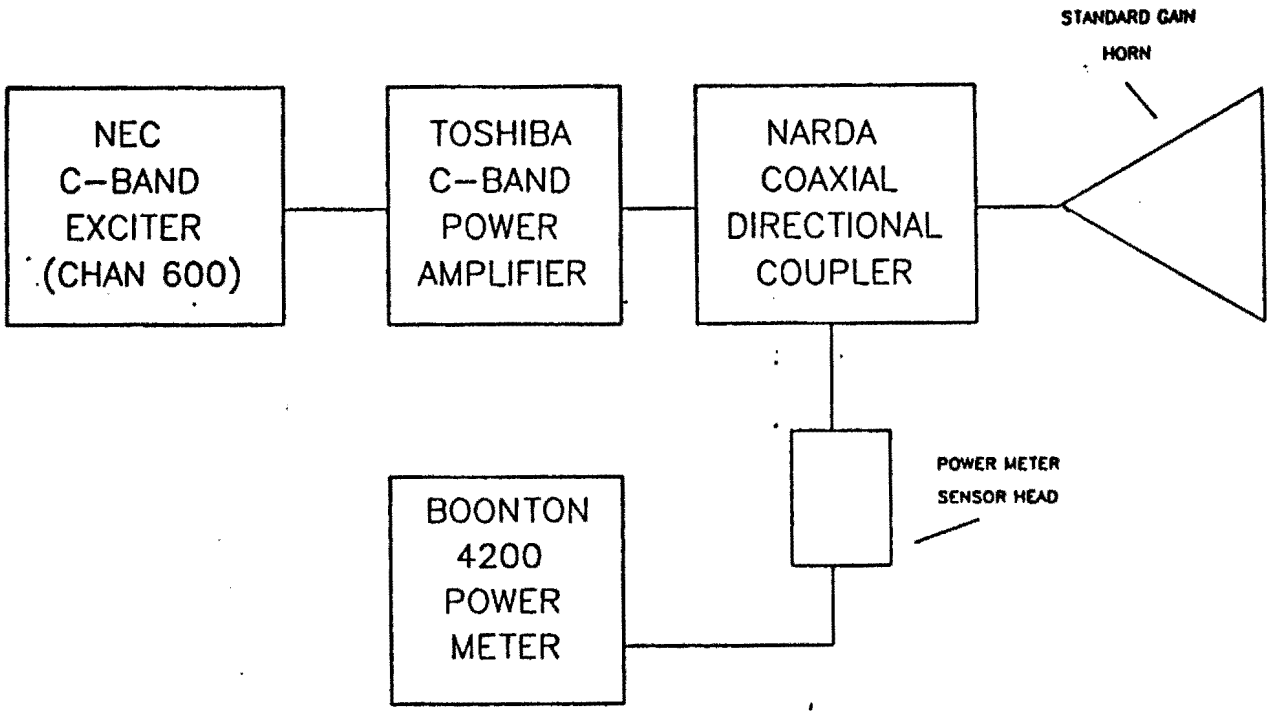


FIG. 2 POWER DENSITY MEASUREMENT TRANSMITTING SYSTEM

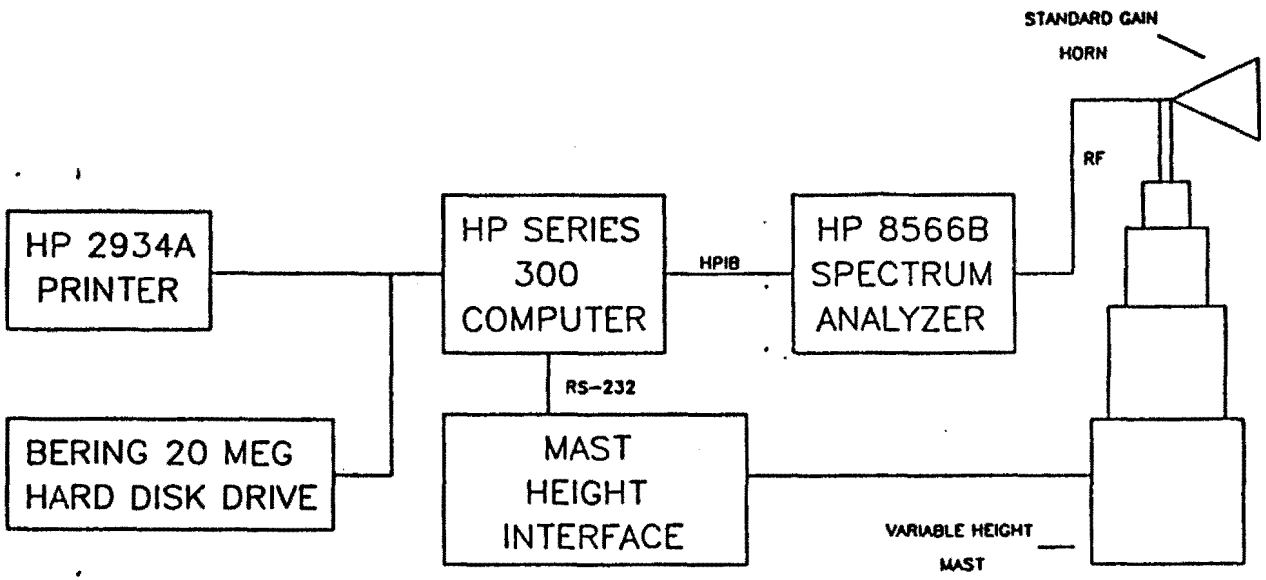


FIG. 3 POWER DENSITY MEASUREMENT RECEIVING SYSTEM

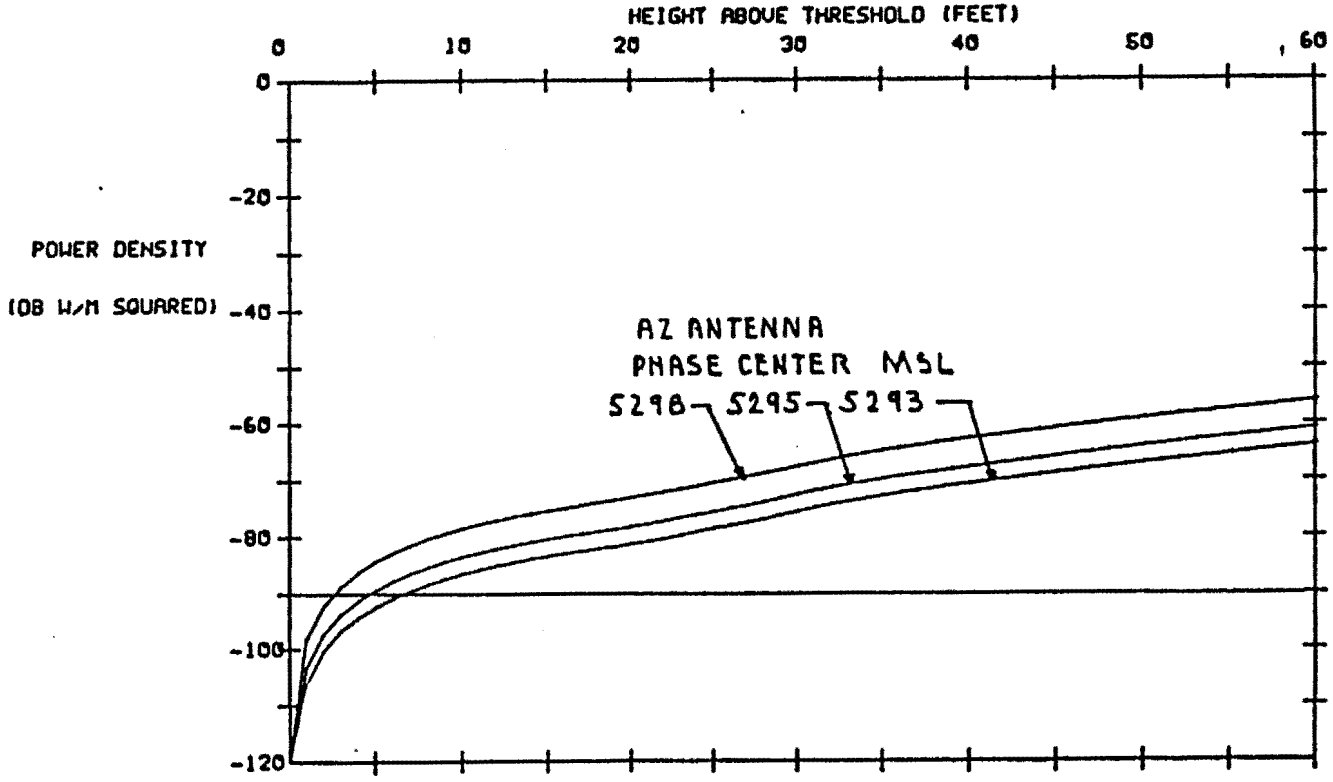


Figure 2. Computed Power Density Above Point PT3

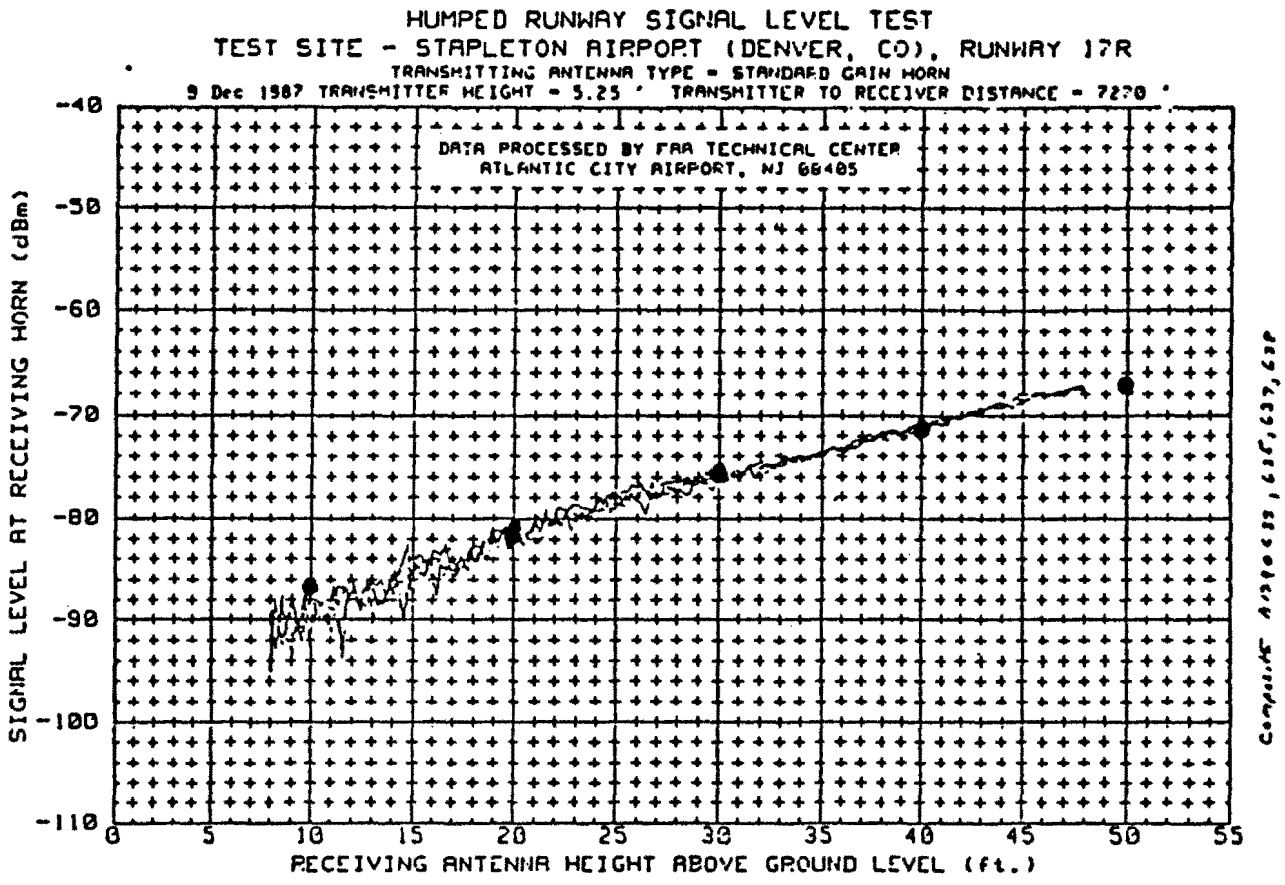
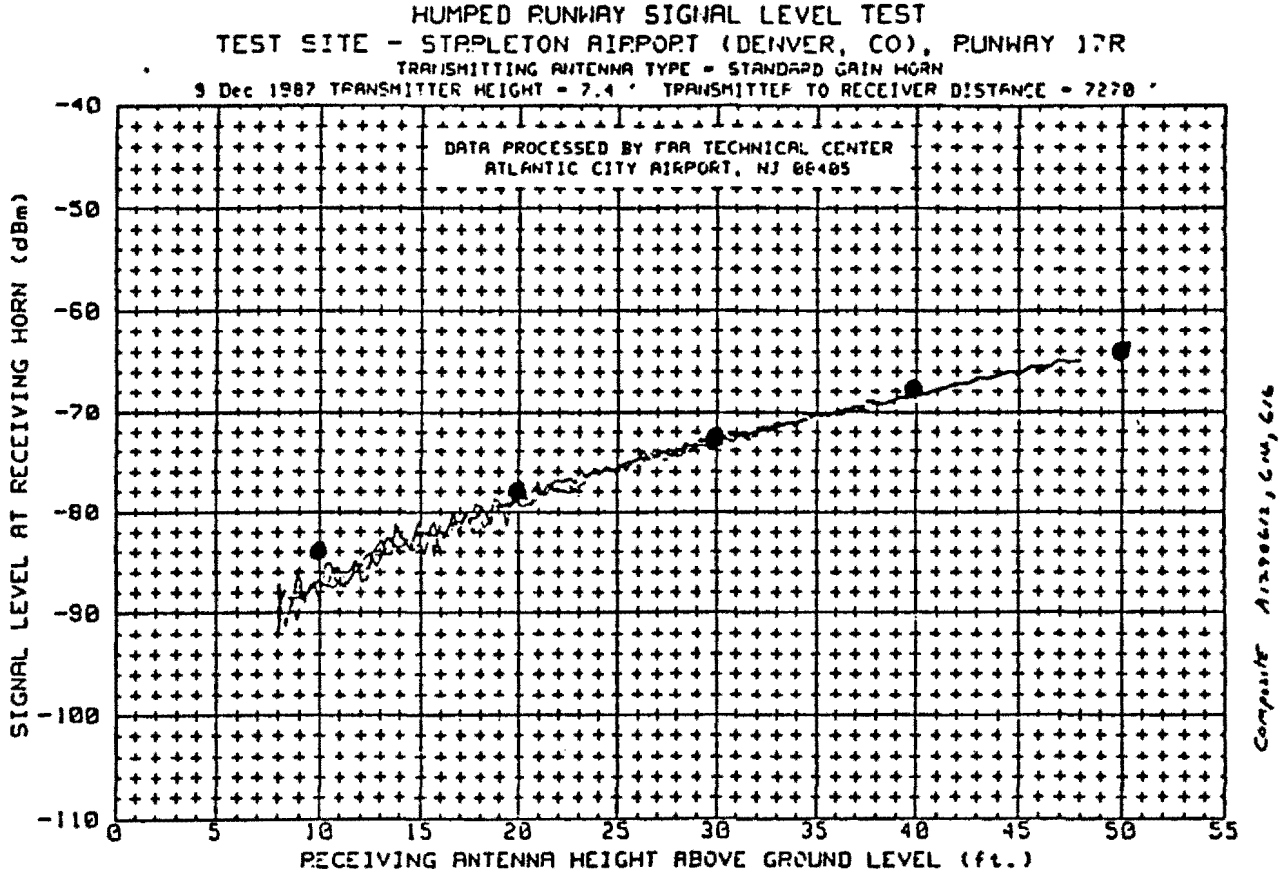
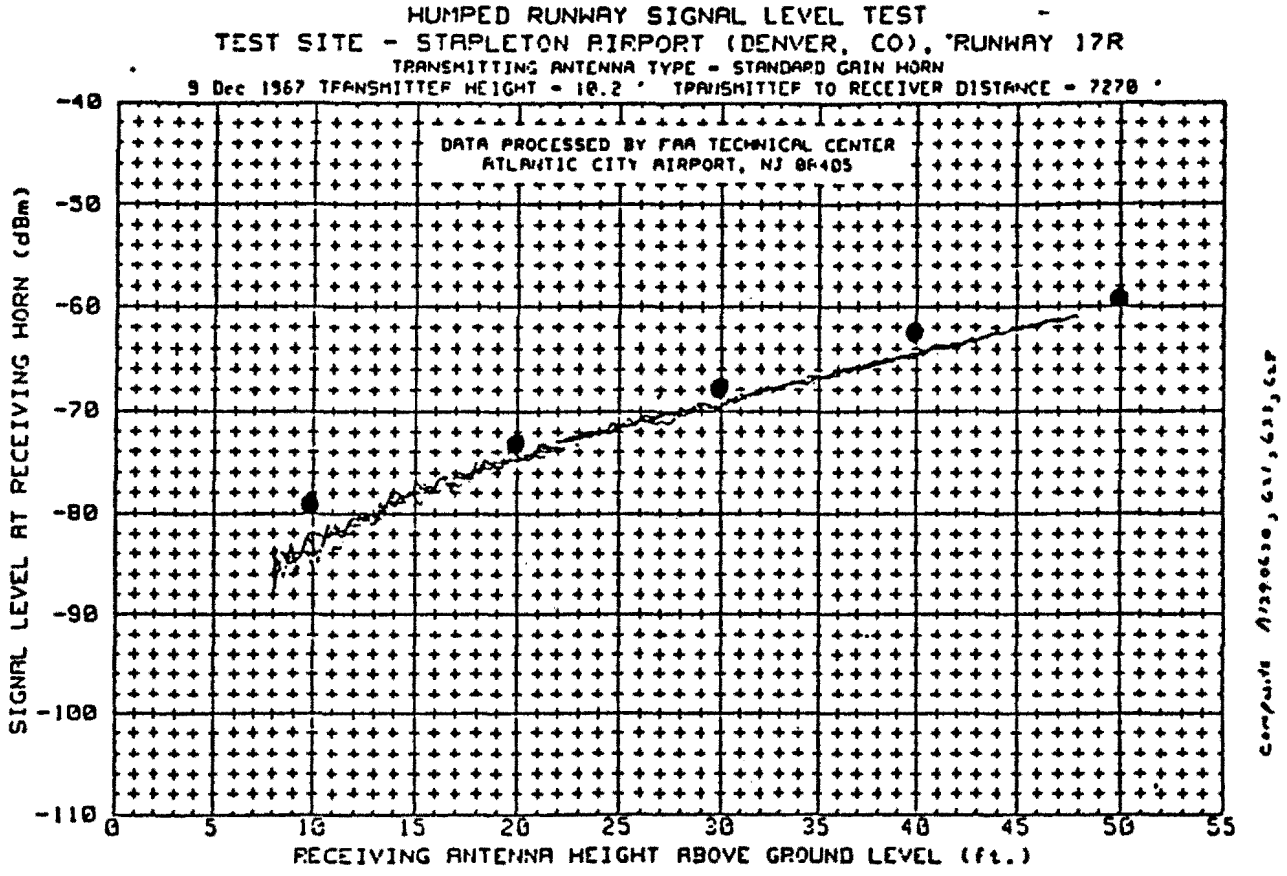


Figure 3. Comparison of Measurements and Computations, Phase Center MSL = 5293 Ft., A/T Distance = 7270 Ft.



● COMPUTED POINT

Figure 4. Comparison of Measurements and Computations, Phase Center MSL = 5295 Ft., A/T Distance = 7270 Ft.



● COMPUTED POINT

Figure 5. Comparison of Measurements and Computations, Phase Center MLS = 5298 Ft., A/T Distance = 7270 Ft.

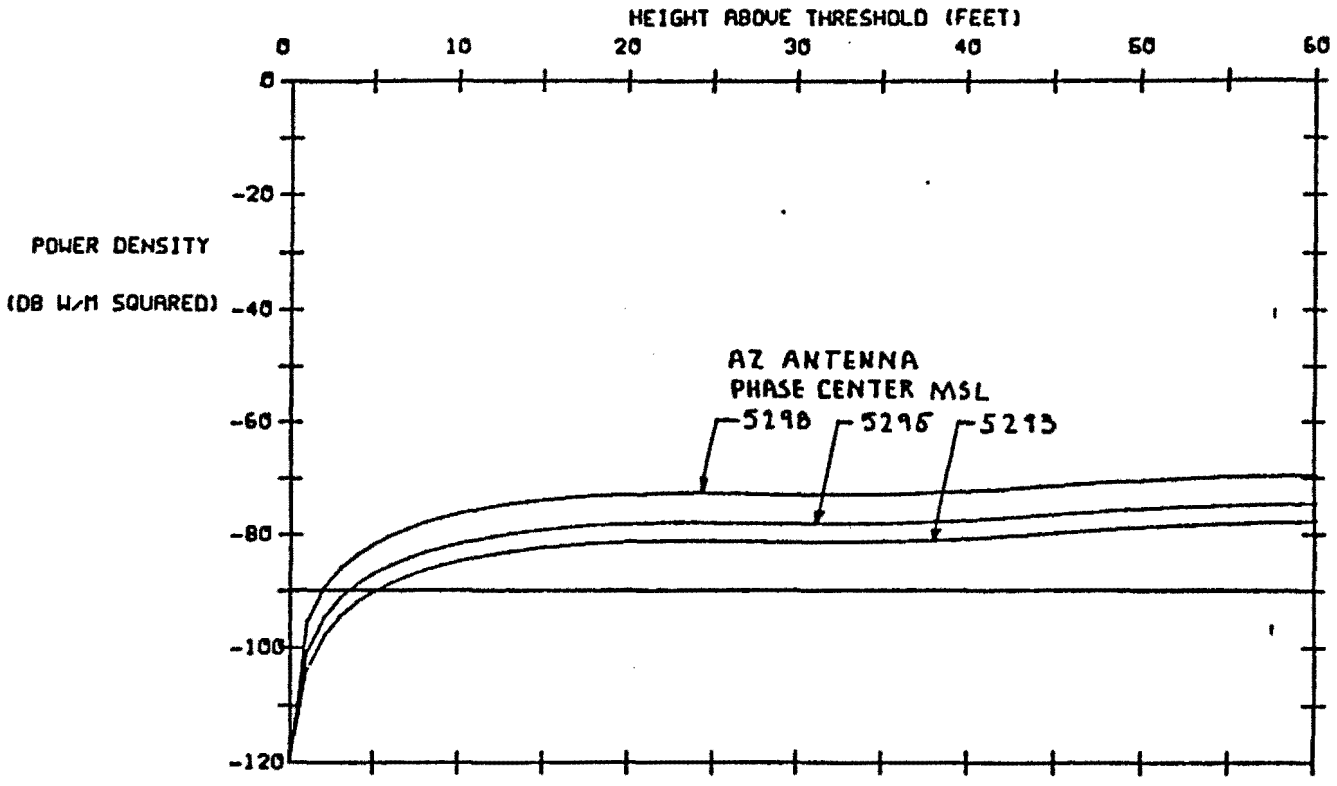


Figure 6. Computed Power Density Above Threshold, PT4

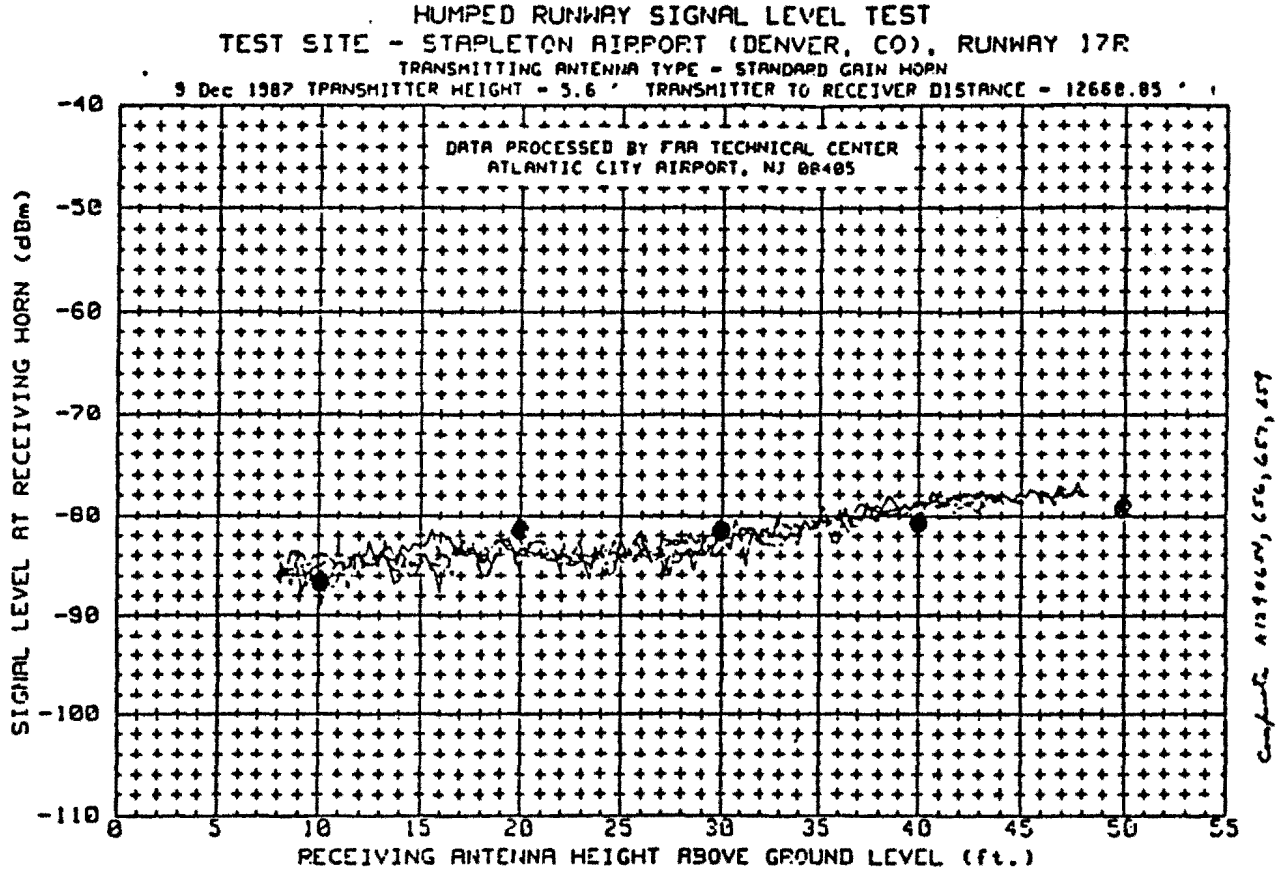


Figure 7. Comparison of Measurements and Computations, Phase Center MSL = 5293 Ft., A/T Distance = 12670 Ft.

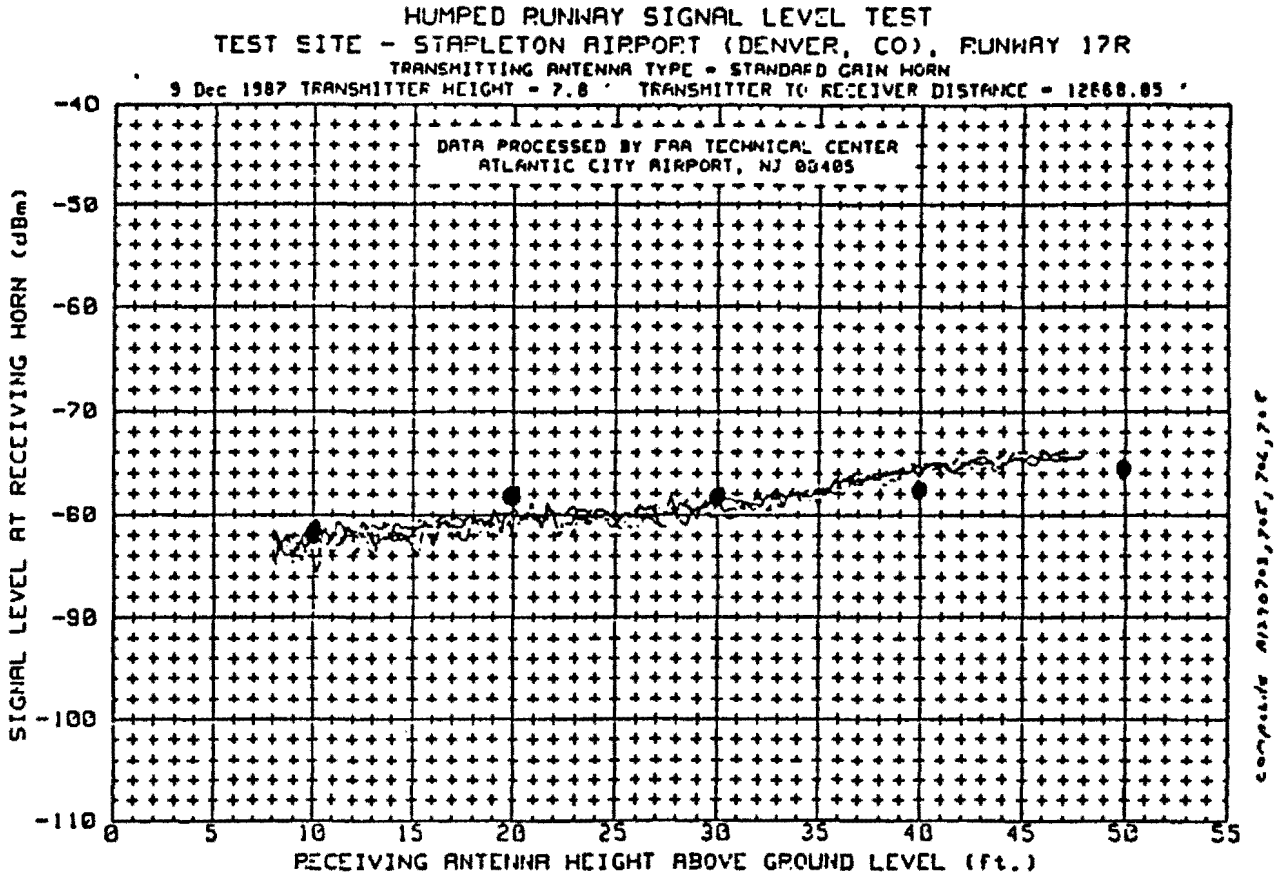
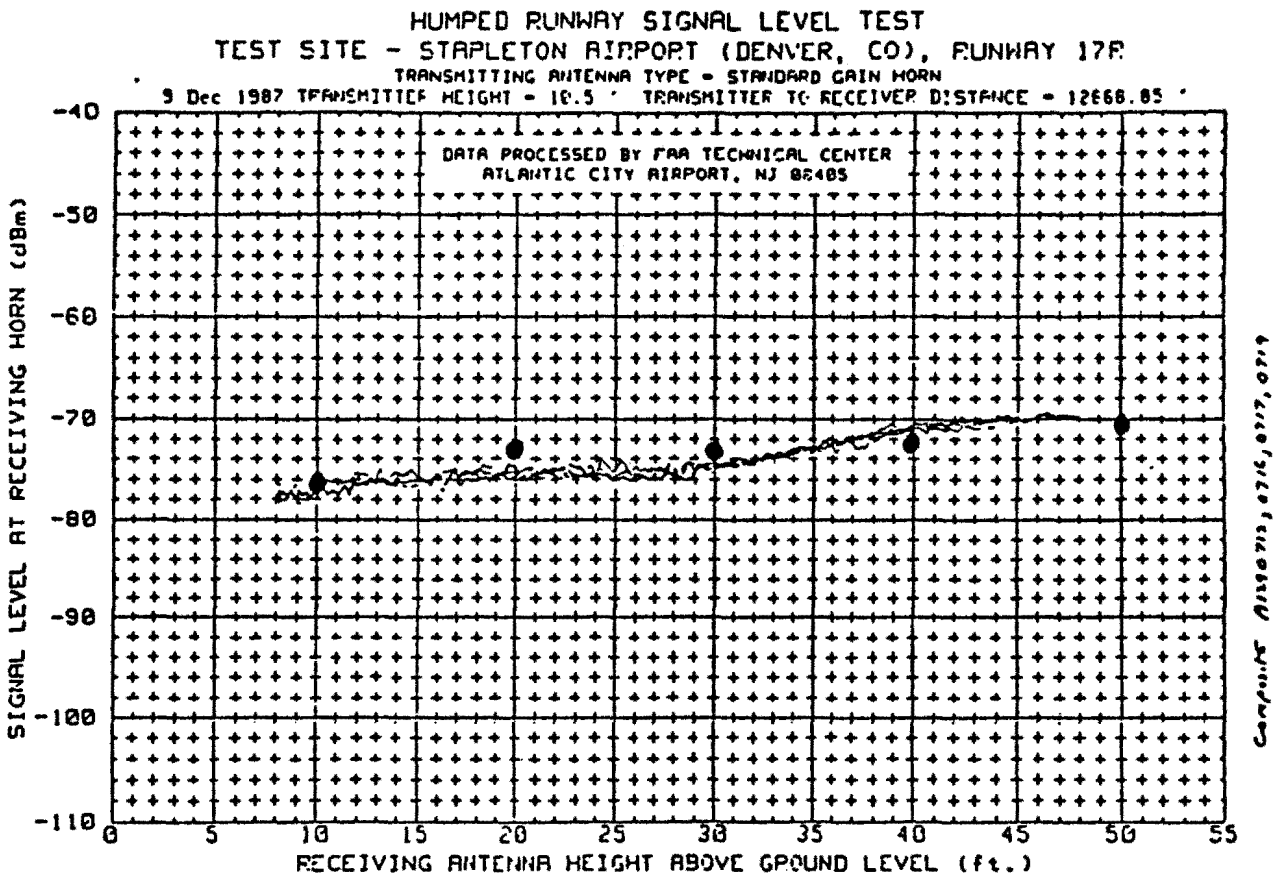
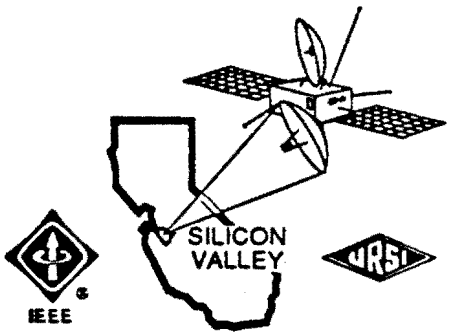


Figure 8. Comparison of Measurements and Computations, Phase Center MSL = 5295 Ft., A/T Distance = 12670 Ft.



● COMPUTED POINT

Figure 9. Comparison of Measurements and Computations, Phase Center MSL = 5298 Ft., A/T Distance = 12670 Ft.



San Jose, CA

1989
IEEE Antennas and Propagation Society
International Symposium and
URSI National Radio Science Meeting
June 26 - 30

ESTIMATING POWER DENSITY ABOVE RUNWAYS WITH COMPLEX CENTERLINE PROFILES

ALFRED R. LOPEZ
HAZELTINE CORPORATION
COMMACK, N.Y. 11725

I. INTRODUCTION

A method, which has special application to the Microwave Landing System, has been developed for estimating power density above runways with complex centerline profiles. The method uses a building block approach where the fundamental flat ground model is augmented with factors which account for the attenuation attributed to the particular centerline profile features. This paper is actually a sequel to the paper "Application of Wedge Diffraction Theory to Estimating Power Density at Airport Humped Runways" [1]. Application of a single wedge surface, as described in the above paper, proved to be adequate for estimating power density at several airport runways. However, at several other runways the centerline profile complexity was such that the single wedge surface proved to be inadequate.

II. THE WEDGE FACTOR METHOD

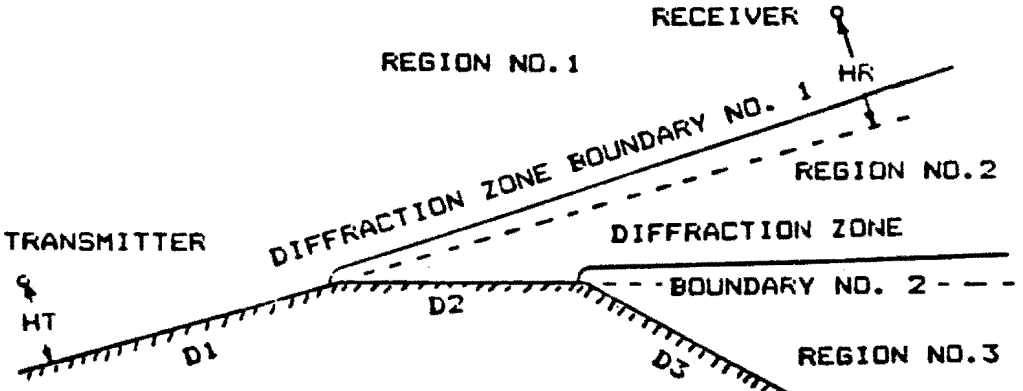
The above referenced paper has shown that if the receiver is near or in the shadow region then the power density can be expressed as a product of the flat ground power density and a wedge factor. For the case of multiple wedges, diffraction from the first wedge excites the second wedge which in turn excites the third wedge and so on. A simple method for estimating the power density in the shadow region is to compute the flat ground case and multiply the result by a factor for each applicable wedge. Figure 1. presents the basic concept. An example is given below for the case of Denver Runway 17R (see Fig. 2) with the receiver 10 ft above the threshold. The wedge factors 1,2 and 3 can be determined by locating the transmitter at heights of HT, 1 and 1 ft. above points 0, 1 and 2 and the receiver at heights of 1, 1 and 10 ft. above points 2, 3 and 4. respectively, and executing the Figure 4 program for the actual and flat ground cases for each of the three wedges.

Factor	Units	Transmitter MSL (ft) 5293	5295	5298
Transmitter power	dB W	13	13	13
Antenna gain	dB	8	8	8
$4\pi/\lambda^2$	dB $1/m^2$	35.5	35.5	35.5
$(HT/R)^2$	dB	-65.1	-63.0	-60.5
$(HR/R)^2$	dB	-62.1	-62.1	-62.1
Wedge No. 1	dB	-14.0	-13.0	-10.8
Wedge No. 2	dB	-11.9	-11.9	-11.9
Wedge No. 3	dB	12.0	12.0	12.0
Power density	dB W/m^2	-84.6	-81.5	-76.3

It should be noted in the table above that the Wedge No. 3 factor is positive. This is because the wedge angle is inverted (i.e. a concave surface). The computer program presented in [1] is modified as indicated in Figure 4 to handle this special case (lines with numbers that do not end with 0 are new; lines 590 and 600 have been changed). Continuous plots of power density versus height above threshold (see Figure 2) where obtained by locating a source above Point No.2 such that the power density was equal to the value computed for the receiver at the 10 ft height. This height was then used as input to the computer program (Figure 4) to generate the plots.

Measurements were made by a team of FAA and Hazeltine personnel at Denver during the period Dec. 7-11, 1987 [2]. A sample of the measurement results are shown in Figure 3. Included are estimated points based on the method presented above. Good agreement is observed.

REFERENCES:
1. A.R. Lopez, "Application of Wedge Diffraction Theory to Estimating Power Density at Airport Humped Runways", IEEE AP Trans., Vol. ap-35, No. 6, June 1987.
2. J.D. Jones, "MLS Signal Strength Measurements and MLS Mathematical Modeling of Runway 17R Hump at Denver Colorado Stapleton Airport", FAA Technical Center Report CT-140-88-9, May 1988.



REGION NO.	POWER DENSITY	
1	$P1 = P*G*(4\pi/\lambda^2)*(HT/R)^2*(HR/R)^2$	R=D1+D
2	$P2 = P1*A1$	R=D1+D2+D
3	$P3 = P1*A1*A2$	R=D1+D2+D3+D

WHERE: P = TRANSMITTER POWER
G = TRANSMITTER GAIN
λ = FREE SPACE WAVELENGHT
D = DISTANCE ALONG EXTENDED WEDGE SURFACE
A1 = WEDGE NO.1 ATTENUATION FACTOR
A2 = WEDGE NO.2 ATTENUATION FACTOR

FIGURE 1. ESTIMATING POWER DENSITY ABOVE RUNWAYS WITH COMPLEX RUNWAY CENTERLINES

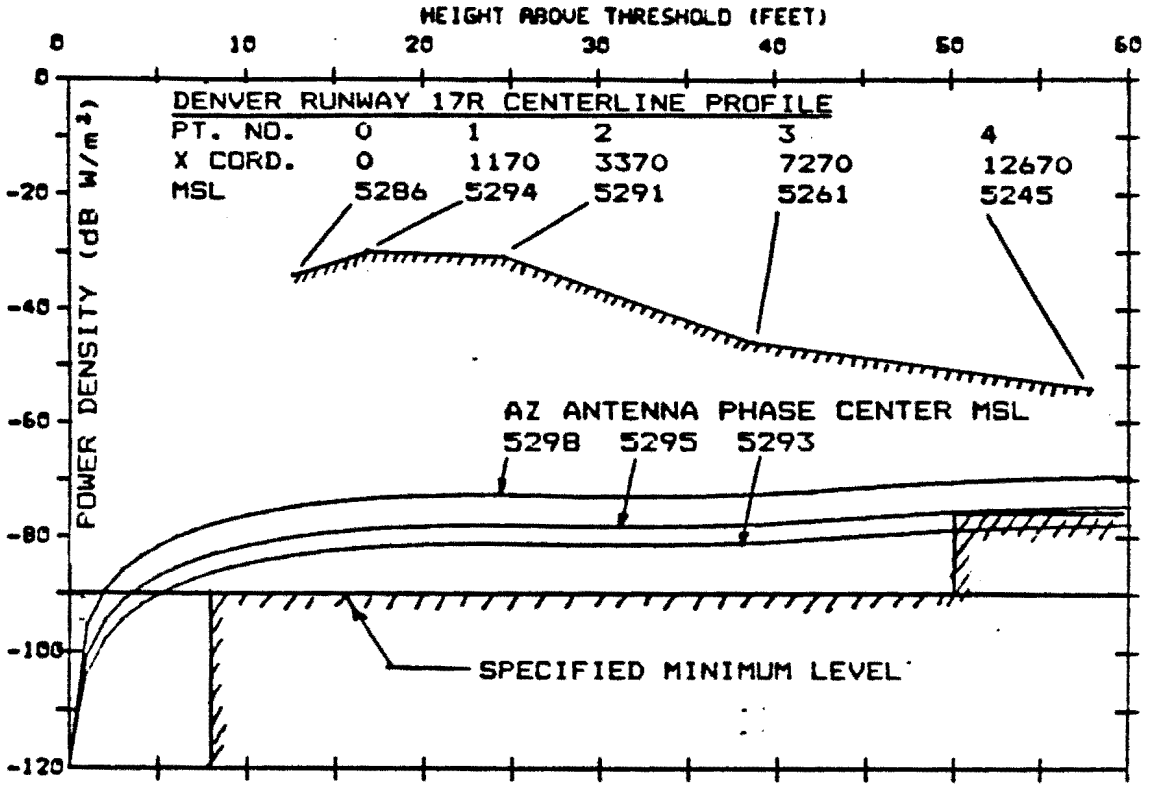


FIGURE 2. COMPUTED POWER DENSITY ABOVE THRESHOLD (POINT NO.4) OF DENVER RUNWAY 17R

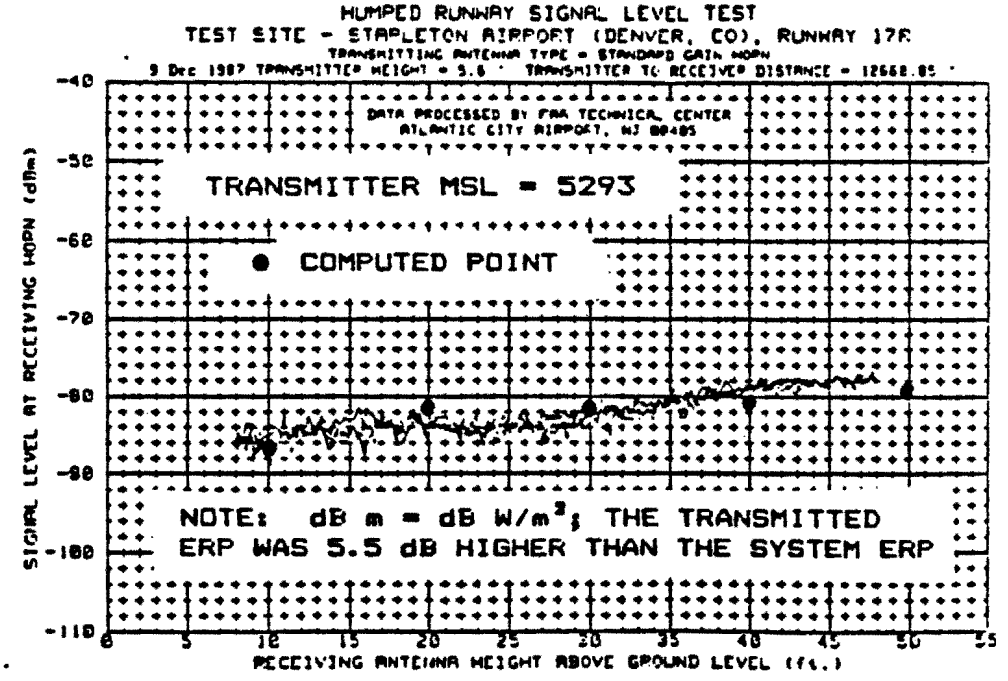


FIGURE 3. COMPARISON OF MEASUREMENTS AND COMPUTATIONS

```
100 DATA 2,0,4000,10,8000,0,.2,13,8,1.215
110 READ ZT,Z1,X2,Z2,X3,Z3,WL,DBW,DBG,VPF
120 INPUT "RECEIVER COORDINATES X,Z = ";XR,ZR
130 PI=4*ATN(1)
140 THETA1=ATN((Z2-ZT)/X2)
150 D2=SQR((ZR-Z2)^2+(XR-X2)^2):D1=SQR((Z2-ZT)^2+X2^2)
160 D3=SQR((ZR-ZT)^2+XR^2)
170 ALPHA=ATN((Z2-Z1)/X2)-THETA1
180 BETA=ATN((Z2-Z3)/(X3-X2))+THETA1
190 ZI=Z2-D1*SIN(2*ALPHA+THETA1):XI=X2-D1*COS(2*ALPHA+THETA1)
200 ZI2=Z2+D1*SIN(2*BETA-THETA1):XI2=X2-D1*COS(2*BETA-THETA1)
203 ZI3=Z2+D1*SIN(2*BETA+2*ALPHA-THETA1):XI3=X2-D1*COS(2*BETA+2*ALPHA-THETA1)
210 D4=SQR((ZR-ZI)^2+(XR-XI)^2)
220 D5=SQR((ZR-ZI2)^2+(XR-XI2)^2)
224 D6=SQR((ZR-ZI3)^2+(XR-XI3)^2)
230 PHE=ATN((ZR-ZT)/XR)-THETA1
240 IF XR>X2 THEN GAMMA=ATN((ZR-Z2)/(XR-X2))
250 IF XR<X2 THEN GAMMA=ATN((ZR-Z2)/(XR-X2))+PI
260 IF XR=X2 THEN GAMMA=PI/2
270 THETA=GAMMA-THETA1
280 W=VPF*PHE*45/ATN(1):GOSUB 650:V1=1+.8*TANH
290 PHE2=ATN((ZR-ZI)/(XR-XI))-THETA1-2*ALPHA
300 PHE3=ATN((ZR-ZI2)/(XR-XI2))+2*BETA-THETA1
304 PHE4=ATN((ZR-ZI3)/(XR-XI3))+2*BETA+2*ALPHA-THETA1
310 W=VPF*PHE2*45/ATN(1):GOSUB 650:V2=1-.8*TANH
320 W=VPF*PHE3*45/ATN(1):GOSUB 650:V3=1-.8*TANH
324 W=VPF*PHE4*45/ATN(1):GOSUB 650:V4=1+.8*TANH
330 D3P=D1*2*(SIN(PHE/2))^2+D2*2*(SIN((THETA-PHE)/2))^2
340 D4P=D1*2*(SIN(PHE2/2))^2+D2*2*(SIN((THETA-2*ALPHA-PHE2)/2))^2
350 D5P=D1*2*(SIN(PHE3/2))^2+D2*2*(SIN((THETA+2*BETA-PHE3)/2))^2
354 D6P=D1*2*(SIN(PHE4/2))^2+D2*2*(SIN((THETA+2*BETA+2*ALPHA-PHE4)/2))^2
360 SN1=SGN(THETA):IF SN1=0 THEN SN1=1
370 SN2=SGN(THETA-2*ALPHA):IF SN2=0 THEN SN2=1
380 SN3=SGN(-THETA-2*BETA):IF SN3=0 THEN SN3=1
390 SN4=SGN(-THETA-2*ALPHA-2*BETA):IF SN4=0 THEN SN4=1
400 E1R=(D1+D2)*V1*(.5+.5*SN1)*COS(2*PI*D3P/WL)/D3
410 E1I=(D1+D2)*V1*(.5+.5*SN1)*SIN(2*PI*D3P/WL)/D3
420 E2R=(D1+D2)*V2*(.5+.5*SN2)*COS(2*PI*D4P/WL)/D4
430 E2I=(D1+D2)*V2*(.5+.5*SN2)*SIN(2*PI*D4P/WL)/D4
440 E3R=(D1+D2)*V3*(.5+.5*SN3)*COS(2*PI*D5P/WL)/D5
450 E3I=(D1+D2)*V3*(.5+.5*SN3)*SIN(2*PI*D5P/WL)/D5
452 E4R=(D1+D2)*V4*(.5+.5*SN4)*COS(2*PI*D6P/WL)/D6
454 E4I=(D1+D2)*V4*(.5+.5*SN4)*SIN(2*PI*D6P/WL)/D6
460 D=D1*D2/(D1+D2)
470 FOR K= 1 TO 4
480 IF K=1 THEN THET=THETA:SN=SN1:GOTO 520
490 IF K=2 THEN THET=THETA-2*ALPHA:SN=SN2:GOTO 520
500 IF K=3 THEN THET=-THETA-2*BETA:SN=SN3:GOTO 520
510 IF K=4 THEN THET=-THETA-2*ALPHA-2*BETA:SN=SN4
520 V=2*PI*SQR(D/WL)*SIN(THET/2):V=ABS(V)
530 IF V=0 THEN E3R(K)=.5:E3I(K)=0:GOTO 580
540 W=V:GOSUB 650:TANH1=TANH
550 W=V/2.4:GOSUB 650:TANH2=TANH
554 IF V<.00001 THEN E3R(K)=.5*SN*COS(PI*TANH2/4):GOTO 564
560 E3R(K)=(TANH1/2/V-V>EXP(-1.5*V)/4)*SN*COS(PI*TANH2/4)
564 IF V<.00001 THEN E3I(K)=.5*SN*SIN(PI*TANH2/4):GOTO 580
570 E3I(K)=(TANH1/2/V-V*EXP(-1.5*V)/4)*SN*SIN(-PI*TANH2/4)
580 NEXT K
590 ER=E1R-E2R-E3R+E4R-E3R(1)+E3R(2)+E3R(3)-E3R(4)
600 EI=E1I-E2I-E3I+E4I-E3I(1)+E3I(2)+E3I(3)-E3I(4)
610 P=(ER^2+EI^2)/4/PI/(D1+D2)^2
620 IF P=0 THEN DBP=-1000 ELSE DBP=10*LOG(P)/LOG(10)
630 DBWM2=DBP+DBW+DBG+10.8
640 PRINT "X = "XR,"Z = "ZR,"DB W/M^2 = "DBWM2:END
650 IF W>10 THEN TANH=1:GOTO 680
660 IF W<-10 THEN TANH=-1:GOTO 680
670 TANH=(EXP(W)-EXP(-W))/(EXP(W)+EXP(-W))
680 RETURN
```

FIGURE 4. REVISED HUMPRWY PROGRAM, INVERTED HUMP CAPABILITY

KENT CHAMBERLIN
UNIVERSITY OF NEW HAMPSHIRE

RUNWAY HUMP SHADOWING

Runway Hump Modeling at the University of New Hampshire

Dr. Kent Chamberlin

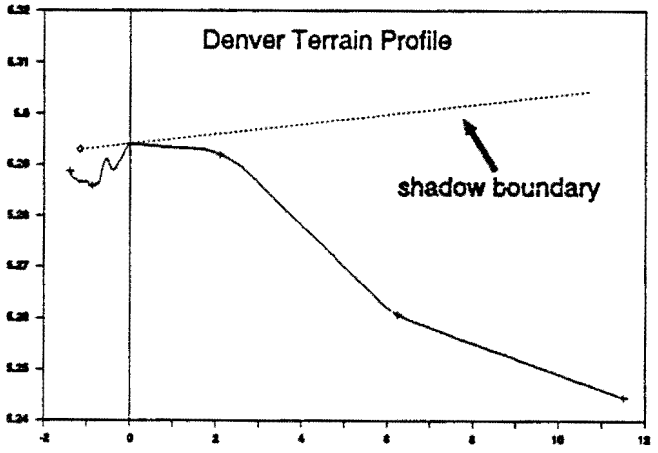
Major Accomplishments

- Implemented State-Of-The-Art Propagation Model (GELTI)
- Validated the Finite-Conductivity Diffraction Coefficient
- Developed a Prototype Terrain Linearization Computer Model
- Began Validation of Double-Edge Diffraction Coefficient

Today's Topics

* Comments on the modeling of high-frequency, short range, and shadowed propagation path loss. A qualitative evaluation of available modeling techniques
* A description of the GELTI propagation model
* Measured and modeled data comparisons
* An overview of diffraction theory
* Validation of the finite-conductivity diffraction coefficient
* Validation of the double-edge diffraction coefficient
* The Automated Terrain Linearization Model (ATLM)

Objective: To model path loss due to runway hump shadowing at MLS frequencies



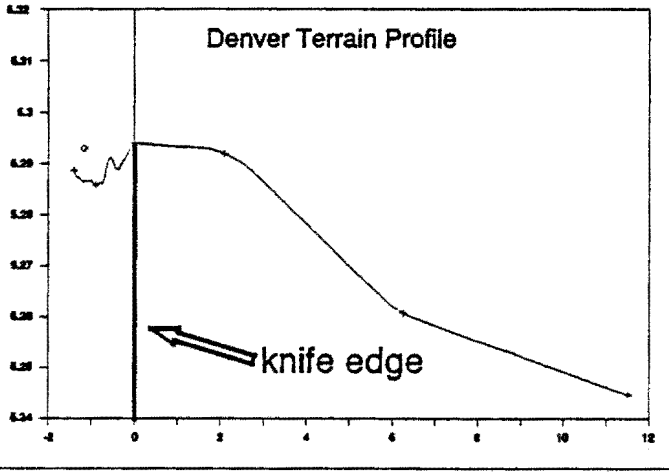
Desired Accuracy: ±2 dB.

Modeling path loss will involve some form of diffraction theory since propagation mechanism is due *primarily* to diffraction

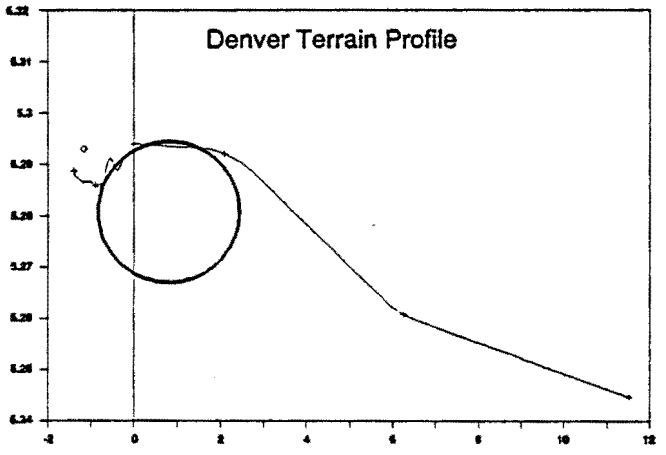
Commonly-Used Diffraction Models

Knife-Edge Diffraction
Wait-Conda Cylinder Scattering
Single-Edge Wedge Diffraction ⇒ GTD
Double-Edge Wedge Diffraction

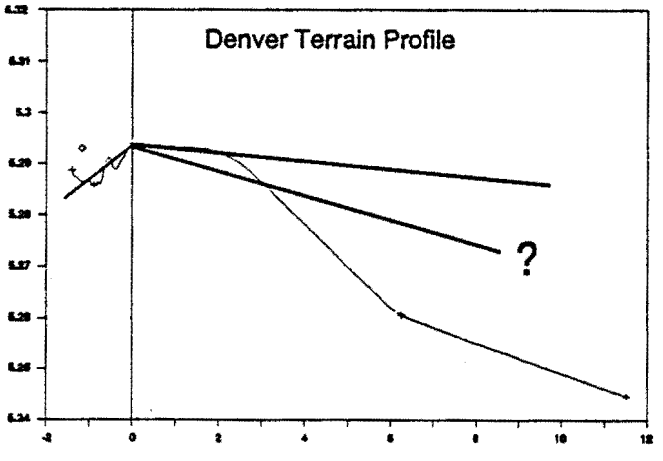
Knife-Edge Diffraction Assumes only mechanism affecting propagation is a single, **conducting edge**



Cylinder (Wait-Conda) Assumes that the only mechanism affecting propagation is a smooth, perfectly-conducting cylinder

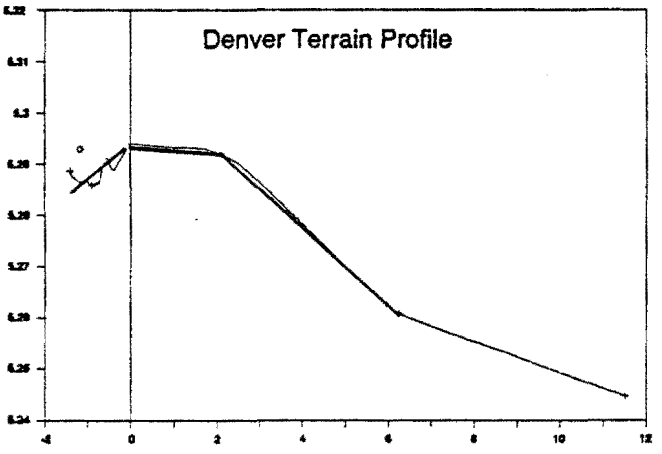


Single-Edge, Wedge Diffraction (GTD) assumes only factor affecting propagation is a single, smooth, perfectly-conducting wedge



Double-Edge Diffraction(GTD)

Accounts for 2 connected edges

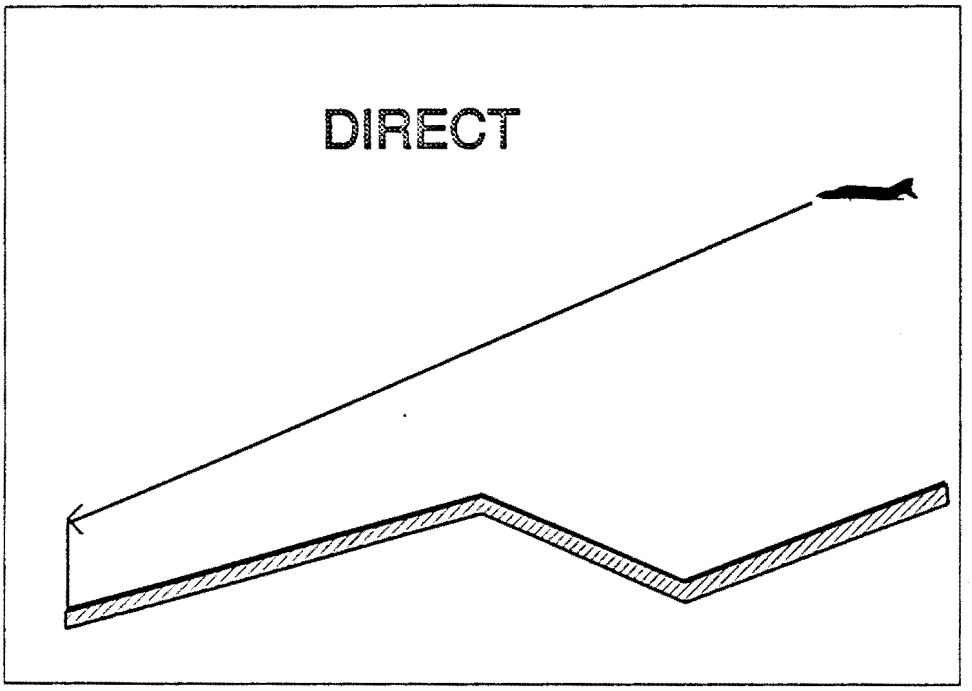


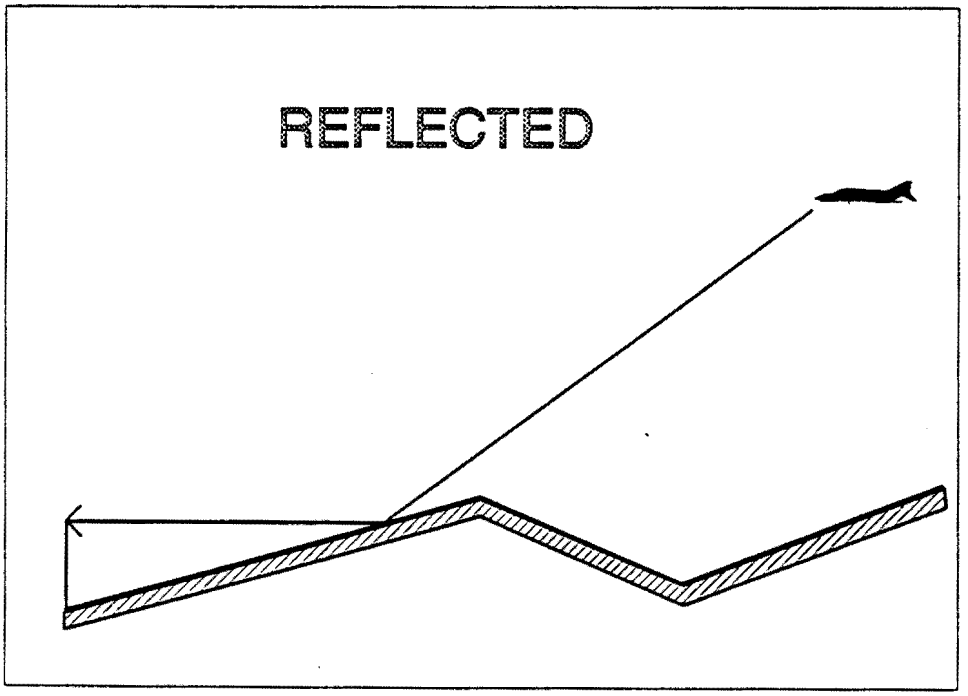
The GELTI Model

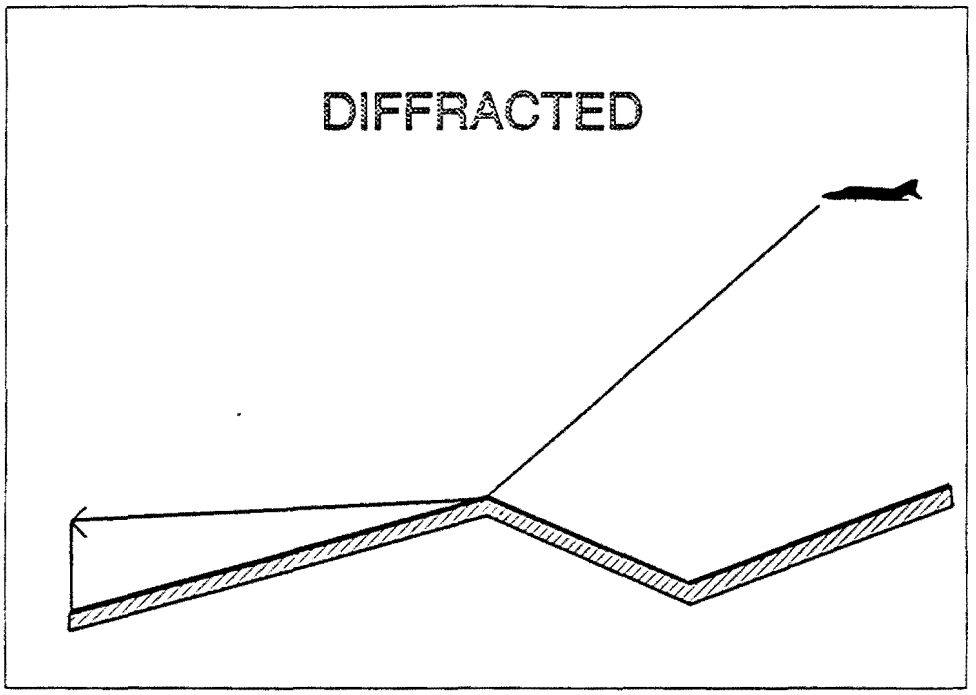
GTD Estimated Loss due to Terrain Interaction

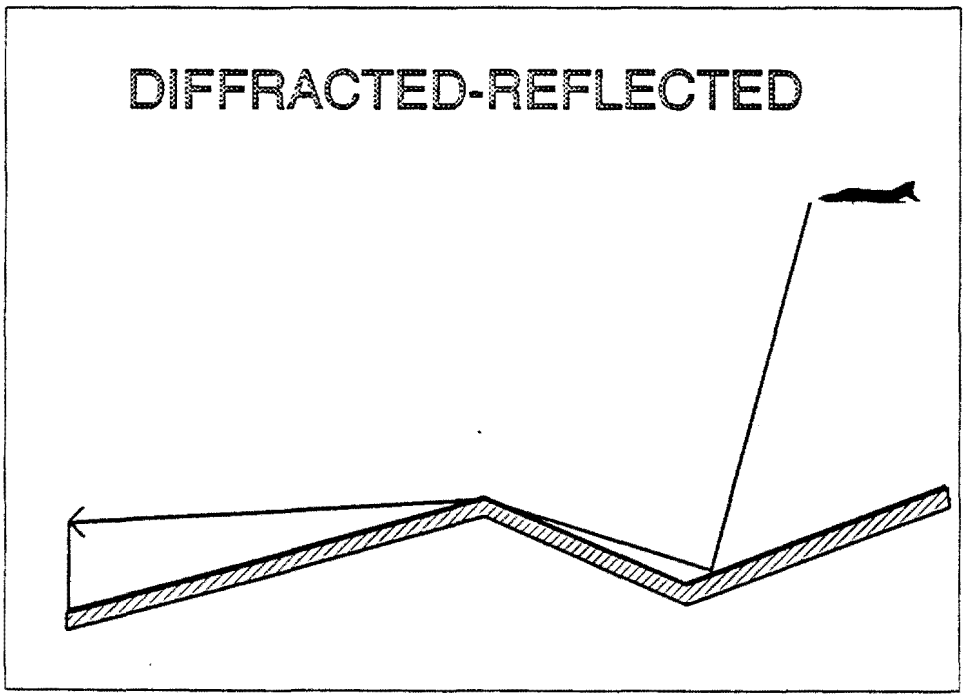
Features

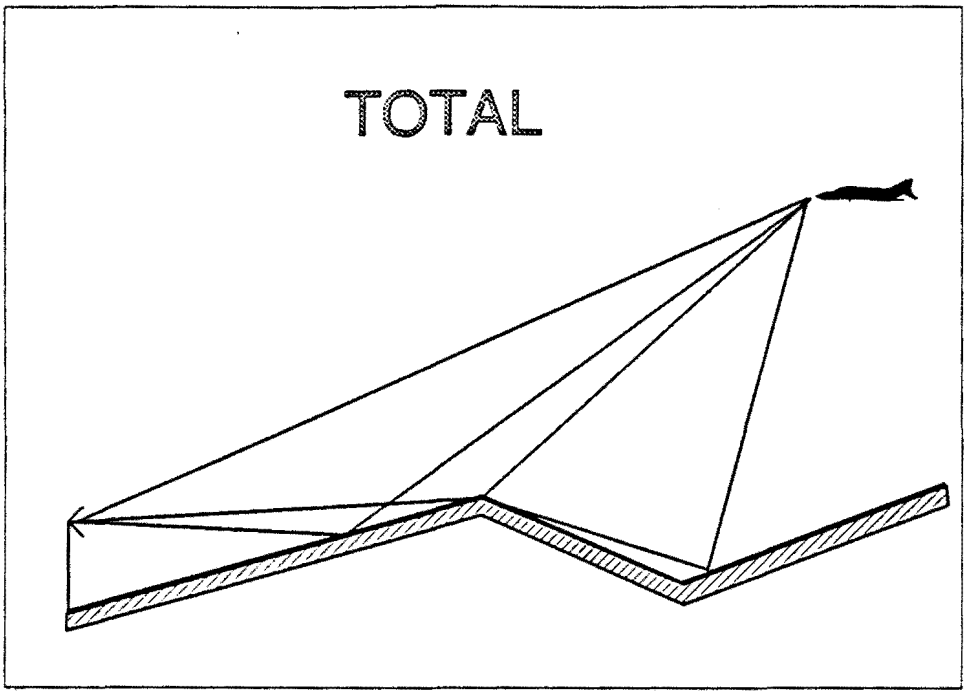
- Considers multiple propagation mechanisms (14 possible ray and ray combinations)
- **Accounts for finite-conductivity and local** surface roughness
- Calculates Double-Edge Diffraction

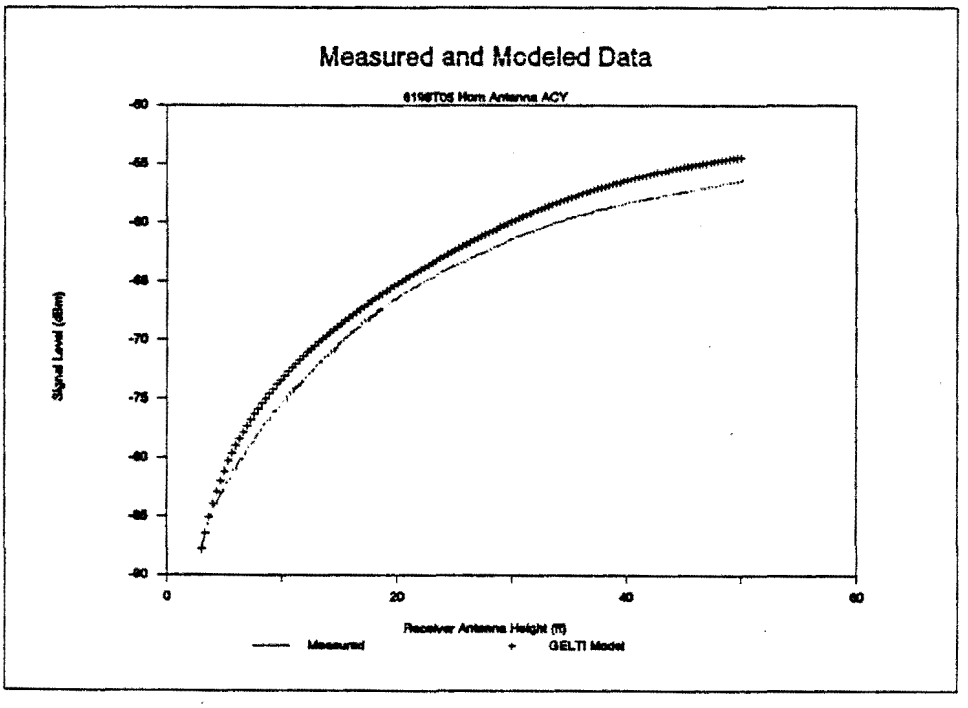

DIRECT

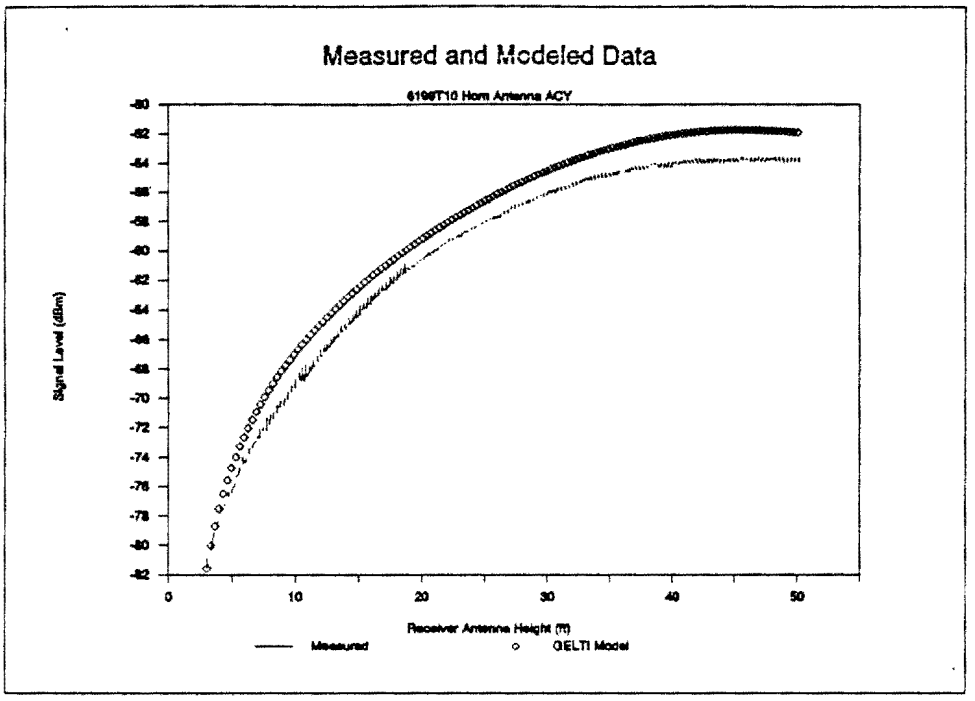

REFLECTED

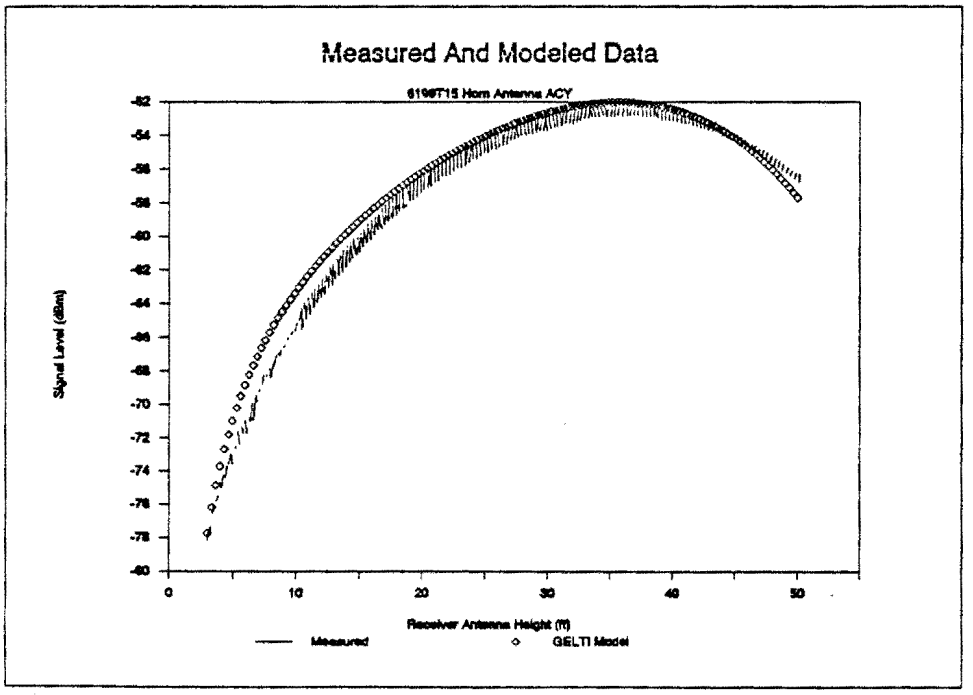

DIFFRACTED

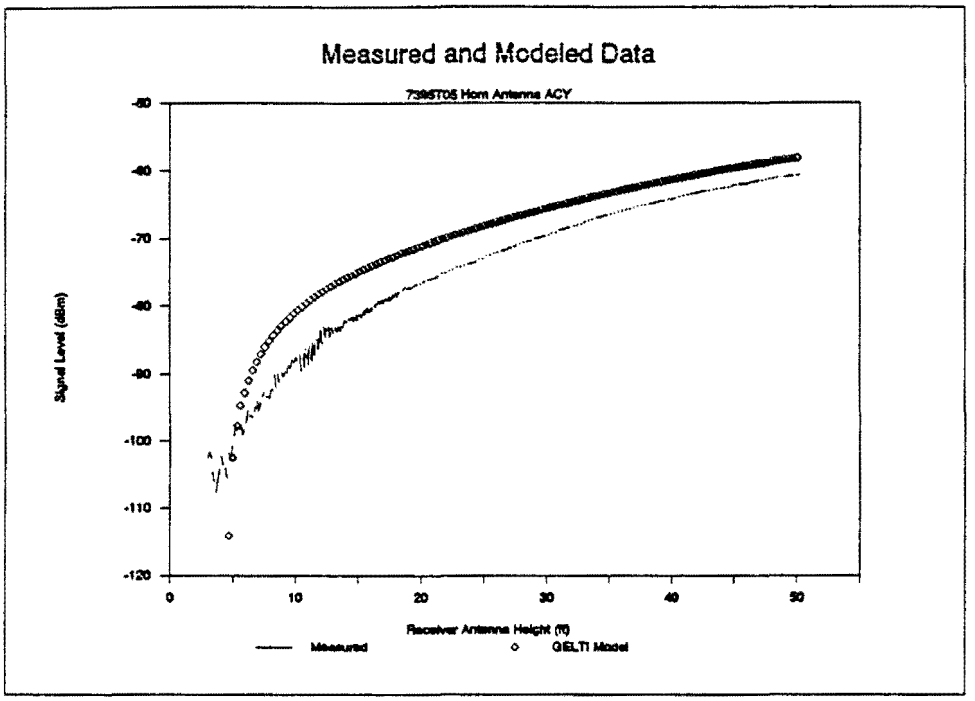

DIFFRACTED-REFLECTED

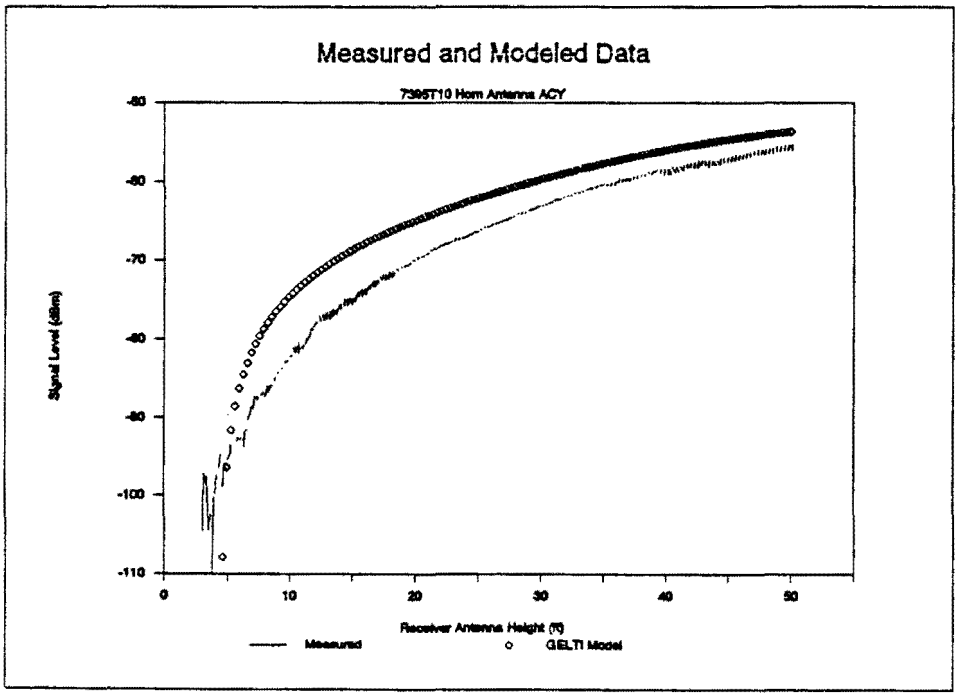

TOTAL

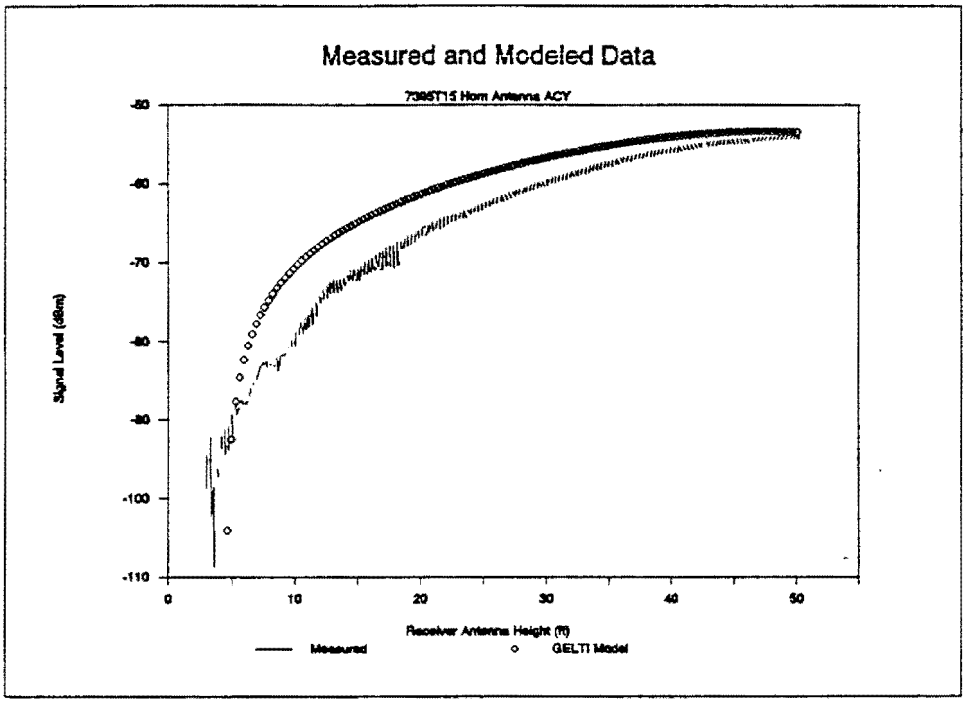

Measured and Modeled Data
619BT05 Horn Antenna ACY
Signal Level (dBm)
-50
-55
-60
-65
-70
-75
-80
-85
-90
0
20
40
60
Receiver Antenna Height (ft)
Measured
GELTI Model

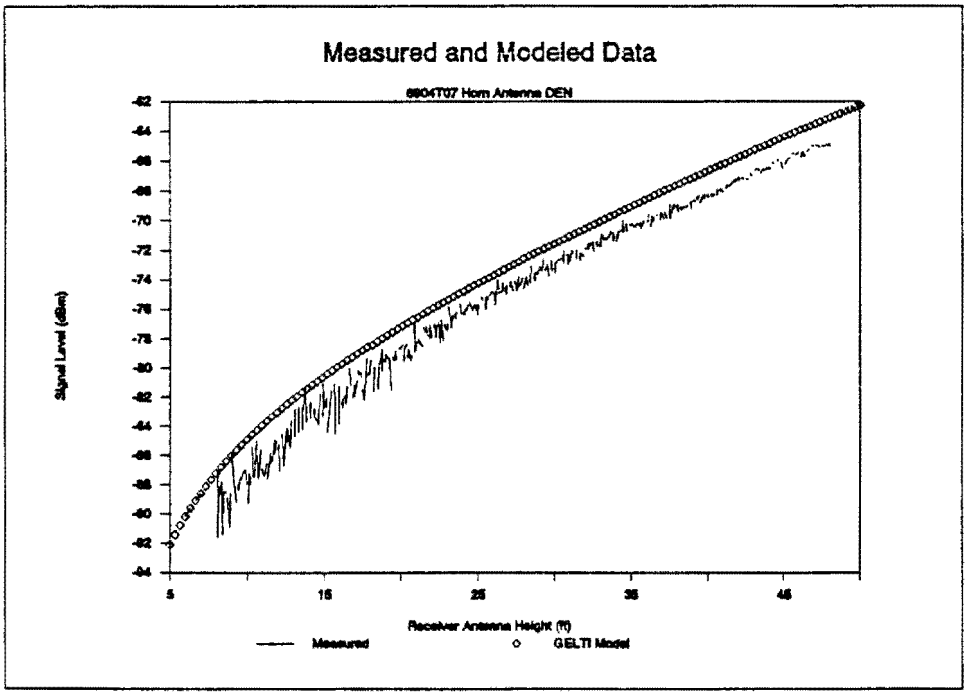

Measured and Modeled Data
6196T10 Horn Antenna ACY
Signal Level (dBm)
Receiver Antenna Height (ft)
Measured
GELTI Model

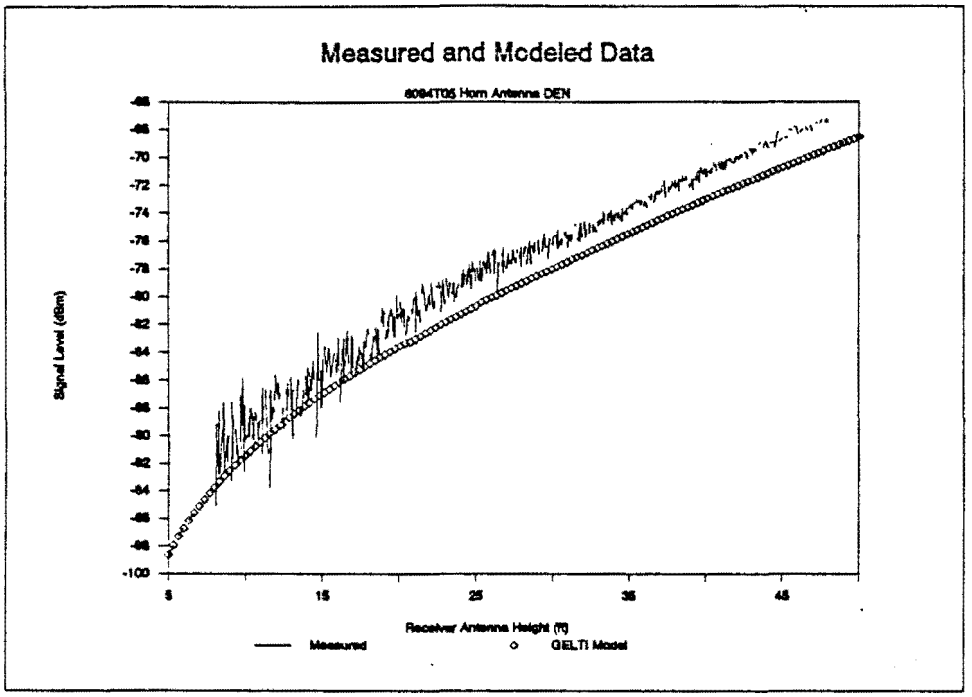

Measured And Modeled Data
6196T15 Horn Antenna ACY
Signal Level (dBm)
Receiver Antenna Height (ft)
Measured
GELTI Model

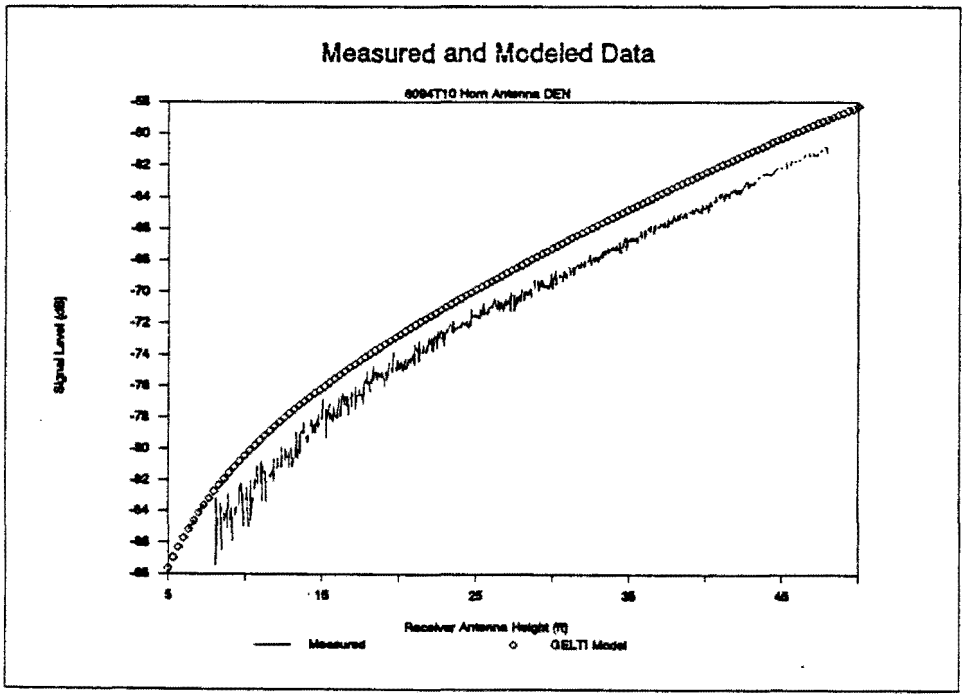

Measured and Modeled Data
7396T05 Horn Antenna ACY
Signal Level (dBm)
-60
-70
-80
-90
-100
-110
-120
0
10
20
30
40
50
Receiver Antenna Height (ft)
Measured
GELTI Model

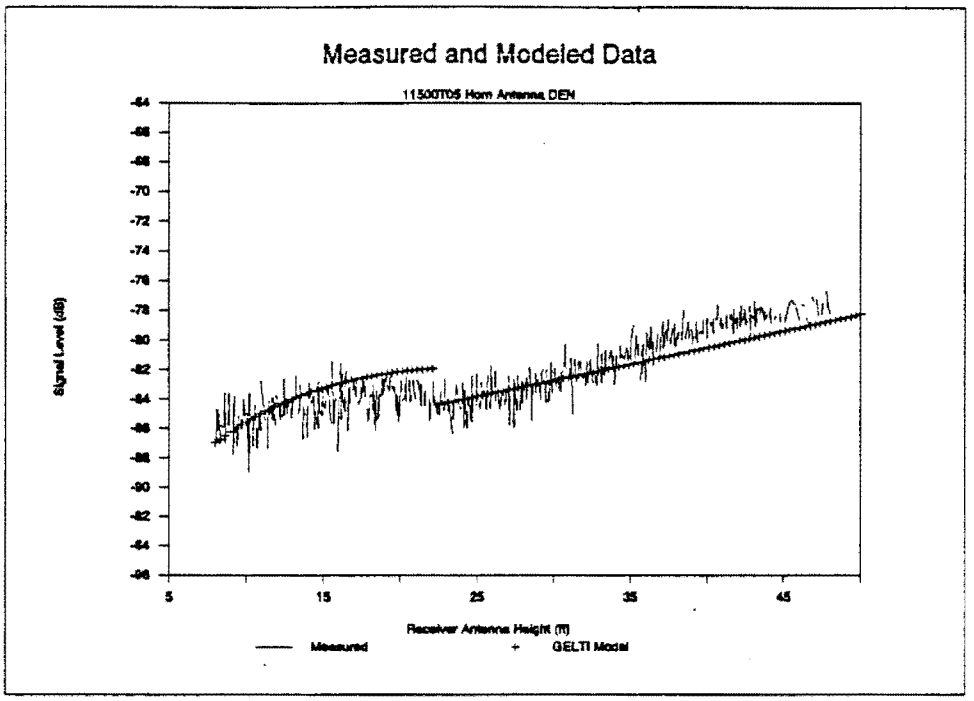

Measured and Modeled Data
7396T10 Horn Antenna ACY
Signal Level (dBm)
-60
-70
-80
-90
-100
-110
0
10
20
30
40
50
Receiver Antenna Height (ft)
Measured
GELTI Model

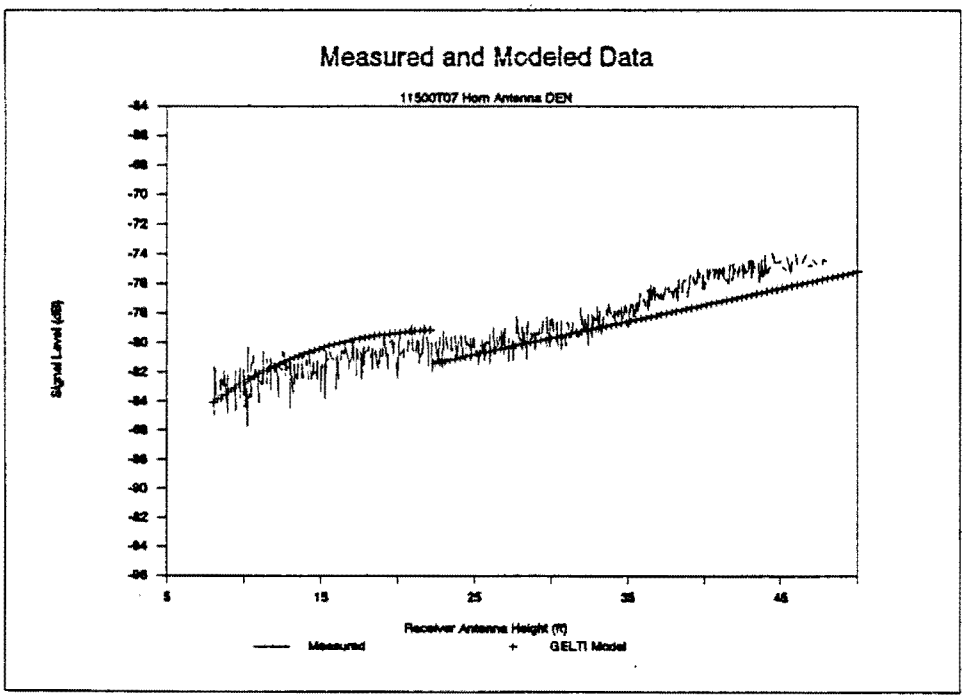

Measured and Modeled Data
7396T15 Horn Antenna ACY
Signal Level (dBm)
-50
-60
-70
-80
-90
-100
-110
0
10
20
30
40
50
Receiver Antenna Height (ft)
Measured
GELTI Model

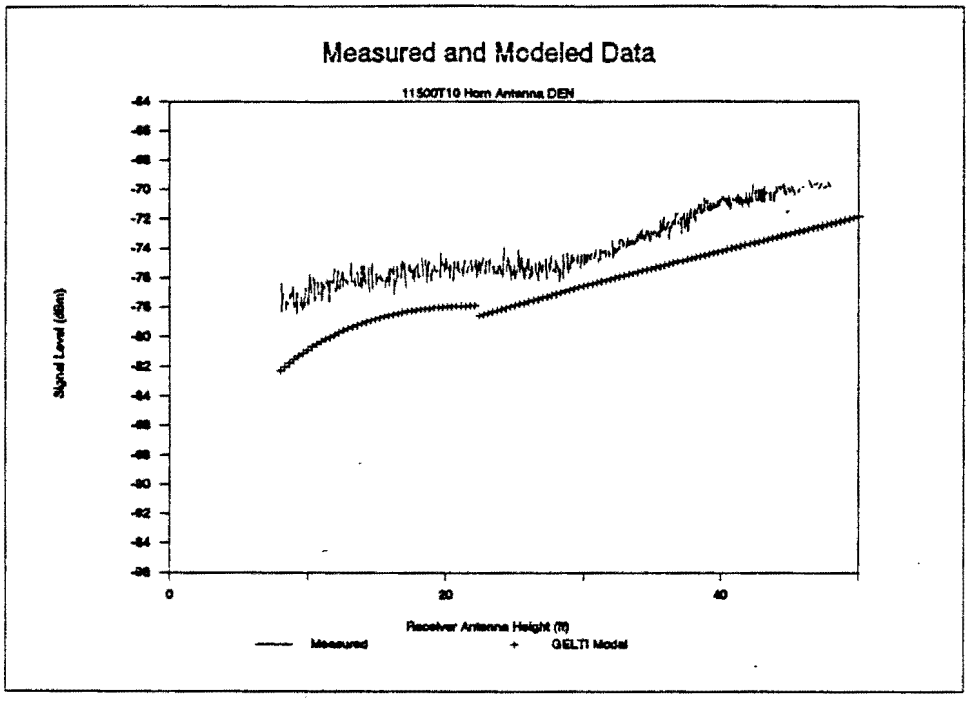

Measured and Modeled Data
6904T07 Horn Antenna DEN
Signal Level (dBm)
-42
-44
-66
-68
-70
-72
-74
-76
-78
-80
-82
-84
-86
-88
-90
-92
-94
5
15
25
35
45
Receiver Antenna Height (ft)
Measured
GELTI Model


Measured and Modeled Data
6094T05 Horn Antenna DEN
Signal Level (dBm)
-66
-68
-70
-72
-74
-76
-78
-80
-82
-84
-86
-88
-100
5
15
25
35
45
Receiver Antenna Height (ft)
Measured
GELTI Model


Measured and Modeled Data
6094T10 Horn Antenna DEN
Signal Level (dB)
-58
-60
-62
-64
-66
-68
-70
-72
-74
-76
-78
-80
-82
-84
-86
5
15
25
35
45
Receiver Antenna Height (ft)
Measured
GELTI Model

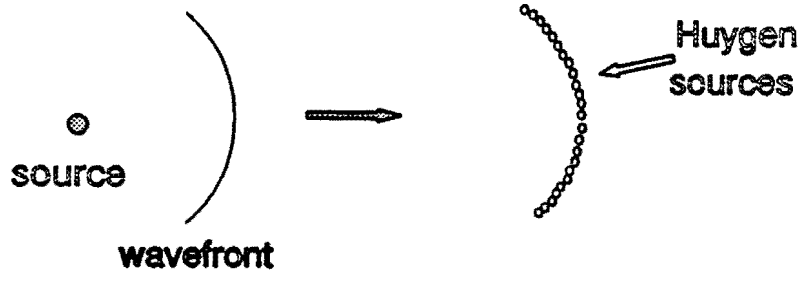

Measured and Modeled Data
11500T05 Horn Antenna DEN
Signal Level (dB)
-64
-66
-68
-70
-72
-74
-76
-78
-80
-82
-84
-86
-88
-90
-92
-94
-96
5
15
25
35
45
Receiver Antenna Height (ft)
Measured
GELTI Model


Measured and Modeled Data
11500T07 Horn Antenna DEN
Signal Level (dB)
-64
-66
-68
-70
-72
-74
-76
-78
-80
-82
-84
-86
-88
-90
-92
-94
-96
5
15
25
35
45
Receiver Antenna Height (ft)
Measured
GELTI Model



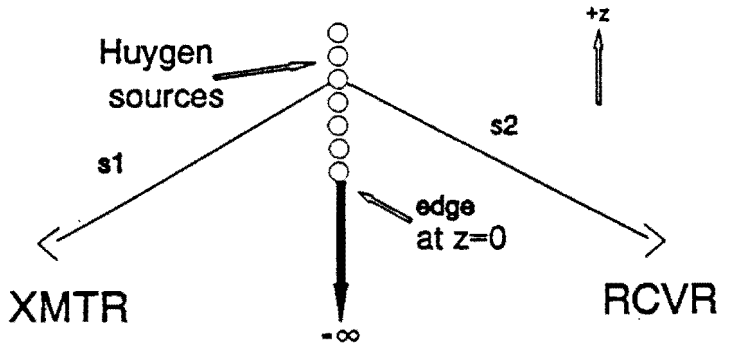
Diffraction Theory

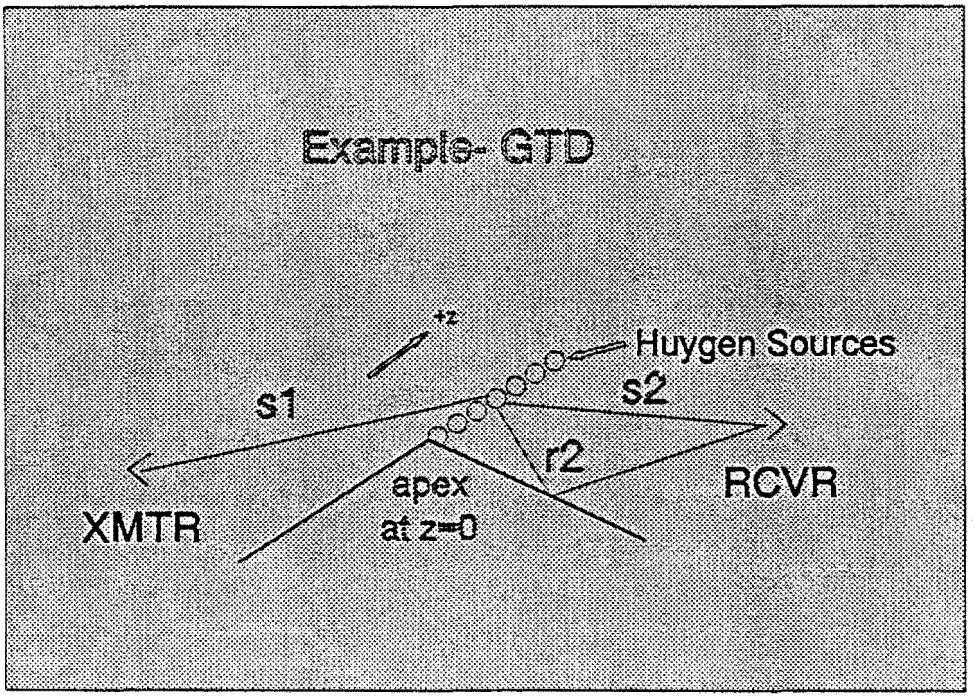
Huygen's Principle: Each point on a primary wave-front can be considered to be a new source of a secondary spherical wave, and that a secondary wave front can be constructed as the envelope of these secondary waves.



Both Knife-Edge Diffraction and GTD are based upon Huygen's Principle

Example: Knife-Edge Diffraction





Validation of the Finite Conductivity Diffraction Coefficient

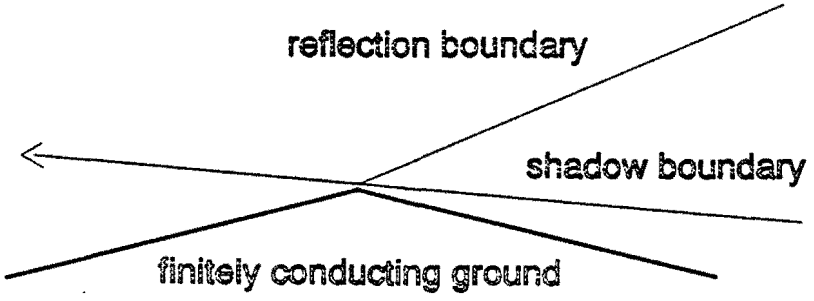
Objective: To verify that the heuristic diffraction coefficient used by GELTI for finitely-conducting, locally rough, terrain is correct

Approach: Implement a theoretically-correct numerical solution

Conclusion: It is correct

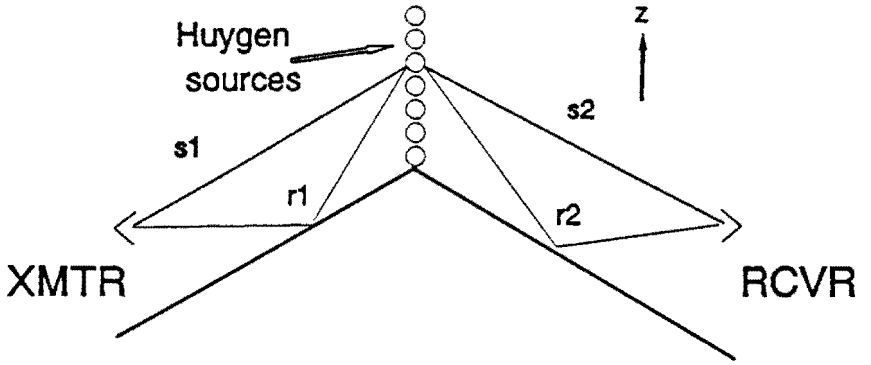
Heuristic approach- Scale diffraction coefficient so as to match reflected ray at reflection boundary and direct ray at shadow boundary

Provided improved model accuracy

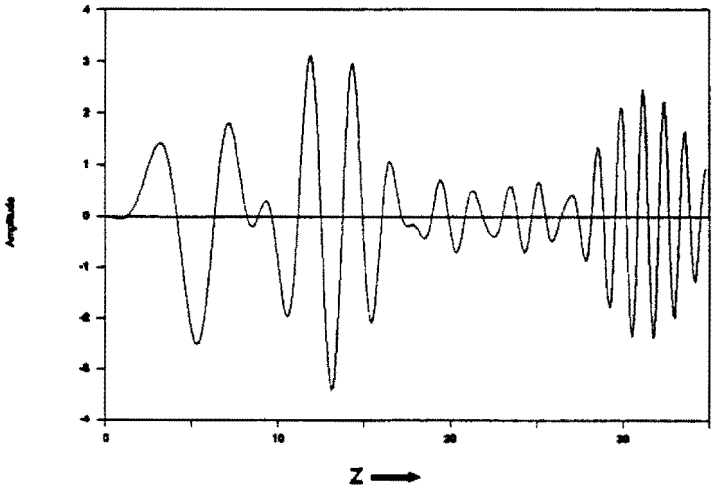


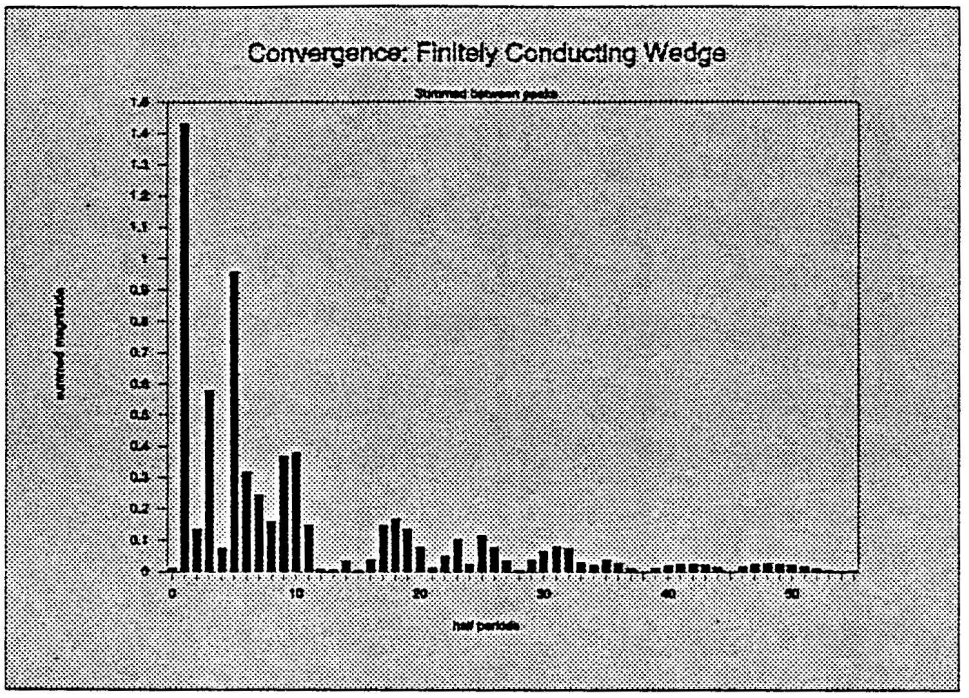
Theoretically-Correct Numerical Approach

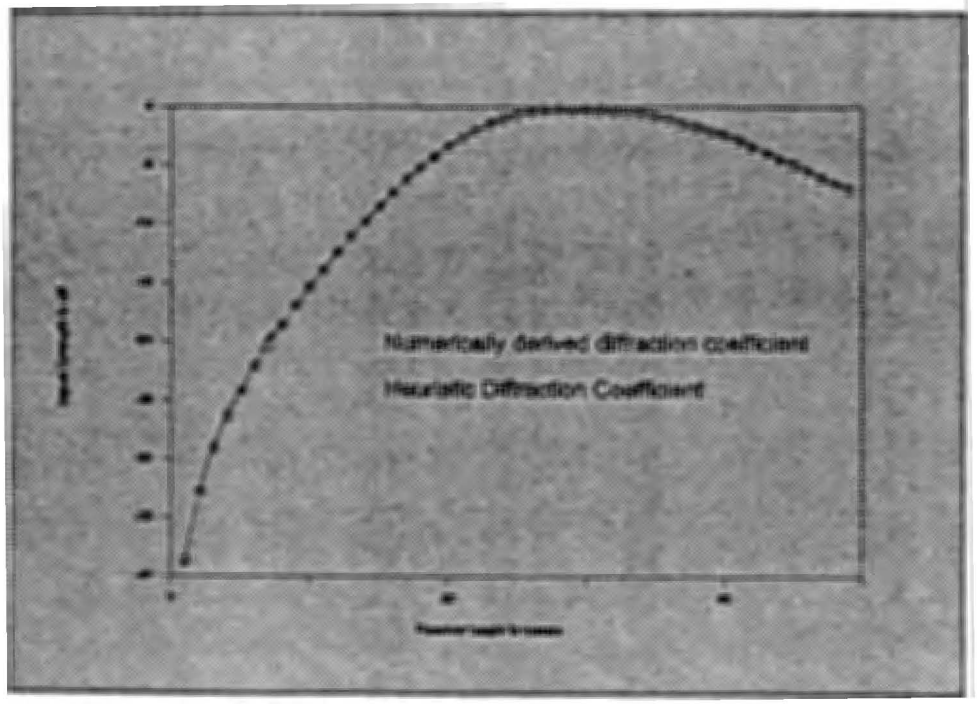
Numerically integrate the contribution of each Huygen source to determine the field at the receiver. Use the finite-conductivity reflection coefficient to calculate reflection



Real part of the contribution from the Huygen source at the indicated height (z). Total received signal is the integral of this waveform.

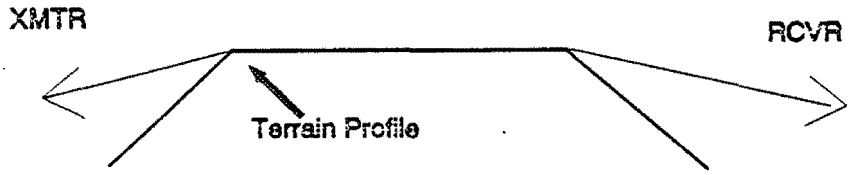



Convergence: Finitely Conducting Wedge
Summed between peaks
scattered magnitude
half periods

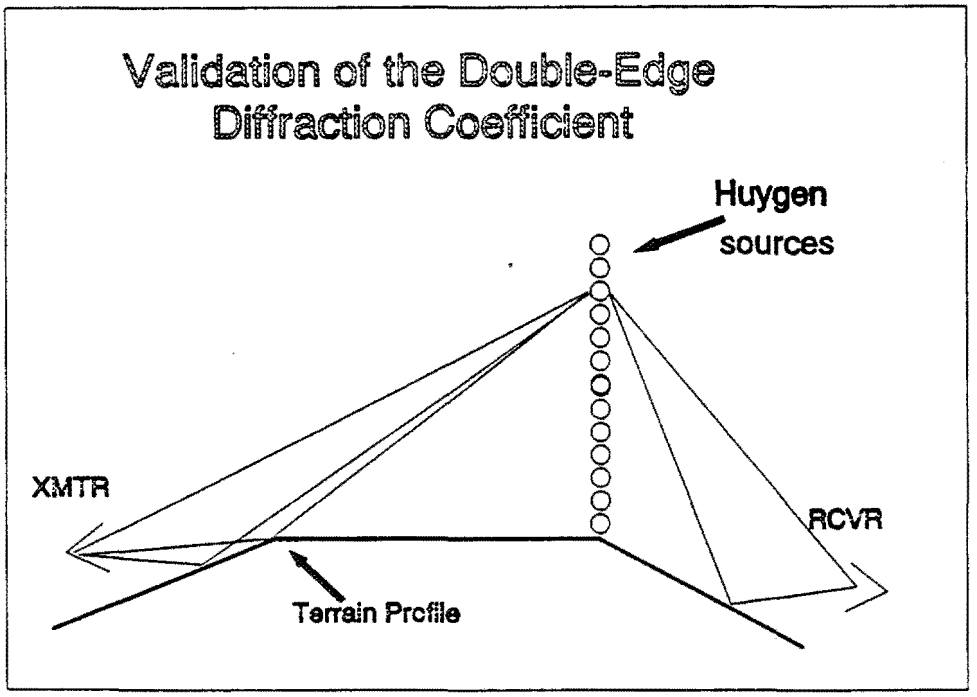

Numerically derived diffraction coefficient
Heuristic Diffraction Coefficient

Validation of the Double-Edge Diffraction Coefficient

A double-edge diffraction coefficient has been developed but does not show close agreement with measured data in some regions



Validation of the Double-Edge Diffraction Coefficient



The Automated Terrain Linearization Model (ATLM)

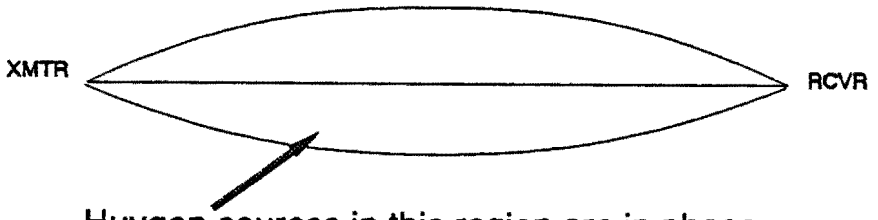
Converts raw terrain data into a GELTI input file
Enables consistent GELTI results from user-to-user

Provides graphical display of data
Aids in error checking of input data and model operation

Requires little expertise on the part of the user
GELTI accuracy is now user independent

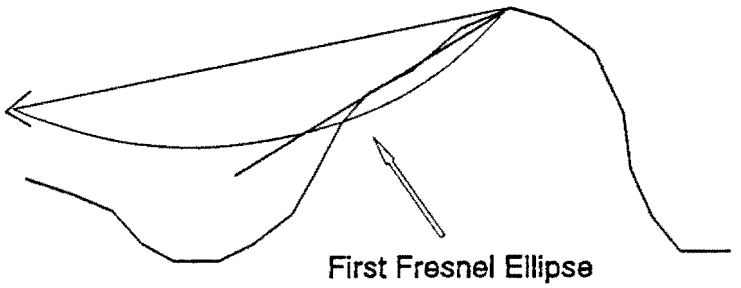
Concept: the Fresnel Ellipse

The region in space between the transmitter and receiver where the majority of energy is transported

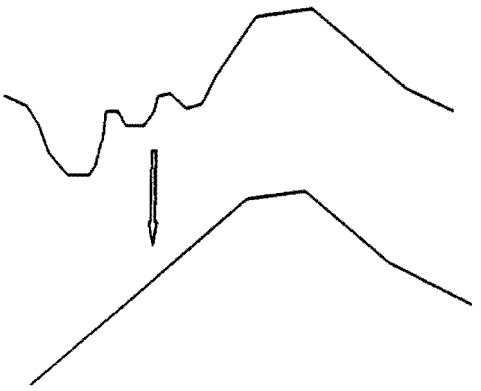


Huygen sources in this region are in phase

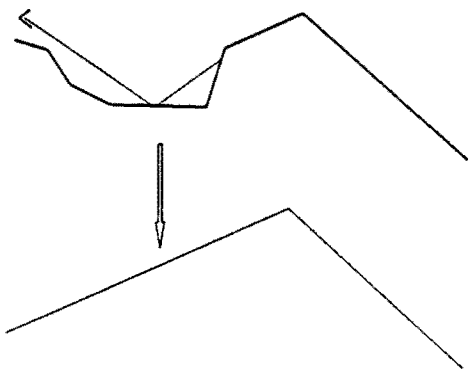
Slope of terrain leading to an edge is determined
by regression of terrain within Fresnel Ellipse



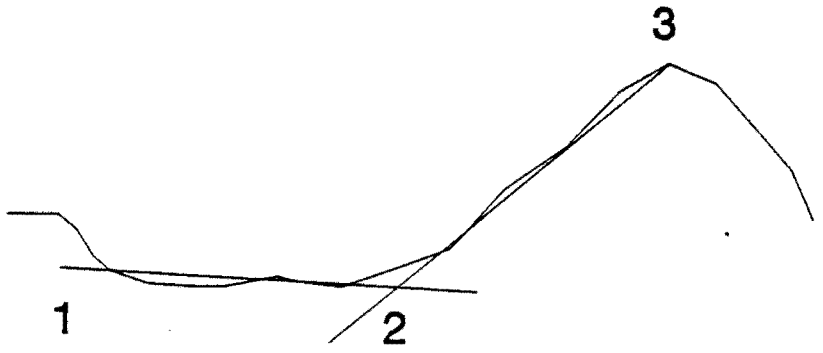
If a region is too rough to reflect
it will not be considered as a separate
terrain segment

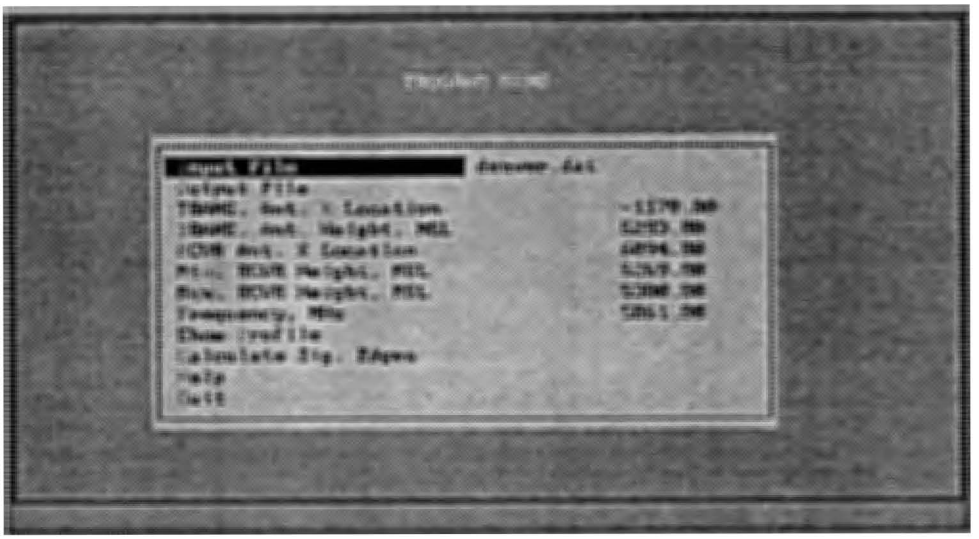


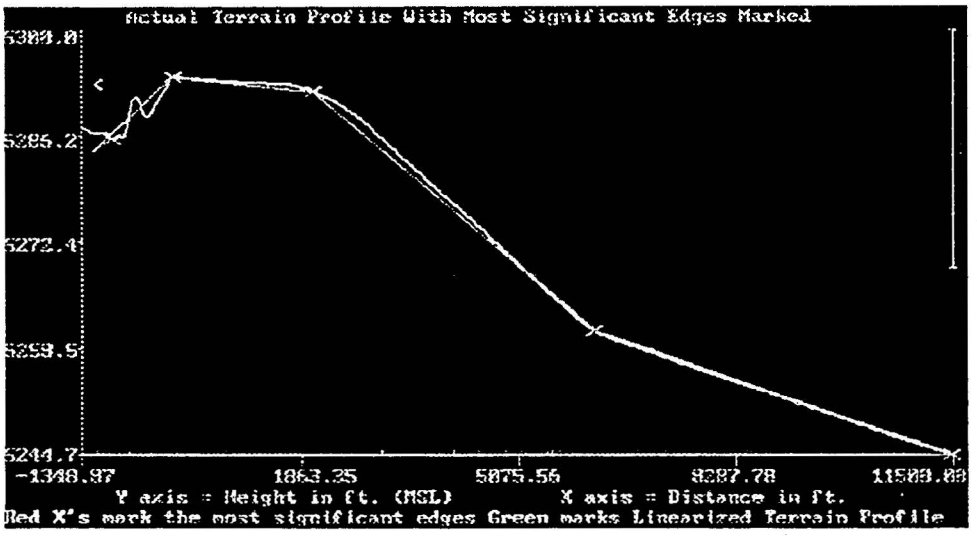
If the reflected ray path from a smooth segment is blocked, that segment will be omitted from the linearized profile

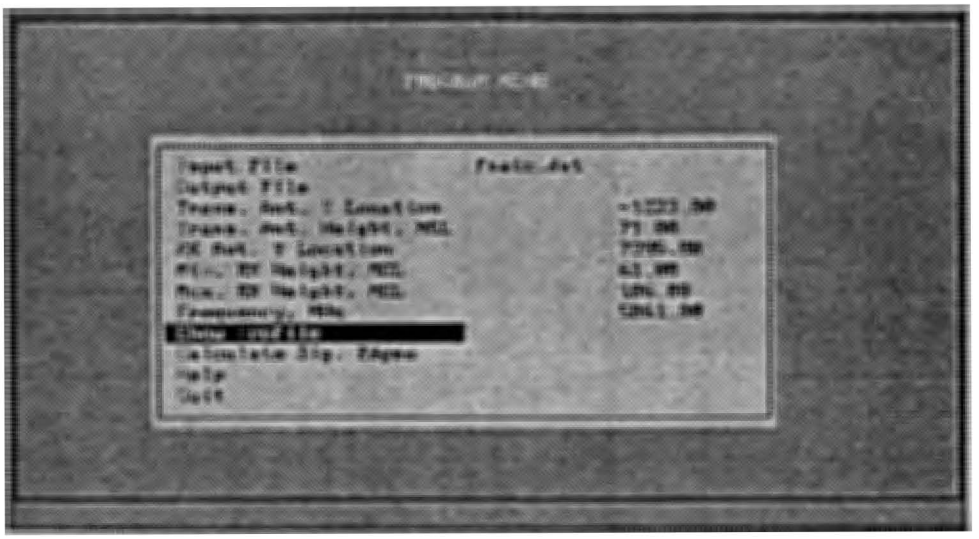


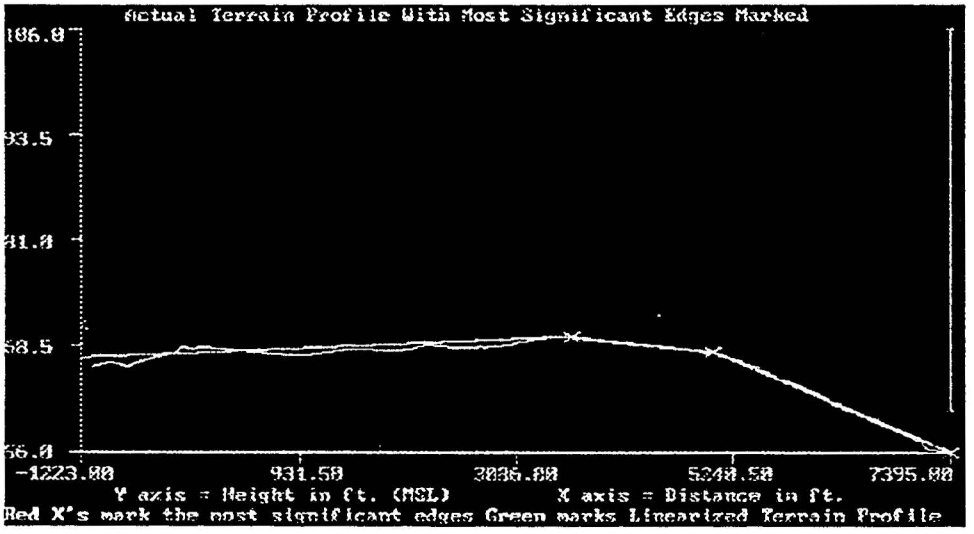
If reflection is possible, edge #2 is determined by intersection of slopes 1-2 and 2-3, which are calculated using linear regression

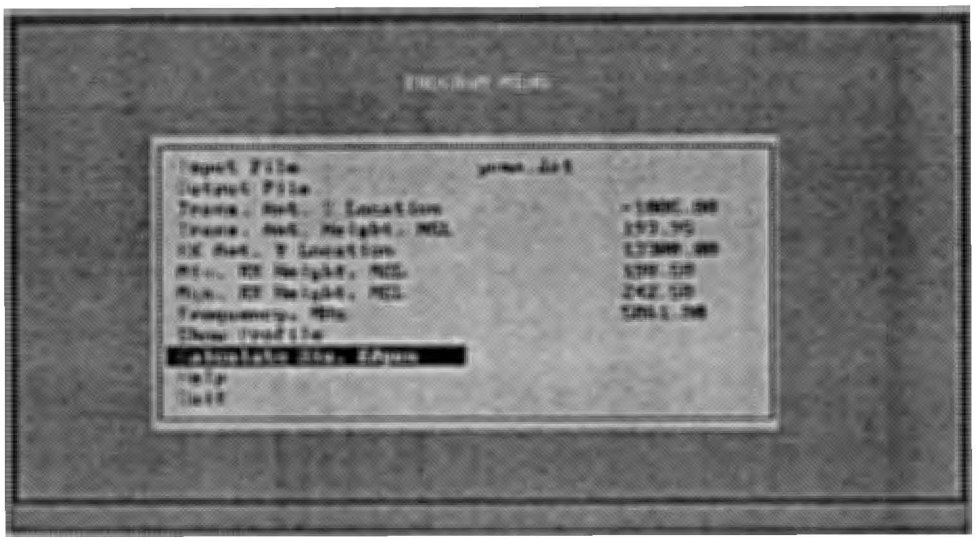


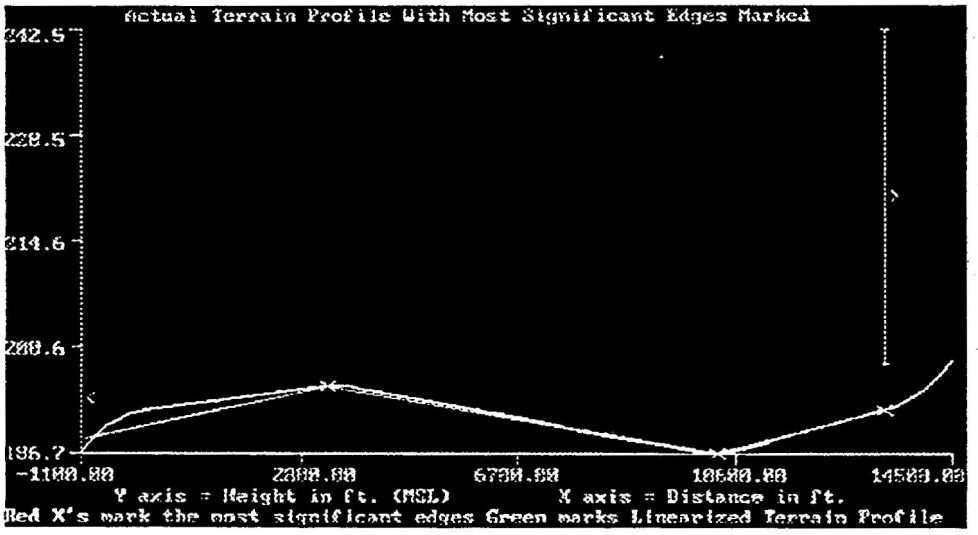



Actual Terrain Profile With Most Significant Edges Marked
5396.2
5272.4
5148.7
-1348.97
1863.25
5075.56
8287.78
11500.00
Y axis = Height in ft. (MSL)
X axis = Distance in ft.
Red X's mark the most significant edges Green marks Linearized Terrain Profile




Actual Terrain Profile With Most Significant Edges Marked
186.0
93.5
41.0
-1223.00
931.50
3086.00
5240.50
7395.00
Y axis = Height in ft. (MSL)
X axis = Distance in ft.
Red X's mark the most significant edges Green marks Linearized Terrain Profile




Actual Terrain Profile With Most Significant Edges Marked
242.5
228.5
214.6
200.6
186.7
-1100.00
2300.00
6700.00
10600.00
14500.00
Y axis = Height in ft. (MSL)
X axis = Distance in ft.
Red X's mark the most significant edges Green marks Linearized Terrain Profile

Conclusions and Recommendations

Accurate modeling results have been obtained for 2 sites

A methodology for terrain linearization has been developed and implemented in computer code

The finite-conductivity diffraction coefficient has been validated

Additional validation should be performed

ROBERT KELLY
BENDIX

THEORY OF DME/P

DME/P SYSTEM DESCRIPTION AND ERROR SOURCE MODELING

MLS MATHEMATICAL MODEL USER GROUP MEETING

JUNE 27-28, 1990
FAA TECHNICAL CENTER
ATLANTIC CITY
INTERNATIONAL AIRPORT, NJ 08405

BY
ROBERT J. KELLY

Allied-Signal Aerospace Company
Bendix Communications Division

DME/P SYSTEM DESCRIPTION AND ERROR SOURCE MODELING

R. J. Kelly
Allied-Signal Aerospace Company
Bendix Communications Division
Baltimore, Maryland

INTRODUCTION

DME is an acronym for Distance Measuring Equipment. The DME associated with the enroute and terminal area navigation, as well as nonprecision approaches, is called DME/N. The Precision DME, called DME/P, is an integral element of the Microwave Landing System (MLS) providing the precision ranging function to complement the azimuth and elevation guidance functions of the system.

The presentation comprises two parts:

- Part I provides the DME background necessary to understand the precision DME. A system description of the DME/P is given in the attached IEEE article, "System Considerations for the New DME/P International Standard."
- Part II introduces the DME/P error source modeling technique. Details are given in the attached paper, "MLS System Error Model Identification and Synthesis."

PART I

In 1978, the International Civil Aviation Organization (ICAO) concluded that the DME/P should be integrated into the existing standards for the conventional DME (DME/N) as a compatible service. The motivation for this was economic. It was reasoned that a single L-band airborne unit could satisfy the need for both existing enroute and the new precision approach and landing services, thereby avoiding unnecessary duplication of on-board ranging equipment. Furthermore, this approach would permit existing conventional airborne equipment to obtain service from the DME/P ground facilities at least during the initial stages of MLS implementation. These compatibility requirements were later incorporated into the DME/P statement of operational requirements which was accepted at an ICAO meeting in April 1981. Further, they were a primary focus in the DME/P ICAO standardization effort.

• Operation and Principles of DME/N

The operation of the DME/N system can be summarized as follows. The airborne unit (interrogator) interrogates a single ground facility that transmits a reply following a known calibrated fixed delay (the zero mile delay). The airborne unit then computes the slant range to that facility by measuring the elapsed time to the receipt of the transponder reply. The measured range is then provided to the pilot and other aircraft systems as required.

Each interrogation consists of a pulse pair where the pulse spacing (or code) together with the RF frequency define the operating channel, thereby allowing the interrogations to be addressed to a specific ground facility. Similarly, the transponder reply consists of a pulse pair having a code and RF frequency corresponding to the channel in use, thereby allowing the airborne unit to distinguish desired ground facility transmissions from those of other facilities within line of sight of the interrogator. The DME/P interrogator and transponder are similar then, in that both must identify valid DME signals using the three discriminates of pulse width, frequency, and code, where the width of the DME pulse is used to discriminate a valid pulse from those due to noise which are of short duration.

The interrogator and transponder differ though in function. An interrogator must accurately measure the time delay between the transmission of the interrogation and receipt of the reply. It does so by starting a clock coincident with the transmission of each interrogation and stopping the clock upon reception of the reply.

Although a reply to its interrogation will only be transmitted by the desired ground facility, the airborne unit will also "hear" replies from other ground stations that are within its line of sight. Consequently, the interrogator must sort out the reply to its own interrogations from the thousands of pulse pairs that it may actually receive. It does so by identifying those beacon transmissions with the proper RF frequency and pulse code that are consistently synchronous with the interrogations.

On the other hand, the transponder must accurately generate a fixed time delay between receipt of the interrogation and the transmission of a reply. This is done by starting the time-delay clock upon receipt of an interrogation, and after a fixed time transmitting a reply such that the round-trip propagation delay is accurately extended by a fixed amount.

A ground transponder will "hear" many interrogations; those from aircraft utilizing the transponder and from other aircraft within line of sight that are utilizing other DME beacons. To minimize the load on the beacon and to ensure unambiguous range information to the user, the transponder must only respond to those interrogations intended for it—those having RF frequency and pulse code corresponding to the assigned channel.

In addition to reply pulse pairs, the transponder radiates squitter and a facility identification signal. Both consist of pulse pairs that are identical to those transmitted in response to interrogations. Squitter consists of random transmissions of on-channel pulse pairs radiated at a rate of 700 to 3600 pulse pairs per second. The intertransmission times are randomized to prevent synchronization with replies to interrogations. Squitter is utilized by many interrogators to determine appropriate automatic gain control (AGC) settings and serves as the source of the TACAN bearing information which is conveyed by modulating the amplitude of the beacon transmissions.

Both airborne and ground DME receivers must handle signal levels from the weakest levels which occur when the aircraft is at the limits of the ground facility coverage (either above, or beyond), to the strongest which can occur when the aircraft is on the ground near a DME facility. Up to an 80 dB variation in signal strength can be expected with levels from -90 dBm on the low end to -10 dBm on the high end. An example system power budget is presented in Table 1.

The dynamic range required of the interrogator receiver is operationally quite different from that of the transponder. Since the interrogator is only concerned with replies from a single source (i.e., the desired ground facility), once the signal level being received from the desired facility is known[1] changes of the level can be tracked by automatic gain control circuitry. As a result, a receiver with a dynamic range on the order of 10 dB is sufficient. As noted above, squitter from the desired transponder often serves as the basis of AGC settings.

[1] The DME system is designed such that the squitter from the desired ground station is the most persistent signal. The AGC voltage is derived on the assumption that the most persistent signal is the desired signal.

TABLE 1. EXAMPLE GROUND AND AIRBORNE DME/N POWER BUDGETS*

	Airborne Receiver ICAO
Power available at antenna airborne	-82.0 dBm
Antenna gain	+2.0 dB
Aircraft cable loss	- 3.0 dB
Signal available at receiver terminals	-83.0 dBm
Receiver noise video noise figure 12 dB; IF bandwidth 0.8 Mhz	-106.0 dBm
Signal-to-noise ratio (video)	23.0 dB
	Beacon Receiver ICAO
Power available at ground antenna	-96.0 dBm
Antenna gain	+8.2 dB
Cable loss	-1.5 dB
Signal available at beacon receive terminals	-89.3 dBm
Receiver noise video noise figure 6 dB; F bandwidth 0.8 MHz	-112.0 dBm
Signal-to-noise ratio (video)	22.7 dB

* Notes: (1) Power density (dB W/m^2) = power (dBm)-7; (2) S/N (video) = S/N (IF) + 10 log (IF noise bandwidth/video noise bandwidth); (3) these budgets are intended as examples only. Other combinations of antenna/cable coupling are possible and should reflect installed conditions.

Such is not the case for the transponder. Since the transponder must be able to process signals from many different interrogators, conventional AGC implementation cannot be utilized, and a wide dynamic range receiver is required. Consequently, logarithmic amplifiers or log/linear hybrid configurations are typically used in the receiver IF to provide the required dynamic range.

The mechanisms which affect the accuracy of the range information are the same for both the interrogator and transponder. The major error mechanisms are simple, controllable, and readily identified. The accuracy and stability of the clocks, counters, and/or shift registers used to measure the round-trip time in the interrogator and to generate the reply delay in the transponder directly affect the accuracy of the range measurement. As the clock-count-to-elapsed-time relationship changes (i.e., oscillator drift due to temperature, age, etc.) from that assumed when performing the range computation, a bias error will result. In addition, since digital timing techniques are typically used, quantization noise error is inevitable. These quantization errors are reduced by utilizing high-frequency clocks. Finally, range measurement errors may also exhibit a dependence on pulse amplitude and rise time. Although such errors are insignificant in the DME/N application, they are of great concern in the design of DME/P equipment (see Section IV, D).

In order to prevent the radiation of erroneous navigation information, the ground facility is actively monitored in real time by what is in essence a high-quality interrogator. The monitor system interrogates the transponder and measures those parameters that affect system accuracy and coverage: mean reply delay, radiated power, receiver sensitivity, frequency stability, and transmitted pulse code. Because mean reply delay can affect safety of flight it is a primary parameter. Primary alerts shut down a ground facility or switch in redundant equipment if available. Shutdown occurs when the reply delay error exceeds predefined limits: nominally 500 or 250 ft when the ground facility is associated with a landing aid such as ILS.

The remaining components of the DME system are the ground and airborne antennas. Ground facilities typically provide horizontal coverage over a full 360°. The vertical lobe of the ground antenna must include the minimum and maximum altitudes of the facility's service volume.

An aircraft requires range information independent of its direction of flight with respect to the ground facility and throughout roll and pitch variations of up to ±30°. Typically, the airborne antenna is a ¼-wave monopole providing nearly uniform gain laterally around the aircraft and maximum gain of 5 dBi in the aircraft's vertical plane. In the power budgets presented later, a gain of only 2 dBi is assumed. This value represents a lower bound on the antenna gain that can be expected over nominal flight altitude and aircraft-to-ground facility geometries and therefore determines the minimum received signal level.

- **Why DME Works So Well**

As a viable navigation aid, DME/N satisfies the following system considerations: service volumes, system accuracy, aircraft capacity/reply efficiency and channel plan

Service volumes are defined with range/altitude coverage characteristics that reflect the intended use of the facility, i.e., high-altitude enroute, low-altitude enroute, and terminal. The minimum available coverage is determined by the radiated power, receiver sensitivity, and antenna characteristics for both the ground and airborne units. Enroute facilities are geographically placed so as to have overlapping service volumes, providing for continuous navigation along defined airways throughout virtually all of the United States. Terminal facilities are associated with airports and are intended to satisfy the need for short-range navigation in the terminal area. Some terminal facilities are associated with landing aides such as ILS and serve as replacements for marker beacons.

Today, the system accuracy of DME/N derived range information is on the order of 0.2 nmi (95% probability). Table 2 is an example DME/N system error budget. By defining a common calibration method, system accuracy is preserved among equipment of different manufacture. Specifically, the ½ amplitude point on the pulse leading edge serves as the reference point for declaring pulse arrival. All time measurements, both for range and pulse code, are referenced to the ½ amplitude point of received and transmitted pulses and are thus independent of pulse rise time and amplitude.

The ground beacon has a finite capacity to process interrogations, a consequence of the "dead time" that results from identifying a valid interrogation and transmitting the reply pulse pair following the appropriate fixed delay. Valid interrogations arriving during this dead time are ignored and result in missed range measurements at the interrogator. This effect defines an important system performance parameter known as the reply efficiency. It is simply the ratio of the number of interrogations from a single interrogator to the number of replies generated by the ground beacon in response to the interrogations. The reply decreases as the total number of interrogations increases, thus limiting the number of aircraft which can be accommodated by a single ground beacon.

The DME/N system is designed to provide a 70% reply efficiency or better in the presence of 100 aircraft. In order to serve all 100 aircraft and satisfy the minimum reply efficiency requirements, both the beacon dead time and interrogation rate must be limited. Dead times are at least 60 microseconds while the interrogation rate for a single interrogator is limited to 30/s for track and 150/s for search. Computations of the peak load capacity typically assume that 95% of the interrogators utilizing the beacon are in track while the remaining 5% are in search.

TABLE 2. DME/N SYSTEM ERROR BUDGET (95% PROBABILITY)

	SPECIFICATION (nmi)		
	SARPs	RTCA	ARINC
Instrumentation Ground (SARPs)	0.08	0.08	0.08
Airborne	0.17	0.17	0.10
RSS total	0.19	0.19	0.13
System error (SARPs)	0.20	0.20	0.20
Margin for site-dependent errors Multipath, garble)	0.07	0.07	0.15

The ground system instrumentation error is 0.04 nmi when the DME is associated with a landing aid (ILS). Total instrumentation error and margin for site-dependent effects are modified accordingly.

Three features of the DME/N system ensure the availability of unambiguous distance information to a known ground location. First, ground beacons are assigned distinct channels characterized by an airborne interrogation frequency/pulse code and a corresponding beacon reply frequency/pulse code. Second, recall that range information is derived by identifying those beacon transmissions (replies) which are consistently synchronous with the interrogator transmissions. In order to prevent synchronization with other interrogators utilizing the beacon which can lead to false range indications, the time between consecutive interrogations is randomized (jittered). Finally, the Morse code identifier transmitted by the beacon allows the pilot to verify that the station in use is indeed the desired one.

Two hundred fifty-two DME/N channels are defined in the L-band portion of the radio spectrum at frequencies from 960–1215 MHz. Each channel consists of an up and downlink frequency pair (63 MHz apart) with adjacent channels spaced on 1 MHz intervals. Pulse codes are utilized to allow multiple channels on a single frequency. The DME/N channel plan is defined in Table 3.

Today's DME system is designed to place the burden of signal integrity in the hands of the ground transponder. In the airborne interrogator, simple modulators generating square pulses are permitted, while rejection of signals and adjacent frequencies is accomplished with simple filters. To allow for this airborne simplicity, strict controls must be placed on the uplink spectrum, and more sophisticated adjacent frequency signal rejection techniques (such as the Ferris discriminator) must be utilized. The four key aspects of interference protection are summarized below.

TABLE 3. TACAN/DME AND VHF NAVAID CHANNEL PAIRING SCHEME

TACAN/DME Channel 200 NAS Channels	VHF Navaid 200 VHF Frequencies
17–59 X and Y 70–126 X and Y	108.0–117.95 MHz 50–kHz spacing
18–56 X and Y even (40 channels)	ILS localizer: 108.10–111.95 MHz odd 100 kHz and next higher 50 kHz (i.e., 18X with 108.10, 18Y with 108.15,...)
17–55 X and Y odd (40 channels)	VOR: 108.0–111.05 MHz even 100 kHz and next higher 50 kHz (i.e., 17X with 108.00, 17Y with 108.05,...)
57–59 X and Y 70–126 X and Y (120 channels)	VOR: 112.0–117.95 MHz 50 kHz spacing (i.e., 57X with 112.0, 57Y with 112.05,...)

Note: ILs localizer frequencies are non–sequentially paired with ILS glide slope frequencies (329.15–335.0 MHz, 150 kHz spacing).

1. Ferris Discriminator

The frequency rejection characteristics of the ground transponder must ensure that off-frequency interrogations will not result in undesired replies and unnecessarily degrade the ground system reply efficiency. Since essentially square pulses can be used by the airborne interrogators, simple IF filters do not provide adequate attenuation of adjacent channel signals. Hence, an alternate means of rejecting an off-frequency pulse is necessary.

Adequate frequency rejection is provided in the ground transponder receiver by comparing the output levels of a narrow and a wide-band IF filter. The narrow-band filter, with a typical bandwidth of 200 kHz, will pass nearly 90% of the energy contained in an on-frequency pulse while an off-frequency pulse is attenuated. The output of the wide-band filter (typically 800 kHz or larger) is needed to make the range measurement since it preserves the high-frequency information contained in the pulse leading edge. A received pulse is declared on-frequency when the output level of the narrow-band filter exceeds a predetermined percentage of the wide-band filter output level. In DME engineering circles, this circuit configuration is called the Ferris discriminator, named after its originator, Hal Ferris.

Rather than simply attenuating the off-frequency pulse as in done in the airborne equipment, the Ferris Discriminator "identifies" the off-frequency pulse, allowing it to be excluded from further processing by the ground transponder receiver. It does so by making use of the fact that 90% of the energy in a DME pulse is confined to within 0.5 MHz of the carrier frequency, a consequence of the fact that a relatively wide (3.5 μs) pulse is used. This technique readily provides the equivalent of 80 dB of frequency rejection, a level greater than that which can be provided by a simple 800 kHz IF filter (see Table 4).

2. Uplink Pulse Spectrum

To accommodate the use of a simple filter in the interrogator, the spectrum of the uplink pulse is strictly controlled. Specifically, as shown in Table 5, the effective radiated power (ERP) in the first adjacent channel is limited to 200 mW, and to 2 mW in the second adjacent channel. This is in contrast to the simple relative adjacent frequency signal level requirement imposed on the downlink waveform. The implication is that any ERP may be utilized as long as the power in the adjacent bands is maintained below the specified absolute levels. This limitation requires careful shaping of the uplink pulse so that adequate signal power can be provided to achieve the desired coverage while simultaneously providing a rise time consistent with system accuracy requirements.

TABLE 4. PROTECTION RATIO D/U (dB)

Type of Assignment	A (before 1989)*	B (after 1989)
Co-frequency		
Same pulse code	8	8
Different pulse code	0	-42
First adjacent frequency		
Same pulse code	$-(P_u - 1)$[b]	-42
Different pulse code	$-(P_u + 7)$	-75
Second adjacent frequency		
Same pulse code	$-(P_u - 19)$	-75
Different pulse code	$-(P_u + 27)$	-75

* The D/U ratios in Column A protect those DME/N interrogators operating on X or Y channels. Column A applies to decoder rejection of 8 dB and a ± 6 microsecond aperture.

[b] P_u is the peak effective radiated power of the undesired signal in dBW. The frequency protection requirement is dependent upon the antenna patterns of the desired and undesired facility and the ERP of the undesired facility.

3. Decoder Rejection Characteristics

Pulse codes are utilized to provide for multiple channels on a single interrogator/reply frequency pair. Thus, although the spectral resource is limited, more facilities can be accommodated in a given geographic area. To obtain a true increase in the number of available channels, off-code signals must be rejected by both the ground and airborne equipment as effectively as off-frequency signals. This is achieved by imposing strict decoder tolerances on both the airborne and ground equipment. These tolerances require that pulse pairs having spacings deviating more than $\pm 2\ \mu s$ be rejected (see Table 4). This ensures that off-code replies received by an interrogator are excluded from consideration as valid replies.

4. Channel Assignment Procedures

Channel assignment procedures are utilized to guarantee that the uplink desired-to-undesired (D/U) signal ratio at all points within a defined service volume falls within the defined signal rejection capabilities of the airborne equipment. This is accomplished by appropriate geographic separation of facilities. Co-frequency/co-code assignments are made such that an 8 dB D/U or greater is provided. Adjacent frequency assignments (both same and different codes) are made such that when the airborne frequency rejection characteristic and ground system radiated spectrum are assumed, a post filter D/U of +8 dB or better is again obtained. On-frequency/off-code assignments are on equal footing with first adjacent frequency assignments—a result of the defined decoder characteristics (see Table 4). This method of frequency protection ensures correct interrogator AGC operation since the desired signal will always be stronger than any decodable undesired signal.

TABLE 5. SPECTRUM CONSTRAINTS ON THE DME TRANSMITTED WAVEFORM

Adjacent Frequency Band Relative to Transmit Frequency	Maximum Ground System Radiated Power	Power with Respect to Peak On-Channel Power
0.55–1.05 MHz	200 mW	-23 dB
1.75–2.25 MHz	2 mW	-38 dB

Using the DME/N summary above as background, the extension of the DME principles to the DME/P is now straightforward.

The DME/P portion of the MLS operates on 200 channels in the standard DME frequency band of 960–1215 MHz. Like the angle portion of MLS, DME/P is an air-derived sampled data system. It uses the familiar interrogator-transponder techniques and estimates range based on the round trip from interrogator transmission to reception of the transponder reply. As in the DME/N case, the interrogator is the airborne and the DME/P ground station serves as the transponder.

The major source of ranging error during the final phases of approach and landing operations is multipath, rather than interrogator and transponder instrumentation errors. In the DME/P application, multipath, i.e., reflections from the ground or airport structures is always received later in time than the desired signals. To minimize these effects, DME/P thresholds the pulses received early, at a point which has not been significantly corrupted by multipath. Thus, the DME/P thresholds very low (about 17 dB below the peak) on a fast rise time (1200 ns) pulse. This is in contrast to the 50 percent (6 dB below the peak) thresholding and slow rise time (2500 ns) pulses used in DME/N. By removing the effects of multipath and by applying self-calibration loops in the ground and airborne equipment to remove bias-like ranging errors, the DME/P achieves 100 ft system accuracy, a twelvefold improvement over the DME/N.

The new DME/P had to be defined in a manner which did not violate the existing DME/N adjacent channel spectrum specifications. Furthermore, interoperability of DME/P with DME/N was a firm requirement. Both constraints were satisfied by a "two pulse/two mode" DME/P signal format: a wide-band, final approach (FA) mode featuring the fast rise time pulse and low thresholding and a narrow-band initial approach (IA) mode, featuring standard 50% thresholding. By reducing the FA mode coverage volume to 5 nmi from threshold, the adjacent channel power constraints could be satisfied. Beyond 7 nmi, the IA mode is used.

As in DME/N, several "channels" share the same RF frequency through the use of different pulse spacings. IA

mode DME/P uses pulse spacings similar or identical to those used by DME/N. FA mode DME/P, on the other hand, is identified by a unique set of pulse spacings. Error budgets, power budget, channel plan, delay and compare techniques, etc., are provided by the accompanying IEEE paper, "System considerations for the New DME/P International Standard."

- **How Does DME/P Achieve Its Accuracy?**

Accuracy is achieved by 1) thresholding low on the first pulse leading edge before 95% of the multipath arrives; 2) making the pulse arrival time processor independent of pulse amplitude and pulse shape variations.

A simple fixed threshold pulse arrival time technique, however, will not satisfy condition 2 above. This is true whether an AGC or log receiver is applied.

For example, assume a linear receiver and let

$$\text{Threshold} = \frac{V}{t_R} t \qquad (1)$$

where t_R is the 10% to 90% pulse rise time, V is the peak pulse amplitude and t is the time that the pulse leading edge crosses the threshold. Equation (1) assumes video processing and that the fixed threshold is within the linear region defined by the DME/P partial rise time specification of 5% to 30%. Let threshold = 0.1 V and assume that t_R = 1000 ns. (ICAO requires that the pulse waveforms have rise times between within 800 ns and 1200 ns.)

The *virtual origin* (or the start of the pulse) t_{vo}, is given by solving (1) for $t = t_{vo}$

$$t_{vo} = \frac{t_R}{V} \text{Threshold} \qquad (2)$$

$$t_{ro} = (1000)\ (.1) = 100 \text{ ns}$$

The important point is that any disturbance (multipath or garble) which occurs after t_{vo} will not affect the pulse arrival time accuracy.

Taking the differential of (1), the pulse arrival time error due to pulse shape is

$$\delta t = \frac{\delta t_R}{V} \text{Threshold}$$

$$\delta t = \frac{200 \text{ ns}}{V}\ (0.1V) = 20 \text{ ns}$$

$$\delta t = 20 \text{ ns or } 10 \text{ ft}$$

where δ_{Q_R} = 20% of 1000 ns = 200 ns.

The error due to -3 dB multipath whose delay > 100 ns and does not perturb the leading edge is

$$\delta t = -\frac{t_R}{V^2} \delta V \text{ Threshold}$$

$$\delta t = (100 \text{ ns})\ (0.7)$$

$$\delta t = 70 \text{ ns or } 35 \text{ ft}$$

where δ_V = 0.7 V.

The 35 ft error is the result of only an amplitude variation which in effect changes the pulse rise time by 70%. There is no multiple error per se because the multipath occurs after Δt = 100 ns. Clearly, a sizable portion of the Standard 1 100 ft error budget has been consumed by only amplitude and incoming wave shape variations. It is desirable then to incorporate a pulse arrival technique which is invariant to pulse amplitude and shape variation. Such an implementation is the Delay and Compare circuit (DAC), which is described in Section 6 of the attached IEEE paper.

PART II

MLS SYSTEM ERROR MODEL IDENTIFICATION AND SYNTHESIS

An activity closely associated with MLS signal modeling is the identification and synthesis of MLS error signals. The attached article entitled "MLS System Error Model Identification and Synthesis" describes three activities: (1) signal error source identification which permits data compression for efficient storage in a signal library; (2) signal generation or synthesis using the library of stored signals; and (3) multivariate hypothesis testing to determine the similarity or dissimilarity of signals at different airports. This identification and synthesis technique applies not only to MLS but to all navigation systems. The DME/P is used as an example.

Modeling of the MLS errors is necessary to:

(1) Certify aircraft for operations using the MLS guidance signals. Due to the high cost of flight testing, the bulk of this certification documentation is developed using aircraft flight control/

dynamics simulations. A critical element in these simulations is the development of the error source generator.

(2) Develop MLS signal error source library from samples of flight error traces collected from worldwide distribution of MLS instrumented runways. Signal synthesis with a data compression of 400:1 permits the records to be stored on a small disk.

(3) Determine the *invariant* characteristics of the MLS signal using Generalized Hotelling T^2 test or the Wilk's likelihood ratio criterion after determinisitic specular multipath sources have been removed.

Signals from different airports (i.e., runways) having similar characteristics reduce the storage requirements of the signal library. Moreover, if certain signal characteristics persist across the ensemble of all airports, then the Aircraft Flight Control Simulations (AFCS) can be more closely matched to the MLS signal-in-space.

(4) MLS equipment performance specifications can be expanded to include the error component identification. Introducing signal error source identification into performance specification would promote a better understanding not only of equipment design but the error mechanisms themselves. Armed with such information, the navigation equipment engineer could implement systems having performance characteristics closely approximating an optimum design. Error source model identification and generation is a tool applicable to ground and airborne equipment as well as flight inspection tests.

Signal model identification will make government regulatory agencies, equipment manufacturers, and the user conscious of the mechanism by which error sources arise in navigation equipment designs. It is our experience that once we identify the error mechanisms, practical means to control them close to their theoretical limits are always discovered. By exposing equipment performance to such analysis, the specifications themselves become consistent and operationally meaningful.

AL LOPEZ
ARL ASSOCIATES

EL SITING CRITERIA

MLS ELEVATION ANTENNA
VERTICAL PLANE SITING CONSIDERATIONS

ALFRED R. LOPEZ

FOUR SARINA DRIVE
COMMACK, NY 11725

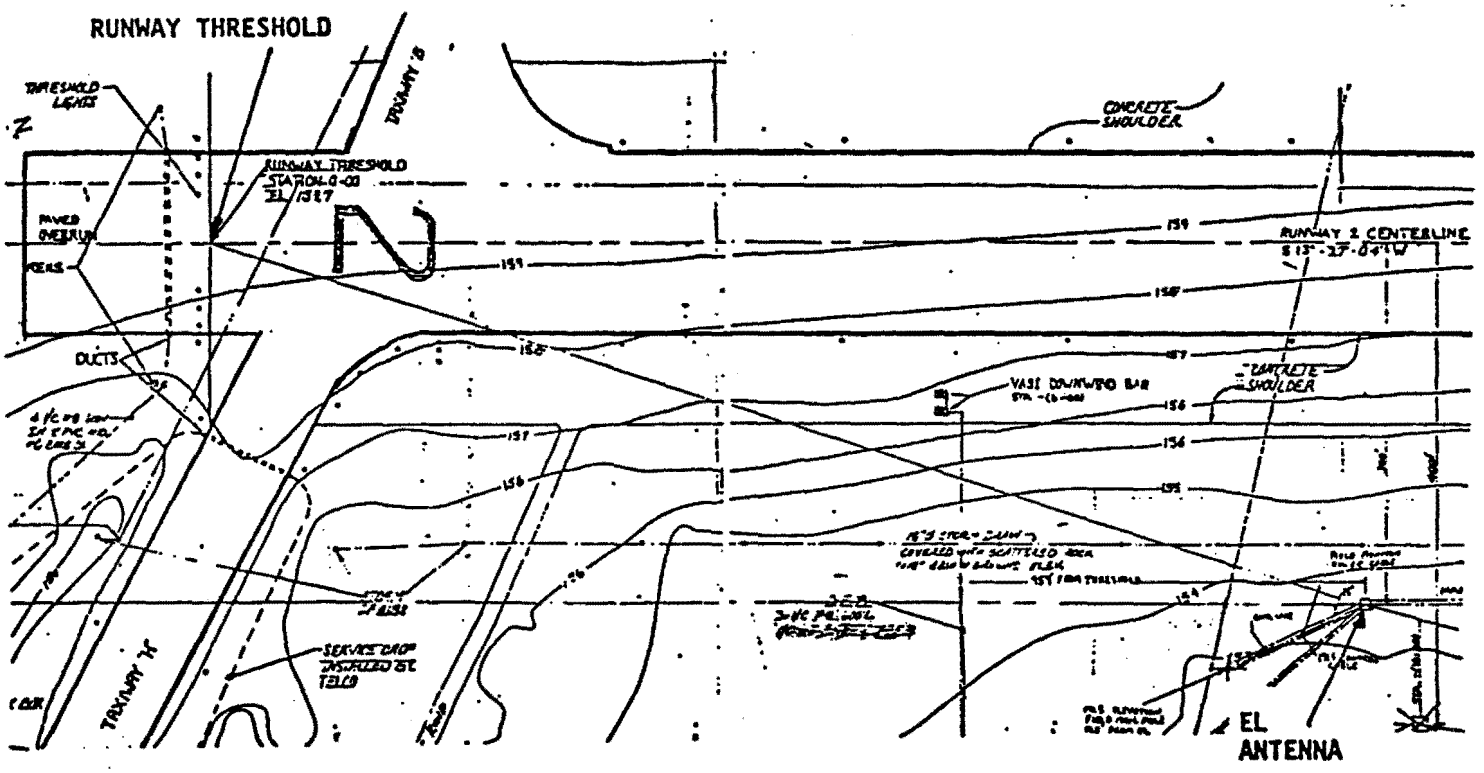
ABSTRACT

A KEY CONSIDERATION IN THE SITING OF THE MLS ELEVATION ANTENNA IS THE VERTICAL PLANE PROFILE OF THE TERRAIN IN THE APPROACH DIRECTION. THE MLS SPECIFICATIONS ALLOW NO DEGRADATION OF THE ACCURACY DOWN TO 60 PERCENT OF THE MINIMUM GLIDE PATH. IMPROPER SITING OF THE EL ANTENNA WITH RESPECT TO THE NEAR-IN TERRAIN PROFILE COULD RESULT IN SIGNIFICANT DEGRADATION OF ACCURACY AT ANGLES NEAR THE 0.6 GLIDE PATH ANGLE. A RELATIVELY SIMPLE METHOD FOR ESTIMATING THE ERROR CAUSED BY THE TERRAIN PROFILE IS PRESENTED. THE RESULTS ARE HELPFUL IN EVALUATING ALTERNATIVES FOR THE SITING OF THE EL ANTENNA.

SOME INITIAL RESULTS INDICATE THAT CERTAIN NEAR-IN TERRAIN FEATURES PRECLUDE THE USE OF A 2° BEAM WIDTH ANTENNA. HOWEVER, A 1° BEAMWIDTH ANTENNA WILL SATISFY THE ACCURACY REQUIREMENTS DOWN TO AN ANGLE THAT IS 60 PERCENT OF THE MINIMUM GLIDE PATH.

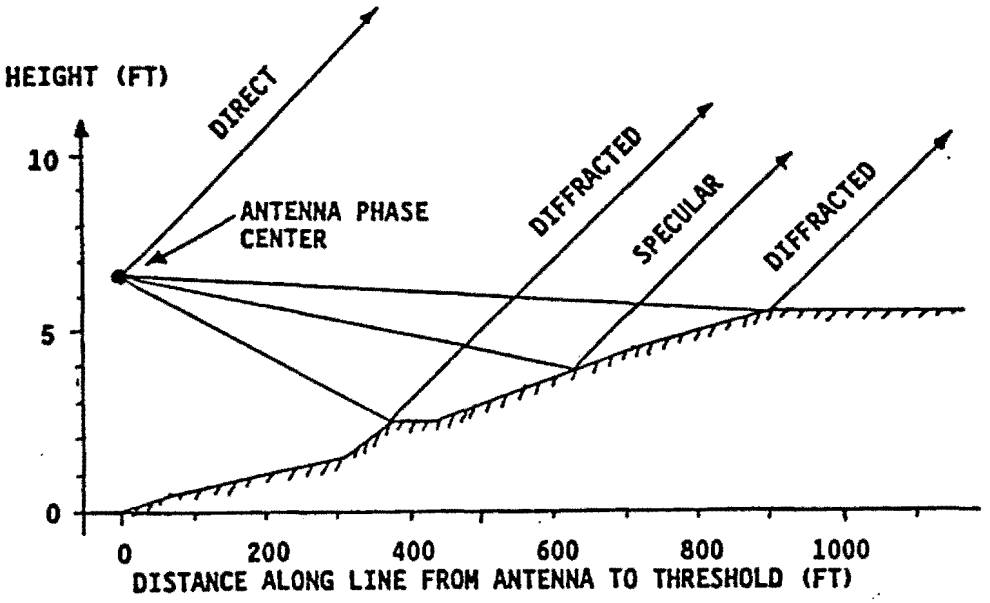
NEAR-IN TERRAIN PROBLEM

RICHMOND, VIRGINIA



THE TERRAIN FEATURES FOR THE EL ANTENNA SITE FOR RUNWAY 02 AT RICHMOND, VA. ARE NOT VERY UNUSUAL. THE SITE, HOWEVER, TURNS OUT TO BE AN UNUSUALLY DIFFICULT SITE, ESPECIALLY FOR A 2 DEGREE BEAM WIDTH ANTENNA. THE GROUND ELEVATION CONTOURS SHOW THAT THE NEAR-IN TERRAIN IN FRONT OF THE EL ANTENNA SLOPES UPWARD IN THE DIRECTION OF APPROACHING AIRCRAFT. DURING FLIGHT INSPECTIONS OF THE MLS FACILITY AT RICHMOND, VA IT WAS DETERMINED THAT THE 2 DEGREE GLIDE PATH HAD ANGLE ERRORS THAT EXCEEDED THE SPECIFIED TOLERANCES. IT IS NOW BELIEVED THAT THE BASIC PROBLEM IS IN-BEAM MULTIPATH CAUSED BY THE NEAR-IN RISING TERRAIN.

PROFILE OF NEAR-IN TERRAIN



THIS VIEWGRAPH SHOWS THE PROFILE OF THE NEAR-IN TERRAIN BETWEEN THE EL ANTENNA AND THE THRESHOLD TO RUNWAY 02 AT RICHMOND, VA. IT IS NOTED THAT THE TERRAIN PRODUCES DIFFRACTED AND SPECULAR MULTIPATH COMPONENTS. OF PARTICULAR SIGNIFICANCE IS THAT THE DIRECTION OF THE SPECULAR COMPONENT IS APPROACHING THE 0° ELEVATION DIRECTION. FOR A FLAT TERRAIN THE SPECULAR DIRECTION IS IN THE NEGATIVE GLIDE PATH DIRECTION.

SIMPLE MODEL FOR ESTIMATING ANGLE ERROR

- ICAO ANNEX 10 GUIDANCE MATERIAL, PEAK ANGLE ERROR

$$\delta\theta = P_R \; P_{ES} \; P_{MA} \; \theta_{BW}$$

- θ_{BW} — BEAM WIDTH
- P_{MA} — MOTION AVERAGING FACTOR
- P_{ES} — EFFECTIVE SIDELOBE FACTOR (OUT-OF-BEAM MULTIPATH)
- P_R — REFLECTION COEFFICIENT

- A MORE GENERAL EXPRESSION, INCLUDES TIME DEPENDENCE

$$\delta\theta = P_R(T) \; P_{SA}(T) \; P_{MA}(T) \; \theta_{BW} \; \sin(2\pi \, PD(T) / \lambda)$$

- λ — WAVELENGTH
- T — TIME
- $PD(T)$ — PATH DIFFERENCE
- $P_{SA}(T)$ — SEPARATION ANGLE FACTOR (IN-BEAM AND OUT-OF-BEAM MULTIPATH)

IN THE MORE GENERAL EXPRESSION THE SEPARATION ANGLE FACTOR ONLY ACCOUNTS FOR THE GROUND ANTENNA ARRAY FACTOR. THE REDUCTION OF SIDELOBE ERROR BY MEANS OF SPATIAL FILTERING (COMPACT OR PHASE CENTER DIVERSITY) IS INCLUDED IN THE REFLECTION COEFFICIENT FACTOR.

REFLECTION COEFFICIENT

- PRODUCT OF FACTORS
  - PATH DIFFERENCE
  - OBSTACLE
    - SIZE
    - DIFFUSE
    - CURVATURE
    - DIFFRACTION
  - GROUND PATH PROFILE
  - GROUND ANTENNA PATTERN
    - HORIZONTAL PLANE
    - VERTICAL PLANE
  - AIRCRAFT ANTENNA PATTERN

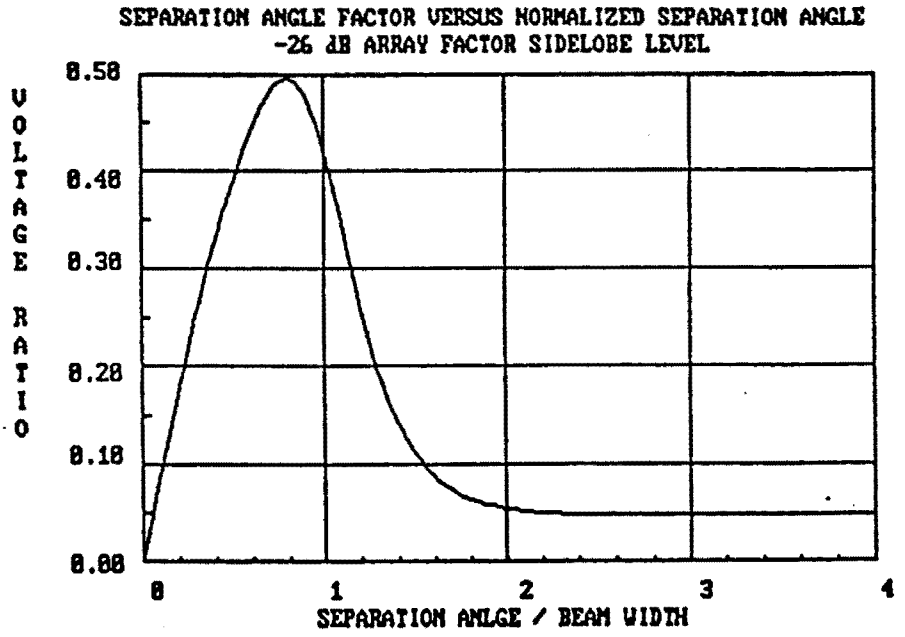
FOR THE CASES BEING CONSIDERED IN THIS PAPER ALL FACTORS ARE EQUAL TO UNITY WITH THE EXCEPTION OF THE:

PATH DIFFERENCE FACTOR,
DIFFRACTION FACTOR, AND
GROUND ANTENNA VERTICAL PLANE PATTERN FACTOR.

THE GROUND ANTENNA VERTICAL PLANE PATTERN FACTOR INCLUDES A COMPACT ELEMENT PATTERN FACTOR OF -14 dB FOR A RECEIVER ON A 3° GLIDE PATH AND A GROUND REFLECTION MULTIPATH SEPARATION ANGLE OF 6°. WITH A RECEIVER ON A 1.8° GLIDE PATH AND A MULTIPATH SEPARATION ANGLE OF 3.6° THE FACTOR IS -8.4 dB.

SEPARATION ANGLE FACTOR

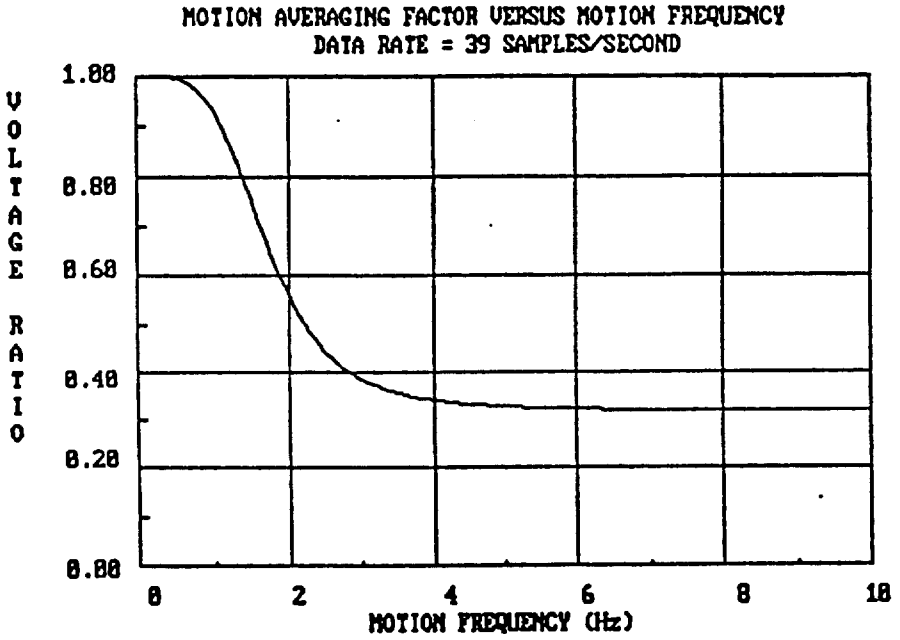
- THE SEPARATION ANGLE IS THE ANGLE IN THE SCAN PLANE BETWEEN THE DIRECT SIGNAL AND THE INDIRECT SIGNAL AS VIEWED FROM THE GROUND ANTENNA.



AS NOTED PREVIOUSLY, THE SEPARATION ANGLE FACTOR ONLY INCLUDES THE EFFECTS OF THE ARRAY FACTOR. ADDITIONAL SUPPRESSION OF SIDELOBE EFFECTS, BY MEANS OF SPATIAL FILTERING, IS INCLUDED IN THE REFLECTION COEFFICIENT FACTOR.

MOTION AVERAGING FACTOR

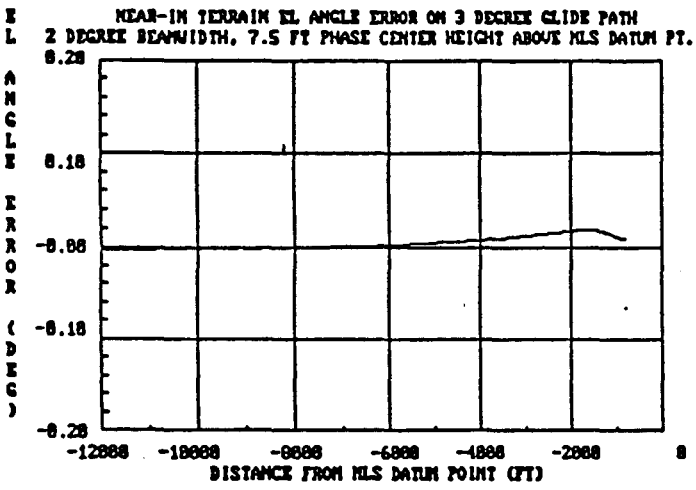
- MOTION FREQUENCY = $\frac{d}{dt} \frac{PD(t)}{\lambda}$



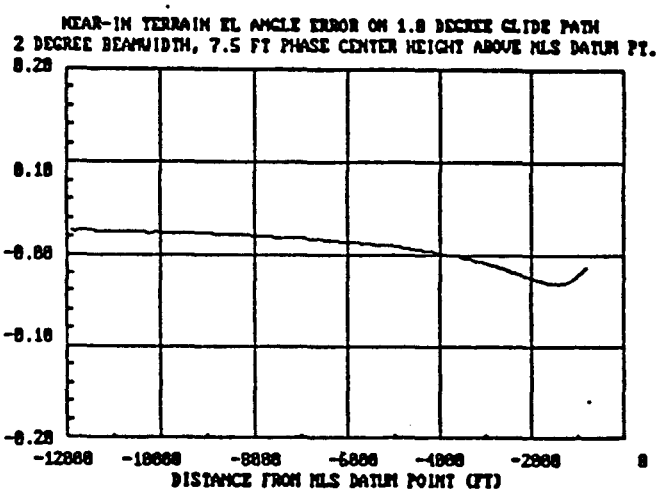
MOTION FREQUENCY IS ALSO REFERRED TO AS SCALLOPING FREQUENCY. THE MOTION AVERAGING FACTOR APPROXIMATES A SINGLE POLE 10 RAD/SEC LOW PASS FILTER FOR FREQUENCIES BELOW 1.6 Hz AND IS THE MOTION AVERAGING FACTOR (SQUARE ROOT OF π X FILTER BANDWIDTH / DATA RATE) FOR MOTION FREQUENCIES ABOVE 3 Hz.

ACCURACY FOR FLAT TERRAIN CASE
2 DEGREE BEAM WIDTH ANTENNA

3 DEGREE GLIDE PATH

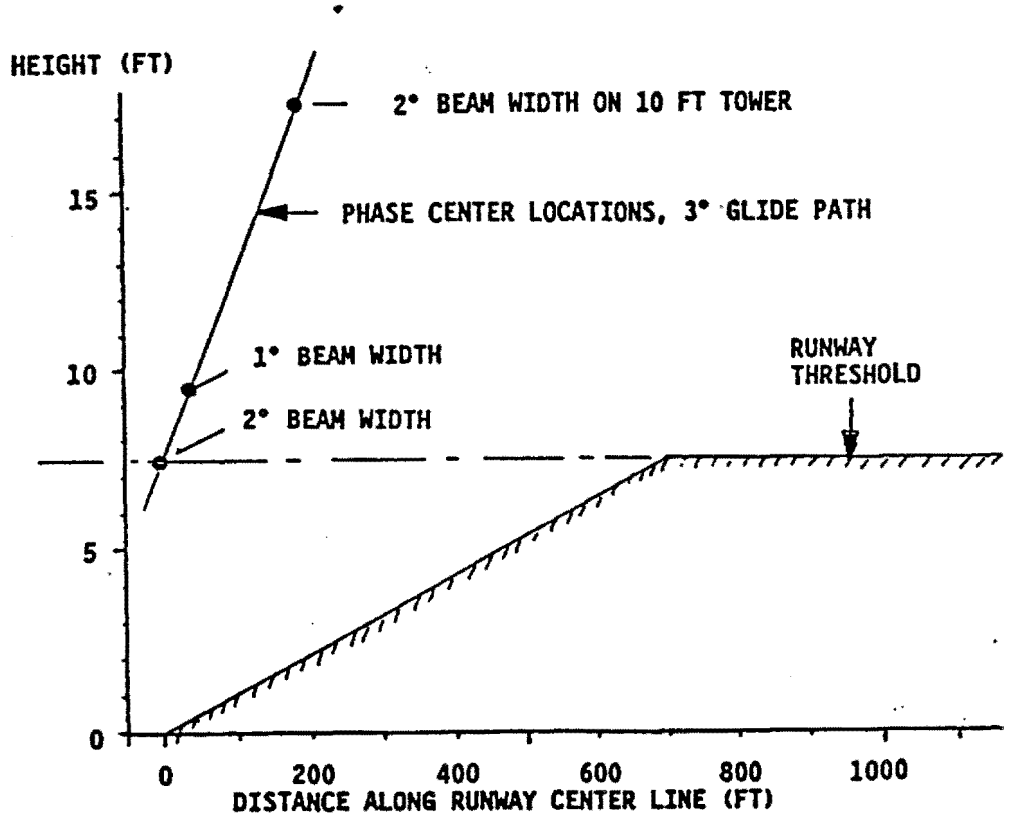


1.8 DEGREE GLIDE PATH



FOR THE FLAT TERRAIN CASE A 2° BEAMWIDTH ANTENNA CAN SATISFY THE ACCURACY REQUIREMENTS AT THE 1.8° GLIDE PATH ANGLE.

WEDGE SHAPE EXAMPLE FOR NEAR-IN TERRAIN

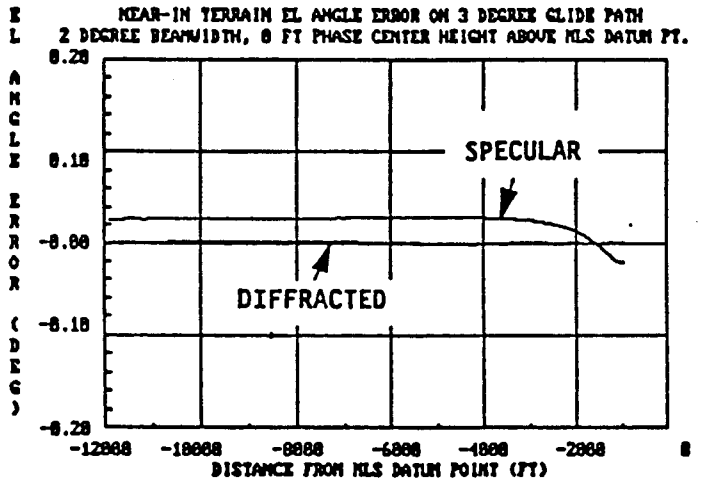


THIS EXAMPLE IS USEFUL IN COMPARING THE PERFORMANCE FOR ALTERNATIVE LOCATIONS FOR 2° BEAM WIDTH ANTENNAS AND FOR COMPARING THE PERFORMANCE OF 2° VERSUS 1° BEAM WIDTH ANTENNAS.

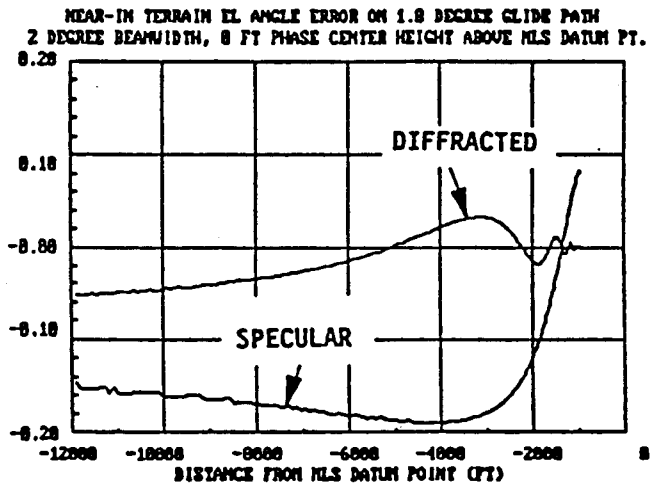
ACCURACY FOR WEDGE TERRAIN CASE

2 DEGREE BEAM WIDTH ANTENNA

3 DEGREE GLIDE PATH



1.8 DEGREE GLIDE PATH

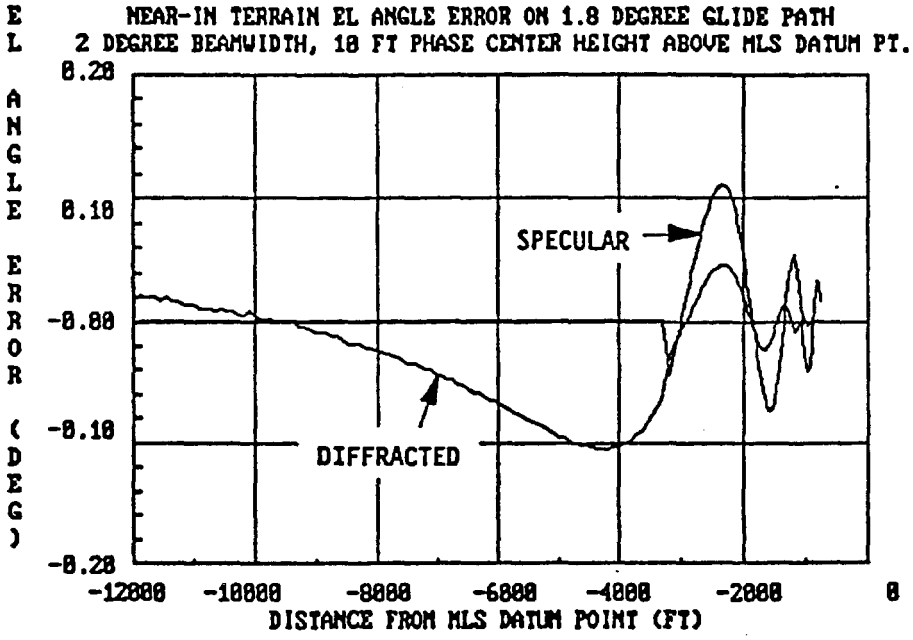


FOR THE 1.8° GLIDE PATH CASE THE SPECULAR MULTIPATH COMPONENT EXCEEDS THE PFE TOLERANCE OF 0.133°. THE RAPID VARIATION OF THE SPECULAR AND DIFFRACTED COMPONENTS NEAR THE RUNWAY THRESHOLD COULD CAUSE DECOUPLING OF AN AUTOPILOT. THIS APPARENTLY WAS THE PROBLEM EXPERIENCED BY FAA FLIGHT INSPECTION AT RICHMOND, VA ON RUNWAY 02 ON 2° GLIDE PATH APPROACHES.

ACCURACY FOR WEDGE TERRAIN CASE

2 DEGREE BEAM WIDTH ANTENNA ON 10 FT TOWER

1.8 DEGREE GLIDE PATH

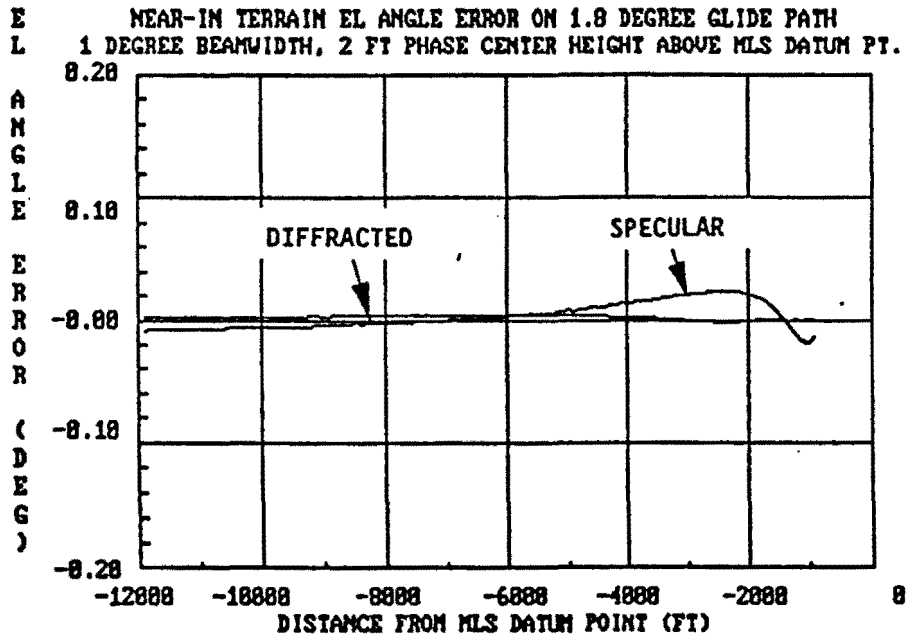


IT WAS INITIALLY THOUGHT THAT MOUNTING OF THE 2° BEAM WIDTH ANTENNA ON A 10 FT. TOWER WOULD IMPROVE THE SITUATION. HOWEVER, AS INDICATED IN THE COMPUTER SIMULATION RESULTS, THERE IS LITTLE OR NO IMPROVEMENT WITH THE ANTENNA ON A 10 FT. TOWER.

ACCURACY FOR WEDGE TERRAIN CASE

1 DEGREE BEAM WIDTH ANTENNA

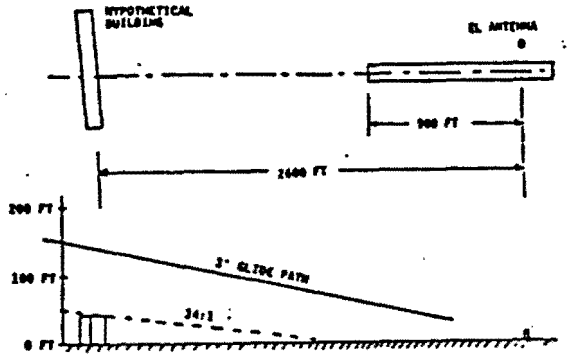
1.8 DEGREE GLIDE PATH

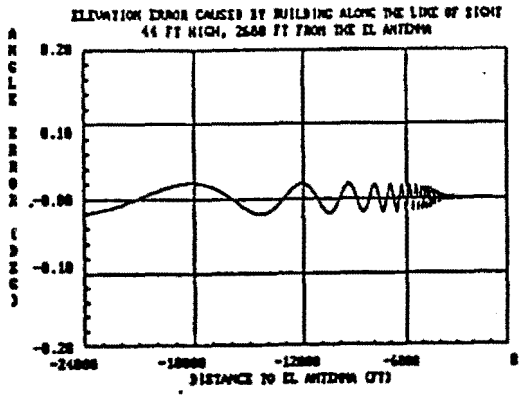


IT IS NOTED THAT THE 1° BEAM WIDTH ANTENNA SATISFIES THE ACCURACY REQUIREMENTS ON A 1.8° GLIDE PATH.

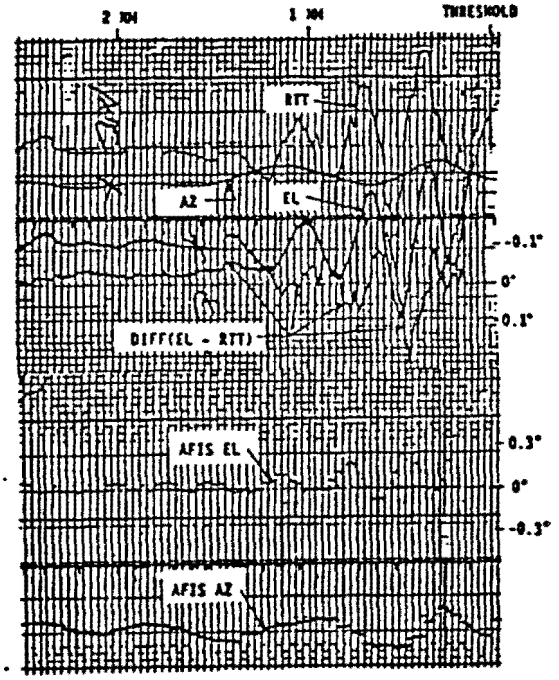
FLIGHT INSPECTION PROBLEM

CADILLAC, MI NOVEMBER 29, 1989





FLIGHT INSPECTION REPORT:
NEW BUILDING CONSTRUCTION BELOW GLIDE PATH HAS CAUSED OUT OF TOLERANCE CONDITION ON 3° GLIDE PATH.



FAA FLIGHT INSPECTION REPORTED AN EXTREME 3° GLIDE PATH STRUCTURE PROBLEM AT CADILLAC, MI DURING A FACILITY CHECK ON 11/29/89. SOME NEW CONSTRUCTION ON MAIN STREET, WHICH WAS DIRECTLY BELOW THE GLIDE PATH, WAS SUSPECTED OF BEING THE CAUSE OF THE GLIDE PATH STRUCTURE PROBLEM. A COMPUTER SIMULATION OF A WORSE CASE BUILDING BELOW THE GLIDE PATH SHOWED THAT THE ERROR SIGNATURE (MAGNITUDE AND TIME VARIATION) DID NOT MATCH THE FLIGHT INSPECTION ERROR SIGNATURE. IT WAS CONCLUDED THAT THE NEW CONSTRUCTION WAS NOT THE CAUSE OF THE GLIDE PATH STRUCTURE PROBLEM.

SUMMARY

- A KEY CONSIDERATION IN THE SITING OF THE ELEVATION ANTENNA IS THE NEAR-IN TERRAIN PROFILE ALONG THE APPROACH DIRECTION.
- A SIMPLE MODEL IS AVAILABLE FOR ESTIMATING THE ERRORS CAUSED BY THE TERRAIN AND OBSTACLES DIRECTLY BELOW THE GLIDE PATH.
- UP SLOPING NEAR-IN TERRAIN MAY CAUSE SIGNIFICANT DEGRADATION IN ACCURACY, ESPECIALLY AT THE LOWER EDGE OF THE HIGH ACCURACY COVERAGE SECTOR AND NEAR THE RUNWAY THRESHOLD.
- AT SEVERAL SITES IT MAY NOT BE POSSIBLE TO SATISFY THE ACCURACY REQUIREMENTS AT THE LOWER EDGE OF THE HIGH ACCURACY COVERAGE SECTOR WITH A 2° BEAM WIDTH ANTENNA. THE 1° BEAM WIDTH ANTENNA IS NOT LIMITED IN THIS REGARD.

JIM EVANS
LINCOLN LABORATORY, M.I.T.

MODELING CONSIDERATIONS

MLS MULTIPATH MODELING CONSIDERATIONS

- **THINK ABOUT POTENTIAL SYSTEM PROBLEMS WHEN DECIDING WHAT TO MODEL**

  AZIMUTH SHADOWING AND/OR IRREGULAR TERRAIN REFLECTIONS

  ELEVATION SHADOWING AT WIDE ANGLES

  ELEVATION MULTIPATH FROM HANGARS NEAR APPROACH END

  REFLECTIONS ON OCI AND/OR CLEARANCE

- **MAKE SIMPLE CALCULATIONS TO DECIDE WHAT IS IMPORTANT**

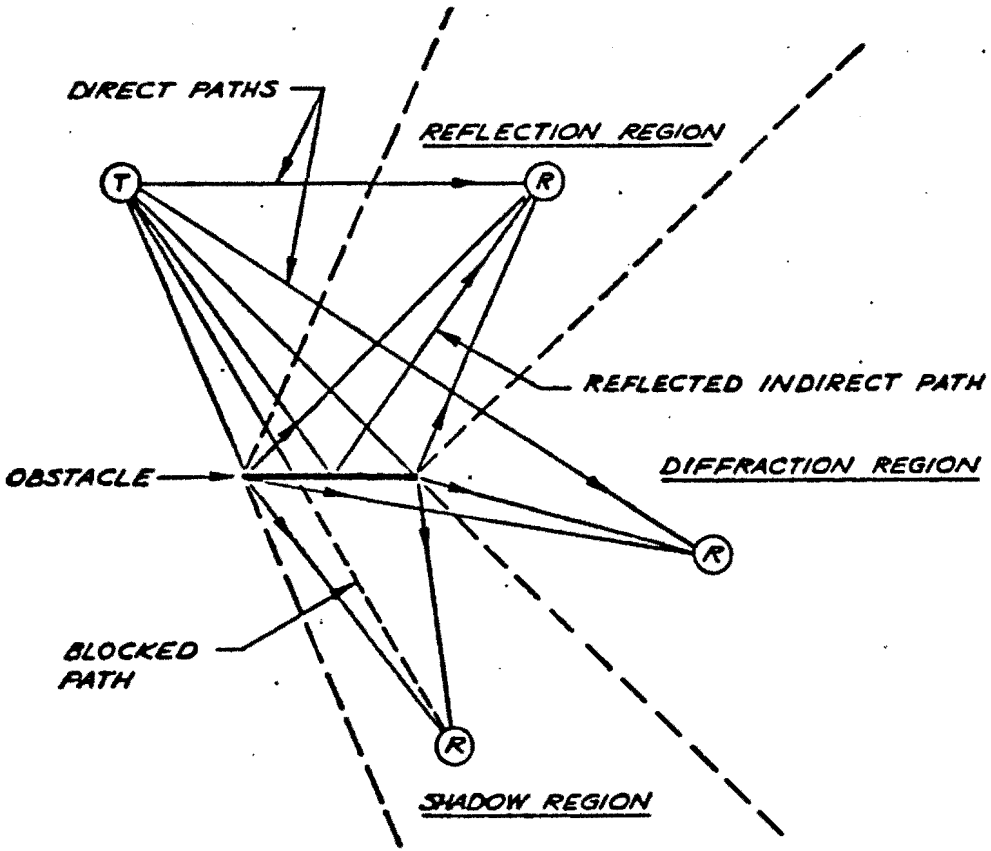
- **WATCH OUT FOR THE PROPAGATION UGLIES**

  SMALL VERTICAL POLES

  CORRUGATED HANGAR SIDES

  DIFFERENTIAL GROUND HEIGHT EFFECTS ON AZIMUTH,OCI,CLEARANCE

Hazeltine
Corporation



NOTE: ALL PATHS NOT LABELED ARE DIFFRACTED INDIRECT PATHS

720804

Figure Q-5. Shadow, Reflection and Diffraction Regions

651

INCORRECT AZIMUTH SECTOR INDICATIONS DUE TO REFLECTED SIGNALS

REFLECTED SIGNAL	REGION INTO WHICH REFLECTED SIGNAL IS ENCOUNTERED			
	SCANNING BEAM	FLY LEFT CLEARANCE	FLY RIGHT CLEARANCE	OCI
Scanning Beam	No problem if $R < 1$ Erroneous angle indication with reversed course sense if $R > 1$ for long time period (e.g., 20 secs) --- High levels of required duration are very unlikely	No problem if $R < A_{CLR}$ Possible erroneous angle indication with reversed course sense if $R > A_{CLR}$ for long time period --- Required reflector geometry may occur with corrugations		No problem if $R < A_{OCI}$ Possible erroneous angle indication with reversed course sense if $R > A_{OCI}$ for ≥ 1 second --- Required reflector geometry will occur in a number of cases and may need to be handled operationally
Fly Left Clearance	No problem if $R < 1/A_{CLR}$ Possible flag when $R > 1/A_{CLR}$ for long time period --- Required levels/durations very unlikely for "normal" values of A_{CLR}	Possible erroneous flag action if $(1-R)A_{CLR} < A'_{OCI}$ Possible erroneous angle indication if $(1-R)A_{CLR} < SL$ and $(1-R)A'_{OCI} < SL$ --- Required reflector geometry is very rare. Motion averaging reduces likelihood of erroneous indication even further.	Possible erroneous clearance indication if $R > 1$ for long time period --- Required levels/durations are unlikely.	Possible erroneous flag indication if $R > A_{OCI} - A'_{CLR})/(A_{CLR} + A'_{OCI})$ for over 1 second --- Required reflector geometry will occur in a number of cases.
OCI	No problem if $R < 1/A_{OCI}$ Possible flag when $R > 1/A_{OCI}$ for over 1 second --- Required levels/durations very unlikely for "normal" values of A_{OCI}	Possible flag when $R > A_{CLR} - A'_{OCI}/(A_{OCI} + A_{CLR})$ for over 1 second --- Required levels and durations are unlikely		Possible erroneous flag action when $(1-R)A_{OCI} < SL$ or $(1-R)A_{OCI} < A'_{CLR}$ for over 1 second --- Required levels/durations unlikely (esp. for scanning beam sidelobes)

A_{CLR} = clearance signal peak level wrt SB peak level

A'_{CLR} = clearance signal peak level in OCI region wrt SB peak level

R = reflected signal level wrt direct signal

A_{OCI} = OCI signal peak level wrt SB peak level

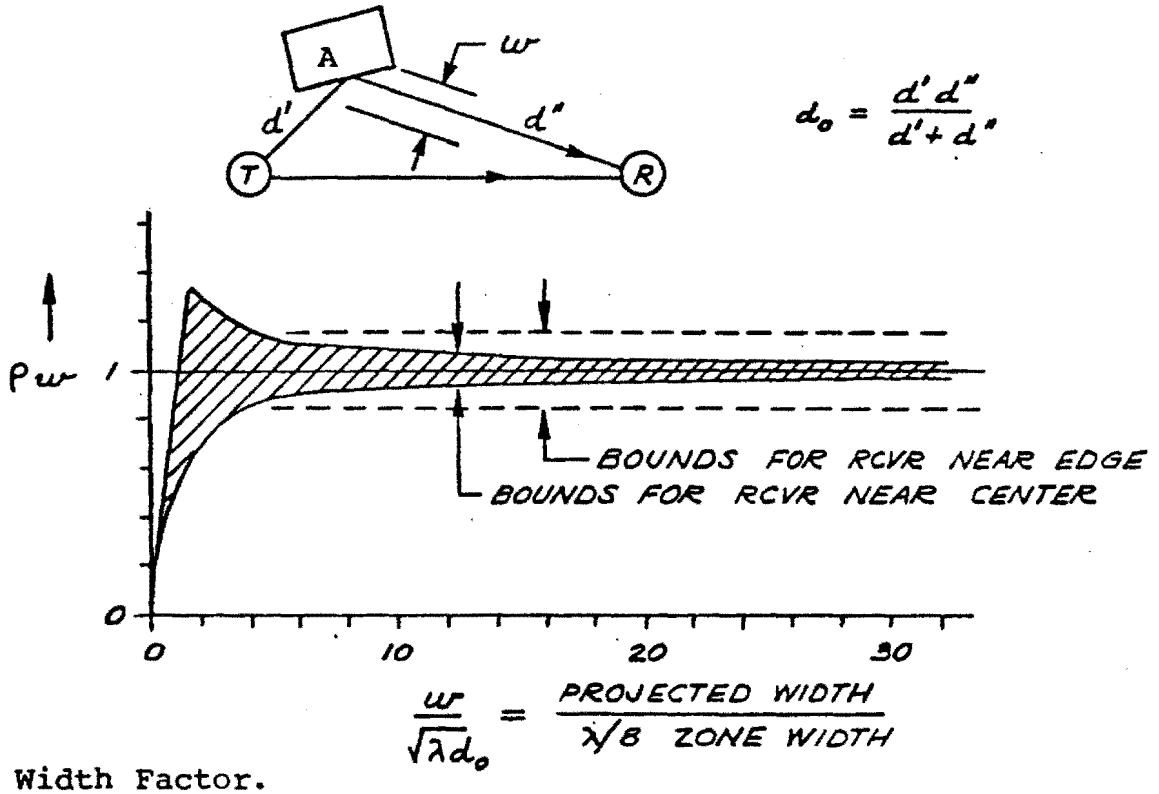
SL = scanning beam sidelobe level in clearance and OCI sectors

A'_{OCI} = OCI signal level in clearance region wrt SB peak level

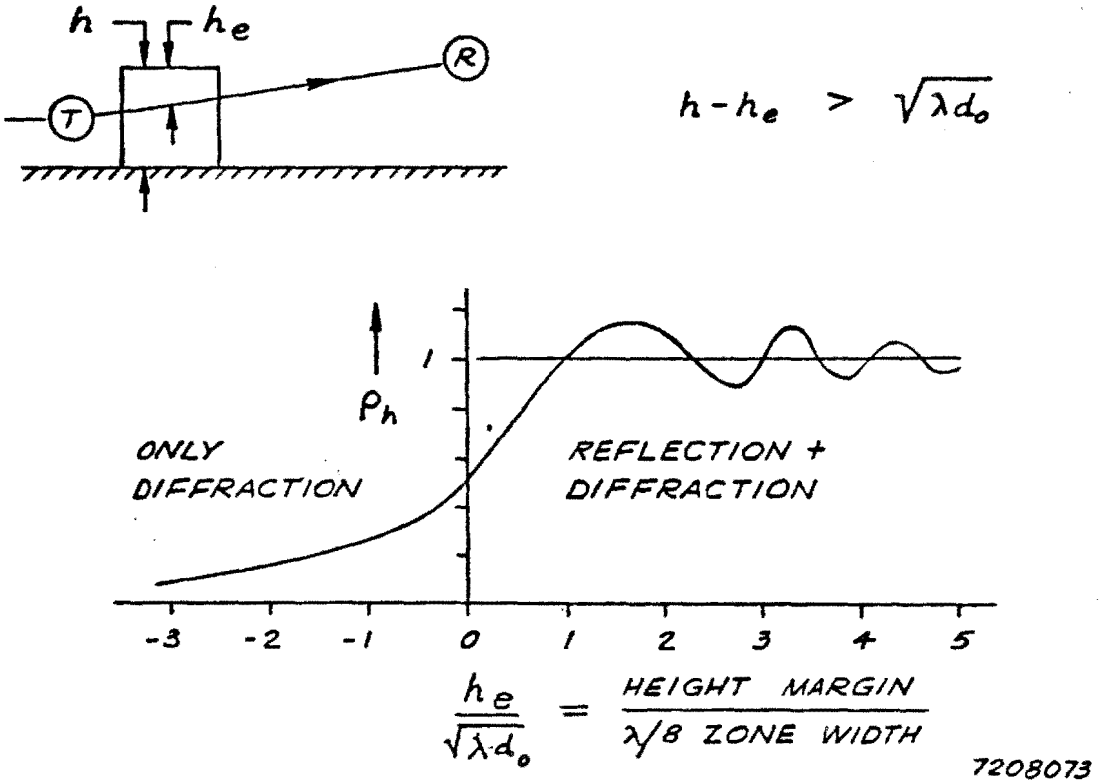
091

SIMPLE EXPRESSIONS FOR MULTIPATH REFLECTION AND DIFFRACTION LEVELS

USE THESE TO BOUND THE PROBLEM BEFORE MAKING A DETAILED SITE SURVEY



(a) Width Factor.

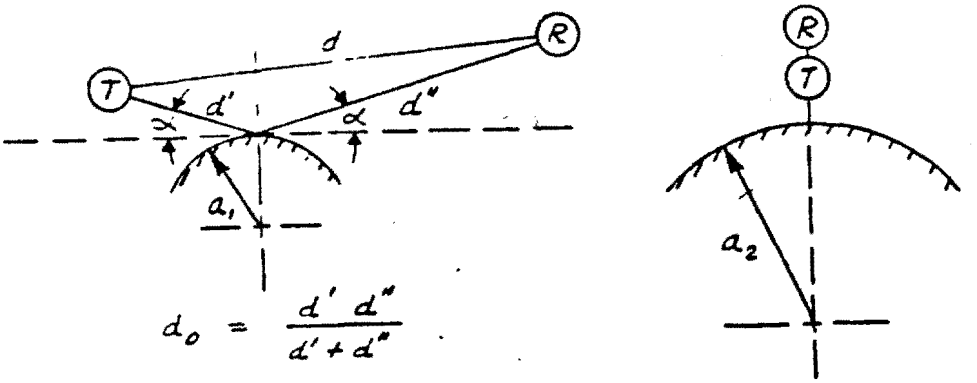


(b) Height Factor.

Figure Q-12. Reflection Factors for a Rectangular Plane Vertical Wall

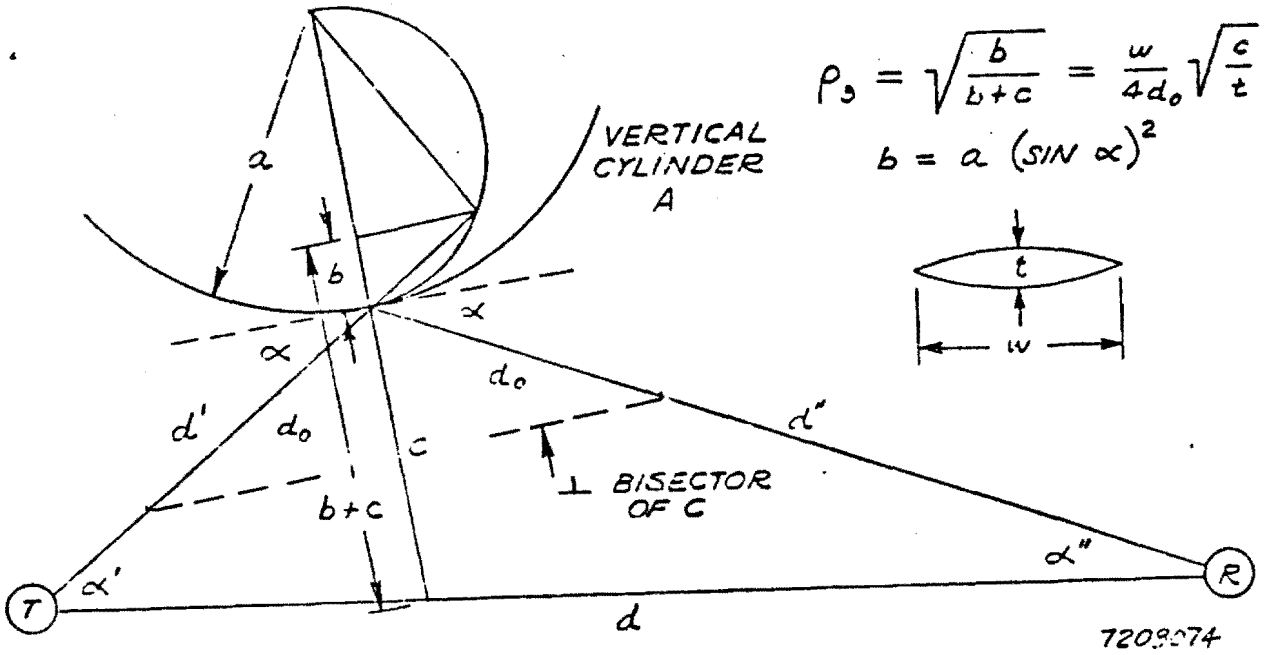
CORRUGATED BUILDINGS - A MAJOR PROBLEM IN ESTIMATING THE LOCATION OF MULTIPATH REFLECTIONS

- HOW OFTEN DO THEY OCCUR
- WHAT IS THE NATURE OF THE CORRUGATION
- AN EXAMPLE OF EXPERIMENTAL VALIDATION



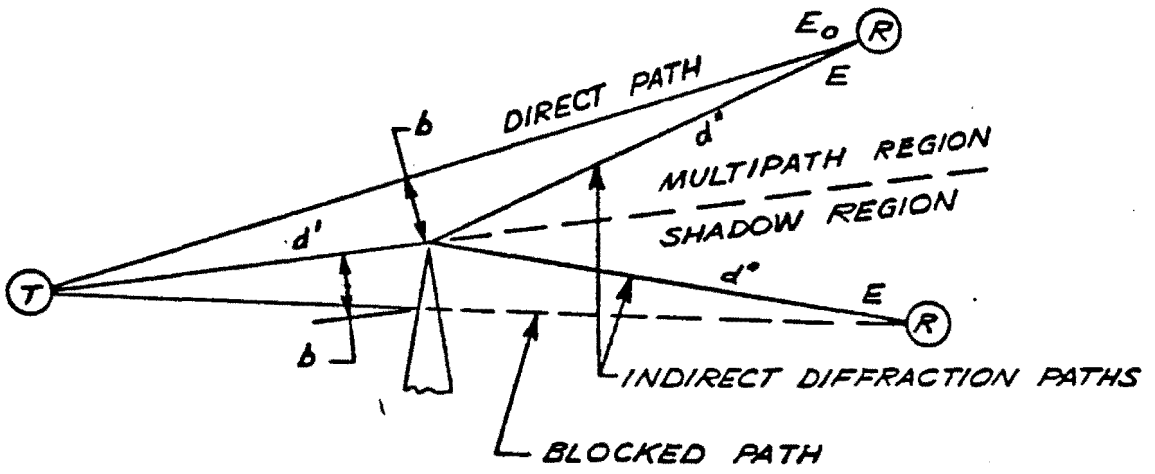
$$\rho_3 = \sqrt{\frac{1}{\left[1 + \frac{2d_o}{a_1 \sin\alpha}\right]\left[1 + \frac{2d_o \sin\alpha}{a_2}\right]}}$$

(a) Formula for Doubly Convex Surface.

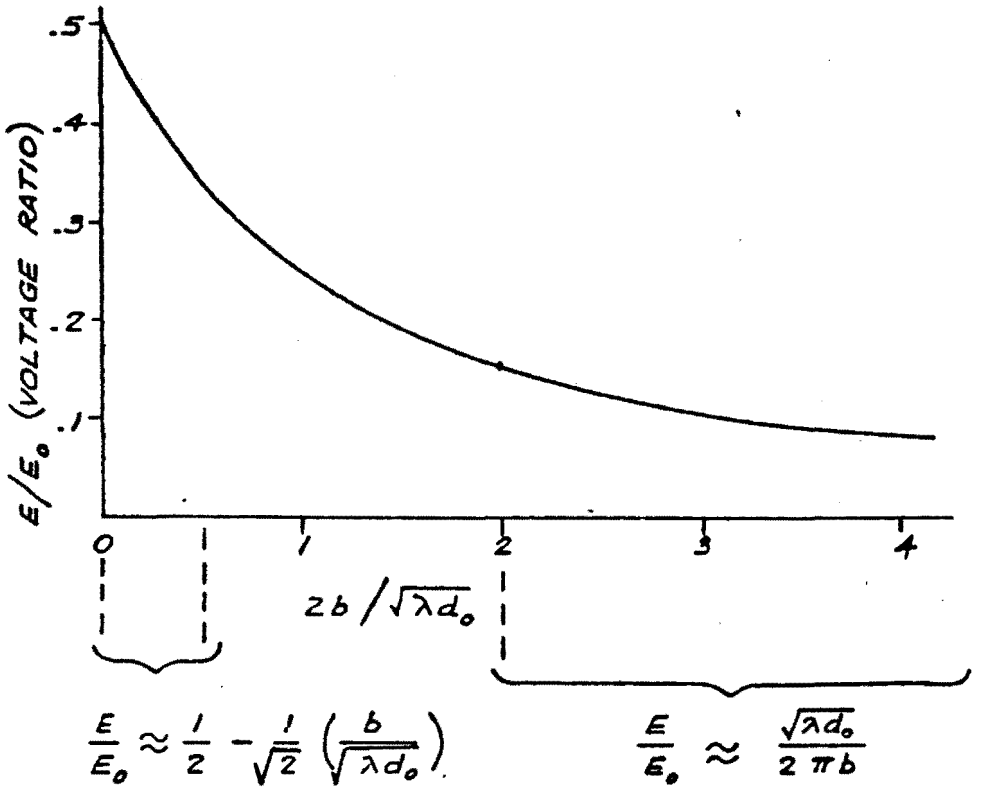


(b) Geometrical Evaluation for Convex Tail Fin.

Figure Q-13. Reflection Factor for a Convex Surface



$$\text{EFFECTIVE DISTANCE} = d_o = \frac{d'\,d''}{d'+d''} \quad \begin{cases} >> b \\ >> \lambda \end{cases}$$



$$\frac{E}{E_o} \approx \frac{1}{2} - \frac{1}{\sqrt{2}}\left(\frac{b}{\sqrt{\lambda d_o}}\right) \qquad \frac{E}{E_o} \approx \frac{\sqrt{\lambda d_o}}{2\pi b}$$

HEIGHT DIFFERENCE BETWEEN EDGE AND STRAIGHT LINE RELATIVE TO 1/2 OF WIDTH OF λ/8 ZONE

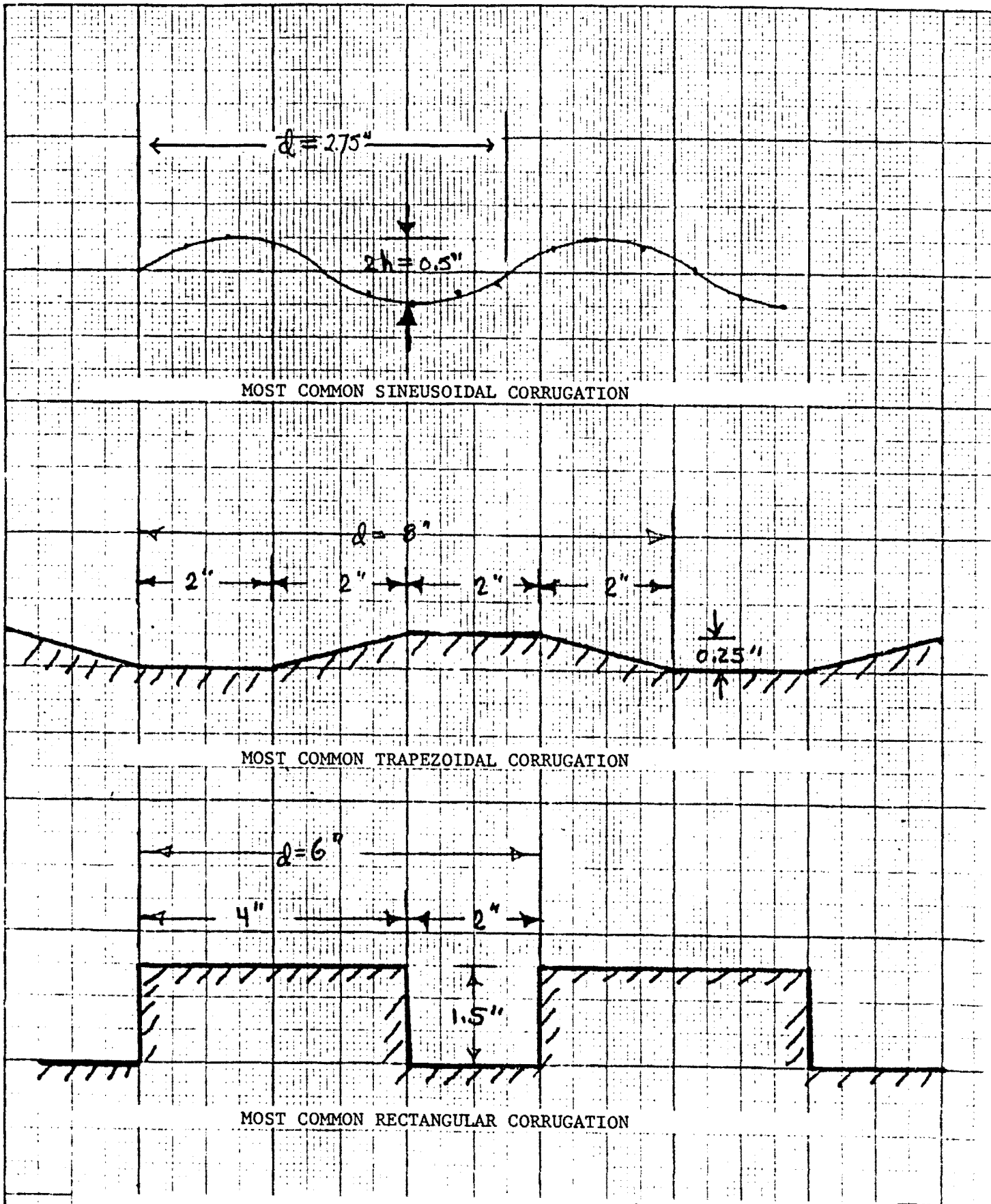
7208067

Figure Q-9. Forward Diffraction from Horizontal Edge, Downward in Shadow or Upward in Multipath Region

TABLE F-1

BUILDING SURFACE TYPE DISTRIBUTION
AT MLS MULTIPATH SURVEY AIRPORTS [12]

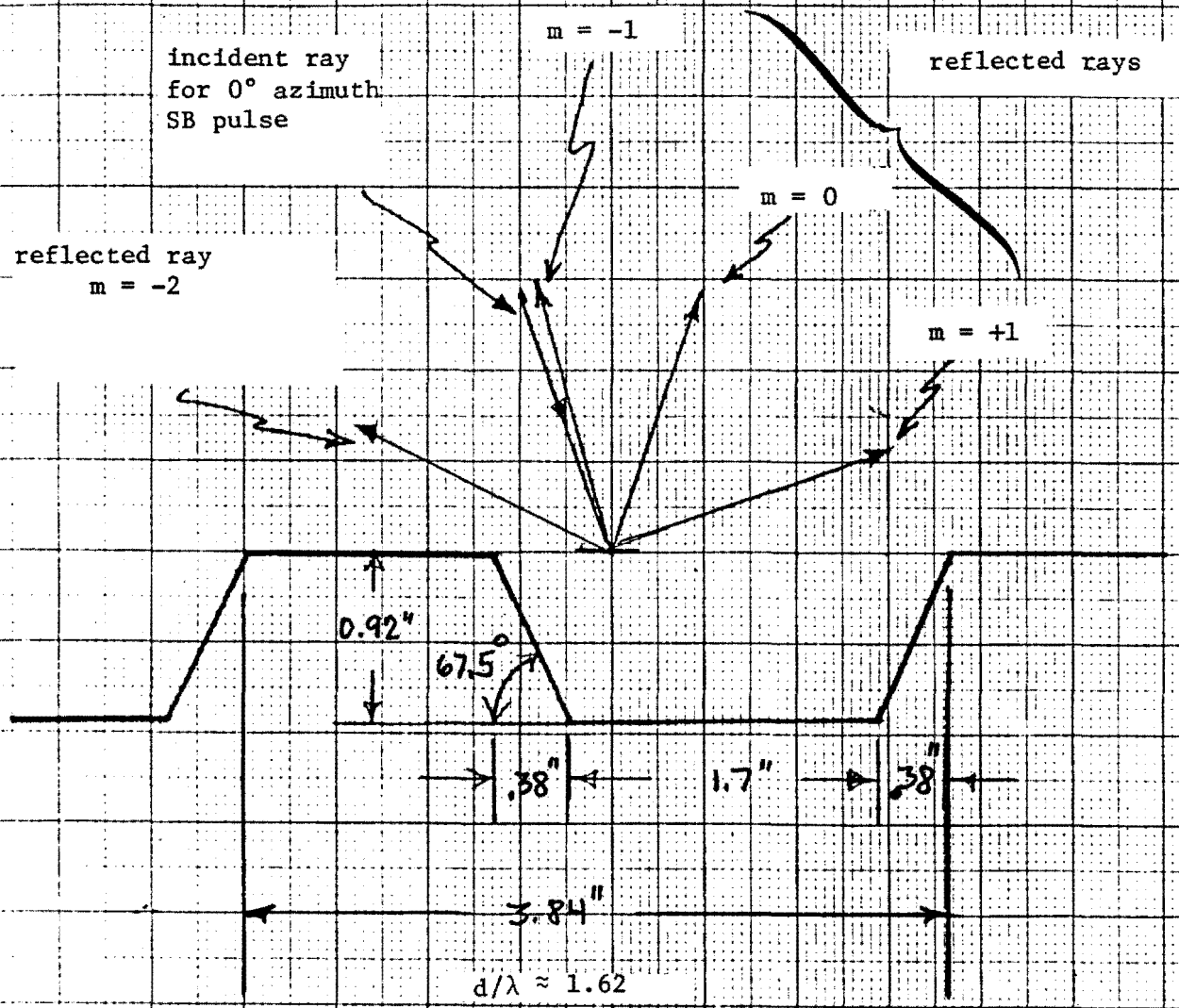
Airport	Buildings	Surfaces	Corru-gated	Cinder Block	Brick	Concrete	Smooth Metal
JFK	19	28	13	3	7	1	4
PHL	12	17	11	3	2	1	
ORD	14	19	14	1	4		
LAX	11	15	9	1		4	1
SFO	4	4	3		1		
MIA	17	20	10	6	1	3	
TUL	10	12	9	2	1	1	
MSP	6	8	5	1		1	1
TOTALS	93	123	74	17	16	11	6



F-2

Fig. ~~2~~ Most common periodic corrugations encountered in MLS airport survey.

F-5



F-8

Fig. ~~2-10~~ Hangar 301 door corrugation profile.

Point a = nearest corner of wall with doors $\theta_i = 11°$

Point b = SB scan limit. $\theta_i = 34°$

	MODE	θ_r	AZIMUTH IN x-y COORDINATE SYSTEM	MLS AZIMUTH
a	0	11°	169°	150°
	+1	53°	127°	108°
	-1	-25°	-155°	-174°
	-2	-90°	-90°	-109°
b	0	34°	149°	130°
	+1	90° *	90°	71°
	-1	- 6°	-174°	+166°
	-2	-46°	-134°	-153°

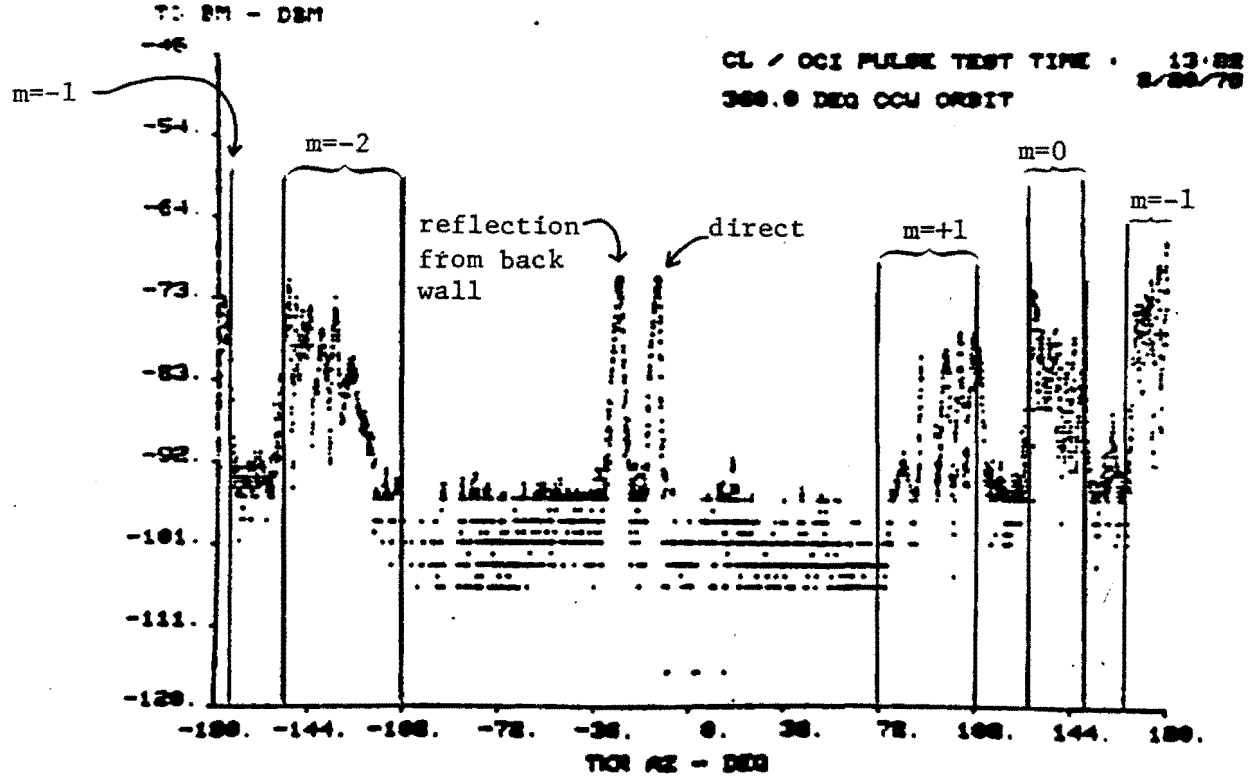
*90° value applies for $\theta_i = 22.6°$ corresponding to a MLS azimuth of +3.6° (i.e., doors corresponding to MLS azimuths from +3.6° to +12° do not have reflection mode +1 for experiment geometry).

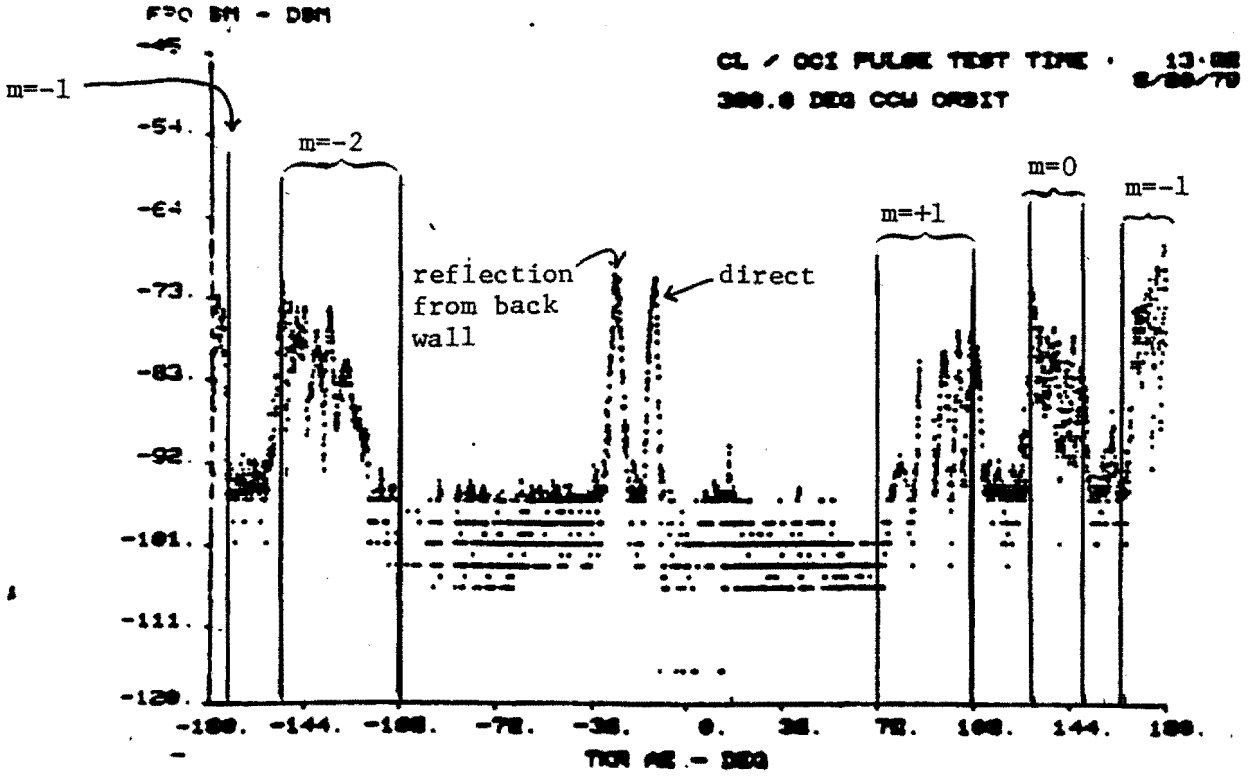
F

TABLE Z-2

COMPUTATION OF SCANNING BEAM REFLECTION REGIONS
FOR HANGAR 301 DOORS

M F-13





F-9

Fig. 2-1 Scanning beam amplitudes on orbital flight 8/20/79.

SUMMARY ON CORRUGATED HANGARS

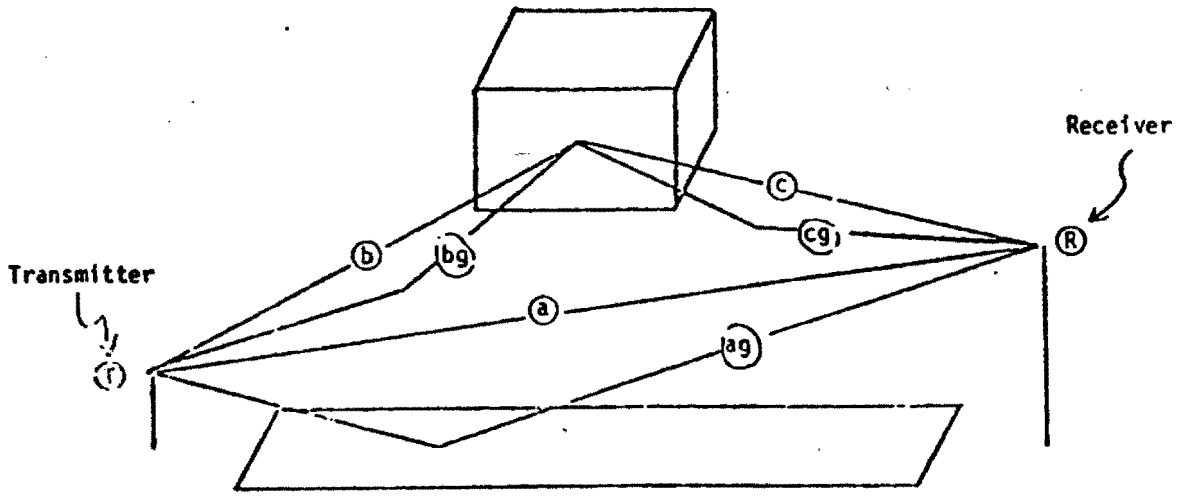
- REFLECTION REGIONS CAN BE PREDICTED FAIRLY EASILY

- PREDICTING THE REFLECTION AMPLITUDE IS A HARD PROBLEM-

    GDT IS NOT APPLICABLE TO THIS CASE SINCE CORRUGATION PERIOD IS COMPARABLE TO WAVELENGTH

    SOMEONE SHOULD REVIEW RECENT PROGRESS IN NUMERICAL COMPUTATIONS

- THE CURRENT MLS PROPAGATION MODEL WILL NOT HANDLE WIDTH FACTOR CALCULATION PROPERLY - THIS WOULD BE A NICE GRADUATE THESIS



Measured "DIRECT" signal level depends on paths a and ag

Measured "MULTIPATH" signal level depends on paths b, bg, c, cg

H-1

Fig. ~~6~~ Role of ground reflections in determining multipath/direct amplitude ratio.

JAN-HEIN VAN DRONKELAAR
NLR

A SPECIAL APPLICATION

MLS MATHEMATICAL MODEL

A SPECIAL APPLICATION

by

JAN-HEIN VAN DRONKELAAR

for

MLS MATHEMATICAL MODEL USERS GROUP MEETING

ATLANTIC CITY, JUNE 27 AND 28, 1990

FAAMMM01



Nationaal Lucht- en Ruimtevaartlaboratorium



National Aerospace Laboratory

FAAMMM02

S41 175



THE NATIONAL AEROSPACE LABORATORY NLR
IS THE CENTRAL INSTITUTE IN THE
NETHERLANDS FOR AEROSPACE RESEARCH

365-02

PRINCIPAL MISSION
TO RENDER SCIENTIFIC SUPPORT AND TECHNICAL ASSISTANCE ON A NON-PROFIT BASIS TO DUTCH AND FOREIGN

- AEROSPACE INDUSTRIES AND ORGANIZATIONS
- CIVIL AND MILITARY AIRCRAFT OPERATORS
- GOVERNMENTAL AGENCIES CONCERNED WITH AVIATION AND SPACE FLIGHT

365-03

FLIGHT DIVISION

Departments:

- **Aircraft instrumentation**
- **Air traffic control and avionics**
- **Operations research**
- **Flying qualities and flight simulation**
- **Flight testing and helicopters**

841

380-07

FLIGHT DIVISION

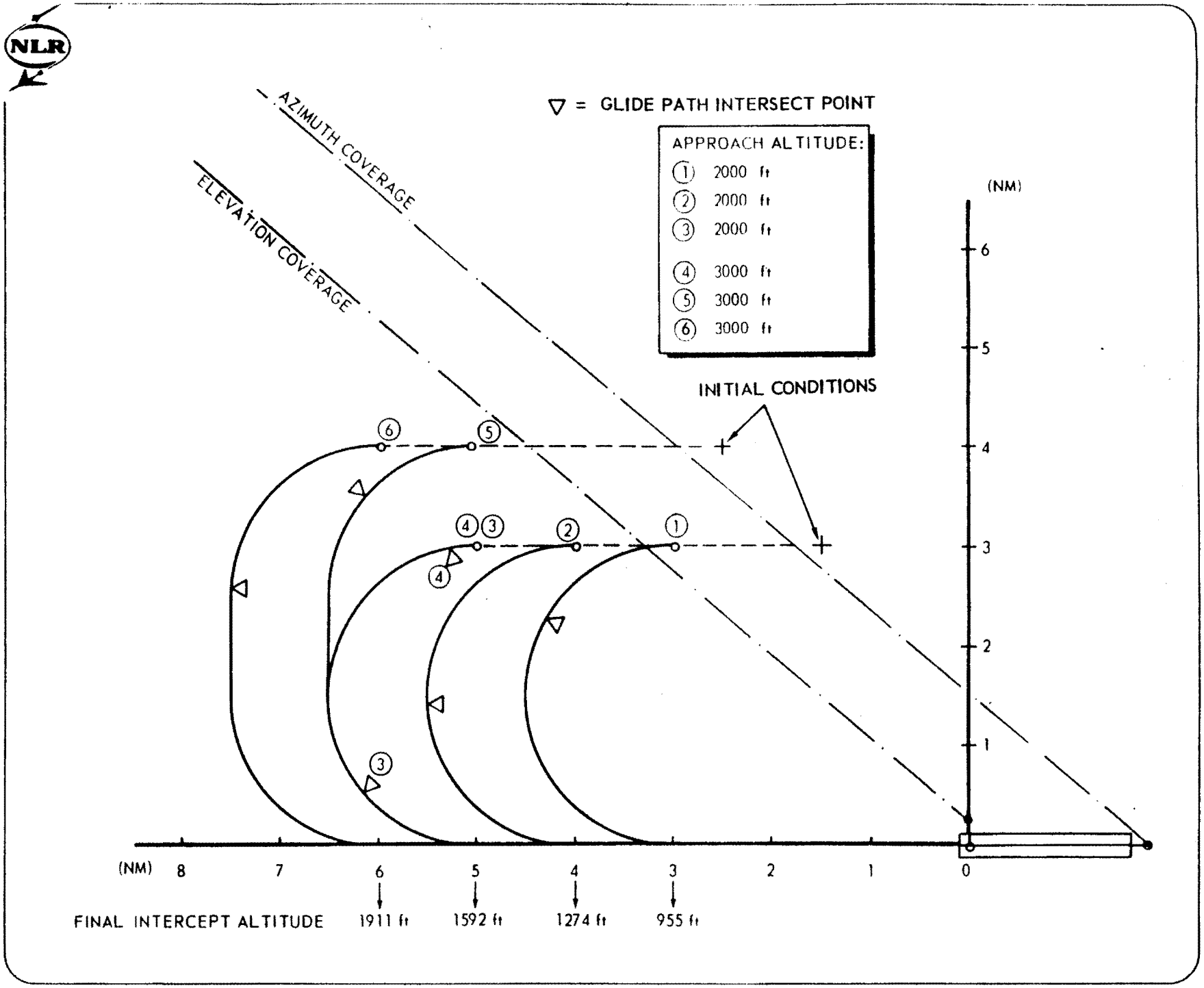
Research areas :

- Handling qualities aircraft / hellcopters
- Performance analysis
- Aircraft systems / Ground equipment
- Avionics
- Flight-testing - Methods / Equipment / Data processing
- Operational Research
- Weapons / Stores certification
- Air Traffic Control
- Human Factors Engineering
- Flight simulator applications

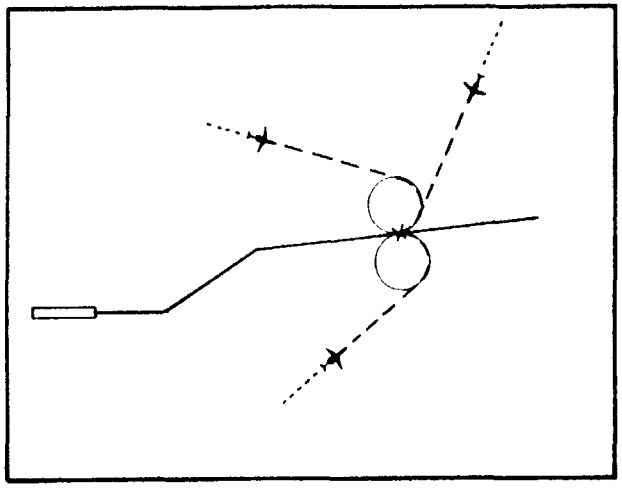
382-009

Flight Simulations on:

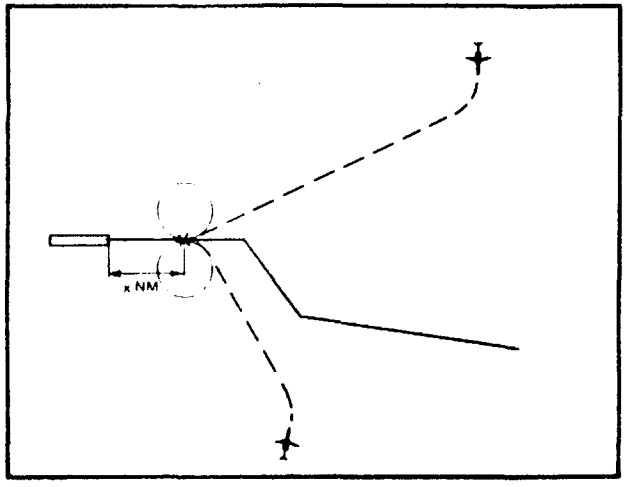
- Laterally curved (segmented) approaches
- MLS interception procedures
- Approach path parameters for curved approaches
- MLS (curved and segmented) departures
- MLS curved approach paths (FAA)


AZIMUTH COVERAGE
ELEVATION COVERAGE
▽ = GLIDE PATH INTERSECT POINT
APPROACH ALTITUDE:
① 2000 ft
② 2000 ft
③ 2000 ft
④ 3000 ft
⑤ 3000 ft
⑥ 3000 ft
INITIAL CONDITIONS
(NM)
6
5
4
3
2
1
0
(NM) 8 7 6 5 4 3 2 1 0
FINAL INTERCEPT ALTITUDE 1911 ft 1592 ft 1274 ft 955 ft

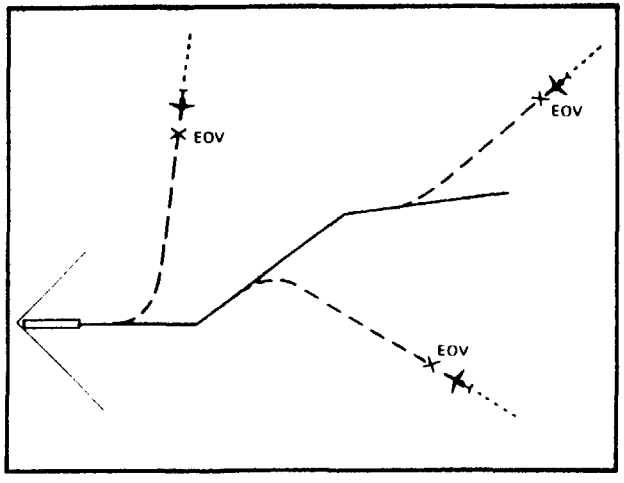
181



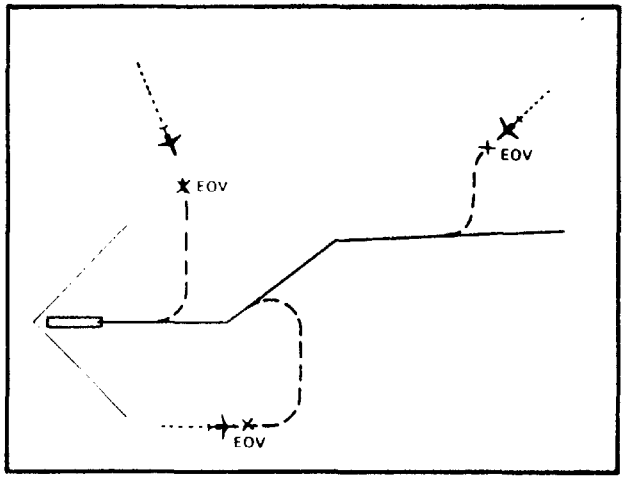
a) Procedural interception



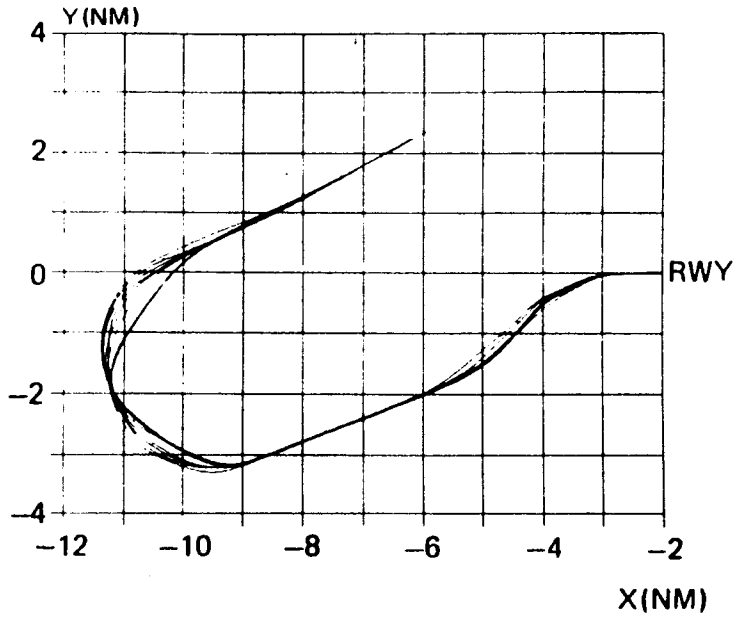
b) Minimum fuel and time interception

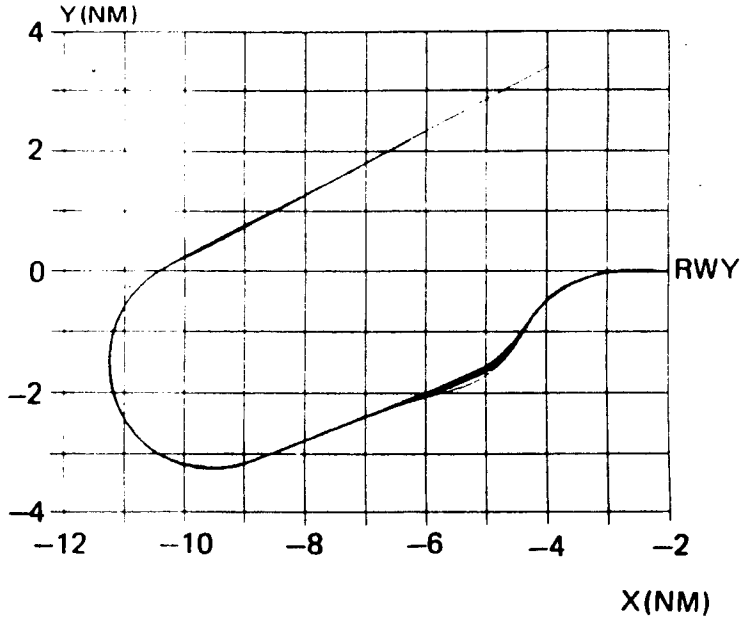


c) Present track interception



d) Fixed angle interception


Y(NM)
4
2
0
−2
−4
−12
−10
−8
−6
−4
−2
RWY
X(NM)


Y(NM)
4
2
0
−2
−4
−12
−10
−8
−6
−4
−2
RWY
X(NM)

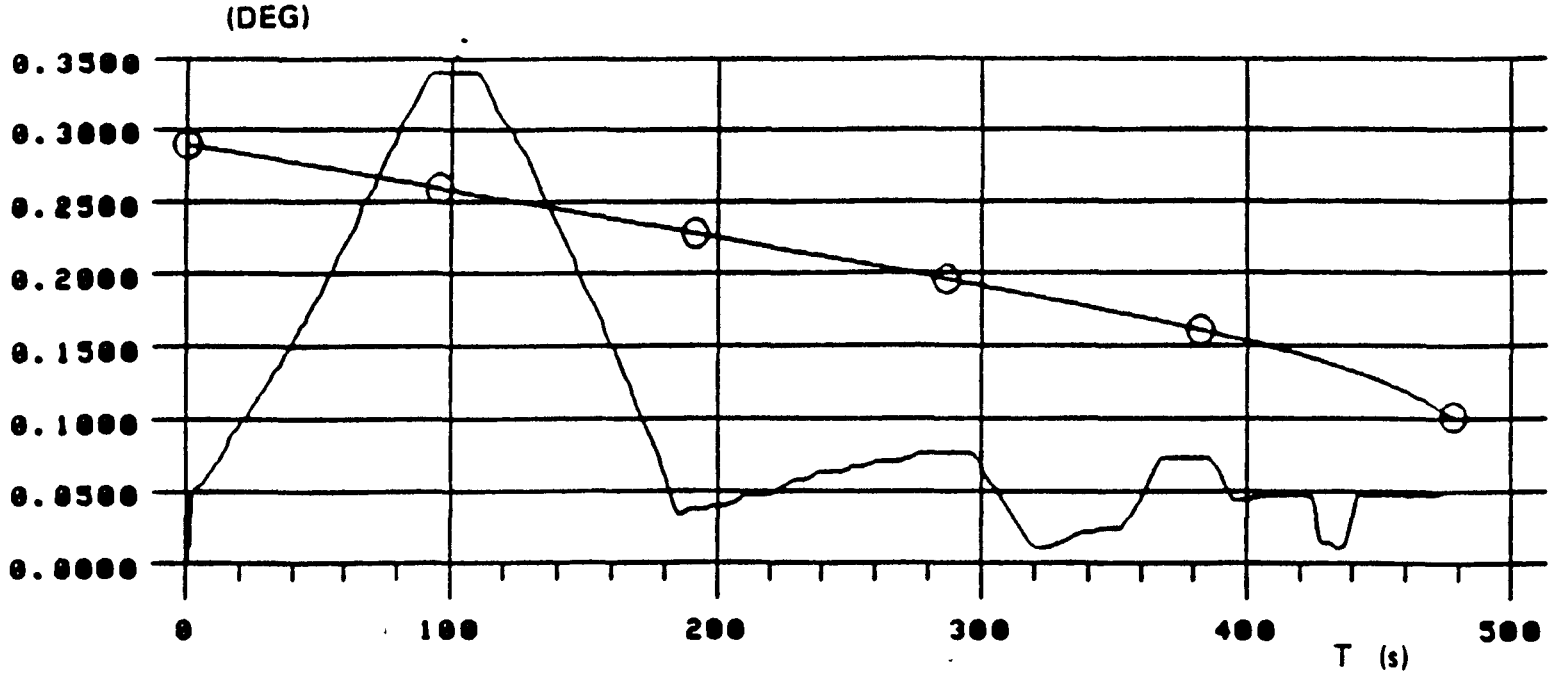
MLS Mathematical Model at NLR

- Implementation
- Validation wrt ICAO Annex 10 limits
- Validation wrt Flight Test Data
- Use in Flight Simulations

FAA/MMDA

481

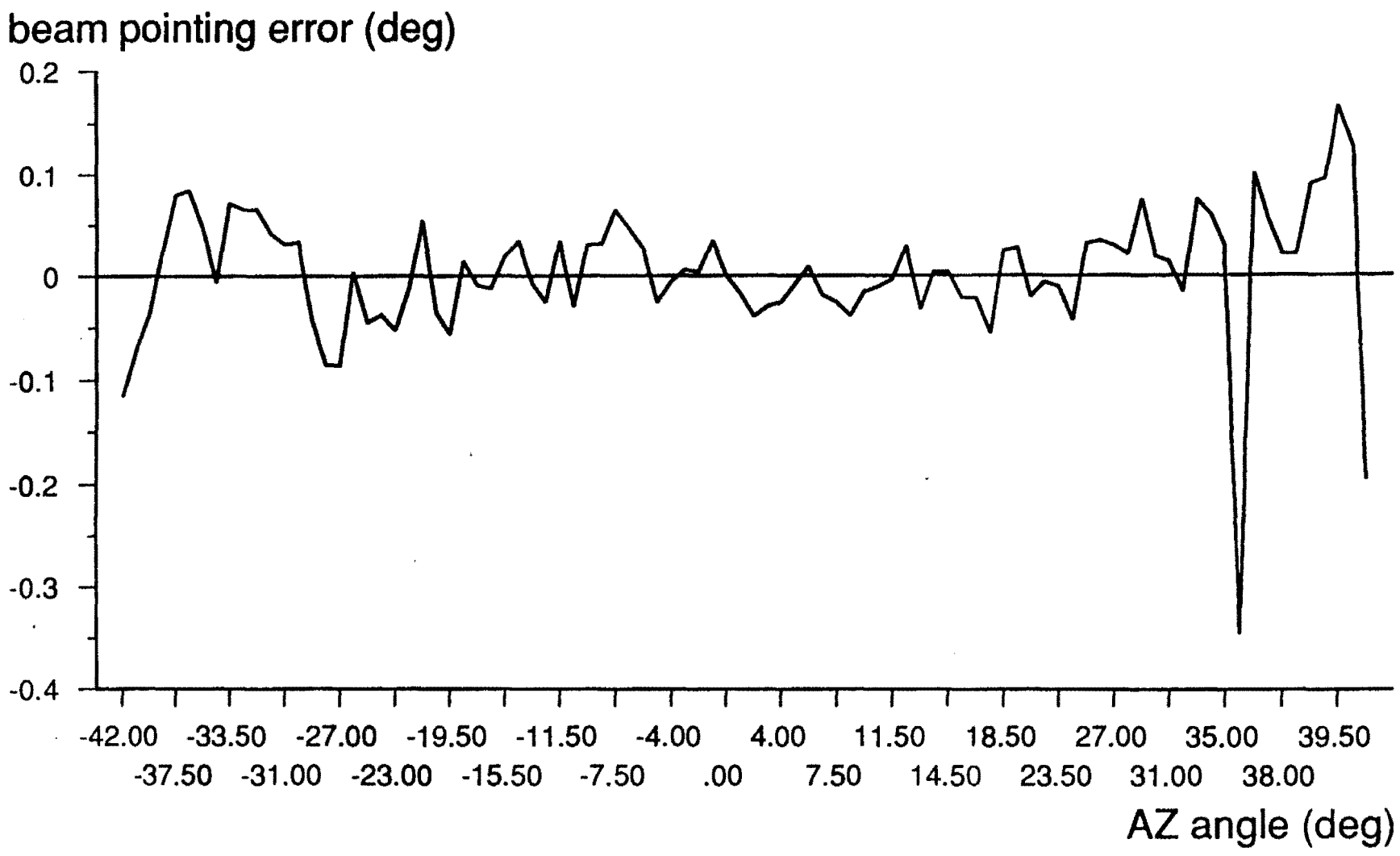
COMPARISON MODEL vs ICAO LIMITS



AZIMUTH Path Following Error

5981

AZIMUTH BEAM POINTING ERROR



FAAMMM05

9811

MATHEMATICAL MODEL vs FLIGHT TEST DATA

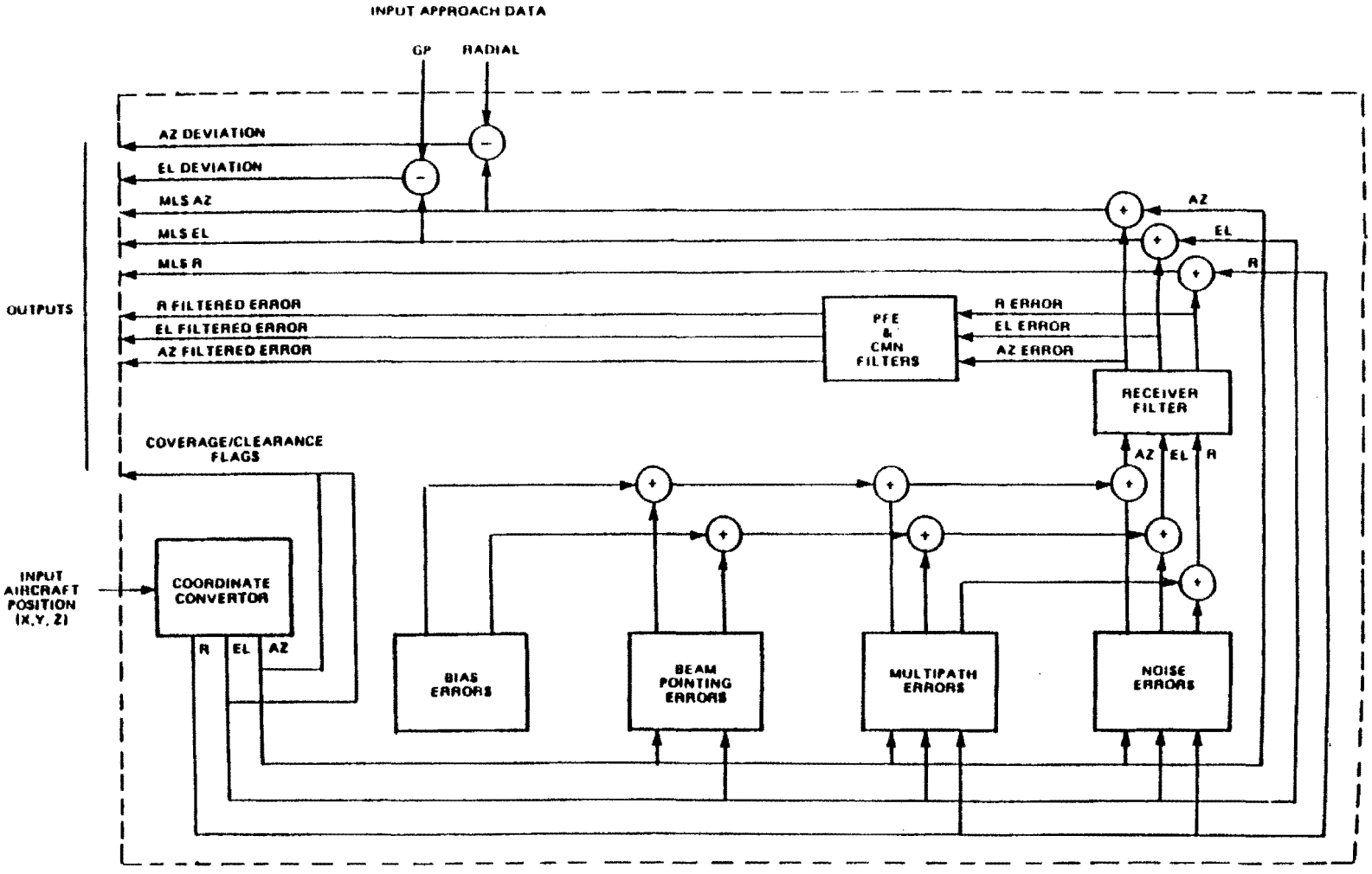
- **AZIMUTH** — **CMN comparable with flight test data**

  PFE somewhat smaller than flight test data

- **ELEVATION** — **CMN somewhat larger than flight test data**

  PFE somewhat larger than flight test data

MLS Mathematical Model Scheme



MLS Mathematical Model Error Components

- **AZIMUTH**
  - bias
  - beam pointing error
  - noise
- **ELEVATION**
  - bias
  - beam pointing error
  - multi-path error
  - noise
- **DME**
  - noise

FAAMMM07

IMPLEMENTATION

Irregularities in the Mathematical Model

- Wrong corner frequencies of PFE filter
- Possibility of mixing units
- Wrong computation of distance A/C - AZ transmitter
- Unnecessary statements in function MYASIN
- Possibility of wrong AZ flags

061

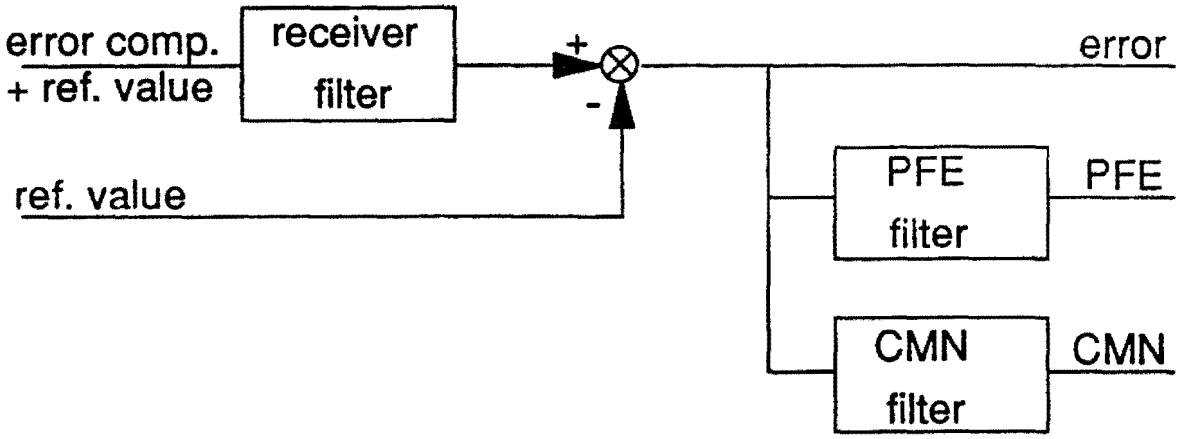
IMPLEMENTATION

Irregularities in the Mathematical Model

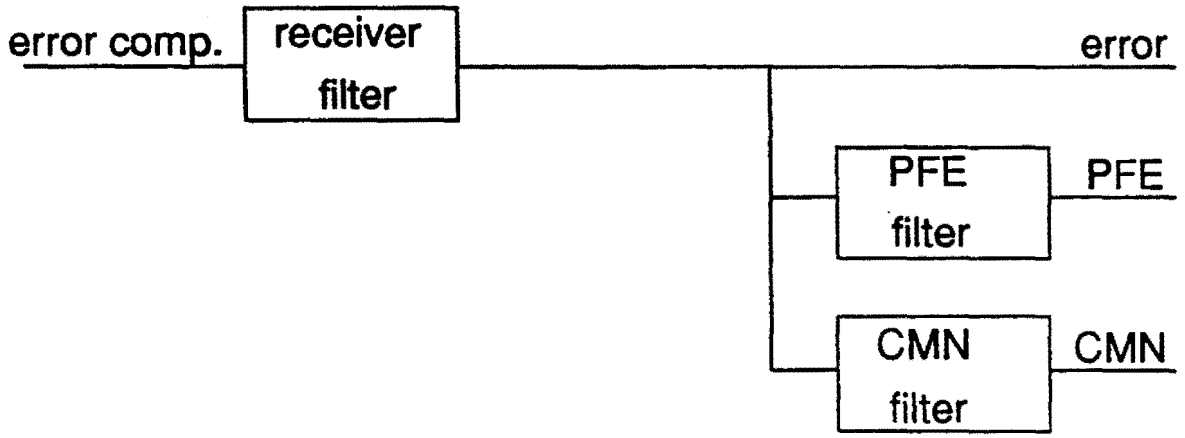
CONT'D

- Limited coverage of AZ beam pointing error table
- Noise exceeds maximum only in less than 3%
- Initialisation of high-pass (CMN) filter
- Input for receiver filter not correct

ICAO


error comp.
+ ref. value
receiver filter
+
-
error
ref. value
PFE filter
PFE
CMN filter
CMN

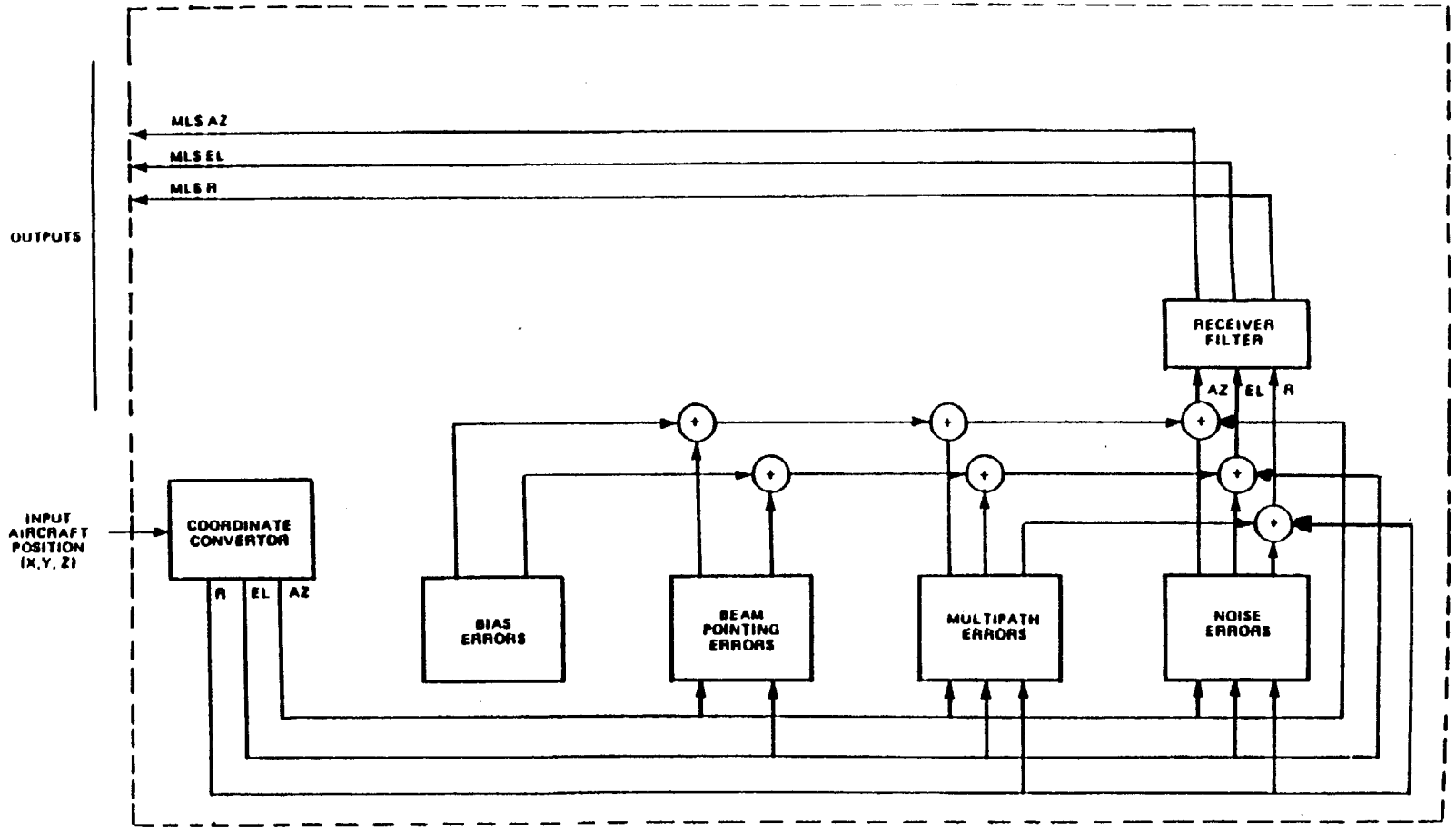
MODEL


error comp.
receiver filter
error
PFE filter
PFE
CMN filter
CMN

PARTS DELETED FOR FLIGHT SIMULATION

- coverage / clearance flags
- PFE and CMN filters
- Reference AZ radial and Glide Slope

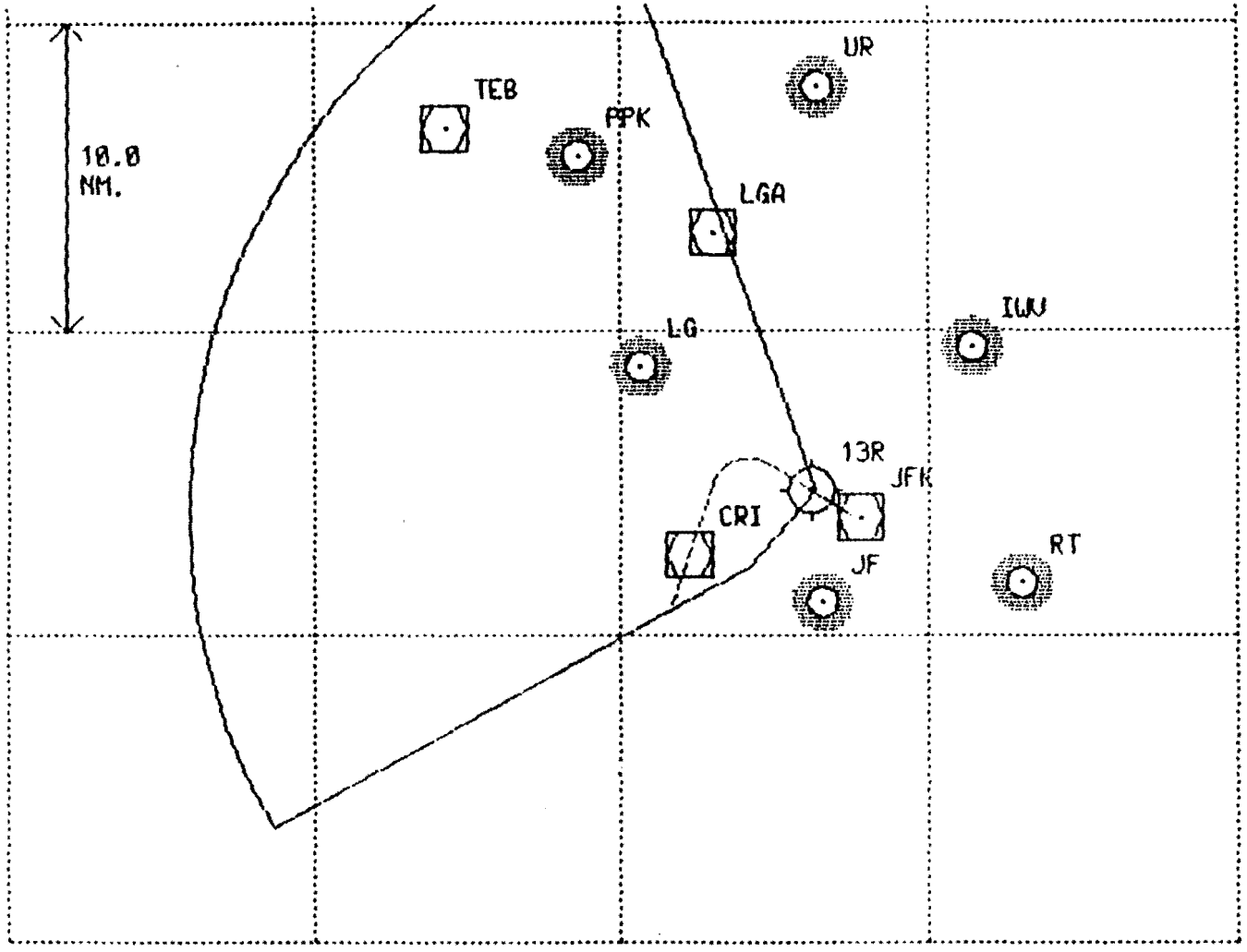
Implemented MLS Mathematical Model



PARTS MODIFIED FOR FLIGHT SIMULATION

- Extension of AZ beam pointing table range
- Calculation of AZ angle
- BAZ application
- Splitting up program

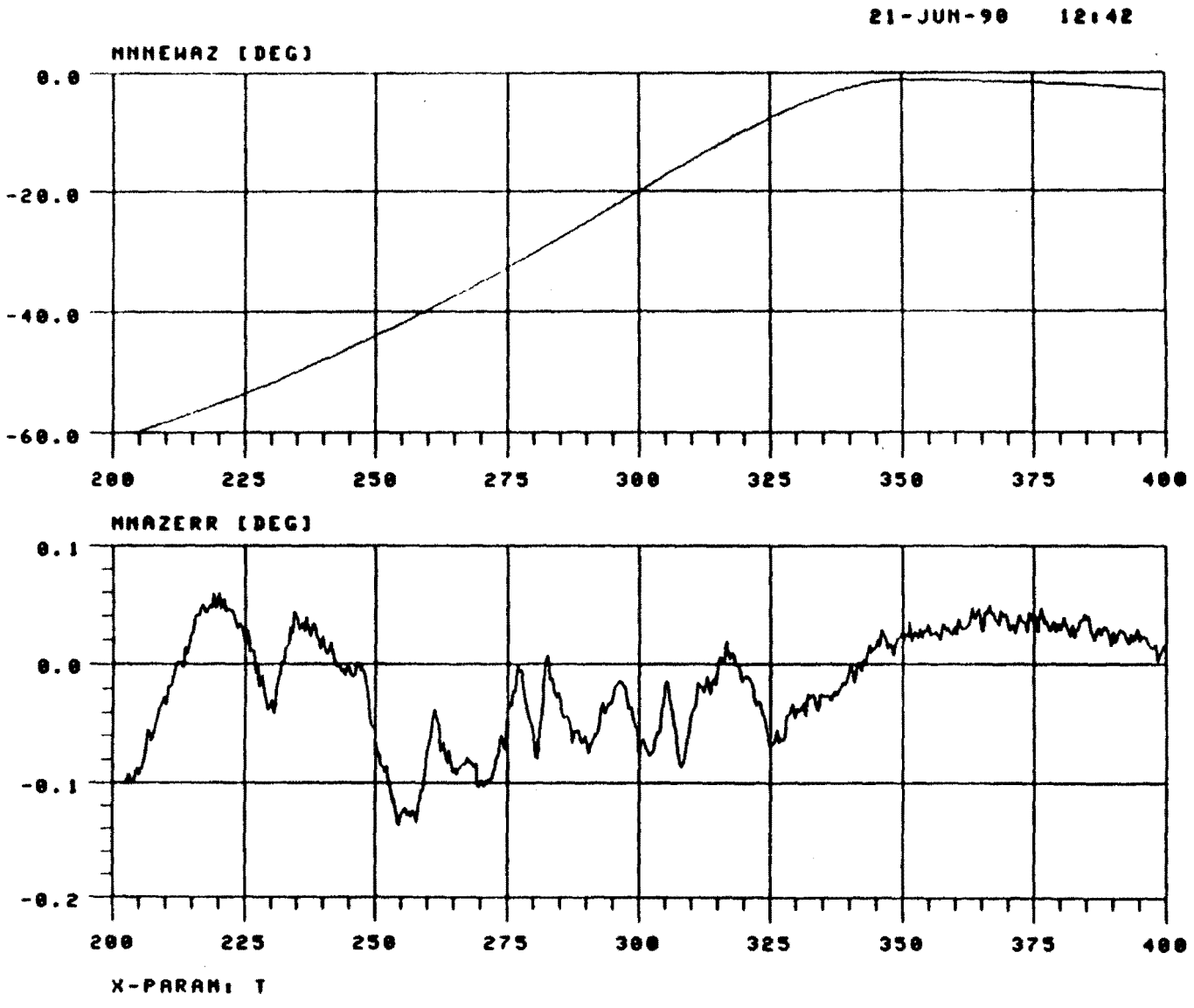
JFK 13R CANARSIE APPROACH



961

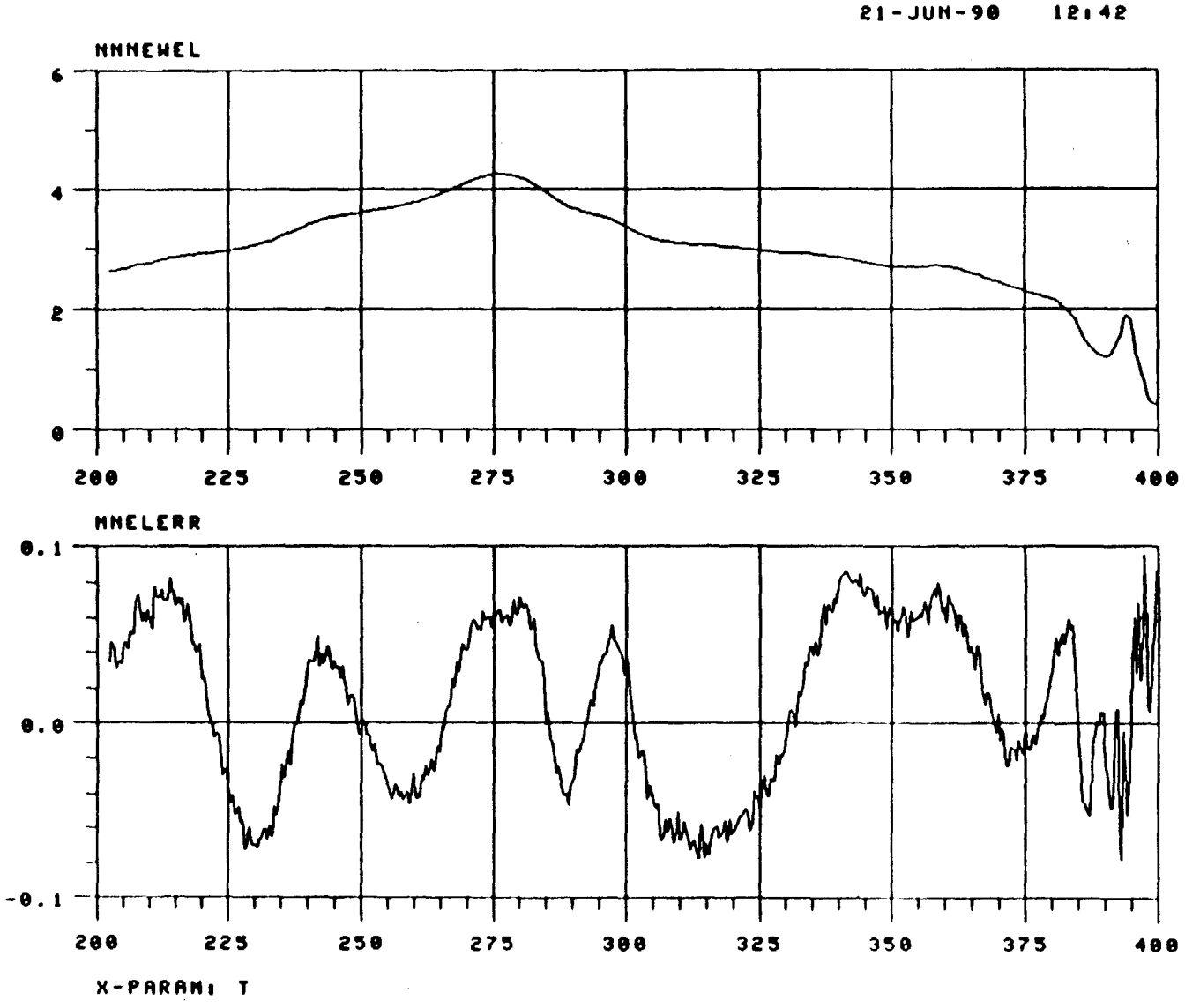
AZIMUTH ANGLE AND ERROR

scenario: JFK Canarsie approach RWY 13R



ELEVATION ANGLE AND ERROR

scenario: JFK Canarsie approach RWY 13R



831

DME VALUE AND ERROR

scenario: JFK Canarsie approach RWY 13R

